PHASE I TOPICAL REPORT

Field demonstration of an active reservoir pressure management though fluid injection and displaced fluid extractions at the Rock Springs Uplift, a priority geologic CO_2 storage site for Wyoming

April 5, 2016

WORK PERFORMED UNDER AGREEMENT

DE-FE0026159

SUBMITTED BY

University of Wyoming Carbon Management Institute
1020 E. Lewis Street, Energy Innovation Center
Dept. 4902, 1000 E. University Ave.
Laramie, WY 82071

PRINCIPAL INVESTIGATOR

Zunsheng Jiao
307-766-6802
jjiao@uwyo.edu

SUBMITTED TO

U.S. Department of Energy
National Energy Technology Laboratory

Contributing Authors

Carbon Management Institute
School of Energy Resources, University of Wyoming

Ramsey Bentley
Kipp Coddington
Evan Egenolf
Yuri Ganshin
Zunsheng Jiao
Fred McLaughlin
Scott Quillinan
Kim Shannon

Lawrence Livermore National Laboratory

Roger Aines
William Bourcier

Los Alamos National Laboratory

Rajesh Pawar
Dylan Harp
Chris Bradley
Lianjie Huang
Jeri Sullivan
Richard Middleton

Battelle

Andrew Duguid

Water System Specialists, Inc.

Chris Haussmann
Tom Wolf

Acknowledgement: This material is based upon work supported by the Department of Energy under Award Number(s) DE-FE0026159.

Table of Contents

I. EXECUTIVE SUMMARY

Commercial-scale geologic carbon dioxide (CO_2) storage sites, tested to safely store billions of tonnes of CO_2 over hundreds of years, will be necessary to meet the United States': (1) 2050 greenhouse gas (GHG) reduction goal of 80% or more by 2050; (2) initial commitments under the 2015 Paris Agreement (an economy-wide target of reducing GHG emissions by 26% - 28% below 2005 levels and to make best efforts to reduce GHG emissions by 28%); and (3) Clean Air Act section 111(b) (GHG New Source Performance Standards for New EGUs) standards, which specifically identify geologic sequestration as a mitigation technology for new coal-fired power plants. More broadly, carbon capture utilization & storage (CCUS) will help to support the Administration's Clean Power Plan goal, which applies to the existing coal fleet, of a 32% reduction in CO_2 emissions from 2005 levels by 2030. Internationally, wide-scale deployment of CCUS on all fossil energy systems – both coal and natural gas, and perhaps in the form of bioenergy with CCUS -- is expected to be necessary by no later than 2050 to meet the 2015 Paris Agreement's goal of "[h]olding the increase in the global average temperature to well below 2°C above pre-industrial levels and to pursue efforts to limit the temperature increase to 1.5°C." *2015 Paris Agreement, art. 2, §1(a), FCCC/CP/2015/L.9/Rev.1 (Dec. 12, 2015).*

However, injecting large volumes of CO_2 into saline reservoirs will result in increased formation pressure. Without proper management, the increased pressure could potentially result in large-scale displacement of in-situ fluids, and geomechanical impacts such as confining layer breaching or fracturing, leading to CO_2 and brine migration beyond the primary injection zone, induced seismicity and contamination of overlying groundwater aquifers. As a result, an active reservoir pressure management strategy is necessary to ensure the safe and efficient operation of commercial-scale geologic CO_2 storage in saline reservoirs (Aines et al., 2010, Sullivan et al., 2013, Surdam and Jiao, 2009). Viable field-scale pressure management strategies will require that research gaps be investigated, and new technologies be developed and validated to: (1) predict differential pressure evolution effects; (2) understand injected fluid-flow migration pathways and distributions; (3) constrain transport simulation; (4) assess geomechanical impacts of fluid injection; and (5) integrate production and injection management strategies.

A key pressure management technique is the production of brines in a controlled manner. Those produced brines, in turn, hold the potential of beneficial uses to include: (1) the creation of usable waters via the use of advanced and economic treatment technologies; and (2) the recovery of potentially economically recovery materials. Making economic use of produced brines in this way thus holds the potential of generating ancillary energy-water nexus benefits including reduced CCUS costs and the production of usable waters.

The primary objective of Phase I is to address technological gaps of reservoir pressure management by developing and validating, through a carefully-designed field project, advanced technologies and engineering approaches for: (1) predicting, monitoring and managing pressure and injectate plumes; and (2) developing a Brine Extraction Storage Test (BEST) facility to validate treatment technologies for extracted brines. The study area is the Rock Springs Uplift (RSU) in southwest Wyoming, an area that already has been intensively studied for CCUS purposes through DOE-funded (DE-FE0002142, DE-FE0009202, DE-FE0026159, and DE-FE0023328) and related efforts.

The following investigations have been conducted to achieve the project goals:

- Refine 3-D reservoir structure and property models of the site that include the known structural complexity and reservoir heterogeneity of the site;

- Evaluate geophysical and geochemical monitoring technologies and techniques to: (1) detect and measure reservoir pressure response to injected fluid; and (2) track fluid migration pathways;

- Analyze the feasibility of extracting formation brine water to mitigate the pressure increase from injection, modify the pressure front, and influence/steer the direction of the migrating pressure/CO_2 plume;

- Develop fluid flow simulation approaches to predict reservoir pressure responses and migration pathways of the injected fluid;

- Implement rock mechanical property and stress calculations, combined with simulations, to help assess geomechanical impacts to the reservoir and confining layers during large-volume injection;

- Develop water management and treatment strategies, and provide a design for the construction of a BEST facility;

- Conduct a produced brine life-cycle analysis, and develop a displaced brine water treatment and management program; and

- Propose an active reservoir pressure and injectate plume management strategy for the study site that could be implemented during field testing in Phase II.

To meet these ambitious goals, the project team completed the tasks outlined in its Phase I application. These tasks included: (1) gathering the information necessary to permit new and existing wells at the RSU and its vicinity for potential use in Phase II; (2) developing a monitoring, verification and accounting (MVA) plan; (3) evaluating the feasibility of repurposing existing wells at the RSU; (4) developing a strategy to manage the produced water; (5) modeling and simulating injections; (6) assessing the geomechanical impacts of comparable CCUS-related injections at the RSU; and (7) developing and validating active reservoir pressure management strategies.

By successfully completing these Phase I tasks, the project team demonstrated the potential for a successful Phase II test center deployment at the RSU with the promise for fundamentally advancing CCUS through advanced pressure management and MVA techniques, while making beneficial use of produced brines, thereby separately advancing the state of water treatment science.

A. Phase I Accomplishments

The steps necessary to re-permit existing wells and/or permit new wells as injection, monitoring, or production wells for use during Phase II were identified. Potential well permitting hurdles and their impact on the project have been identified along with strategies to overcome them.

Required State of Wyoming, federal (if any) and local approvals for Phase II of the project were identified. Identified approvals include those related to: (1) surface and subsurface use permitting; (2) state land section access; (3) the Underground Injection Control (UIC) program; (4) water treatment center permitting; (5) storm water permitting; (6) API number applications for injection and production wells; (7) water rights permissions; (8) air quality permitting; (9) electrical service permitting; and (10) county approval. During Phase I key regulators were contacted and the requirements for granting these permits/approvals were clarified.

Variables that are most critical to assessing the reservoir's response to CO_2/water injection were evaluated. These variables -- chosen to reduce project uncertainty and risk as much as possible -- include: (1) porosity and permeability heterogeneities; (2) shear strength/rheologic properties; (3) reservoir fluid geochemistry/physical properties; (4) reactive minerals; (5) clay mineral composition and content; (6) pore architecture/pore throat distributions; (7) facies architectures; (8) capillary pressure properties; and (9) fracture/faults systems. These variables were analyzed using core, wellbore, and seismic data, much of which were generated during prior DOE-funded investigations of the RSU. With an eye towards Phase II, the team's evaluation of these reservoir variables at the study site greatly improved confidence relative to: (1) pressure and injectate plume management plans; (2) MVA; (3) long-term injectate/CO_2 containment; and (4) the production of suitable brines to meet the project's Phase II water treatment objectives.

Extensive research of case studies was performed to identify MVA and related techniques capable of monitoring pressure propagation resulting from a sizable fluid injection at a depth of more than 12,000 ft. Identified monitoring technologies included: (1) three-dimensional vertical seismic profiling; (2) downhole pressure and temperature gauges; and (3) crosswell seismic surveys. Three-dimensional vertical seismic profiling (3-D VSP) acquired along the well bore can be used to characterize the rock and fluid properties in the vicinity of injection, production and monitoring wells. The 3-D VSP data set will provide an opportunity to make in-situ, time-lapse measurements of seismic amplitude, velocity, anisotropy, and attenuation (Q factor). From this same data set, fracture orientation information can be derived; hence, the VSP must be capable of recording not only P-waves but also shear waves. Downhole pressure and temperature gauges at both the injection and the production/monitoring wells will collect data in real time. The other valuable monitoring technology includes crosswell seismic surveying between production and injection wells, and between injection and monitoring wells. The time-lapse inter-well tomography can be used to image the pressure changes and injectate plume movement as a sizable amount of water/CO_2 is injected into the targeted reservoir. The use of chemical tracers to track the flow pattern of the injection reservoirs as well as connectivity from the injector to the producing wells was also investigated. There is a wide array of materials and methods used for tracer testing. Some of these methods include injecting stable isotopes, radioactive chemical species, organic dyes, and fluorocarbons into the injecting well and measuring the quantity (and time) of material received at the producing well. The project team

has a contact (with funding) from the National Energy Technology Laboratory (NETL) that is interested in exploring its novel tracer design at the RSU study site.

Candidate wells at the study site and within its vicinity, including the existing RSU#1 well, were analyzed for repurposing. The results of the technical analyses were used to estimate costs associated with drilling, completion or recompletion. Well integrity analysis was based on existing logs and records, and will provide a picture of potential risks to the Phase II project. The utility analysis used the vital statistics of each well (size, material, depth, cement, etc.) to analyze its expected performance as an injection/production well. The analysis included nodal modeling to calculate injection volumes and rates, and establish tubing size. This well design analysis ensures the well can handle the new stresses associated with sizable injection; well scale assessment ensures that precipitation in the well will not significantly impede injection further; and corrosion modeling ensures existing materials in the well will provide for a successful operation.

Water in the targeted formation is of high salinity -- more than twice that of seawater -- so treatment processes require special handling. Chemical modeling of the Madison Formation brines was conducted in order to help guide treatment technology selection and possible scaling issues with brine reinjection. The chemical analysis results of the targeted formation water were assembled and the analytical self-consistency was verified. All available treatment technologies are reviewed in detail in this report. Five conceptual water treatment trains were selected for further evaluation: (1) nanofiltration (NF) alone operated at low recovery; (2) nanofiltration followed by reverse osmosis (RO); (3) NF plus RO followed by thermal softening of the reject for $CaSO_4$ reduction prior to reinjection; (4) NF plus RO followed by thermal evaporation and crystallization; and (5) thermal evaporation and crystallization. Spreadsheets to predict RO and NF membrane stream quality and cost were generated. Such baseline quality and cost information is necessary to determine water quality for reuse as well as potential reservoir scaling issues of the returned concentrate streams.

Preliminary water life cycle analysis (LCA) indicates that minimizing transportation distances, brine disposal costs (via volume reduction) and pretreatment costs will be important components of cost control. Influent flow rate to the treatment system may also create increased cost variance. Market forces will dictate the potential for use of some products from water treatment. Maximizing the extraction of fresh water from the brine stream will greatly reduce disposal costs (and transportation costs), unless a market is found for "clean brine" products. Minimizing the use of hydrocarbon fuels and optimizing energy uses in site operations are expected to reduce the project's carbon footprint. A full understanding of the effects and impacts of these processes on the overall system life cycle can be achieved with ongoing LCA, cost measurement, and site-specific analysis during Phase II testing.

A numerical model was developed using the Los Alamos National Laboratory's (LANL) FEHM reservoir simulator for a 6 km x 6 km subsection of the RSU 3-D seismic survey domain. The numerical model was based on the geologic data available for the area of interest through previous geological CO_2 storage site characterization efforts. The data were used to generate tops for five formations of interest at the RSU: Weber, Amsden, Madison, Madison reservoir zone, and the bedrock Darby Formations. The tops for all formations were used to generate a

numerical mesh using LANL's LaGriT toolkit (http://lagrit.anl.gov). A number of preliminary flow simulations were performed to simulate injection of water, assuming the same injection location as the existing RSU-1 well. Multiple runs simulating water injection with injection rates of 1 tonne, 100 tonnes, and 1,000 tonnes per day (tpd) in the Madison Limestone for a period of 10 years were performed to generate an understanding of the scale of pressure changes that could result from such injections. The preliminary simulation results indicate that pressure changes extend over a considerable horizontal distance. The pressure change could be on the order of 1MPa at a distance 3 km away from the injector. The predicted pressure change at any location in the reservoir is lower for a low injection rate (e.g., 100 tpd) compared to a higher rate (e.g., 1000 tpd); the extent and time-dependence of the pressure change display similar trends. The simulation results indicate that production from the reservoir and reservoir compartmentalization have a significant effect on overpressures and represent a major source of risk and uncertainty for pressure management design.

Research on various fluid injection/production scenarios shows that a variety of options for placement of wells exists for effective plume management control, formation pressure control, implementation of MVA, and production of brines for treatment. Production wells can be placed up-dip or down-dip from injection wells, for example, or wells can be converted from production to injection as the project progresses. Research on engineered fluid barriers utilizing dense brine waste streams did not produce a great amount of information. This method of plume control is generally used in very shallow pollution control situations. Problems such as unanticipated plume migration events were researched as well. Information from various enhanced oil recovery (EOR) operations provides insight into this problem. This project is somewhat different from an EOR operation in that breakthrough of injected fluids to production well(s) would not be acceptable and would diminish the fluid storage effort. Placing production well(s) down-dip to take advantage of the density difference of the fluids might be a way to avoid breakthrough and will be further investigated.

Based upon all of these analyses conducted during Phase I – including how best to leverage DOE's prior investments at the RSU, minimize project risks, and maximize the successful completion of objectives in light of Phase II's budget constraints -- the project team has concluded that:

- The proposed field test site for Phase II will be within the area of the existing Jim Bridger 3-D seismic survey (State section, T20N, R101W, Sec. 16). Better known as the RSU and the location of the existing DOE-funded RSU#1 well, this site carries with it numerous tangential benefits to advancing CCUS, including: (1) it has been the subject of numerous prior DOE-funded investigations; and (2) it sits in close proximity to existing CO_2 pipeline infrastructure and PacifiCorp's Jim Bridger power station, one of the largest sources of CO_2 in the Rocky Mountain region. As it has done in the past and did for Phase I, PacifiCorp has committed to support Phase II objectives.

- Project infrastructure will be constructed to minimize costs while maximizing the data that can be collected regarding reservoir differential pressure changes. Injectate plume movement can be controlled through variation of subsurface gradients created by injection and production. As a result, the Phase II project will have two wells: one

injector and another well that can serve both production and monitoring tasks. This well design is the minimum configuration that can validate the control of subsurface plumes. Injection and production in a single well validate pressure management by simply increasing or decreasing pressure. Plume management requires injection in one well and production/monitoring from other wells. A tracer will be injected along with the brine and production will alternate between wells and/or rates will vary between the producer/monitoring well to show that tracer concentrations and pressure can be steered. The project team will spend the remainder of Phase I evaluating other pressure management strategies that may be implemented within the Phase II budget.

- Novel MVA strategies may be deployed under these conditions to advance the state of science and generate data to enable effective updating of the relevant geologic models.

- A BEST facility may be constructed directly onsite to validate, through use of slip streams from the production well, a variety of treatment technologies for extracted brines. The water situation in Wyoming makes placement of such a facility here ideal.

In conclusion, the project team, through its Phase I analyses and leveraging DOE's prior investments at the RSU site through the use of data such as WY-CUSP core, has met all Phase I objectives and advanced the state of the science on pressure management, MVA and brine treatment through the analyses presented in the report. The project team has thereby laid the groundwork for successful implementation of Phase II at the RSU site. The team remains confident that continued investment in the RSU holds promise for advancing CCUS through implementation of advanced pressure management techniques, MVA, and water treatment technologies at a site with strategic importance for CCUS generally and the Rocky Mountain region specifically.

II. STUDY SITE

Building on DOE-funded characterization studies (DE-FE0002142, DE-FE0009202 and DE-FE00026159) at the same location, the project team has an ideal field test site: the RSU. The RSU: (1) has distinct saline reservoirs; (2) offers unique opportunities to test pressure response and pressure management strategies for a wide-range of reservoirs; and (3) is home to the RSU#1 stratigraphic test well that was drilled by the University of Wyoming under DE-FE0002142. Located approximately 34 miles east of the town of Rock Springs, Wyoming, 1 mile southeast of the 2100 megawatt Jim Bridger coal-fired power plant, and approximately 12 miles to the northwest of the Black Butte coalmine (**Figure 1**), the 5 mi x 5 mi area of review (AOR) is centralized to prime industrial activity. In addition to the power plant and coalmine, approximately 60 oil and natural gas wells are located within the AOR, with 20 of those still actively producing. Several of these wells could potentially be repurposed, if necessary, to meet Phase II subsurface objectives including a dry hole drilled approximately 1,800 ft. to the northeast of the RSU#1 test well. (Wyoming Oil and Gas Conservation Commission http://wogcc.state.wy.us/). Four different producing fields were established including Deadman Wash, Masterson, Point of Rocks, and Shiprock with targeted producing zones in Cretaceous age rocks. Several shallow groundwater monitoring wells are located in close proximity to the study site. Access is simplified by a heavy-duty haul road through the northeast quarter section and several proximal two-track roads.

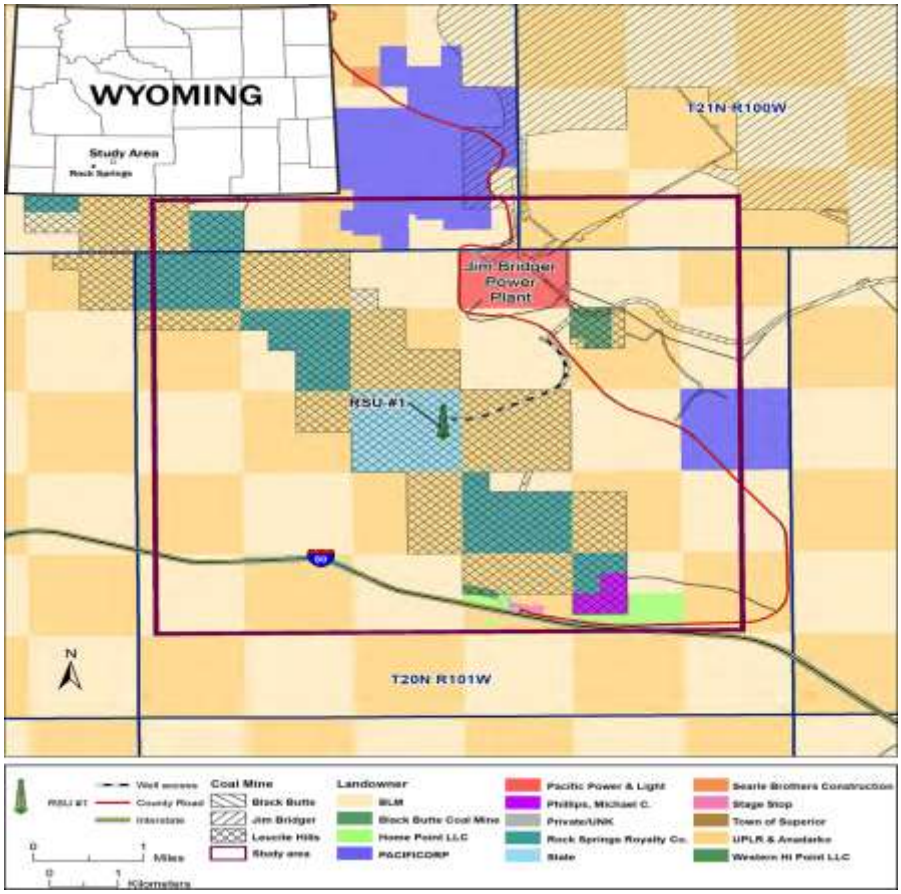

Figure 1: Map of southwest Wyoming showing the RSU#1 study site.

III. SITE CHARACTERIZATION

Building on DOE-funded characterization studies (DE-FE0002142, DE-FE0009202 and DE-FE00026159) at the same location, in the RSU the project team also has a well-characterized field test site. The site characterization was achieved through field investigation, the acquisition of a 5 mi x 5 mi seismic survey, drilling of the RSU#1 test well, multiple downhole tests, logs and extensive analyses. Previous analysis of subsurface data has allowed identification and definition of prime injection zones, sealing capacity, reservoir and confining layer heterogeneity, rock mechanics, stress vectors, geochemistry and compositional variance of the formation fluids, pressures, temperatures, geologic history, fluid characteristics, diagenetic history, burial history, micro-seismic variance, reservoir response to limited step-rate injection, seismic character and attributes, seal by-pass systems, and preliminary responses to injected fluids (Surdam, 2013).

Geologically, the RSU is a large (50×35 mi, 80×55 km) doubly-plunging asymmetric anticline with the steeper limb on the west side. It has four-way closure with over 10,000 feet of structural relief (Surdam and Jiao, 2007). The targeted Mississippian Madison

Limestone reservoir at the site is approximately 400 ft (120 m) thick and occurring at depths greater than 12,200 ft (3,700 m) below the land surface (McLaughlin et al., 2014). Overlying thick and laterally extensive Paleozoic and Cretaceous marine sediments are documented to seal and hydraulically isolate the targeted reservoirs (Frethey and Cordy, 1991; Bartos and Hallberg, 2010; McLaughlin et al., 2014). Most of the site has a fairly shallow surface slope having sufficient space to drill additional wells and place surface facilities for monitoring activities, brine production, and water treatment.

Several sets of subsurface data were gathered at the study site during the DE-FE0002142, DE-FE000044 and DE-FE00026159 projects that were and will continue to be valuable to this project. The data sets include: (1) the 5 mi x 5 mi 3-D seismic survey; (2) 916 ft. of core, cuttings and thin sections from target reservoirs and seals; (3) a comprehensive suite of petrophysical well logs (Multipole Array Acoustic, high definition induction, mud, photoelectric, caliper, spectral suite, compensated z-density, compensated neutron, resistivity, gamma ray, earth imager/CBIL); (4) a zero-offset VSP for correlation with the seismic survey; (5) various in-situ reservoir tests including a vertical interference test, step-rate injection and fracture gradient testing; (6) multiple brine samples from targeted formations and analysis results; and (7) a micro-seismic survey.

As noted, the RSU has distinct saline reservoirs that offer unique opportunities to test pressure response and pressure management strategies over a wide-range of geologic settings. These include: (1) reservoirs with different lithologies (sandstone and limestone); (2) different reservoir types (conventional reservoirs: porosity > 15% and permeability >10 mD; and tight reservoirs: porosity < 10%, and permeability 1 mD); and (3) different in-situ fluid qualities (salinities from 30,000 ppm to > 100,000 ppm and temperature from 80 to 110°C). The characterization data from the projects listed above will be used to further define estimated injectivity, storage capacity, pressure responses, CO_2 plume migration, and fracture characteristics of the selected reservoir interval through actual field experiments.

Target reservoirs in the Madison Limestone were defined on the basis of lithology and reservoir/sealing characteristics, including permeability, porosity, reservoir heterogeneity, and sealing intervals. These data were correlated with seismic and petrophysical data to identify prime injection zones. This information will greatly reduce the risk associated with the pressure management program and provide a greater understanding of plume migration. The prime injection zone in the Madison is identified as the middle 170 ft. of the dolostone/ limestone, though there are three additional dolostone zones lower in the section. The average porosity and permeability within the middle Madison are 13.1 % and 22.7 mD, respectively. Reservoir heterogeneity within the dolostones is related to porosity type (intergranular and/or moldic/vuggy), diagenesis and cementation. Dolostone with intergranular porosity has permeability that ranges from 0.001 mD to 82.6 mD, and porosity ranges from 0.3 to 22.4 %. Pore sizes and distribution are relatively homogeneous. Permeability in moldic and/or vuggy dolostones ranges from 0.001 mD to 2245 mD, and porosity ranges from 0.3 to 19.8 %. Pore sizes and distribution within vuggy and/or moldic zones are highly variable, with pores as large as 3000 µm. Porosity in the Madison mostly associates with early dolomitization. Due to a higher permeability and overall holding capacity, the Madison is identified as the prime target for fluid injection and extraction for this project.

Formation fluid samples were collected from the Madison reservoirs and tested for minor and major elements, radionuclides, organic acids, volatile organics, organic characteristics and flash gas compositions. Brines from the Madison reservoir are a sodium-chloride type with measured total dissolved solids concentrations 75,000 mg/L (*see Appendices:"Complete Madison Formation Water Analyses"*). Ionic strength ranges from 1.44 molal to 1.61 molal. Brine temperatures is 95°C, with a formation pressure of 5,312 psi.

Core from caprock was analyzed for porosity, permeability, and mercury capillary displacement pressure. Main confining layers are the Triassic Red Pick Formation, the Pennsylvanian Amsden Formation, and the upper portion of the Mississippi Madison Limestone. Porosities of the major confining layers range from 0.62% to 1.4 %, and permeability is less than 0.001 mD at reservoir conditions. Pore throat radii are <2 µm, ranging between 0.001 µm and 1.6 µm. Displacement pressures in the reservoir condition, calculated from mercury capillary injection tests, range between 65 psi and 252 psi (448 kPa and 1,737 kPa) for the oil-water system, and 126 psi to 488 (869 kPa and 3,365 kPa) for the gas-water system. This indicates the overlying seals can effectively confine injected fluids within the reservoir.

The Jim Bridger 3-D seismic survey, covering an area of about 25 mi^2, was shot as a baseline study for possible future CO_2 injection. More than a dozen seismic attributes were systematically analyzed, concluding that curvature, interval velocity, acoustic impedance, iso-frequency amplitude, and mean frequency were particularly useful in mapping structural trends, performing seismic facies analysis, and determining porosity and permeability distributions within the target horizons (**Figure 2**). Seismic data were interpreted with respect to the RSU#1 test well petrophysical and core data, as well as to surrounding wells. The seismic data allowed for numerous interpretations of the reservoir, seal, and fluid properties within the study site, which will be used to further define the pressure management program.

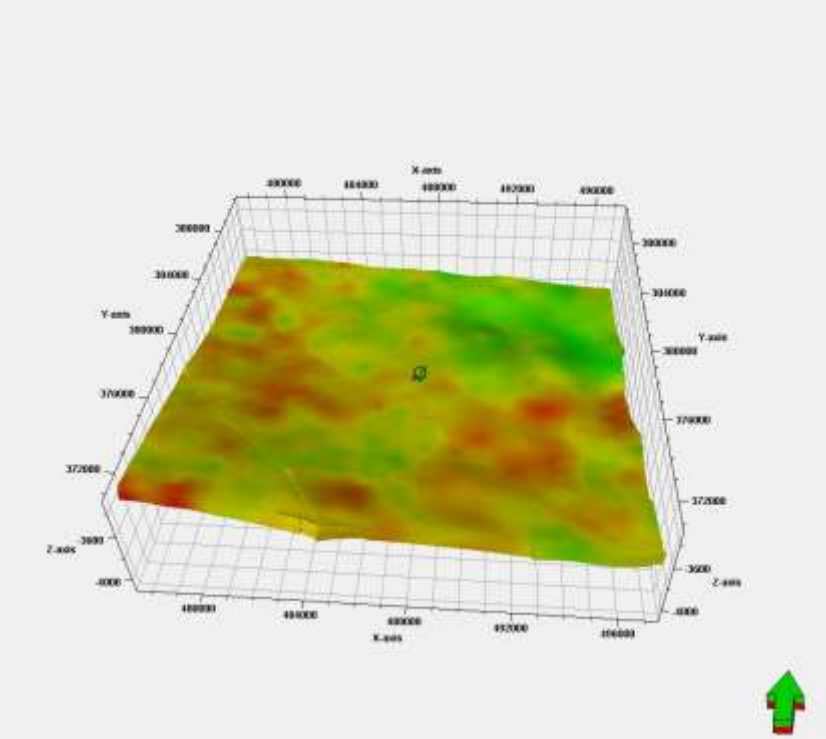

Figure 2: **Madison Limestone Porosity** - The porosities derived from the seismic interval velocities for the Madison Limestone for the RSU site show significant heterogeneous characteristics in the study domain.

The dominant trend of unfilled subsurface fractures at the RSU site is ENE-WSW, correlative to the trend of regional structural features. The Madison Formation is slightly under or normal- pressured, and the stress state is transitional between strike-slip and normal faulting. The results of the step rate test calculated a fracture pressure gradient of 0.84 psi/ft. With pore pressure increase, the fractures could become critically stressed and hydraulically conductive. Higher injection pressures could cause a wider range of fracture orientations to become permeable.

For both the VIT and the Mini-DST, a partially penetrating wellbore model in a homogeneous infinite acting reservoir was used. The VIT results indicate a horizontal permeability value of 4.16 mD, a vertical permeability of 0.48 mD, and a radius of investigation of 74 ft.; the model calculated the initial pressure of 5312.47 psi at the depth of 12,361 ft.

Using the aforementioned data, a preliminary numerical fluid flow simulation model was created and CO_2 injection simulations were performed using LANL's multiphase porous flow simulator (Finite Element Heat and Mass transfer code, or FEHM). These simulations tested various injection scenarios over differing periods (**Figure 3**). These simulations reveal that the greatest uncertainty in the quantitative assessments of the storage capacity, reservoir pressure responses, and plume migration pathways for a selected storage site highly depends on characterizing geological heterogeneity in three dimensions (Jiao and

Surdam, 2013). The simulation results also demonstrated that brine production would be necessary to reduce pressure buildup resulting from large-scale CO_2 injection at the RSU.

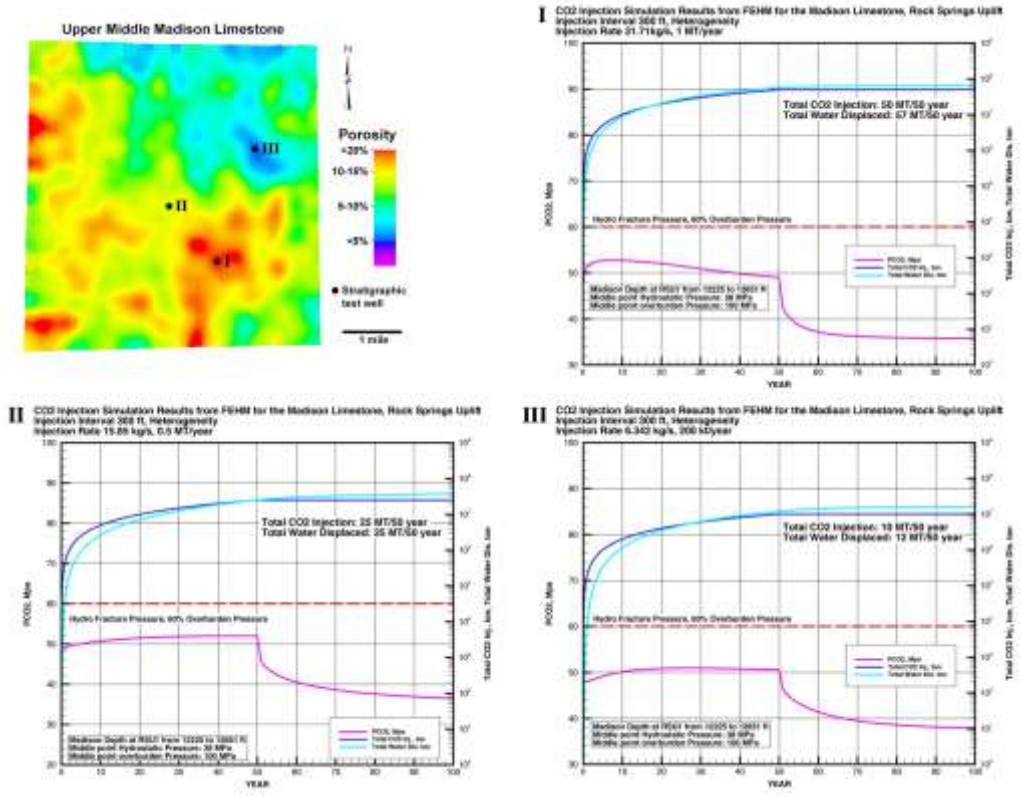

Figure 3: **FEHM Injection Simulation Results** - FEHM CO_2 injection simulation results for the Madison Limestone, RSU.

The simulations are set up for a heterogeneous reservoir. The injection rates of 31.71 kg/s, 15.85 kg/s, and 6.34 kg/s are constant for 50 years for wells in the high, medium, and low reservoir quality areas, respectively. Simulated injections modeled 50 years, stopped, and the simulation modeled another 50 years without CO_2 injection. The reservoir pressure quickly elevates when injection begins but is kept below the hydro-fracture pressure through the entire injection time. After modeled injection ceased, the reservoir pressure is attenuated back to original pressure within ten years.

Currently, the RSU study site has been reclaimed, but utilizing relationships built under DE-FE0002142, the project team already has enlisted qualified assistance in re-establishing appropriate well-sites and drilling areas. In addition, the project team identified potential team members under DE-FOA-0001238 that are interested in furthering project goals and objectives by assisting with water treatment facilities.

IV. EVALUATION OF PERMITTING REQUIREMENTS UNDER WYOMING CODE RELATIVE TO POTENTIAL APPLICATIONS OF THE INJECTION WELL

The steps necessary to re-permit existing wells or permit a new well(s) as an injection, monitoring, and/or production well for use during Phase II were identified. Potential permitting hurdles and the impact on the project were identified along with the lowest risk classes of injections wells with respect to the success of the project.

The program team evaluated the permitting of wells identified for Phase II broadly to include not only well permitting but also site access, site preparation, certain ancillary facilities, potential water treatment facilities, and reasonably foreseeable permitting needed to fully permit and operate the wells at the site. Our criteria for assessing potential permitting needs were principally (1) the prior experience with the WY-CUSP permitting for the RSU#1 test well; (2) team meetings to ascertain the scope and potential facilities needed for the project; and (3) personal communications with regulatory agencies and landowners who will provide necessary access and support for the project. Details follow.

A. Surface and Subsurface Use for Siting and Conducting Project Activities

The project is proposed for siting on state trust land administered by the Wyoming Office of State Lands and Investments (OSLI) located in Section 16, Township 20 North, Range 101 West, Sweetwater County, Wyoming. This is the same location previously permitted for the WY-CUSP project and drilling of the RSU#1 test well. Existing uses of the parcel have not changed and there are no apparent conflicting uses.

Use of the site for an integrated facility will require a Temporary Use Permit (TUP) or a Special Use Lease (SUL) from OSLI as approved by the State Board of Land Commissioners (Board). Whether a TUP or SUL is most appropriate will depend on the combined duration of construction, operations and decommissioning, the scope of use of the state parcel, and OSLI preference upon review of a complete plan of development for the integrated facility. On February 23, 2016, team members met with the OSLI Director and staff members to review the project and the necessary permitting requirements. Application for a TUP or SUL involves an application to OSLI, which is reviewed by staff and the Director. The Director makes a recommendation to the Board on the application, which is then presented to the Board for consideration at a public meeting. From application to permit approval should be between three and six months; associated filing fees and rentals are anticipated to be modest (less than $3,000.00 annually). Because the land is managed in trust for generation of revenue for designated beneficiaries, the Board cannot waive fees and rentals.

B. Access to the State Land Section

Access to the project site will be by the same access road used utilized in the WY-CUSP Project, entering from Sweetwater County Nine-Mile Road in Section 10, and crossing Sections 10 and 15 to reach State Section 16. There is a current haul/access road utilized by Black Butte Coal Company (Black Butte) crossing lands owned by Anadarko Petroleum Corporation (Anadarko), and the Bureau of Land Management (BLM).

Both Black Butte and Anadarko have provided letters of commitment to CMI indicating their support for the project and their willingness to enter into formal letter agreements or rights of way to allow CMI to use the existing roads for the Phase II project at no cost. A right of way (ROW) will also be required from the BLM to cross federal surface in Section 10, E1/2E1/2 along the same access road. BLM granted a three-year ROW to use the same road for the WY-CUSP project without incident; the ROW grant expressly exempted the University of Wyoming from cost recovery and rental fees. We anticipate BLM approval within six months of submission of a complete SF299 application, without additional cost. Because the ROW would provide access across an existing road, no National Environmental Policy Act (NEPA) processes or analysis are anticipated.

C. Underground Injection Well (UIC) and Water Treatment Bed Permitting

The project potentially envisions drilling and completion of two wells: one for injection and another for production/monitoring. On February 22, 2016, team members met with the Wyoming Department of Environmental Quality (WDEQ), Water Quality Division (WQD) Administrator and WQD staff to review the Project and permitting process within the WDEQ/WQD. The WDEQ/WQD maintains primacy over Class I UIC injection wells.

The same WDEQ principals involved in the permitting of the RSU#1 test well for the WY-CUSP project were at the meeting and would likely be involved in the permitting for this project. The WDEQ confirmed that all requirements for the RSU#1 test well were met and there were no compliance issues with that permit.

Because the Phase II project does not contemplate injection of CO_2 into the formation, Class I UIC permitting would apply. Class VI was investigated further despite the fact it is not relevant for Phase II as the team will be injecting water. WDEQ does not presently have to permit Class VI wells; therefore, and again hypothetically, if injection of CO_2 were to occur, Class VI permitting through the US Environmental Protection agency (EPA) would be required until such time as a WDEQ Class VI primacy application is submitted to and approved by the EPA. WDEQ/WQD staff did discuss the possibility that it may be feasible to permit the project as a Class I UIC facility, but construct the facilities to Class VI standards (while also complying with Class I standards), in the event there is a future opportunity to convert the demonstration project into an actual CO_2 injection project.

After discussing the general project concepts, WDEQ/WQD staff indicated that it would be possible (and appropriate) to streamline the application for the two wells and process them in a single UIC Class I application. Staff also indicated they could further streamline permitting by including other project components under the same UIC application, such as the planned BEST facility (i.e., the Rocky Mountain Brine Treatment Test Center). While the water treatment bed would require technical review by the WQD Construction Permit Program staff, design reports and supporting information could be submitted as part of the UIC application and issued under a single UIC permit with the other project facilities. If the water treatment bed produced a waste stream that is discharged to surface waters of the state rather than being injected back into the formation, a Wyoming Discharge Pollution Elimination System (WYPDES) permit also would be required; we do not envision surface discharges to occur.

UIC permit applications are processed under Chapter 27 of the Wyoming Water Quality Rules and Regulations (WQRR). Upon submission of an application with the requisite supporting information, WQD conducts an initial review within 60 days, and, if complete, prepares a draft permit for issuance or denial, prepares a fact sheet on the proposed operation, and provides public notice of the permit. (If the application is deficient WQD provides the applicant notice of the deficiencies.)

All Class I permits require a thirty-day public notice and opportunity for comment, pursuant to WQRR Chapter 27, Section 21. In addition to publishing notice of the draft permit, notice is also provided to the EPA, Wyoming Game and Fish Department, Wyoming State Engineer, State Historical Preservation Officer, Wyoming Oil and Gas Conservation Commission, the WDEQ Land Quality Division, persons requesting notice of such applications, and local governments having jurisdiction in the area where the facility is proposed to be located (e.g., Sweetwater County). Any interested person may request a public hearing on the draft permit. The WQD Administrator is required to hold a hearing when he determines, on the basis of requests, there is a significant degree of public interest in a draft permit, and may elect to hold a hearing if it may clarify issues involved in a permit decision.

The WDEQ Director is required to render a decision on the draft permit within thirty days after the completion of the comment period if no hearing is requested. If a hearing is held, the Director makes a decision as soon as practicable after the receipt of the transcript of such hearing or after the expiration of time set to receive written comments. No public hearing was requested or conducted prior to approval of the WY-CUSP RSU#1 Class I UIC permit. We are not aware of any stakeholders likely to request a hearing or challenge a Phase II UIC Class I permit application. WDEQ/WQD staff indicated that they typically can approve a Class I UIC application within six months of receipt of a complete application.

All Class I wells require financial assurance. The amount of financial assurance cannot be less than the estimated cost of plugging, abandoning, and post-closure care for each well. Based on our discussions with WDEQ/WQD staff, financial assurance is estimated at approximately $$13 per foot for any Class I injection well. Currently, the financial assurance for the RSU#1 test well (a $140,000 letter of credit) remains on file with the DEQ, even though the well has been plugged and abandoned. CMI could transfer the RSU#1 financial assurance to one of the other Project wells. In addition to posting financial assurance for any Class I injection wells, WDEQ

has indicated financial assurance would also be determined for associated surface facilities (such as the water treatment bed) and the amount of bonding would be addressed at the time of permitting.

OSLI also has authority to require bonding of facilities constructed on State Lands; however, we discussed with both OSLI and WDEQ the possibility of posting financial assurance with only one agency, rather than both agencies. Bonding with the WDEQ and not OSLI for the RSU#1 test well was allowed for the WY-CUSP Project; accordingly, we anticipate the two agencies would coordinate to avoid duplicate bonding for the Phase II project as well.

D. Storm Water Permitting

Phase II project construction will require storm water permitting through the WDEQ/WQD, which administers the federal storm water program. There are two possible storm water permits that could apply to the project: (1) a construction storm water permit (either small activity or large activity); and (2) an industrial storm water permit. The construction storm water permit pertains to clearing, grading and excavating activities associated with the project. Whether an industrial storm water permit will be required will depend on the nature of the activities on and the potential for industrial pollutant run-off from the site.

The construction storm water permit is required to ensure that sediment and other pollutants do not leave the site during facility construction. One of two construction storm water permits could apply, depending on the size of the project's construction footprint. If construction activities are more than one but less than five acres, permit coverage for a small construction activity will be required. If construction activities exceed five acres, permit coverage for a large construction activity will be required. For purposes of determining the construction footprint acreage, the disturbance areas for all construction activities associated with the project will be aggregated.

The WDEQ/WQD has developed both small and large construction storm water general permits. Thus, individual permits are not required (absent conditions that are not likely to be present for the project). Instead, CMI will have to ensure it follows the requirements of the applicable general permit. The small and large general permit requirements are the same, with the exception that for any project larger than five acres, a Notice of Intent (NOI) must be submitted to the WDEQ/WQD and approved prior to commencing construction.

For both large and small general permits, a Storm Water Pollution Prevention Plan (SWPPP) must be in place prior to commencing construction. The SWPPP is a document prepared by the applicant (or its consultant) that identifies how storm water runoff will be controlled at the construction site, and requires identification of best management practices (BMPs) that will be employed to minimize and prevent the discharge of pollutants to waters of the state during surface water runoff events.

An industrial activity storm water permit will be required if the project facilities are characterized as an industrial plant and such facilities include a conveyance used for collecting and conveying storm water directly related to manufacturing, processing or raw materials storage areas. The possible need for an industrial storm water permit can be evaluated and an application

can be submitted, if necessary, at the same time it is determined whether the project requires a large or small general storm water permit. WDEQ also has an industrial storm water general permit that operates similar to the large construction general permit and contains similar requirements (submission of a NOI, preparation of a SWPPP and WDEQ approval before operations commence).

There is a $500 fee for large construction activity and industrial activity NOIs, which is paid at the time of NOI submission. Authorizations are issued for a maximum of five-years. (Underlying general permits are issued for five years, and if the general permit expires sooner than five years from the NOI authorization, a new NOI authorization must be obtained when the general permit is renewed.) If the project life is less than five years (construction through reclamation), as is the case here, the construction permit fee can be reduced by $100 per year. Small activity construction permits do not require a fee. The processing time for approving NOIs for large construction and industrial storm water permitting is usually within thirty days.

E. Obtaining an API Number

CMI will need to submit a "courtesy" application for permit to drill (APD) to the Wyoming Oil and Gas Conservation Commission (WOGCC) in order to obtain an API number for each well (production/monitoring and injection). The assignment of an API number to each well is necessary to include each well in the state's database of well records. Accordingly, the WOGCC also requests continuous communication as to the status of each well (e.g. recompletions to different depths, plugging, and abandonment). The WOGCC waives APD fees for API number assignments and there is no additional bonding required through the WOGCC. API numbers typically are assigned within a few weeks following submission of the courtesy APD.

F. Water Rights for the Project

The sources of water that will be used for drilling and injection may include water: (1) withdrawn from the project's production well; and (2) produced from the mine dewatering system at the Bridger Coal Company (a division of PacifiCorp) operated as part of its underground coal mining activities. CMI must acquire water rights from the State Engineer's Office (SEO) for both sources for use in the project. The project team foresees two types of water rights, as follows: (1) permits to appropriate groundwater for any project production well from which water will be withdrawn for re-injection purposes; and (2) a permit to appropriate by-product water sourced from the Bridger Coal Company mine dewatering system for project purposes. Each is discussed below.

For any project well that will produce groundwater for a beneficial use, a permit to appropriate ground water from the SEO is required. (Wyo. Stat. 41-3-930). The beneficial use for water from the project's production well would be to withdraw and reinject water for the purposes of maintaining or regulating formation pressures and to direct the injection plume within the formation. We anticipate both of these purposes would be described as industrial categories of "beneficial use." If any of the produced water is treated and put to beneficial use on the surface rather than reinjected (as would be the case here), the permits would also identify the beneficial surface use(s).

The SEO does not have a commonly-established ground water permitting protocol for the type of beneficial uses to which project water will be put. Thus, a pre-application meeting in advance of submitting permit applications will help ensure the necessary project information is provided so that the SEO can efficiently process the applications. We do not anticipate a lengthy permitting process, particularly if a pre-application meeting is held to discuss the applications. The project area is not in a designated ground water control area where special permitting procedures and additional notice requirements apply. The application would be reviewed by staff, and if the necessary information is present, a permit should issue as a matter of course. Typical ground water applications are processed and permits issued in 4-6 weeks. The permit application fee is $75.00 per well for ground water applications for industrial use wells.

Water from the Bridger Coal Company mine dewatering system appears to fit within the statutory definition of "by-product water" under Wyo. Stat. 41-3-904. A SEO permit is required to appropriate by-product water for beneficial use for project purposes. The by-product water appears capable of being intercepted for use at the project before it has commingled with the waters of any live stream, lake, reservoir, surface watercourse or groundwater aquifer. Under such circumstances, CMI may seek to permit the use of the water through the SEO in the same manner that groundwater rights are applied for, but CMI must also file an agreement signed by Bridger Coal Company granting CMI permission to appropriate the water for the Project. (Wyo. Stat. 41-3-914(a)(ii)). (CMI already has a letter of commitment from PacifiCorp for this purpose.) In the event that water from the mine dewatering system commingles with any live stream, lake, reservoir, surface watercourse or groundwater aquifer prior to being intercepted for project purposes, CMI may seek to permit the water under the laws pertaining to surface water appropriations, subject to use by existing priority rights. Since the Bridger Coal Company mine dewatering system utilizes several permits and related water infrastructure, we envision holding a pre-application meeting with the SEO staff to review permitting issues prior to submitting any applications.

G. Air Quality Permitting

The project may require a New Source Review (NSR) Construction Permit from the WDEQ Air Quality Division (AQD) under Chapter 2 Section 6 of the Wyoming Air Quality Standards and Regulations (WAQSR). If an NSR permit is required, it likely would be issued to cover the project, rather than individual project components. NSR requirements apply to new construction projects that may cause an increase in air contaminants. A permit is required before construction commences.

NSR applications are made on forms provided by the AQD and require identification of project components or processes that may result in air emissions (e.g., generators, engines, tanks, heaters, boilers, well completion emissions, etc.), and an estimation of project emissions. Based on the information submitted, the AQD will determine whether a permit is required, or whether a waiver may be issued. Under the NSR program, sources are required to be equipped with the Best Available Control Technology. In this case, until all project components are identified and evaluated, it is not possible to predetermine whether the project will be eligible for a waiver. These issues would be determined at the time the AQD reviews the application.

Upon submission of a complete application, when the AQD Administrator has reached a proposed permitting decision to grant or deny a permit, AQD will provide public notice of the proposed approval or disapproval and allow 30 days for public comment, and may hold a hearing on the application prior to making a determination on permit issuance. In addition to publishing notice of the proposed decision, notice is also provided to the EPA, any affected comprehensive regional land use planning agency, affected county commissioners and any state or federal land manager or Indian governing body whose lands may be significantly affected by emissions from the proposed facility. If the applicant or agency anticipates a hearing will be required, the processing time can be minimized by including the notice of the hearing with the publication of the application.

If the AQD determines that a waiver applies, it notifies the applicant of the waiver determination and no public notice is required. The AQD can impose conditions on a waiver as necessary to ensure compliance with legal requirements.

With a complete application, the typical permitting timeframe is four to five months. There is a standard application fee of $464.00, and the AQD also charges $58.00/hour for time spent reviewing the application.

The project also envisions hauling water from the Jim Bridger plant to the project injection well. Hauling activities will need to be carried out in compliance with the AQD regulations in Chapter 3, Section 2(f) of the WAQSR, which require minimization of fugitive dust from hauling operations. Control measures can include application of asphalt, oil, water, or suitable chemicals on unpaved roads and other surfaces which can give rise to airborne dusts.

H. Electrical Services

If electrical services are secured through a third party utility provider under a contract for service negotiated between CMI and the utility provider (here, Rocky Mountain Power), as is envisioned for Phase II, it is typical for the utility provider to contract for delivery of power to a drop point, at which point it can be distributed to project facilities. The utility provider typically arranges access and routing for its facilities to get them to the power drop, thus avoiding any additional CMI permitting requirements relating to electrical services. CMI has had fruitful initial discussions with Rocky Mountain Power (through PacifiCorp and the Jim Bridger power station) regarding these aspects.

I. County Approvals

The RSU#1 stratigraphic test well required an oil and gas well permit from Sweetwater County. As none of the proposed wells fall within the jurisdiction of the Wyoming Oil and Gas Conservation Commission, a county oil and gas well permit may not be required for either of the two project wells. Moreover, so long as no CO_2 is to be injected and no man camp is to be constructed to house workers on site, no county conditional use permit should be required. CMI nevertheless should and will (if approved under Phase II) communicate with Sweetwater County regarding Phase II project plans and timelines, and should be prepared to submit all requested

hazardous chemical and emergency planning information to the County for emergency management and response purposes. Sweetwater County was an interested and supportive stakeholder of the WY-CUSP project and we anticipate the same will be true for Phase II project activity.

V. DEFINE CRITICAL SUBSURFACE DATA AND MODEL INJECTATE GEOCHEMICAL RESPONSES

A. Select Critical Variables to Define Reservoir Characteristics

There are numerous geological and physical variables that are most critical to assessing reservoir pressure response to fluid injection at the RSU study site. Our analysis considered critical reservoir variables/parameters from core, petrophysical, and formation fluid chemistry, wellbore and seismic data. Variables were selected and analyzed as they proved most effective at reducing geologic uncertainty, risk, and increasing total storage capacity and successful injectivity. Nearly a decade of work by the project team evaluating and characterizing these reservoir variables at the study site has and will continue to greatly increase confidence relative to low-risk fluid injection/storage. **Table 1** defines critical reservoir variables needed for characterization of the Madison injection zone for Phase II. These data were used to build and populate 3-D geologic property models, dynamic fluid models, and develop geologic history.

This research team has extensive research experience evaluating the reservoirs and seals of the study site (DE-FE0009202; DE-FE0026159; Surdam, 2013; McLaughlin et al., 2014; Pafeng et al., 2014; Shukla et al., 2015; Wu et al., 2015). In these studies, our team has evaluated and analyzed the critical reservoir variables in **Table 1**, as well as other relevant data. These studies have given us an unprecedented understanding of the Madison reservoir and associated seals, and two current investigations (Phase I of this project and DE-FE0023328) will help to further define geomechanical and modeled reservoir pressure responses. The Madison Limestone is the best target for CO_2 storage at the RSU study site. Though heterogeneous, the Madison has the highest permeability and porosity of Paleozoic formations (**Figures 4 and 5**). The Madison is overlain by numerous sealing lithologies including the upper limestone facies of the Madison Limestone, the Amsden Formation, the basal marine facies of the Weber Sandstone, and the siltstone and claystone of the Triassic Chugwater Group.

Table 1: A listing of general reservoir properties defined for Phase 1.

Critical Variable/Parameter for Reservoir Characterization	**Generalized Data from the RSU study site**		
1. Reservoir property heterogeneity			
Dykstra-Parsons coefficient of permeability variation		0.99	
2. Porosity (%)	*Minimum*	*Maximum*	*Average*
Core measured, at reservoir pressure	5.9	22.4	14.2
Seismically-derived porosity		Qualitative	
3. Permeability (mD)	*Minimum*	*Maximum*	*Average*
Core measured, at reservoir pressure and Klinkenburg corrected	0.2	2,245.7	22.7
Seismically-derived permeability		Qualitative	
4. Relative permeability			
Core measured, CO_2 flooding experiments[1]			
5. Shear strength/rheologic properties	*Minimum*	*Maximum*	*Average*
Compressive strength from traixial shear tests (psi)	22,046	47,677	34,542
6. Formation pressure			
Measured in-situ from vertical interference tests (psia)		5,312.5	
7. Formation temperature		*Maximum*	
Maximum measured at total depth (TD), degrees fahrenheit		201.6	
8. Density	*Minimum*	*Maximum*	*Average*
Measured, in g/cm^3	2.77	2.87	2.82
9. Reservoir fluid geochemistry/physical properties	*Minimum*	*Maximum*	*Average*
Total dissolved solids, measured from reservoir samples	81,346	89,931	85,865
10. Gas content/composition			
Ratios, as measured from fluid samples	82.9% CO_2	16.7% N_2	0.4% Alkanes
11. Bulk mineralogy			
Primarily dolostone, calcium, silicate minerals, anhydrite, and pyrite			
11. Reactive minerals			
Primarily carbonates and sulfates			

*Akbarabadi, Morteza, and Mohammad Piri. "Relative permeability hysteresis and capillary trapping characteristics of supercritical CO 2/brine systems: An experimental study at reservoir conditions." Advances in Water Resources 52 (2013): 190-206.

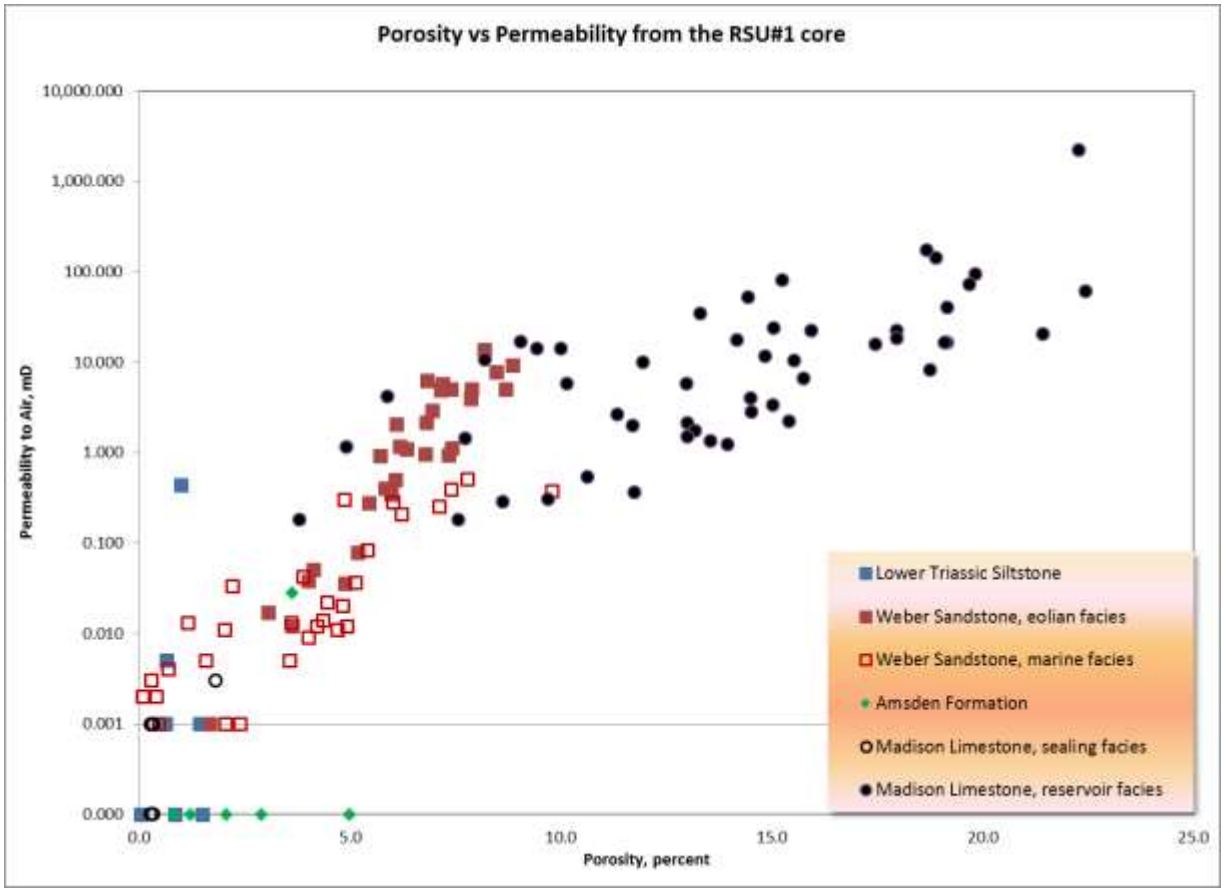

Figure 4: Porosity vs. permeability distribution measured from the RSU#1 test well. These data show that there are two distinct reservoirs in the Paleozoic section: (1) the eolian Weber Sandstone facies, and (2) the Madison Limestone reservoir facies. There are also four formations/facies that act as sealing lithologies (low permeability and porosity). Note that porosity correlates to permeability much more strongly in the Weber Sandstone than the Madison Limestone. This indicates a higher order of geologic heterogeneity in the reservoir portion of the Madison formation.

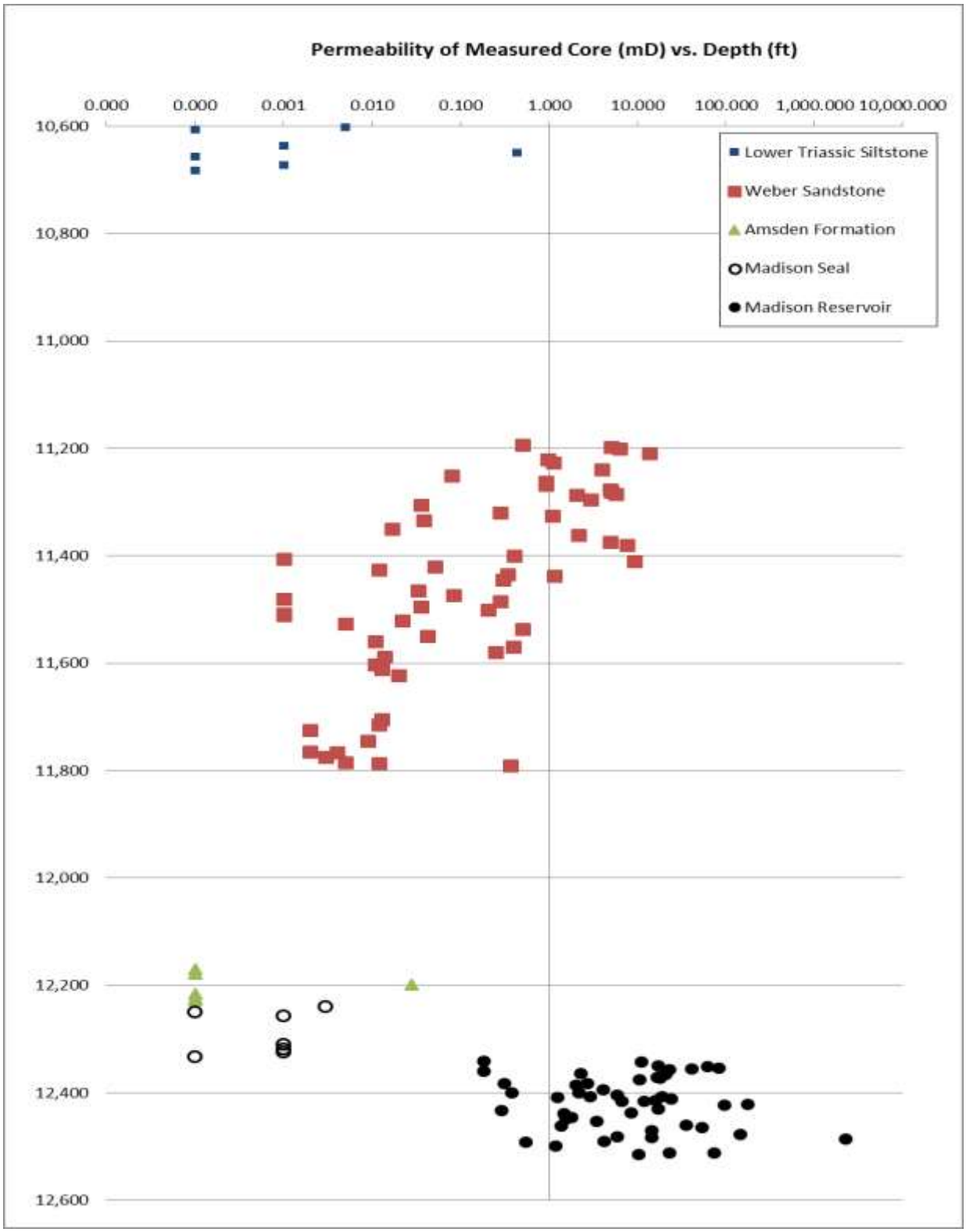

Figure 5: Permeability by formation and depth at the RSU#1 test well. This shows that the Madison Limestone reservoir facies has exponentially greater reservoir properties than other formations at the study site.

Previous RSU#1 test well injectivity tests: Several small-scale injectivity tests have been performed at the RSU#1 test well. These include a mini-DST (drill stem test), VIT (vertical interference test) and a step-rate injection test. The VIT, run during the well's completion, showed that the Madison had vertical permeability anisotropy, and that the reservoir recorded pressure disturbances/responses during drawdown and build-up periods. This is an absolute necessity for Phase II experimentation, and helps to validate the use of the Madison reservoir for our injection target. This test also showed that permeability was at least 13 mD at the packer interval, and that fluid infiltrated at least 74.0 feet into the reservoir.

During a second entry of the RSU#1 test well, a step-rate injection test was performed. This test identified pressure build-up in the well, as well as the fluid response from the Madison reservoir. **Figure 6** shows the results of temperature log profiling before and after set-rate injection. The large blue spike identifies the zone (previously perforated) in the Madison reservoir wherein most of the fluid was injected. This shows that the Madison will act as an ideal test reservoir for pressure management; fluids can be injected into the formation and injection is differential.

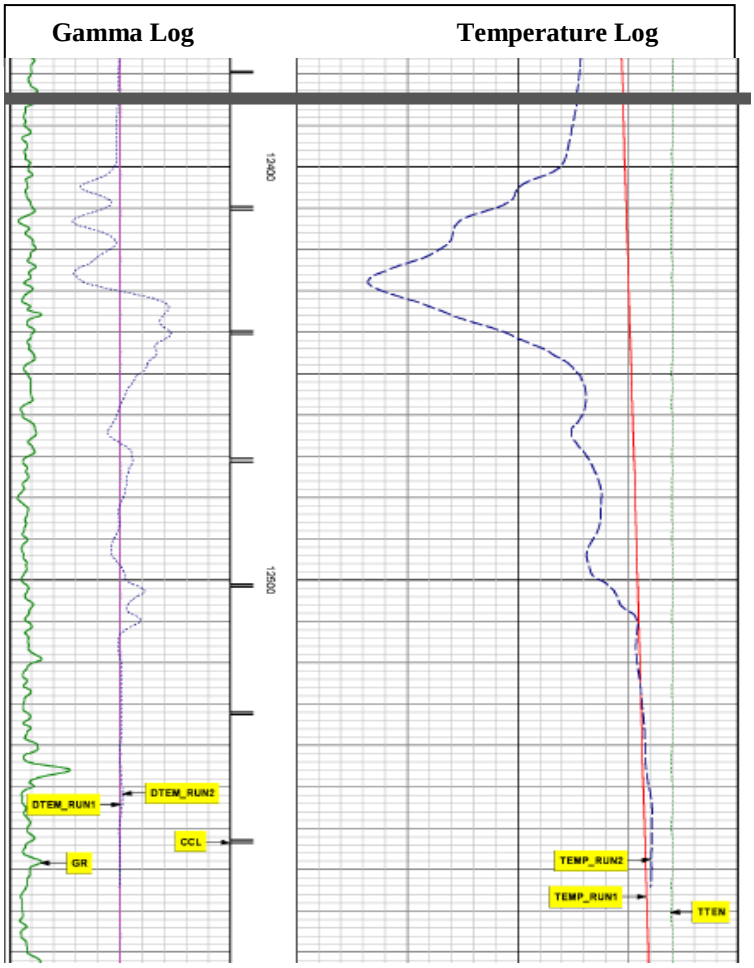

Figure 6: Sequential temperature log from the step-rate injection testing. The dashed blue line highlights the zones where cooler surface waters infiltrated the Madison reservoir. This suggests a relatively high permeability heterogeneity.

VI. DEFINE THE COMPOSITION AND RANGE OF INJECTATES FOR THE TARGET FORMATIONS

Outlined in detail below, there are four candidate injectates available for Phase II reservoir pressure tests in addition to recycled formation fluid from the water treatment test center (the Rocky Mountain Brine Treatment Test Center). All of the potential injectates are water. We investigated the potential of obtaining and using nitrogen, CO_2, and flue gas for injectation; none of them proved to be pragmatic for this project. Both nitrogen and CO_2 would have necessitated expensive shipping fees, as well as crippling purchasing costs. The project team could have likely obtained flue gas from the nearby Jim Bridger power station, though the engineering and regulatory challenges of capturing and compressing a flue gas slipstream during Phase II's compressed schedule eliminated that option, too. In Phase II, all of the four injectate types could be provided courtesy of the Jim Bridger power station, thereby negating the need for drilling additional water wells or trying to buy water rights in one of the driest regions of the Colorado River basin. Additionally, obtaining an injectate from the Jim Bridger power station should significantly reduce transportation costs, thereby preserving Phase II resources to focus on science objectives.

The four candidate injectates can all competently meet the volume requirements of the Phase II test phase. They also all have variable water chemistries. The four candidate injectates are sourced as follows: (1) mine water from the Jim Bridger coal mine; (2) circulation water from the Unit 1 tower at the Jim Bridger power station; (3) "raw" water destined for the plant's cooling towers; and (4) water from the plant's ash disposal ponds. Specific chemistry is displayed in **Table 2**.

1. *Mine water from the Jim Bridger coal mine*: Mine water, sourced from Tertiary coal beds of the Jim Bridger mine, has the second lowest overall salinities. This water has relatively low total dissolved solids, with sodium as the dominant cation and carbonate and sulfate as primary anions. Trace metals concentrations are very low.
2. *Circulation water from the Unit 1 tower*: Circulation water, sourced from the Unit 1 tower at the Jim Bridger power station, has the second highest overall salinity. This water has higher total dissolved solids, with calcium and sodium as dominant cations and carbonate and sulfate as the dominant cations.
3. *"Raw" water destined for the cooling towers*: Raw water, sourced from the Green River, has the lowest salinity of all candidate injectates. This water has low total dissolved solids, with calcium and sodium as primary cations and sulfate and carbonate as primary cations.
4. *Water from the ash disposal ponds*: Pond water, sourced from ash disposal ponds, has the highest salinities of all candidate injectates. This water has total dissolved solids that would likely complicate scaling and geochemical reactions in the wellbore and reservoir.

A. Select Optimal Injectate for Injectivity Testing

During the pressure testing of Phase II, upwards of 100,000 tonnes of fluid will be injected into the Madison reservoir per year for the two-year operational phase (BP3). It is therefore critical to research injectate reactions relative to reservoir fluids and conditions. Much of the injectate used for this project will be recycled brines from the target formation (Madison Limestone; detailed water chemistry available in Quillinan and McLaughlin, 2013). Additional waters will be needed for drilling, increasing reservoir pressure, and to supplement in-situ well tests. The Jim Bridger power station can provide four candidate injectates for Phase II pressure experiments, as noted above. **Table 2** shows the chemical constituents of the potential injectates.

Table 2: Geochemistry of the different waters available from the Jim Bridger power station as potential injectates

Constituent	Unit	Raw Water	Mine water	Unit 1 Circulation Water	Pond 2 water
Al+++	mg/l	–	0	2.2	–
B(OH)3	mg/l (as B)	0.03	–	–	542
Ba++	mg/l	0.07	0.07	0.8	0.23
Ca++	mg/l	56	25	770	57
Carbonate alkalinity	mg/kg_as_CaCO3	180	810	76	–
Cl-	mg/l	6.1	26	130	4680
Cu+	mg/l	nd	0	0.07	0.05
Electrical conductivity	uS/cm	470	1900	4600	–
F-	mg/l	–	–	–	422
Fe++	mg/l	–	0.12	2.1	0.89
Hardness	mg/l_as_CaCO3	212	63.5	3500	–
HCO3-	mg/l	0	–	–	19600
K+	mg/l	2	4.4	25	1020
Li+	mg/l	0.01	0.46	0.2	–
Mg++	mg/l	17	6.4	210	110
Mn++	mg/l	–	0	0.19	0.61
Na+	mg/l	28	500	410	39200
Ni++	mg/l	–	0.03	0.01	0.31
NO3-	mg/l	–	2.4	–	–
Pb++	mg/l	–	nd	–	0.03
pH		8.4	8.4	7.7	9.3
SiO2(aq)	mg/l	3.23	7.63	50	–
SO4--	mg/l	94	250	2900	42500
Sr++	mg/l	0.468	0.496	9.3	–
Zn++	mg/l	–	0.04	–	0.22

B. Compatibility

To identify the potential injectate compatibilities with the Madison formation fluids we generated flash diagrams. Flash diagrams can be instructive to determine mineral scale that may occur from the result of mixing two fluids. These calculations show mineral scale as a function of mixing fraction between to the two fluids, and are designed to evaluate reactions in the wellbore. **Figures 7a-d** demonstrate the mixing responses from 100% formation fluid (0% injectate) to 1% (99% injectate) for each of the four candidate injectates.

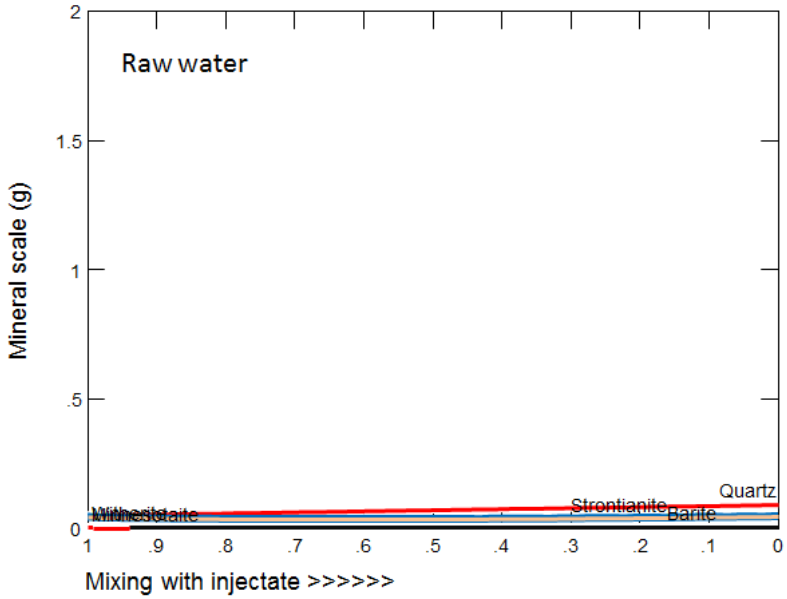

Figure 7a: Mineral scale growth as a mixing fraction of Madison formation water to the raw water injectate. Note that very little mineral scale is expected at all mixing ratios.

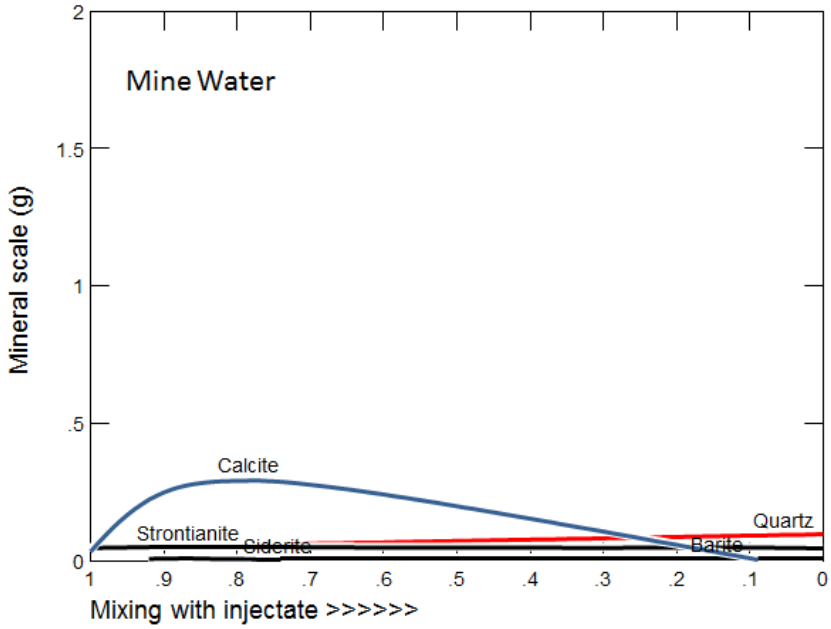

Figure 7b: Mineral scale growth as a mixing fraction of Madison formation water to the mine water injectate. Calcite scale will form at most mixing ratios but is most prominent at 90 -60% formation water and 10-40% mine water.

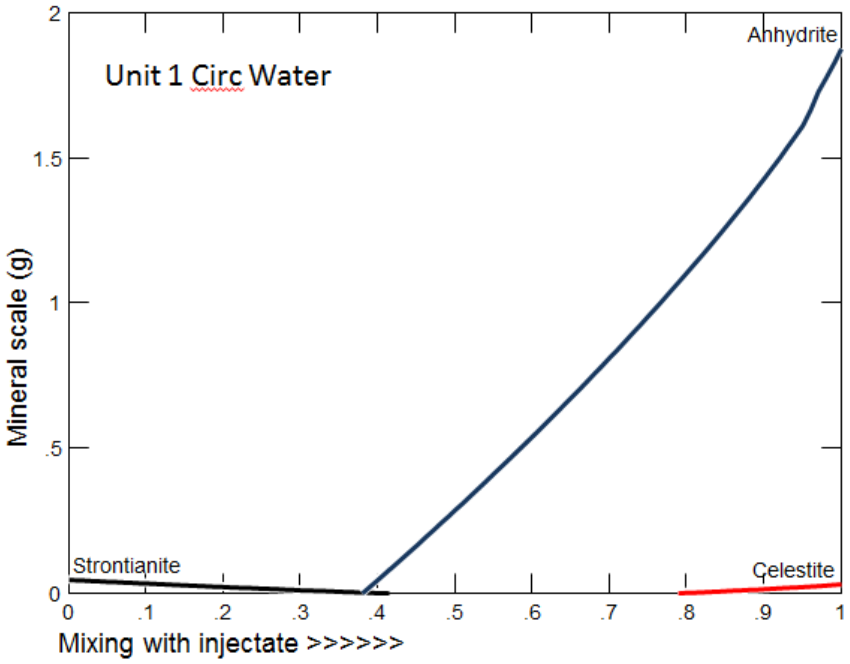

Figure 7c: Mineral scale growth as a mixing fraction of Madison formation water to the Unit 1 Circ water injectate. Anhydrite scale will form will begin to form once the formation water is diluted to beyond 40%.

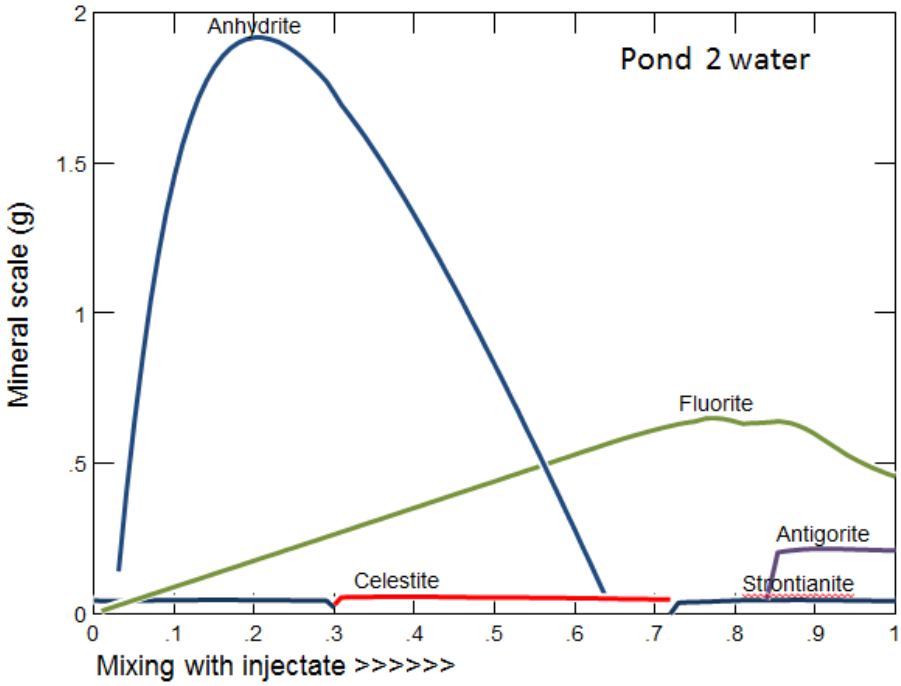

Figure 7d: Mineral scale growth as a mixing fraction of Madison formation water to the Pond 2 water injectate. Significant anhydrite scale begins to form even at very low mixing fractions. Fluorite scale is also a concern high ratios of injectate to formation fluid.

On the basis of these calculations, the injectate with the lowest potential for mineral scale is the "raw" water. The mine water also suggests a high compatibility with the formation fluids, as only minor calcite scale is estimated. The circulation water from Unit 1 has a low probability for mineral scale, as long as it is mixed in fractions that don't exceed less than 40% formation water. Beyond the ratio of 40% in the formation water significant anhydrite scale is anticipated. The water from Pond number 2 presents the highest scale potential of all of candidate injectates. This injectate would have significant anhydrite scale with less than 10% mixing. Fluorite scale is also a concern if the formation water is mixed with the Pond 2 water.

These data show that the "raw" water and Jim Bridger mine water have the lowest potential for mixing-related scaling, negating the need for well treatments and workovers. On the basis of these analyses and in concern for not disrupting Jim Bridger's current operational strategy, we suggest using the mine water for injectate during Phase II of this project.

VII. DEVELOP A MONITORING PROGRAM

A. Seismic Acquisition Strategies That Will Provide Optimal 3-D Raypath Coverage

One of the project objectives is to develop geophysical technologies to monitor the reservoir pressure responses due to fluid injection. It is a well-known fact that seismic velocities depend on pore pressure. This fact has been used for predrill pore-pressure estimation for a long time. As such, time-lapse seismic observations can serve as a tool for monitoring injection. However, there are several principal and site-specific challenges that must be considered. Importantly, the burial depth and thickness of the reservoir zone must be in reasonable proportion to each other for a velocity change to be detectable. The seismic noise content that increases with the burial depth is another important factor to consider. In case of injecting fluids that do not differ much in physical properties with the target reservoir brine (e.g., fresh water or brine from a different subsurface reservoir), we will face an extremely challenging situation.

For a study site consisting of only two wells, as we propose for Phase II, information between the wells is scarce so seismic monitoring techniques are essential to provide data on lateral variations between wells. Pressure and fluid changes are the important factors in monitoring injection/production processes. In this study we want to quantify the seismic sensitivity to changes in saturation and pressure. But first the best seismic attribute to monitor the reservoir changes must be identified. Formation P-wave velocity is our first candidate, but we are also planning to analyze shear-wave velocity as well as seismic amplitude and frequency. The changes in velocity are attributed to both changes in fluid saturation and the increase in pore pressure. Numerous case studies show an increase in velocity near the production well due to the increase in effective pressure and decrease in velocity near the injection well due to decrease in effective pressure and change in saturation. As the effective pressure of the rock increases, the rock becomes stiffer and so the velocity increases. The velocity decrease due to pore pressure increase is due to the opening of a number of closed pores or microcracks thus making the rock softer. Changing pore pressure can change the saturation as gas goes in and out of solution making velocities sensitive to saturation.

For the purpose of pressure change monitoring in three dimensions, we propose acquiring 3-D VSP. Unlike surface seismic techniques, VSP utilizes measurement of rock properties (in particular, wave propagation velocity) along the vertical (or near-vertical) well bore that provides: (1) an improved resolution due to increased frequency content; and (2) an improved signal/noise ratio due to the subsurface recording of seismic waveforms. We propose to deploy an array of 3C geophones over a depth of 8,500 feet from the base of the Madison Limestone to the top of the Baxter Shale. To ensure a good acoustic coupling and repeatability of measurement conditions, we suggest installing permanent down-hole geophone arrays or a fiber-optic cable. The geophone level spacing should be of 50 feet or less (distributed in case of fiber-optic cable) over the reservoir intervals and a coarser spacing could be used over the Baxter Shale interval. Our design suggests using multiple shot points around the injection wellhead. We propose to use vibroseis sources with a peak-force allowing recording of reflections from a 14,000-foot depth

with maximum offsets up to 12,000 feet. The vibrators should produce a broad range of sweep frequency, e.g. from 10 to 200 Hz. We propose acquiring data from a set of multiple concentric circles with a maximum radius of 12,000 feet that is centered on the wellhead (**Figure 8**). The minimum amount of surface stations that we are planning for the baseline acquisition should be within the range 1,000-2,000 source points. This recording geometry should produce a wide range of offset and azimuth fold coverage of the subsurface. Another unique aspect of this project is the use of downhole 3C arrays. The sensor spacing is chosen to be 50 ft, comparable to typical wireline tools. The maximum deployment depth of approximately 12,500 ft is limited by the proposed borehole's depth. Our design remains an iterative process that is dependent on the final design of the field scale test (well placements, geochemistry data, etc.).

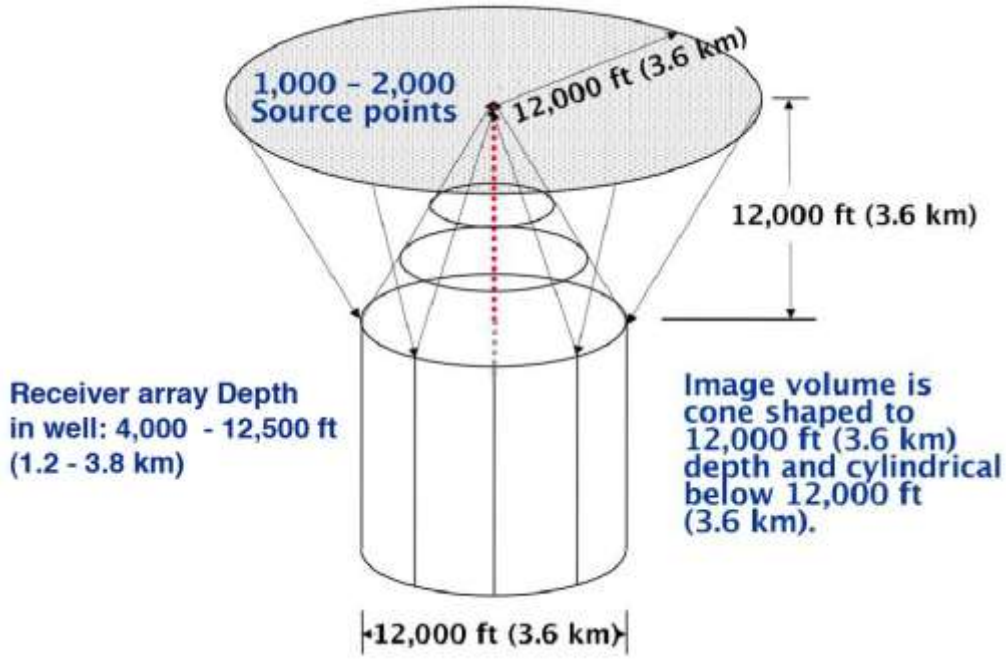

Figure 8: Schematic drawing depicting an example image volume obtainable from a 3-D VSP acquisition in a vertical well.

For time-lapse (4-D) reservoir monitoring new challenges and opportunities arise beyond static VSP imaging. One key question is repeatability of data acquisition conditions. For the proposed field experiment, we consider a fixed downhole geophone tool to be an excellent answer for acquiring the time-lapse VSP. Recently, fiber-optic technology has been developed for reservoir monitoring using permanent in-well seismic sensors. Initial trials of fiber-optic technology demonstrated that the technology works and the signals of comparable fidelity to standard geophones could be obtained using fiber-optic-based sensors deployed on tubing (e.g. Mateeva A. et al., 2013; Daley T.M. et al., 2013). Another question is this – can we acquire borehole seismic data during injection/production of a well? As demonstrated by Knudsen et al. (2006), excellent-quality seismic data were acquired with single-phase (water) flow. For the multiphase

(water/air) flow, good-quality data were acquired, with more noise on the radial (x, y) sensors. For the proposed field experiment, we see permanent instrumentation of wells with seismic sensors to be a strong candidate for reservoir monitoring that will enhance seismic illumination and signal-noise ratio as compared to a surface 4-D acquisition scheme. In this case we might deploy permanent seismic sensors in multiple wells to give a larger, reservoir-scale coverage.

This task also identified some special processing steps required for advanced analyses of time-lapse seismic data. Changes of geophysical properties caused by fluid/CO_2 injection are usually small, ranging from a few percent up to approximately 20% of changes. Therefore, some special data processing steps that are different from those for conventional data processing are needed for time-lapse seismic data in order to preserve time-lapse changes in seismic data. These processing steps and output datasets are often not in the routine seismic data processing steps used by seismic data processing companies. For advanced seismic imaging and inversion of time-lapse seismic data, we need to obtain prestack (before stack) seismic data in common-shot or common-receiver or common-midpoint gathers with the following processing steps employed:

- statics corrections (for VSP and surface seismic data);
- amplitude corrections for source coupling;
- denoising (noise attenuation);
- deconvolution;
- cross-equalization/balancing of time-lapse seismic data; and
- amplitude-friendly processing steps.

Some processing steps such as automatic gain control (AGC) and spectrum whitening are not amplitude friendly as they cannot preserve amplitudes of seismic data. However, these processing steps are essential for seismic migration imaging. Therefore, the output datasets from seismic data processing should include a copy of data for migration imaging and the other copy of data for full-waveform inversion that requires amplitude-friendly processing.

The processing output datasets should also include:

- a copy of data with multiples removed as in the conventional data processing for migration imaging; and
- a copy of data without removing internal multiples (processing in the tau-p domain for a few walkaway lines for VSP data after denoising).

This is because internal multiples in time-lapse seismic data carry much more information on reservoir changes than primary reflections.

When applying band-pass filtering to seismic data, the low-frequency components of data need to be retained as much as possible according to the vibroseis and borehole source sweep frequencies. It may work to just apply a low-pass filter instead of a band-pass filter. Low-frequency components of seismic data are helpful for full-waveform inversion to avoid converging to local minima of the objective function for the inverse problem. **Table 3** lists the processing output datasets/products needed for advanced time-lapse seismic data analyses.

Particularly, a 3-D velocity model obtained using prestack depth migration velocity analysis is crucial for reverse-time migration and full-waveform inversion of seismic data to obtain a high-resolution subsurface structure image and a high-resolution velocity model.

Table 3: A list of output datasets/products from processing of various seismic data.

3-D/walk-away VSP data	**Crosswell seismic data**	**3-D surface seismic data**
Downgoing P and S data	Downgoing P and S data	Common-shot P- and S-wave gathers
Upgoing P and S data	Upgoing P and S data	Common-shot rotated three-component data in East, North, and Vertical coordinates
Rotated three-component downgoing data in East, North, and Vertical coordinates	Rotated three-component downgoing data in East, North, and Vertical coordinates	P- and S-wave velocity models obtained using prestack depth migration velocity analysis.
Rotated three-component downgoing data in East, North, and Vertical coordinates	Rotated three-component downgoing data in East, North, and Vertical coordinates	Source wavelets extracted in P- and S-components and in rotated three components.
Traveltime picks for the downgoing data for all shots	Travel picks for transmission data	
P and S-wave velocity models built from ray tomography inversion or others using traveltimes for all shots.	P and S-wave velocity models built from ray tomography inversion or others	
Source wavelets extracted in P- and S-components and in rotated three components.	Source wavelets extracted in P- and S-components and in rotated three components.	
Processed zero-offset VSP data and traveltime picks together with 1D velocity model reconstructed using the zero-offset VSP data		

B. Pressure Distribution Volume for the Investigated Domain on the Basis of existing 3-D Surface Seismic

CMI acquired a 3-D surface seismic dataset at the RSU. LANL obtained a copy of the data in SEGY format and conduct some preliminary analyses. From the SEGY headers of the data, we obtained the distributions of seismic sources and receivers used for acquiring the data (**Figure 9**).

Figure 10 is an example of common-shot gather of the dataset. It shows coherent seismic reflection events with high data quality. **Figure 11** shows an averaged spectrum of seismic traces in a sample common-shot gather. It shows that the data: (1) contain a "water" level (or a DC component) because the spectrum has a non-zero amplitude at the zero frequency; (2) have a peak frequency of around 10 Hz; but (3) have a very broad frequency band up to 200 Hz even though the peak frequency is very low, which is very usual. For prestack depth migration imaging using such as reverse-time migration to obtain high-resolution subsurface structure images, seismic data have to be processed such that the spectrum is as flat as possible within the useful frequency band, as shown by the blue curve in Figure 11. For full-waveform inversion to build a high-resolution velocity model, seismic data have to be processed using amplitude-friendly processing steps. Both seismic migration and full-waveform inversion need to use an initial velocity model obtained using prestack depth migration velocity analysis. However, such a velocity model is not available yet. It is a crucial task for Phase II to obtain a 3-D velocity model using prestack depth migration velocity analysis. Most of large seismic data processing companies, such as Schlumberger, WesternGeco, CGG, TGS, have advanced velocity analysis tools to process the 3-D seismic data from the RSU.

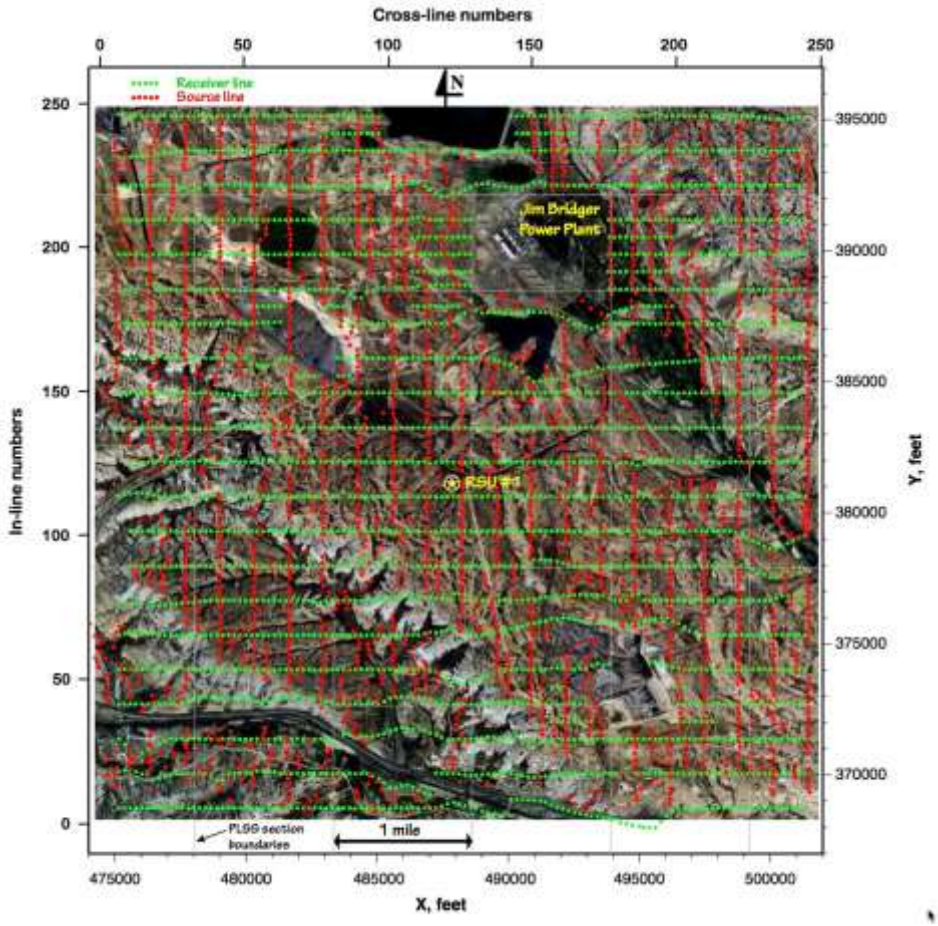

Figure 9: Distributions of seismic sources and receivers used for acquiring the 3-D surface seismic data at the RSU.

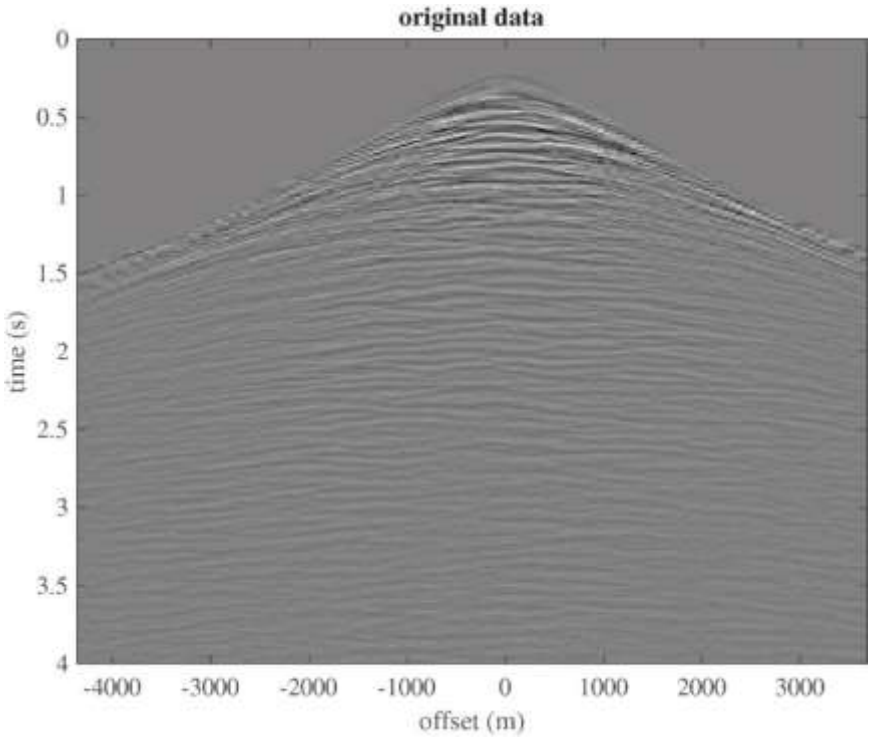

Figure 10: An example common-shot gather of the 3-D seismic data acquired at the RSU.

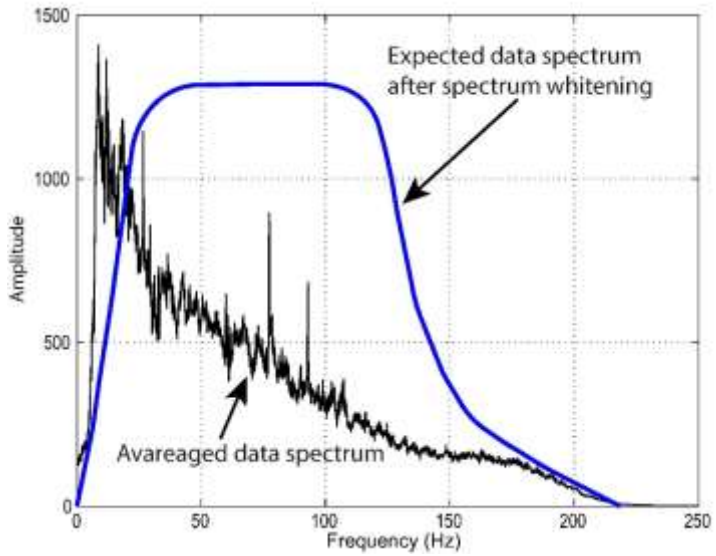

Figure 11: Averaged spectrum of seismic traces from a sample common-shot gather of the 3-D seismic data acquired at the RSU. The blue curve is the expected data spectrum after spectrum whitening processing of seismic data for high-resolution seismic migration imaging.

Basic pressure concepts and definitions: Knowledge of the formation pore pressure is required for the safe and economic injection of water or CO_2 into low permeability fractured rocks such as those occurring at depth in the RSU. On one hand, injection rates must be low enough to prevent reservoir damage from over pressuring and inducing unwanted fractures. On the other hand, these rates must be high enough to make the costly fluid injection process economic. In the exploration stage, knowledge of the pore pressure will ensure better assessment of the trap integrity and reservoir geometry, as well as fluid migration pathways. In the drilling stage, the safety requires that the wellbore pressure be maintained between the formation pore pressure and the maximum pressure the formation can withstand without fracturing.

Besides drilling a well, seismic survey is the only way to predict a subsurface pore pressure distribution, and hence a potential geo-hazard, a priori. Because variation in formation pore pressure affects the amount of sediment compaction, seismic wave velocities can be used to predict pore pressure. Petrophysical properties of porous rocks are controlled by effective stress and rock composition: as effective stress increases, rocks compact, and the effects of compaction can be observed as a general increase of rock velocity and density with depth (normal compaction trend). Where pore pressure exceeds normal hydrostatic pressure, effective stress is reduced and sonic/seismic velocity is less than that expected from a normal compaction trend. Over the years, numerous methods have been developed to perform velocity-pressure transform, among which the empirical methods of Eaton (1975) and Bowers (1995) are most widely used in the industry. It is not the intention of this study to explain the concepts of pore pressure prediction, as extensive literature exists (e.g., Dutta, 2002; Bell, 1998; Bowers, 2002; Sayers et al., 2002, Chopra and Huffman, 2006); however, the main practical steps are outlined below.

Following the effective stress principle first formulated by Terzaghi (1943), we assume that elastic wave velocity is a function only of the vertical effective stress σ, defined by:

$$\sigma = S - pp \qquad (1)$$

Here, *pp* is pore pressure and *S* is the overburden pressure or total vertical pressure produced by the combined weight of the rock matrix and the fluids in the pore space overlying the depth of interest:

$$S(z) = g\sum_{0}^{z}\rho(z)dz \qquad (2)$$

where $\rho(z)$ is the density at depth *z* below the surface, and g is the acceleration due to gravity. In this study, the overburden pressure variations with depth $S(z)$ are determined by integrating the continuous density log available for the RSU #1 well.

If the relationship between elastic wave velocity and vertical effective stress is known, the pore pressure *pp* may be calculated from equation (1), employing equation (2) to calculate the total vertical stress. In this study we utilize Eaton's (1975) method to estimate effective stress σ from the seismic velocity v, via the relation:

$$\sigma = \sigma_{normal}(v/v_{normal})^n \qquad (3)$$

where σ_{normal} and v_{normal} are the vertical effective stress and seismic velocity expected if the sediment is normally pressured, while the exponent n describes the sensitivity of velocity v to effective stress. Combining (1) and (3), the final form of the equation used in this study for pore pressure prediction is the following:

$$pp = S - (S - pp_{normal}) \left(\frac{v}{v_{normal}}\right)^n \qquad (4)$$

where pp_{normal} is the hydrostatic or normal pressure in a borehole.

To use equation (4), not only are the accurate measurements of seismic velocity required, but also the normal compaction trend and the corresponding velocity function, v_{normal}, which must be estimated. To assure the plausibility of transform given in equation (3), the results must be calibrated using available pressure measurements. In this study, mud weights from the RSU#1 test well were used to calibrate the velocity to pore pressure transform, as described below.

Seismic processing and velocities: This study utilizes the publicly available Jim Bridger 3-D seismic survey, acquired by Geokinetics Service Co., Houston, Texas, during November 2010 together with the suite of wire-line logs, VSP, and mud weight measurements from the RSU#1 test well. Seismic data conditioning and detailed velocity analysis resulted from the DOE-funded WY-CUSP project (Ganshin and Surdam, 2013). The accuracy of predrill pore pressure prediction largely depends on the type of seismic velocity used for the velocity-pressure transformation and the quality of the data conditioning. We used pre-stack time-migrated common mid-point (CMP) gathers as input for velocity analysis. Velocities have been manually picked on a coarse grid from velocity spectra displays to produce a preliminary 'guide' velocity function. This guide velocity function was later used to define a corridor of physically reasonable trial stacking velocities (V_{rms}) for an automated velocity analysis routine. The high-density velocity analysis was performed at every time sample and at every CMP location using conventional semblance-based technique to estimate stacking velocities by maximizing a coherence measure with respect to the reflection's hyperbolic parameter (Taner and Koehler, 1969). Automatic velocity picking process is associated with uncertainties that notably increase with the increase of two-way traveltime, and depend on acquisition parameters such as the spread length, the CMP fold, and the signal-to-noise ratio. To decrease the noise in stacking velocity cube, the velocity analysis was performed with an internal filtering step. This internal filter was designed with a time-variable operator to keep the velocity uncertainty unchanged within a time range of interest. Because of the fixed velocity uncertainty, resolution of the resultant velocity volume considerably decays with depth (time). This property is an expression of the Heisenberg uncertainty principle with respect to seismic processing. To enable use of regularly sampled seismic velocity field for pore pressure prediction, it has to be converted from stacking to interval velocity, which was done using the Dix approximation (Dix, 1955). A spatial smoothing window consisting of 11 x 11 traces was used to decrease velocity instabilities associated with the Dix method. The west-east section extracted from the interval velocity volume at the RSU #1 test well location is shown in **Figure 12**. Overall, the interval velocity

field is conformal to geological bedding and demonstrates a reasonably good correlation with sonic velocities at the well location. Note also that the rock beds of the Cretaceous section (above 1.7 seconds two-way traveltime) are better resolved in interval velocity compared to the pre-Cretaceous strata that make pressure prediction for the deeper formations less reliable.

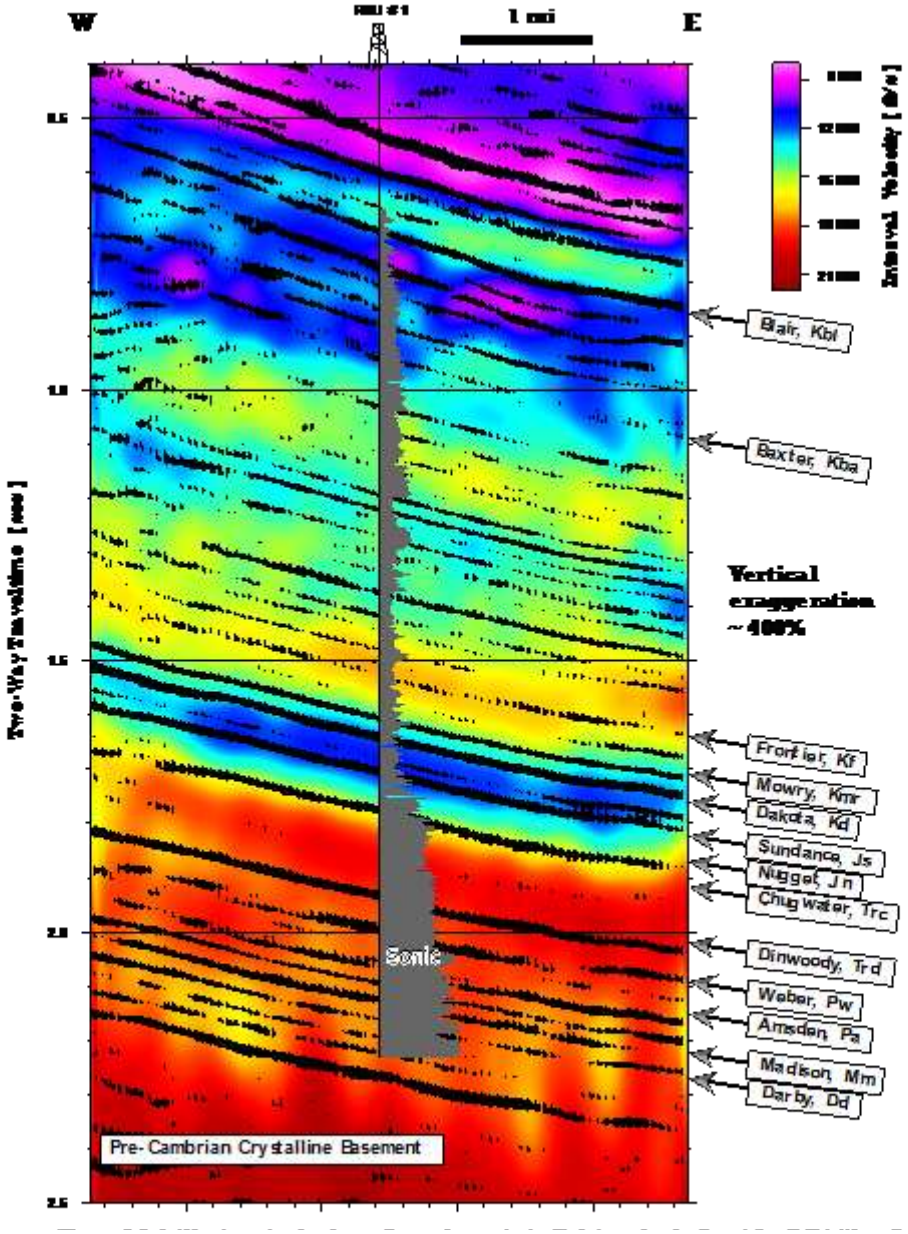

Figure 12: West-east seismic section color-coded with interval velocity at the RSU#1 test well location. Geological interpretation (formation tops with symbols with done based on integrated analysis of the wireline logs and VSP.

Further processing steps and calibration: The essential steps undertaken in this study of pressure prediction using high-density seismic velocity volume are as follows:

1. *Time-to-depth conversion of interval velocity volume.* Seismic velocities were picked from reflections in the time domain. In order to compute spatial volume, these time picks need to be converted to depth and calibrated to well markers and VSP. The task is to first find the corresponding depth value for each time velocity pair. That is done by depth converting the time value. The resulting depth value is then paired with the same velocity. This is done for all time velocity nodes in the time velocity cube to produce a large set of depth velocity values. These values are then gridded into the depth velocity cube using a vertical interpolation scheme for those grid nodes that have to be filled in.

2. *Construct a normal compaction trend line for the area under investigation*. Empirical approaches such as Eaton's are good as long as a normal compaction trend can be constructed for all depths of interest. This trend suggests a gradual increase of velocity with depth. In this study, we assume that v_{normal} varies linearly with depth as follows:

$$v_{normal}(z) = v_0 + kz \qquad (5)$$

where z is depth measured from the seismic datum (7,500 feet AMSL) and v_0 is the velocity of sediments at the datum. The representation of seismic velocity as a linear function of depth is one of the most widely used in industry (Sayers, 2002). The parameters v_0 and k of linear relationship (5) can be estimated using, for example, sonic log data. For the RSU#1 test well, the sonic velocity is characterized by strong fluctuations that result in a poor fit of the linear velocity model even within lithologically equivalent units (**Figure 13**). In this study we used a different approach. Velocities were picked from the depth-converted volume along seismic horizons corresponding to the Weber and the Amsden stratigraphic units. Because of the structural relief along these horizons within the study area, the range of depths was sufficient to estimate the normal compaction trend-line within the lithologically similar units (see the rightmost panel in **Figure 13**). The deviation, $(\frac{v}{v_{normal}})$ of seismically derived interval velocity at a given depth from the normal compaction trend is used as an indicator of abnormal pressure. Of course, this procedure tactically assumes that the interval velocities indicate porosity (and compaction) variation rather than variation in lithology.

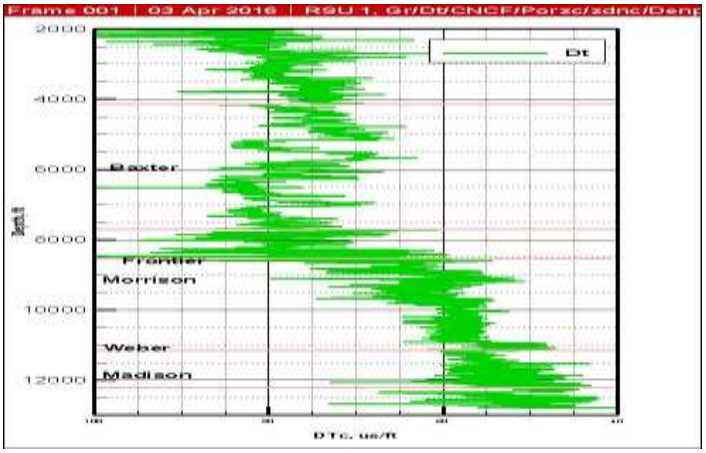

Figure 13: The sonic velocity (RSU #1) is characterized by strong fluctuations that result in a poor fit of the linear velocity model even within lithologically equivalent units.

3. *RSU#1 test well using the U.S. customary units, pounds per gallon.* Using the same units of measurements, the force per unit area caused by a column of fluid is calculated using the equation: P = MW*DEP*0.052, where MW is the drilling fluid density, DEP is the true vertical depth in feet, and 0.052 is a unit conversion factor chosen such that P results in units of pounds per square inch (psi). **Figure 14** shows the wellbore pressure computed at depths of available mud weights (the red dots). It should be noted that mud weights represent an imperfect estimate of pore pressure. They are most reliable when it is clear from drilling records that mud density has been increased in response to increased gas levels at a given depth. The pore pressure can then be deduced from the mud weight required to prevent gas from entering the wellbore.

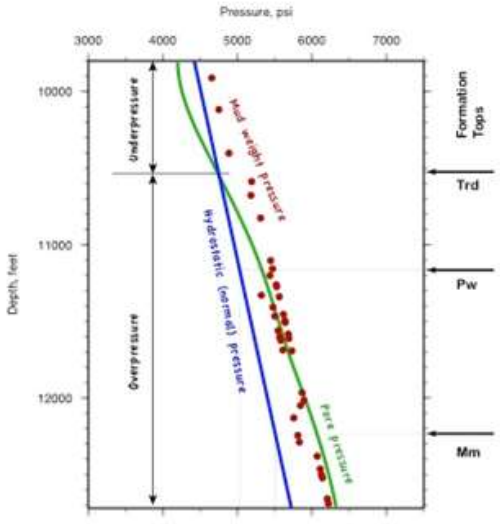

Figure 14: Pressure regimes for the target depth interval at the RSU#1 test well location. The normal pressure profile (blue curve) is plotted assuming 0.45 psi/ft hydrostatic pressure gradient. The wellbore pressure (red dots) was obtained from mud weights (MW) using the equation: P = MW*Depth*0.052 (psi). The pore pressure (green curve) was estimated from seismically derived velocity profile at

4. *Calibration of the velocity-to-pore-pressure transform.* Using the 3-D estimates of velocity v together with the trend-line v_{normal} and the overburden pressure (S) variations, the distribution of pore pressure was first determined for the vertical profile corresponding the RSU #1 test well location (the green curve in **Figure 14**). We used the trial and error method to derive the Eaton's exponent *n* while solving equation (4). After a satisfactory match between the

measured mud-weight pressures and the predicted, velocity-derived pressures was obtained, we used the derived value of *n* to model pore pressure for each cell in the 3-D model.

Results and discussion: A pre-drill estimate of formation pore pressure was obtained from seismic interval velocities for the study area in the vicinity of RSU#1 test well. **Figure 15** shows a vertical section through the predicted pore pressure volume, while **Figure 16** shows horizon slices extracted from this 3-D volume along the Weber and the Madison stratigraphic units.

In the calibration of the pore pressure model for this area, it is important to note that methods for pore-pressure prediction are based on the theory of undercompaction of argillaceous sediment (e.g., Bowers, 1995). When empirical methods such as Eaton's method are applied to carbonate rocks, they can lead to significant errors. As noted by Yu et al. (2014) this is due to inability to identify key parameters linking the P-wave velocity response to the pore-pressure change. Despite all the difficulties, it seems that a successful attempt has been made in predicting the pressures in this structurally and lithologically complex area. The main challenges are: (1) the pressure compartmentalization; (2) non-pressure related influences on seismic velocity; and (3) carbonate rocks composing the Madison Formation. It is still required to undertake real time prediction of pore pressures while drilling. The predicted pore pressure volume can be used as a reference and can be updated when new well data becomes available.

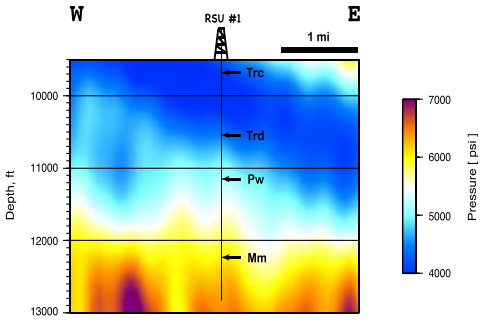

Figure 15: West-east section through the predicted pore pressure volume at the RSU#1 test well location. Pore pressure was modeled using Eaton's method with seismically derived interval velocities. The Chugwater (Trc), Dinwoody (Trd), Weber (Pw), and Madison (Mm) formation tops are shown with arrowheads along the well's shaft.

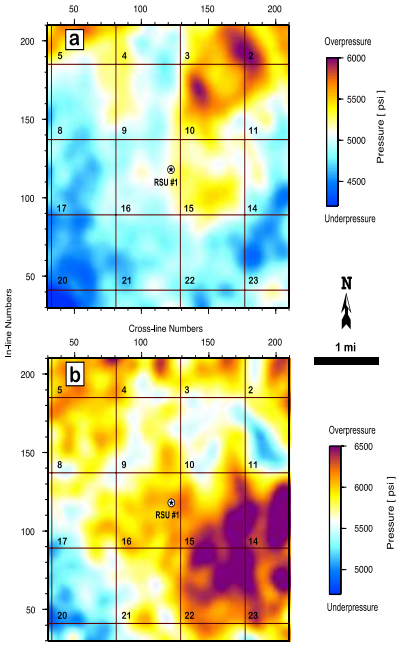

Figure 16: Estimated pore pressure distribution maps for the Weber (a) and the Madison (b) stratigraphic intervals around the RSU#1 test well. Pore pressure was modeled using Eaton's method with seismically derived interval velocities. White color on both maps correspond to the areas with normal formation fluid pressure. A rectangular grid with numbers displays the PLSS sections of T20N, R101W.

C. Downhole Monitoring

Team member WellDog will deploy its temperature and pressure gauges to provide continuous downhole pressure and temperature measurements in all of the wells during Phase II. Their gauge systems are safe, reliable, cost effective, and present minimal problems for installation in the wellbore. The other major WellDog technology that will be deployed is their proprietary raman spectroscopy. This tool will be lowered in the wellbore to detect the different types of brine and/or substances that will be entering the production well. WellDog will also participate in research by trying to detect various injected tracer particles in real time. Typically, tracer programs use periodic sampled produced waters and are then taken back to the lab for analysis. The possibility of real time detection of injected tracers offers real time data, higher levels of accuracy, and time and cost efficiency.

Along with WellDog employing its downhole monitoring tools, Silixa will be present with its distributed acoustic fiber optic cable along with a fiber in the cable for temperature readings. Since the cable runs the entire length of the wellbore, all formations will be monitored for strain on the cable and for temperature in real time. This, coupled with WellDog's monitoring techniques, will add fault tolerance and more areas and opportunities for data collection.

D. Design a Baseline Crosswell Seismic Survey

Horizontal-to-horizontal crosswell outline: Crosswell profiling is a proven high-fidelity seismic imaging technology due to its ability to provide unusually high-frequency content conventionally unattainable neither by 3-D surface seismic nor by 3-D VSP surveys.

Historically, crosswell seismic had been recorded in vertical wellbores having several hundred feet in horizontal separation. For the first time the novel idea of recording crosswell seismic data from horizontal wells was first implemented at EnCana Corporation's Weyburn Field in the year 2000, when the horizontal drilling became a common practice in field optimization (Majer et al., 2001; Washbourne et al., 2001). Since that time, the necessary equipment (such as downhole sources and/or receivers) and a robust deployment technology for use in a horizontal well environment were developed and probed. With the permanent fiber-optic cables installed in wells, the time-lapse horizontal-to-horizontal crosswell seismic profiling promises to become the leading method for monitoring reservoir changes due to fluid injection/production cycles.

The primary objective of our crosswell survey is to acquire high-resolution baseline seismic information for a better understanding of the small-scale reservoir rock features in the inter-well space, whose effects on fluid flow behavior may be of importance. Our secondary objective is to create a dataset from subsequent time-lapse surveys to provide more detailed in-situ information about water and pressure front movements and their interactions with reservoir features such as fractures.

For the objectives outlined above, we propose to drill two reasonably parallel, horizontal legs (sections) from the injection and production wells as shown in **Figure 17**. Both horizontal legs will be located within the most porous part of the carbonate Middle Madison reservoir and will be separated by 1,000 to 1,200 feet. The lateral extent of these horizontal legs will be as much as 3,500 feet, with the opposite direction relative to each other to maximize the coverage area of the data to be recorded. **Figure 18** shows the proposed wells location overlain on the interpreted porosity distribution map built for the Middle Madison reference horizon (Ganshin and Surdam, 2013).

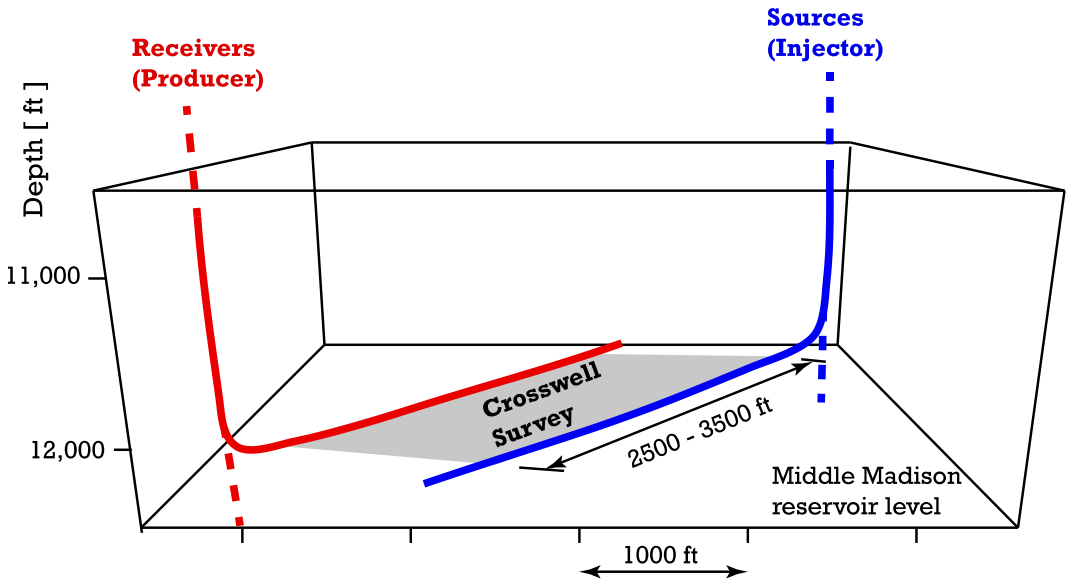

Figure 17: A perspective view of the proposed crosswell acquisition geometry. The injection and production wells are reasonably vertical and parallel. Both wells have horizontal legs starting at the Madison Limestone level and extend through the Middle Madison for about 3,000 feet. The horizontal legs of both wells are equipped with fiber-optic sensors and their direction may run against each other as shown. We propose a 1,000 ft separation between the horizontal sections. For seismic energy sources (within the injection well) we consider to use either small explosive charges (in form of perforation gun carrier) or piezoelectric sources. The shaded area represents lateral coverage at the Middle Madison reservoir level.

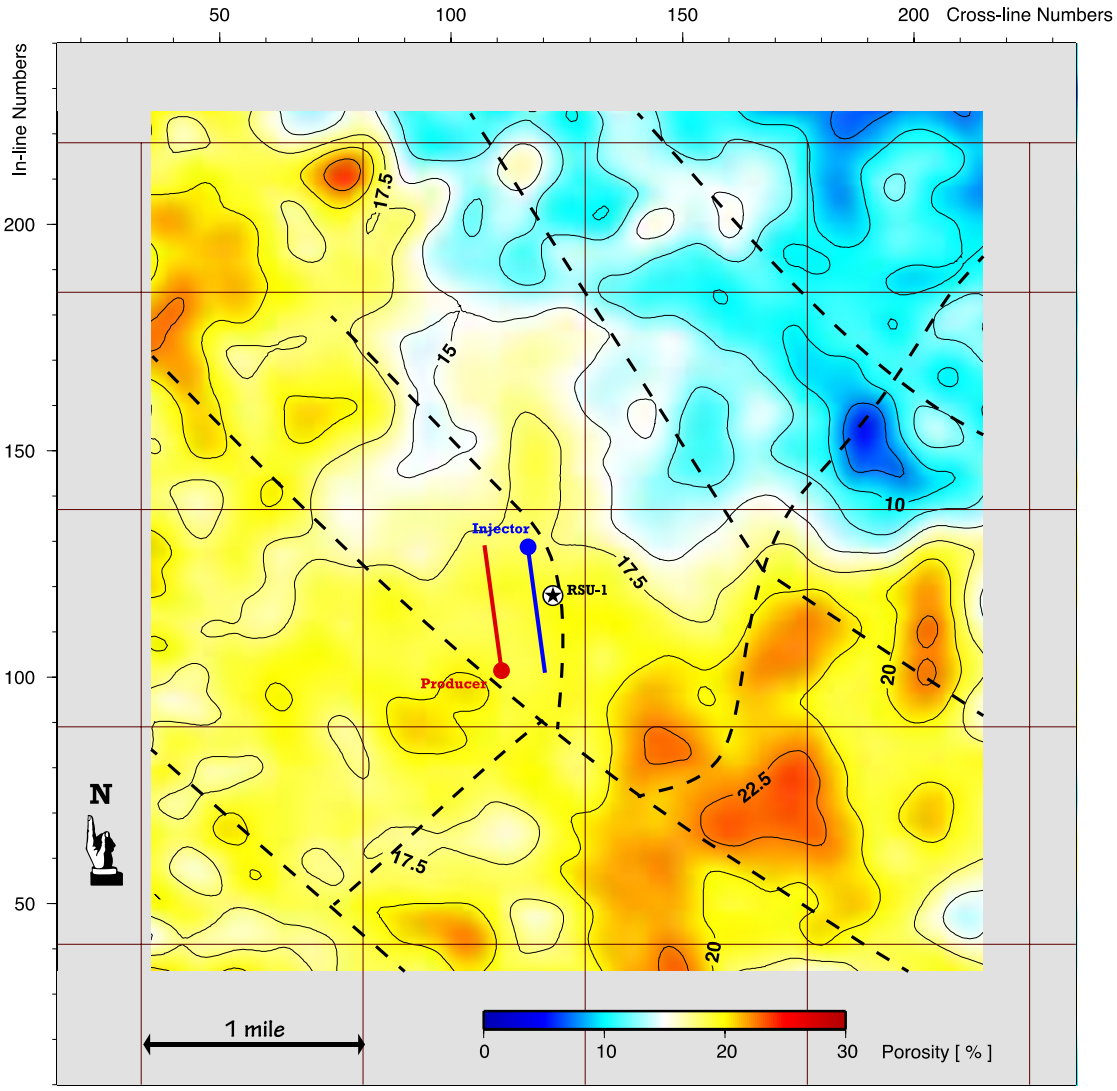

Figure 18: Porosity distribution map for the Middle Madison reference horizon derived from seismic interval velocity volume. Black dashed lines represent the interpreted fold axes with possible faulting or zones of intense fracturing. The proposed injection well with a horizontal leg is shown in blue color next to the RSU#1 well location. The production well is shown in red color. The up-dip direction is the south-west.

Virtual source technique applied to crosswell geometries and VSP: Virtual Source (VS) redatuming is a new seismic acquisition and processing method based on interferometry (e.g., Bakulin and Calvert, 2006; Korneev and Bakulin, 2006). The technique allows generating data independent of the overburden complexity and the time-lapse changes therein. It should be applied in the areas where seismic monitoring from the surface is problematic, not only due to imaging issues but also due to near-surface changes that create false 4-D responses. The VS procedure cross-correlates downgoing energy with upgoing energy to redatum surface source

records to downhole receiver locations. By cross-correlating these two records, virtual source traces can help resolve time-lapse changes occurring between a given pair of buried receivers (**Figure 19**). Besides, when properly applied, this technique allows overcoming severe repeatability issues.

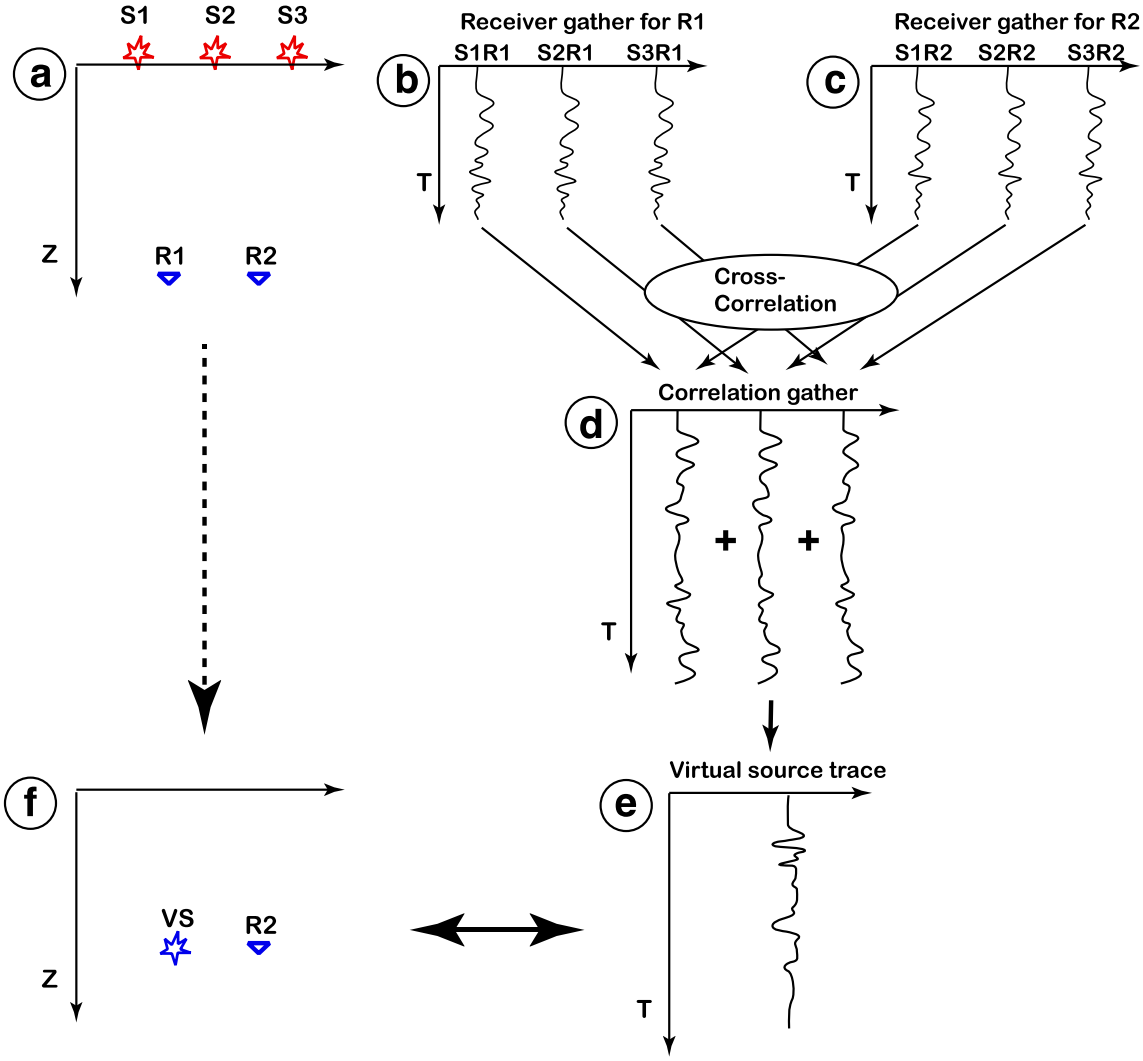

Figure 19: Processing steps for generating a virtual source. (a) Seismic experiment with surface shooting and subsurface recording. After cross-correlating the receiver gather (b) and (c), and summing the correlated data (d) over the sources, the resultant trace (e) represents the signal recorded by receiver R2 as if there were a virtual source (VS) at the location of receiver R1 (f).

The VS technique can be applied to crosswell geometries, whereby a virtual crosswell survey can be simulated by shooting a line of surface shots passing through two boreholes instrumented with downhole sensors. By using this acquisition geometry, receivers in one of the two wells are turned into virtual sources (**Figure 20**). Correlating the wavefield recorded by those receivers with the recording at receivers in the other well, and summing the correlated data over the surface shots could do this. An important feature of such virtual crosswell surveys is the possibility to customize the virtual source radiation type (P- or S-wave), its strength, and pattern. Unlike real crosswell surveys where the radiation pattern of the downhole source is fixed, we can control the radiation pattern of the virtual source by appropriate selection of the surface shots that illuminate the virtual source location. The VS technique enables both vertical and horizontal virtual crosswell surveys.

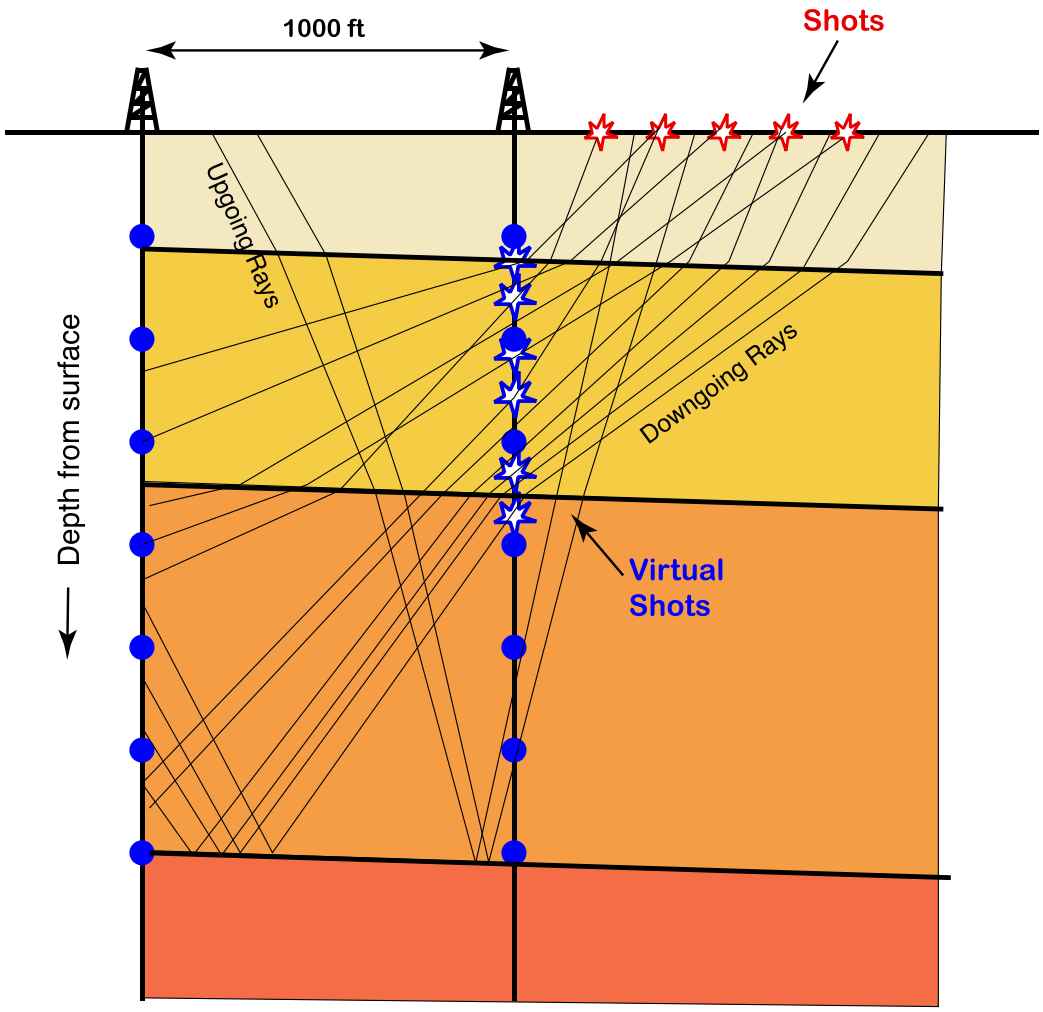

Figure 20: A sketch showing transformation of dual-well VSP geometry into a virtual source crosswell imaging scheme.

VIII. DEVELOP WATER MANAGEMENT AND TREATMENT STRATEGY

In Phase I separate analyses were conducted to identify suitable water treatment technologies that can be used to process the requisite amount of formation water which must be removed from the reservoir to make room for the injected carbon dioxide. Among those considered were treatment technology types that were funded under DOE sister awards *AOI 5 of DE-FOA-0001238* and *AOI DE-FOA-0001095*.

Because the formation water is hot and contains a very high level of total dissolved solids (TDS), including some problematic components, the treatment of this brine poses a number of challenges. In developing suitable treatment scenarios, the project team looked at a combined goal of not only treating and removing the formation water, but also doing so in a manner to make water available for beneficial use.

As a result of the adverse characteristics of the extracted water, most treatment concepts would consist of a string of several treatment processes operating in a series. Both conventional off-the-shelf and almost off-the-shelf technologies were reviewed for the applicability, as were promising technologies that may be worth consideration.

The evaluation was done by viewing the formation water treatment to be integral with the associated power plant (Jim Bridger), with the latter considered to be the main benefactor of the recovered water. Other beneficial uses for the recovered water were also considered, including other large industrial users, agricultural, and domestic use.

The current operating experience for the desalination of hot and high salinity water, including this formation water, is extremely limited. Only a few technologies could be considered off-the-shelf for this application. For most treatment processes, this water will be pushing the boundaries of the known processing envelope. As such, bench testing, pilot testing, and demonstration will be required to qualify most of the technologies cited in this study.

Because the formation water contains relatively high levels of components such as lithium and other species, the economic potential to extract these elements are reviewed in this study. The budgetary economics for both the full-scale and pilot-scale operations are addressed and presented.

A. Goal and Scope

The goal of the water treatment aspects of Phase I was to identify one or more viable scenarios for the treatment and recovery of the requisite amount of formation water that must be removed from the formation to manage pressure in the reservoir(s) as water (as a proxy for CO_2) is injected. The identified treatment options must be capable of purifying the high TDS brine to a degree where it is acceptable for beneficial use at either the associated power plant or for other needs. The treatment must be technically and economically viable without significantly adding to the environmental and carbon footprint. The potential of constituent recovery from the formation water is also of interest.

The scope of the Phase I efforts in this regard was to review existing and promising water treatment technologies, with the latter offering promise to be operational by project maturity. The recommended technologies were required to meet the criteria defined by the project goal.

B. Baseline Assumptions

The baseline assumptions of this produced water treatment study are:

- The produced water chemistry used as the basis of this study is presented in **Table 4** below. They represent the average of the three (3) Madison test well samples previously collected by the University of Wyoming;
- The produced water temperature at the wellhead is ≤ 90°C (194°F);
- A net total of 500 gpm (113.5 m3/h) of produced water must be removed from the reservoir;
- Process residual wastewater, consisting of concentrated brine, can be disposed of by reinjecting it into CO_2 storage formation or other geological strata as long as this brine is non-scaling, non-precipitating and compatible with the receiving geological formation;
- The purified water will be used in either the associated power plant or have other beneficial purposes; and
- Power and utilities will be available from the associated power plant.

In evaluating the potential technologies, the beneficial use of the recovered brine was assumed to be the following:

- High-quality water, i.e., water of low TDS that can be used to satisfy power plant or other local water needs;
- Non-scaling and non-precipitating brine containing no or low levels of suspended solids that can be used in drilling or fracking operations; and
- Recovered components of value, such as lithium, from the produced water.

C. Research Gap Analysis for Brine Treatment Technologies

Here we briefly consider new technologies and improvements to existing technologies that might lower the costs associated with brine management at CO_2 storage sites and may merit further R&D funding to make them available for use. In order to guide our analysis, we begin with a summary of current cost data for reverse osmosis in order to identify those areas where greatest cost improvements are possible.

A cost breakdown for desalination of sea water using reverse osmosis (RO) is shown in **Figure 21a**. Electrical energy is a fairly large fraction (30-40%) of total costs of which about 85% of the total is used to drive high pressure pumps. The rest is used to provide feed, distribute the product water, and return the concentrate.

Although the energy use is considered large, an improvement in energy use of desalination would not lead to a dramatic reduction in overall cost. The current energy use for reverse osmosis including energy recovery is about 2-3 times the theoretical minimum (NRC, 2008). This energy use is five times lower than was the case 20 years ago, with the reduction due primarily due to the development of energy recovery devices for RO.

So regardless of technology the largest reduction that could be expected, even for an "impossible" 100% energy efficient desalination technology, would be to cut the energy costs in half (vs. current technologies that use twice the minimum energy). This improvement in energy efficiency would reduce the overall desalination cost by about half of 30% or 15%. This fact is important when considering new types of membranes for RO, such as graphene, aligned carbon nanotubes, and others. Even if they were infinitely permeable while still having good salt rejection, the maximum benefit in overall costs would only be about a 15% reduction (assuming all the other costs in **Figure 21a** remain the same). This suggests that energy use alone is probably not the best target for reducing desalination costs.

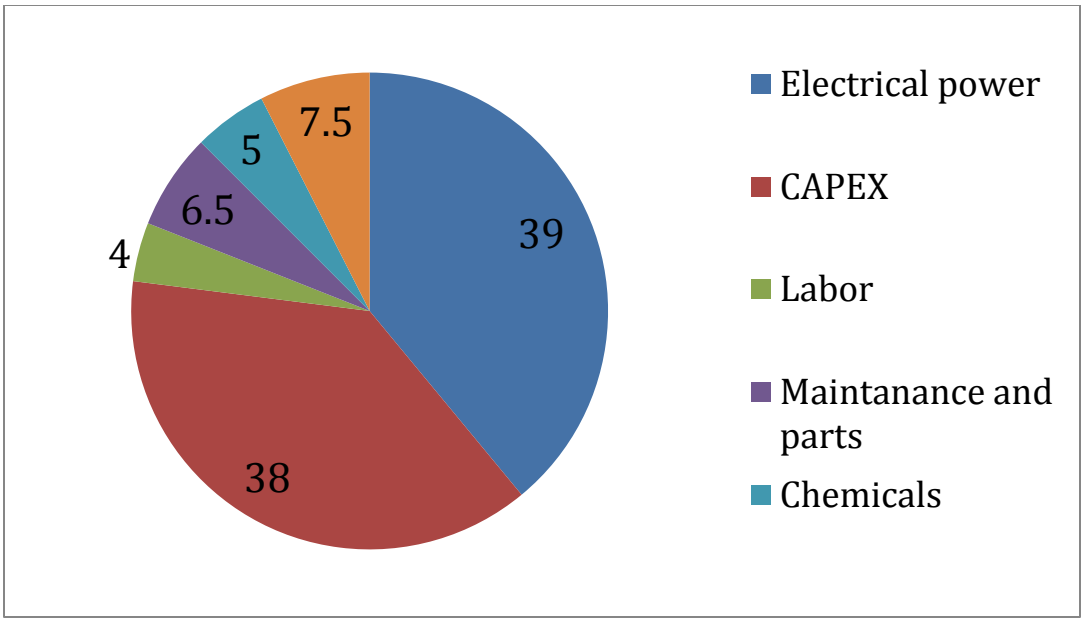

Figure 21a: Breakdown (in %) of total costs for typical sea water reverse osmosis desalination.

The other main RO cost is CAPEX which here includes cost of funds and site costs as well as purchase of hardware. RO tends to be expensive because of the equipment needed to run at high pressures, such as pressure vessels and pumps, as well as the cost of the membranes. Use of epoxy pressure vessels and gradual lowering of the costs for the polyamide (Nylon) membranes has driven membrane module costs down. But in spite of this, CAPEX remains high and technologies that run at ambient pressure and thus avoid high-pressure pumps, pressure vessels, and expensive membranes are desirable from the point of view of lowered CAPEX that may even offset a higher energy use. Technologies such as capacitive deionization and other electrostatic approaches might have an advantage in CAPEX given they operate at ambient pressure and potentially could have very low equipment costs.

The other area to look at to reduce costs has to do with the fragile nature of RO membranes, and their need for a high degree of upstream cleaning (pretreatment) to prevent fouling. Pretreatment may involve using additional membranes, dosing with anti-scalants and cleaning chemicals, and sometimes softening steps. These costs can add up to 10-15% of total cost (chemicals, maintenance, and membrane replacement). A major limitation of RO is the fact that the polyamide membranes are damaged by oxidants such as chlorine, so are particularly susceptible to biofouling. Much of the pretreatment cost for RO is a consequence of the need to avoid biofouling. Technologies that are chlorine tolerant therefore have an advantage, as well as all "robust" technologies that can function with limited pretreatment and have long service lives. The potential payoff of reduced capital cost and technology robustness for membrane systems is probably comparable or greater than that achievable by energy reduction.

The final cost consideration has to do with the need for skilled operators and the degree to which a desalination plant can run unattended. Simple technologies that can run unattended and which are stable even with changing feed compositions are attractive for treatment of carbon storage

fluids that are likely to change over time. Such technologies also would allow switching between various feed wells or blended feeds as the reservoir is managed. RO is sensitive to changing feed composition and each implementation is optimized for a particular feed salinity. Also, RO plants tend to be most problematic at startup and shut down. Desalination technologies that do not have these limitations would be preferred.

Improved membrane methods:

Temperature and pressure limits of membranes. There are pressure limits that restrict the salinities for which membranes can desalinate feed. Membranes must be constructed of materials that can support a pressure difference across the membrane equal to the osmotic pressure plus a driving pressure of 10-20 bars to provide the flux of water through the membrane. For seawater, the total pressure across the membrane is on the order of 50 to 70 bars. Even at these pressures there is some compaction of the polymer support (**Figure 21b**) which reduces flux through the membrane. In order to desalinate more saline waters, stronger membrane materials are needed or the desalination process needs to be staged so that the overall pressure is broken down into manageable steps.

In addition, RO performance is improved as temperature is increased. The flux of permeate through the membrane increases as the viscosity of water decreases. Water viscosity decreases such that the permeate flux doubles as the temperature is raised from 25 to 50^{o}C.

R&D goal: develop reverse osmosis and nanofiltration membranes that can operate continuously at temperatures as high as boiling and at higher pressures than are normally used for sea water desalination

Advantages:

- Membrane systems will operate at higher flux – fewer modules needed
- Eliminates the need for cooling of the produced water
- May allow geothermal energy extraction

Current temperature limits for RO and NF membranes are determined not by the active polyamide layer (the layer that separates salt from water) but by the polymers that compose the backing and spacer materials. The use of polymers that retain their strength at high temperature as backing and spacer materials could increase the thermal limits to 100^{o}C or more.
In addition, there may be opportunities to use additive manufacturing to make permeable spacer fabrics more resistant to permeability loss with compaction due to applied pressure.

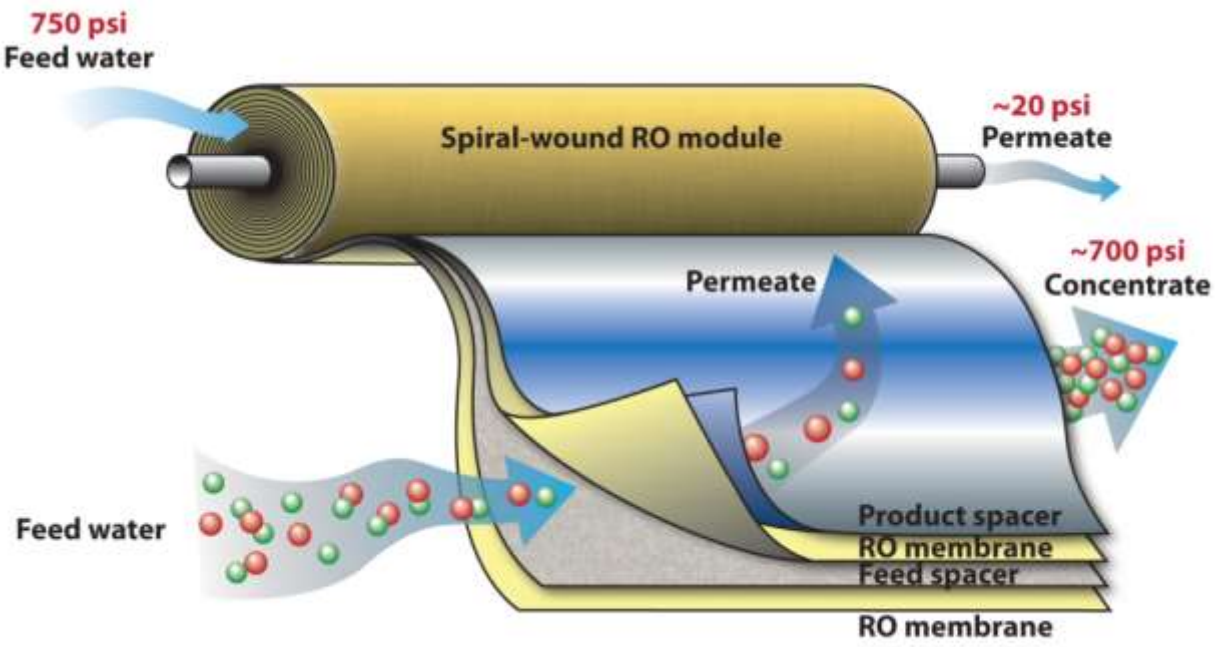

Figure 21b: Cut-away of reverse osmosis membrane module construction. Feed spacer is under pressure; product spacer is at or near ambient pressure. A high driving pressure causes compression of RO membrane and product spacer (between feed spacers) and limits maximum pressure, and therefore maximum feed salinity.

Staged membrane desalination. Membrane methods can be extended to higher salinities by staging the membranes and allowing some salt passage with each step (DOE, 2015). This breaks the osmotic pressure down to a series of manageable steps for each stage of membrane treatment. For this technique to work well, the membranes need to be optimized for this use. A set of membranes that allow sequentially less and less salt passage are needed.

R&D goal: NF and RO membranes optimized for staged membrane systems

Results have shown acceptable performance using NF and RO membranes designed for other purposes (DOE, 2015). What is needed are membranes designed specifically for staged systems. Whereas most RO membranes are designed to allow minimum salt passage, a staged system would utilize membranes having a range of salt rejections in order to evenly split the salt gradient between each step. Such membranes are possible to make, but have not been the target of developmental work because of the lack of a known commercial application.

Improved thermal methods:

The workhorse thermal technologies of multi stage flash (MSF) and multiple effect distillation (MED) have been optimized over decades and it seems unlikely they could now be improved significantly. But the one area that might be considered is the use of new materials with favorable heat exchange, corrosion, or reduced cost relative to conventional materials. Of particular interest here is vapor compression (VC) which historically has shown the lowest

energy use of the thermal methods, and for which material properties are the most critical. The need to desalinate large volumes of brines significantly more saline than sea water (and beyond the range of reverse osmosis) may merit an effort to improve the current state of VC technology using advanced materials. In particular, there may be potential for additive manufacturing methods to create efficient but non-corrosive heat exchange materials needed for VC.

R&D goal: investigate new materials of construction of thermal systems that are corrosion resistant and thermally conductive to replace the expensive alloys currently in use

These materials might include:

- Conductive polymers
- Low-cost titanium fabricated using new powder metallurgy or additive manufacturing technologies
- New composite nanomaterials such as those composed of titanium-graphite

Emerging technologies:

Capacitive deionization. Capacitive deionization (CD) uses an electric field to desalinate water. CD functions much like a capacitor, an electric field causes positive and negative charges (salt ions) to move in opposite directions to charged electrodes where they are held by electrostatic forces (**Figure 21c**). Periodic release by removing the applied electrical potential allows removal of a concentrated waste brine.

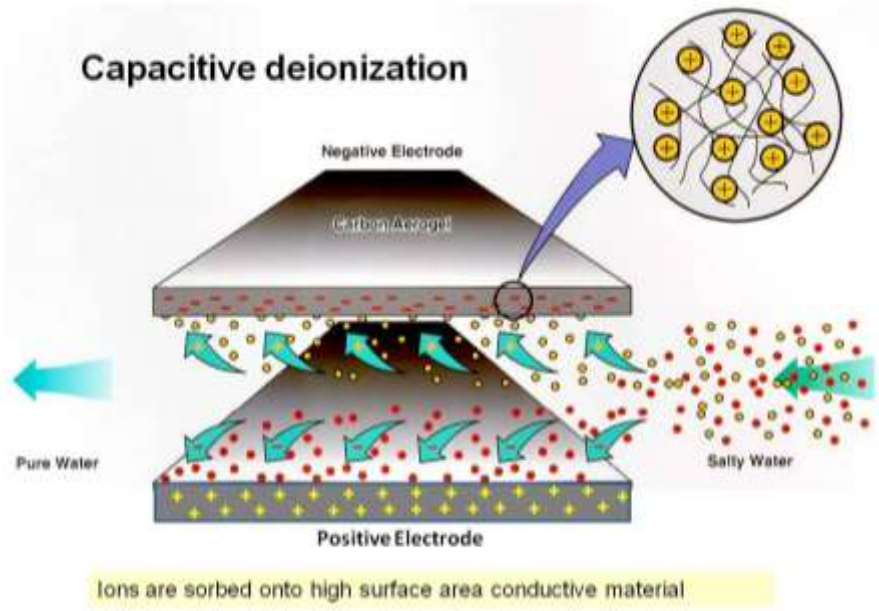

Figure 21c: Schematic of conventional capacitive deionization (CD).

CD was first developed in the mid-20th century (Oren, 2008) and has not yet had a great degree of commercial success. Recent improvements in material properties, in particular the mesoporous carbon (aerogel) electrode materials, and the concept of a flow-through electrode

which greatly reduces ion travel times has significantly improved CD performance relative to RO (Suss, et al., 2012). The technology is still limited in salt capacity, and for high energy efficiency needs to employ efficient energy recovery between cycles by re-using the energy stored in the salt 'capacitor' for use in the next charging cycle. But recent work (Stadermann pers. com.) tends to show costs at least comparable to RO, with the potential to be lower.

Forward osmosis: Forward osmosis (FO) uses a very saline draw solution to remove water from a less saline feed solution. The draw solution must have some property such that the clean water can be efficiently separated. For example, ammonium carbonate solution will upon heating decompose to ammonia and carbon dioxide gases leaving relatively pure water as a liquid phase.

The FO membrane itself has identical separation properties as an RO membrane; it should pass water but not allow salt transport. FO membranes look like RO membranes in that they are composed of a film of polyamide cast onto a macroporous layer of some other polymer, commonly polysulfone.

A major limitation of FO in general is concentration polarization. No matter how the membrane is oriented (film to feed or film to draw where film is the active polyamide layer) there will be a buildup at the polyamide-backing contact that will tend to slow water transport. For example, if the film-backing contact is on the draw side, water coming through the membrane will dilute the saltiness of the draw and reduce the osmotic driving pressure. Unless this water can be flushed or mixed efficiently inside the porous backing, the overall flux will slow down. This is a main topic being addressed by current FO membrane developers.

A major benefit of FO vs. RO is that FO membranes are much less likely to foul than conventional RO membranes. This is probably due simply to the pressure gradient across RO membranes that drives fouling materials through the membrane whereas with FO there is no pressure gradient, just a concentration gradient (= osmotic pressure gradient) that pushes water through the membrane. This characteristic makes FO membranes attractive for difficult feeds such as those common in produced waters from fossil fuel production. In some cases, it is economic to use FO to pull water out of such feeds and then use conventional RO to desalinate the draw solution to get back out the water because these waters would otherwise not be treatable due to fouling.

Solvent extraction. Solvent extraction is a method that uses a solvent in which water is soluble and salt is not soluble to pull water out of a salty feed. The feed and solvent are vigorously mixed to maximize surface contact. They are then allowed to separate where now much of the water originally present in the feed is now in the solvent phase. As with FO, the solvent must then be easily separable from the water, which is generally accomplished by heating or cooling. Solvent extraction generally is not used for potable water production because of the remaining solvent in the purified water, which is likely to either taste bad, small bad, be toxic, or all of the above. But applications where the water is used for industrial use such as cooling towers or steam makeup the technology could work well. More work to commercialize this technology seems warranted.

Membrane distillation. Membrane distillation is a method that uses a thermal gradient to drive water vapor through a membrane that allows water vapor but not liquid water transport. As with all distillation processes, the product is freshwater.

Passive membrane methods such as membrane distillation and FO are all limited by relatively low flux and thus need large areas. This technology has been around for quite some time without many large-scale deployments, and no commercial success. Like FO it is limited in flux by concentration polarization and materials that have the right thermal as well as flow properties remain elusive.

Next generation antiscalants. Recent work to understand early stages in the precipitation of scale-forming solids suggests a new approach to developing antiscalant chemicals. Work by Gebauer et al., (2008) shows that prior to crystallization of carbonate solids, there exists a population of amorphous hydrated colloidal clusters that over time decomposes to form a crystalline solid. Some types of polymers have been shown to stabilize these clusters and delay their transformation to crystals. It is likely that the chemicals that stabilize the clusters are in fact identical to "threshold inhibitor" antiscalants. Previously, there had been only speculations to how these antiscalants prevented scale formation. It now appears that they stabilize the hydrated clusters long enough to avoid precipitation of scale. The addition of antiscalant causes the clusters to remain in solution for a long enough time to exit the desalination membrane or evaporation tube without causing scale.

This new understanding of the molecular mechanism of scale formation and the functionality of known antiscalants should be used to attempt to identify improved methods of scale control.

D. Approach to Selecting Technologies

Formation Water Chemistry:

The formation water chemistry used in this study is shown in **Table 4** below. It is an average of the Madison formation water analyses conducted on 8/27/2011, 8/27/2011, and 12/3/2012. Only those components that are pertinent to this technology evaluation are presented.

A review of this water chemistry shows several characteristics that will have to be accommodated and potentially mitigated by or ahead of each of the candidate technologies considered. These characteristics include:

- High temperature
- High TDS
- High chloride level
- High alkalinity level
- High silica level
- Saturated in $CaCO_3$
- At or near saturation in $CaSO_4$ anhydrite
- Presence of sulfide

- Relatively high in boron concentration
- Moderate presence of iron in ferrous form

Formation Water Temperature:

Although the high produced water temperature will be advantageous for evaporative processes, it does pose a problem for the membrane-based technologies and cooler temperatures must be utilized. Therefore, some of the processes evaluated make use of produced water temperature to flash off steam and, thereby, producing a small portion of the desalinated stream.

The use of high temperature membranes may, however, be possible which would not require the prior produced water temperature reduction.

Table 4: Formation Water Chemistry Used as the Basis for all Technology Calculation of This Study

COMPONENTS			Formation Water Chemistry Used
Major Ions			
Alkalinity, Total as $CaCO_3$ (mg/L)	Alk		1,895
Carbonate as CO_3 (mg/L)	CO3		0
Bicarbonate as HCO_3 (mg/L)	HCO3		2,073
Calcium (mg/L)	Ca		1,367
Chloride (mg/L)	Cl		51,397
Flouride (mg/L)	F		6
Magnesium (mg/L)	Mg		174
Nitrogen, Ammonia as N (mg/L)	NH3		41
Nitrogen, Nitrate+Nitrite as N (mg/L)	NO2/NO3		0.05
Nitrogen, Nitrite as N (mg/L)	NO		0
Phosphate	P		0
Potassium (mg/L)	K		3,995
Silicon (mg/L)	Si		48
Silica	SiO2		102
Sodium (mg/L)	Na		29,907
Strontium (mg/L)	Sr		59.1
Sulfate (mg/L)	SO4		2,300
Metals			
Aluminum (mg/L)	Al		1.9
Arsenic (mg/L)	As		1.068
Barium (mg/L)	Ba		2.74
Boron (mg/L)	Ba		98.1
Borate (mg/L)	BO3		120
Bromide (mg/L)	Br		127.5
Copper (mg/L)	Cu		1.35
Iron (mg/L)	Fe		13.6
Lithium (mg/L)	Li		96.2
Manganese (mg/L)	Mn		2.7
Zinc (mg/L)	Zn		1.3
Physical properties			0
pH			6.6
Total dissolved solids @ 180 C (mg/L)	TDS		86,642
BOD (mg/L)	BOD		142
Chemical oxygen demand (mg/L)	COD		2,495
Non-Metals			
Dissolved inorganic carbon (mg/L)	DIC		540
Dissolved organic carbon (mg/L)	DOC		2.7
Total organic carbon (mg/L)	TOC		2.8
Total cyanide (mg/L)	Cn		0.1695
Sulfide (mg/L)	S		55
Sulfide as hydrogen sulfide (mg/L)	H2S		58

E. Discussion of Technologies for Consideration

All Technologies Considered and Reviewed:

This section contains a listing of the "conventional" and "potential" technologies that were considered and evaluated for their capability and applicability to produce a net total of 500 gpm from the targeted formation at the RSU. All technologies types awarded under Area of Interest 5 of DE-FOA-0001238 and Area of Interest 1 of DE-FOA-0001095 were also considered and evaluated under this section (though not named specifically). To be a viable treatment candidate, the individual process or process combinations had to meet the previously stated process goals from a technical perspective and had to be economically competitive in their application.

Conventional technologies are deemed off-the-shelf processes that can be readily adapted to the treatment requirements, either directly or possibly after some pilot demonstration to identify peculiarities that may require design adjustment.

Potential technologies are processes that do not have a proven track record in power plant or related applications. Their use would require more intensive bench and pilot testing to demonstrate their technical process merit in addition to showing economic feasibility.

Challenges for Formation Water Treatment

With the high TDS and high levels of some of the components (see **Table 4**), plus the high formation water temperature at the wellhead, the number and types of water treatment technologies for potential application are rather limited. Although the high temperature can be readily mitigated, the high TDS poses a more significant challenge. Related experience in EOR and Steam Assisted Gravity Drainage (SAGD) operations has shown only a few treatment technologies to be successful. Research and development is, however, currently underway to expand this list of candidates, but most alternative technologies are in their very early stages of development or demonstration.

Some of these alternative technologies -- the ones that hold promise for RSU BEST applications -- are included in the discussions below. It must be noted that the EOR and SAGD produced waters involved in the water treatment development efforts are of significantly lower TDS.

Conventional Technologies

The power plant and related industries have a long track record of using state-of-the art technologies in dealing with their overall plant water management. Because the focus of this study is on how to deal with the very saline formation water brine, most of the treatment candidates for consideration would be used in wastewater and desalination applications. The specific technologies investigated that fall into conventional category are as follows:

- Flash evaporation of the formation water
  - Flash Chamber to evaporate the requisite amount of water and condense it in a heat exchanger/condenser.
  - Dedicated cooling tower to evaporate the required water by direct contact with the circulating cooling water.

    - Flash Chamber in conjunction with a surface condenser to condense the flashed steam.
- Membrane separation
    - Nanofiltration (NF) – a softening type of membrane system to extract formation water, but producing a high-salinity water of limited beneficial use.
    - NF as pretreatment for RO to extract the water yielding a significantly higher quality permeate compared with NF alone.
- Evaporation
    - Mechanical Vapor Compression Evaporator (MVR Evaporator) – produces a high-quality distillate.
    - Multiple effect evaporator (MED Evaporator) – distillate quality similar to that for MVR.
    - Multistage Flash Evaporator (MF Evaporator) – distillate quality similar to that for MVR.
    - MVR Evaporator combined with a crystallizer – distillate quality similar to that for MVR, but no brine reinjection required.
- Electro Coagulation (EC) in place of or to supplement front-end softening or use for specific component removal.

More detailed discussion of the above cited technologies are found later in this report.

Potential Technologies

The specific technologies investigated that fall into the potential treatment system category are as follows:

- Membrane Distillation (MD)
- Forward Osmosis (FO) as applied to NF or RO
- Solvent-based desalination systems
- Ion Exchange
- Electro Deionization (EDI) and Electrodialysis (ED)
- Capacitive Deionization (CDI)
- Solar-based desalination systems
- Supercritical waste destruction/desalination

Conventional Technologies:

The following are technologies that have a proven track record in treating saline waters in power plants and related industries. Although the "difficult to treat" nature of the formation water may pose a challenge and a stretch to the existing experience of some of the processes, it can be anticipated that many of the conventional candidates can be successfully applied as treatment options. Special conditioning or pretreatment may, however, be required, and all should be subjected to demonstration testing.

Flash Extraction

Flash extraction takes advantage of the produced water's high temperature by flashing off and condensing the needed amount of water. This process could be done in a direct contact chamber,

a cooling tower, or surface condenser operated at a vacuum. In all cases, the heat of condensation would have to be dissipated via an on-site cooling tower or as part of the power station's cooling system. The unflashed, residual produced water, now concentrated by about 1.1 times, would be reinjected into the formation. The advantage of this process is its simplicity. All components are "low-tech", simple to operate, and easy to maintain.

The big disadvantage of this scenario would be that a large amount of produced water will be needed, with most of it having to be reinjected into the formation after flashing. The construction costs for the numerous high-capacity wells may prove to be prohibitive.

Direct-Contact Cooling Tower

Use of a direct-contact cooling tower would provide the same low-tech simplicity as in the flash evaporation approach. In this case, the produced water would be fed to a cooling tower where the brine would recirculate through and over the tower slats until the requisite amount of water was evaporated to atmosphere.

The advantage of this approach is that it would be a stand-alone system that would not require cooling water from the power plant.

The disadvantage would be as above -- i.e., the high amount of formation water needed and reinjected. Additionally, because of the high TDS of the recirculating water, cooling tower drift may create an air quality issue.

Membrane Separations

Membrane separations in the form of Micro- (MF), Ultra- (UF) and Nano-(NF) filters as well as RO systems have been successfully applied in the power, desalination, and other industries for water recovery and purification. The most common high-salinity RO membrane application is the desalination of seawater, where the feed TDS is about 40% that of our formation water.

NF and RO have been applied for volume reduction as well water recovery. Successful wastewater and process applications have typically used upstream MF or UF to remove turbidity and particulate fines from the NF or RO feed streams.

The most commonly membrane type in use today is of a polymeric construction and has, according to the product data advisories, a maximum continues operating temperature of 35°C (95°F). There are high-temperature polymeric membranes available, with the capacity to operate at 90°C (194°F) or more. The high temperature capability is acquired by using a standard polyamide membrane, but assembling the modules using high temperature compatible components (glue, spacers, product water tube, etc.).

While not in wide use at this time, high temperature modules are being considered for specialty applications, including produced water treatment. In a related application, high temperature membranes have been successfully demonstrated for silica and lithium recovery from geothermal waters. The obvious advantage of using such membranes in our application is that it would obviate the need to cool the formation water for the membrane treatment process.

Membranes consisting of ceramic or other materials of construction are also marketed, but these are costly and are mainly in MF and UF configurations.

In the past 40 years, RO has displaced evaporation as the most common means of seawater desalination. Special high-pressure membranes, capable of withstanding (1200 psi) operating pressure have been developed to process seawater, which typically has a salt content of 33,000 to 44,000 mg/l. Such membranes can recover up to 60% of the seawater feed stream, resulting in a permeate quality that meets EPA or WHO drinking water standards.

More recently a membrane type (Nanofiltration) was developed that has high rejection for divalent ions, such as calcium, magnesium, and sulfate, but a lower rejection for monovalent ions, such as sodium and chloride. This membrane, often referred to as a softening membrane, has found wide application in the treatment of brackish ground water to make drinking water by removing hardness and 40% to 60% of salinity.

These low-rejection NF membranes have also been employed to effectively separate sulfates from monovalent anions. For example, in offshore platforms, these membranes process seawater to reduce the sulfate in the drilling muds, preventing barium sulfate precipitation in the formation. With the correct ratio of monovalent to divalent anions, and with low water fluxes, negative rejections of monovalent anions can be achieved. This phenomenon, known as a Donnan Ion separation, has been demonstrated at scale in Australia (4,000 l/min) but with much lower TDS (15,000).

With the high salinity of the formation water, a NF membrane could be used to extract a permeate stream from the high-salinity, high-hardness formation water. Because the salt content of the permeate would still be high, however, its beneficial use would be questionable unless a use for such a water could be found. Further purification of the permeate using RO membranes may be in order.

The advantage of the membrane approach is that this technology typically offers a cost effective means of volume reduction and desalination.

The disadvantages of the membrane scenario is that the permeate from NF alone may not be of sufficient use to make it practical. Although adding a RO system to the process stream will produce an industrial quality makeup water, it also adds cost and complexity. Furthermore, because both the NF and the RO leave a large rejected brine residual, the amount of formation water needed and the brine volume for reinjection are relatively high.

Additionally, the off-the-shelf approach for using standard membranes requires the formation water to be cooled from 90°C (194°F) to 45°C (113°F) before entering the membrane systems. The use of high-temperature membranes could be considered.

Evaporative Technologies

Water treatment using evaporation has been state of the art in the power industry for many years. The Brine Concentrator, which is the workhorse for concentrating power plant wastewater, was

introduced at three southwest power plants in the mid 1970's. There are currently more than 150 such units operating at generating stations worldwide.

Mechanical Recompression Evaporator – Brine Concentrator

Evaporators in power plant wastewater applications are usually Mechanical Recompression (MVR) Evaporators, commonly called Brine Concentrators (BC). They are defined by three main design characteristics:

- The design is a long-tube, falling film evaporator
- It uses a Mechanical Vapor Compression power cycle (MVR)
- It uses a seed slurry process to prevent scaling of the heat transfer tubes

The MRV cycle allows the evaporator to operate at a relatively high steam economy equivalent to of about 35 to 45 BTU/lb (81to 128 kJ/kg, or ~100 kWh/kgal) of water evaporated, translating to a Gain Output Ratio (GOR) of about 25.

Brine Concentrators achieve wastewater volume reductions of 8 to 40 times and are capable of operating in a calcium sulfate crystallizing mode, which minimizes scale deposition on the heat transfer service. The typical feed water TDS ranges from 1,000 to 35,000 mg/l. The main limiting factors for the amount of volume reduction possible are the need to stay below sodium chloride saturation and to limit the brine's boiling point rise (BPR) to the capacity of the (centrifugal) vapor compressor.

The same type of evaporator, but operating without crystallization and at a much lower water recovery, could be applied to the formation water treatment. The percent water recovery would also be limited mainly by the concentrate's boiling point rise (BPR).

The main advantages of the evaporator option are that the formation water salinity would be well within the processing envelope and that the formation and reinjection well demand would be much smaller compared with the previous options discussed. Additionally, the formation water would not have to be cooled. This technology is the most off-the-shelf process for use in this application.

The disadvantages of this approach are that the feed water would have to be softened, and evaporators are costlier in both operating expenses (OPEX) and capital expenses (CAPEX) compared with membrane treatment systems. The presence of boron in the formation water may require special design adjustments to prevent carryover into the distillate.

Multiple Effect Evaporator

Multiple Effect Distillation (MED) evaporators are not common in power plants, but they are used in industrial and pulp and paper applications, especially where "waste" heat or low grade heat is available. Although the MVR systems usually consist of a single evaporator body powered by a compressor, the MED systems consist of at least two vapor bodies, smaller in size compared with an MVR system, that are connected in series. The brine enters the first body where a portion of the brine is evaporated, creating steam for the next effect. This steam, lower

in pressure than the previous source, now provides evaporative energy for the next body, and so on, until the final effect, where the emitted (lowest pressure) steam is condensed in an outside condenser. The steam to the first effect is supplied by an outside source. The cascading steam direction, depending on the process, can run parallel or counter to the brine's flow path.

The steam source is typically waste heat generated within the plant. In this application, however, the energy source for evaporation would be the formation water's latent heat so that no or only little outside steam would be required. To provide enough heat transfer driving source, the system would have to be operated at a relatively high vacuum at the final effects.
The steam efficiency of a MED evaporator is approximately equivalent to the number of effects present * 0.9. A two-effect system would have a steam economy or GOR of 1.8, whereas six effects would roughly translate to a GOR of 5.4. This compares with a GOR of 25 for a MVR system.

Crystallizer

Crystallizers in power plant applications typically take evaporator/brine concentrator blowdown and evaporate it to a dry salt residual, which can usually be deposed of in a conventional landfill, subject to passing the Paint Filter Test (PFT) and Toxic Characteristic Leaching Procedure (TCLP). The use of crystallizers in the power generating industry is common, especially where Zero Liquid Discharge (ZLD) is part of the water management requirement.

The advantage of using a crystallizer to convert the evaporator blowdown to dry salts cake is that it would result in the lowest formation water well extraction and would require no brine reinjection. It may also allow the extraction of such constituents as lithium from the recirculating crystallizer brine.

The disadvantage of adding crystallization to the evaporation treatment is that it adds complexity to the operation, and crystallizers are the costliest in both OPEX and CAPEX of any of the technologies discussed. Furthermore, with the high salt content of the formation water, the salt cake generation would require sizable landfill space for deposition.

Electro Coagulation (EC)

Electro Coagulation (EC) is an old technology that has only recently been resurrected for use in the water treatment industry. The applications to date have been mostly for smaller systems in the metals finishing and oil production industries. One of the largest operational EC to date is a 227 m3/hr (1,000 gpm) system that was installed at El Paso Electric's Newman Power Station in Texas. EC has been used in fracking operations to purify the water sufficiently to allow its reuse.

Based on some test data and vendor claims, EC is capable of achieving significant reductions in turbidity, TSS, iron, aluminum, and barium, as well as silica and organic components. Claims of water softening are also made. The basic principle of the process is that it uses an electric current, supplied through sacrificial iron or aluminum electrodes, to introduce minute metal flocculants into the water; it generates hydrogen gas to help in the separation process, which acts as a dissolved air flotation process. The sacrificial electrodes are periodically replaced.

Potential Technologies:

The following technologies may also be considered for this application. Many of them are, however, in their R&D stages and would not be ready for service until a thorough demonstration program was conducted.

Membrane Distillation (MD)

Membrane Distillation (MD) is one of the furthest developed of the technologies for potential application to high-salinity brines. The technology is a marriage of membrane separation and thermal processing, with the latter requiring a source of heat. MD proponents suggest that MD can utilize waste heat, possibly even from the temperature differential of the reservoir to surface temperature.

MD is similar to the MED evaporation process previously described, where the steam generated in one effect becomes the heat source for evaporation in the next. The main difference is that MED uses solid heat transfer surfaces (high-alloy or titanium tubes) to impart the necessary energy for evaporation to the brine, and MD uses a semipermeable membrane barrier which acts as both a barrier and a heat exchange surface, which allows steam to permeate from the brine to the distillate side, driven by the condensing steam's energy from a previous effect: thus the term Membrane Distillation. The thermal portion of the process occurs once the pure water has penetrated the membrane and is then vaporized and carried away to provide energy to the next effect.

Forward Osmosis (FO) and FO/RO/NF Combinations

Forward osmosis (FO), like RO is a membrane separation processes. Whereas in conventional RO the saline water permeates the membrane driven by the hydraulic pressure applied to the feed (which is in excess of the osmotic pressure), in FO the water molecules penetrate through the membrane into the "draw solution" by natural diffusion without application of hydraulic pressure. The driving force for FO is the osmotic pressure difference between the lower salinity feed and the higher salinity of the draw solution. Pure water from the low-salinity feed water penetrates the membrane barrier, trying to achieve an energy balance between both sides by diluting the more concentrated draw solution side. The draw fluid, therefore, must be of higher salinity than the feed side.

FO and its close cousin, Pressure Retarded Osmosis (PRO), with combinations of RO and NF for additional desalination could be considered. FO is alleged to have much greater scaling resistance than conventional RO, but requires a draw solution. A special case of FO could be worth consideration if the associated carbon capture process uses ammonia to capture CO_2 as ammonium carbonate. In these ammonia capture systems, the nearly saturated ammonium carbonate solution is heated to separate the NH_3 for reuse and the CO_2 for liquefaction. An interim step involving FO, using the ammonium carbonate solution as the draw solution, could offer substantial energy savings in the desalination process, because in the CO_2 capture process most of the heat energy is expended breaking the $NH_4 – CO_3$ bonds. The resulting extra water when the NH_3 and CO_2 are separated is the desalinated product.

Other FO processes utilize "directional solvents" which are organic solvent which are miscible with water at one temperature and immiscible at higher temperatures. Water passes through the FO membrane into the draw solution solvent. The solvent and the water are separated by raising the temperature, which makes the solvent immiscible with water. A gravity separation is possible, however the separation is not 100% and delivery of a product free of solvent is difficult and expensive. More development is needed.

Although interesting in concept, FO, which is in its infancy, has too many drawbacks, including the accumulating high-salinity draw solution (brine), which would have to be dealt with. Forward osmosis is a technology of general interest, but the desalination of the high-salinity formation water is not considered a good application at present.

Solvent-Based Systems

The methodology of using a "directional solvent", as noted with FO above, to extract water from a brine solution is based on using a solvent that has a different density from water and has the peculiar characteristic of being water soluble at one temperature but hydrophobic at another. When the brine is contacted with the cold solvent, it dissolves in the solvent forming a single-phase liquid. Salt and other impurities do not accompany the water but stay separated in the residual concentrate phase. The lighter solvent/water portion is decanted and then reduced in temperature, which causes the water and solvent to separate again into 2 distinct phases, leaving a relatively pure water layer. The water is withdrawn and the solvent returned to the process cycle. The salts remain behind as a concentrated brine.

This idea has had numerous reincarnations over the years with so far little commercial success. Originally, the Boeing Company's RCC (now RCC is part of GE) tried this approach using trimethylamine to separate oil or water from oily sludges. More recently the process has been tested in other applications. Because of the inefficiencies of separations and the need to augment the process with additives, this process has not yet found commercial favor in desalination applications.

Ion Exchange

Ion exchange could possibly be used to remove salts from the brines. The end product, however, is simply a salt residual for disposal amounting to at least twice as much, and in practice at least 2.25 times, as the amount removed from the produced water. Exchanging divalent cations and divalent anions with NaCl, using anion and cation resins, will result in a high concentration of salty water with mostly NaCl. The only realistic means of disposal of this brine would be to inject the brine into the formation. Adding additional brine to the formation would require more formation water to be processed. Alternatively, the brine could be used as makeup to a high TDS cooling towers or in oil field brine applications. Use in cooling towers would generate high cooling tower blowdown rates and may lead to scaling as a result of the regenerated hardness of the ion exchange. Additional resin-based deionization is possible using HCl and NaOH, but costs become substantial for chemicals and disposal. Desalination of the formation water using ion exchange is, therefore, not deemed to be practical.

Electrical Deionization (EDI) and Electrodialysis (ED)

Both EDI and ED are well-established commercial processes. EDI is suited for low TDS operations, and ED is generally considered not cost effective above a few thousand ppm. The reason is that salt removal is strictly an amperometric process. Although ED is used for concentrating salt from seawater, particularly in Japan, the power requirement is in the order of 240 kWh/ton of salt removed. Japan has no natural salt deposits and limited land space so in Japan special ED membranes are used in approximately 7 large scale plants to make nearly saturated NaCl (22 to 24 wt percent) from seawater ready for evaporative crystallization. The process is utilized to avoid the necessity of the large tracts of land typically associated with recovery of sea salt and to maintain substantial NaCl production in the homeland. Recovered water is discharged back to the sea at about 10,000 ppm.

A brief review of the removal of KCl and NaCl from 500 gpm of the Madison Formation water shows that there would be approximately 242 tonnes of KCl plus NaCl per day, requiring approximately 58,000 kWh, or about 2.4 MW. The recovered water (the ED dilute) would not be pure and would be enriched in divalent ions. Additionally, there would be a stream of near saturated KCl and NaCl, which would require disposal or could potentially be used in oil field operations. In summary, EDI or ED would not be a good fit for this application.

Capacitive Deionization (CDI)

CDI, while not a new process, has never been applied in large-scale operations. It will have some of the same limitations as ED, although there is a possibility of operation in a "multiple effect" style, where the charging current and voltage is "recaptured" in several stages. This technology is, however, far too early in its large-scale development for consideration.

MD Solar thermal area analysis. Area needed to produce 500 gpm with a six (6) effect MD system.	
5.3	Presumed MD GOR
46,909	Steam - lbs/hr
46,908,921	btu/hr to first effect steam
13,744	kw equivalent
5.20	kwh/m^2/day per NREL Rock Springs
217	watts/m^2 solar insolation 24 hr avg
75%	Collector Thermal Efficiency
84,580	Minimum Area, m^2
21	Acres

Table 5: *Solar Requirement for Evaporation*

Solar-based desalination systems

Solar-based systems can be considered, although the thermal energy requirement is high. Consider also that a solar system must of necessity be designed to capture energy at least 3 times the 24-hour rate and, depending on the location, perhaps 4-5 times as much. Looking at the MED and MD designs shows that at least 93.8 gpm of steam at >81 °C will have to be generated.

Table 5 illustrates the solar requirement to drive an evaporation system. Twenty to even fifty acres or more of solar collectors is not infeasible. A hot oil or hot pressurized water system with molten salt could potentially provide the required energy to drive the first effect of either an MD

or MED system. The significant advantage here is that potentially the brine requirement is greatly reduced to be nearly the same as an MVR type system. We could presume that land is relatively low cost in the target areas. When and if evaporation systems are considered to be viable solutions, the solar ideas should be revisited. The solar capture technology is a separate development issue not affecting the evaporator design.

The above does not fully address the needs of solar driven evaporators as some heat storage facility or alternate heat source is required to make the operation continuous. However, if RO/NF proves acceptable, a much smaller solar field based on PV technology with night grid supply would be applicable to powering the RO/NF systems.

Waste Destruction and Desalination at Supercritical Conditions

Another potential method for removing formation water salts is a process in which the brine is elevated to supercritical conditions, i.e., P ≥ 221 bar (3,200 psi) and T≥ 374 °C (≥ 706 °F). At supercritical conditions, salts are only minimally soluble in the supercritical fluid and crystallize out. The salts can then be separated and removed with the single-phase supercritical fluid subsequently cooled.

This technology has been used for chemical weapons destruction and is currently being investigated for salt removal and organics destruction in municipal waste sludges as well as for the desalination of produced water in EOR operations. These technologies for waste destruction and desalination are, however, in their infancy of development. Several have been recently patented.

Aside from generally being a costly approach, the high salt content of the produced water will pose a serious issue. The water's high chloride content at high temperatures would result in a very corrosive environment, and the high calcium and sulfate content may lead to plugging problems within the supercritical heater. Because of the sum of these reasons, this technology was not further considered.

F. Technologies Reviewed in Detail

The treatment scenarios described in this section are options considered to have sufficient merit to warrant a more detailed analysis. Most of the treatment methodologies described consist of several processes arranged in series, where each process step conditions the feed water for the next downstream unit operation. All of the scenarios presented will generate one or more residuals, consisting of waste brine concentrate, sludge or salt cake, which must be disposed of. The disposal of these wastes will figure into the overall technical and economic ranking.

Some of the concentrated brine residual may be suitable for beneficial use in drilling operations. Although identified in the following discussion, such brine disposal is considered to be of an intermittent nature so that it is not integrated into the overall technical or economic evaluations.

Option 1: Evaporation or Flash Extraction:

The scenarios of Option 1A, 1B, and 1C below take advantage of the produced water's latent heat to evaporate or flash off and remove the required amount of produced water.

Option 1A: Dedicated Direct Contact Cooling Tower

Figure 22 shows the simplest of all of the options presented. The hot produced water is fed to a dedicated mechanical draft cooling tower, which uses the produced water as the circulating media. The 500 gpm of produced water evaporates in the mechanical draft tower and is thereby removed from the system. A large cooling tower blowdown, which is about 1.1 times the feed concentration, is needed since this is all the energy available (reducing the produced water temperature to approximately 90 °F provides only enough energy to evaporate 10% of the water). This discharge, which is of lower volume compared to Option 1B and 1C, will be reinjected into the formation.

The only technology involved in the approach is the use and operation of a seawater type of cooling tower.

Option 1A: Advantages

The advantages of Option 1A include:

- Option 1A, along with all of the other Option 1 scenarios, is by far the simplest and cheapest approach from both a CAPEX and OPEX point of view, not counting the size and operation of the wells need to support this plan.
- Option 1A is the simplest of all the options and the cheapest of all three Option 1 approaches.
- Option 1A's produced water and reinjection flow requirements are less than those for Options 1B and 1C.
- Option 1A is a total stand-alone system requiring a minimum of supporting equipment and instrumentation.
- This option is the lowest-tech approach of any of the scenarios presented in this study.

Option 1A: Disadvantages

The disadvantages of the dedicated cooling tower approach include:

- The major disadvantage of the dedicated cooling tower is the high formation water feed and brine reinjection volumes, amounting to approximately 5,500 gpm and 5,000 gpm, respectively.
- Although not adding to the power plant's heat load, the stand-alone cooling tower must reject approximately 300 MMBTU/h, which translates to a refrigeration load of about 30,000 cooling tower tonnes. A tower of this capacity will have a footprint of about 20 x 100 ft.
- Because of high salinity, the cooling tower will be a seawater type, which is more costly than a conventional cooling tower. Seawater cooling towers are in common use, however, and are considered to be state of the art.
- The use of scale inhibitors and chemical control of the cooling tower is expected to be sufficient to prevent scaling. As the concentration factor is low, the chemical control

dosage rates may be low. Because the produced water is saturated in both calcium carbonate and calcium sulfate (anhydrite), scaling is a concern, so that a careful review of water chemistry will be in order. As the water cools from the 90°C to 65°C, the anhydrite may, with time, begin to transform to the gypsum form, which has a higher solubility.

- Any formation water impurities, such as H_2S, would enter the cooling water loop, which, depending on the amount of H_2S or other impurities present, may lead to air quality issues.
- If the formation water temperature were lower than the 90 °C expected, then these feed and discharge flow rates would increase. Should, with time, the feed water temperature decline beyond the design envelope then the overall process would fail unless supplementary steam were added to the formation water feed to maintain the temperature at 90°C.

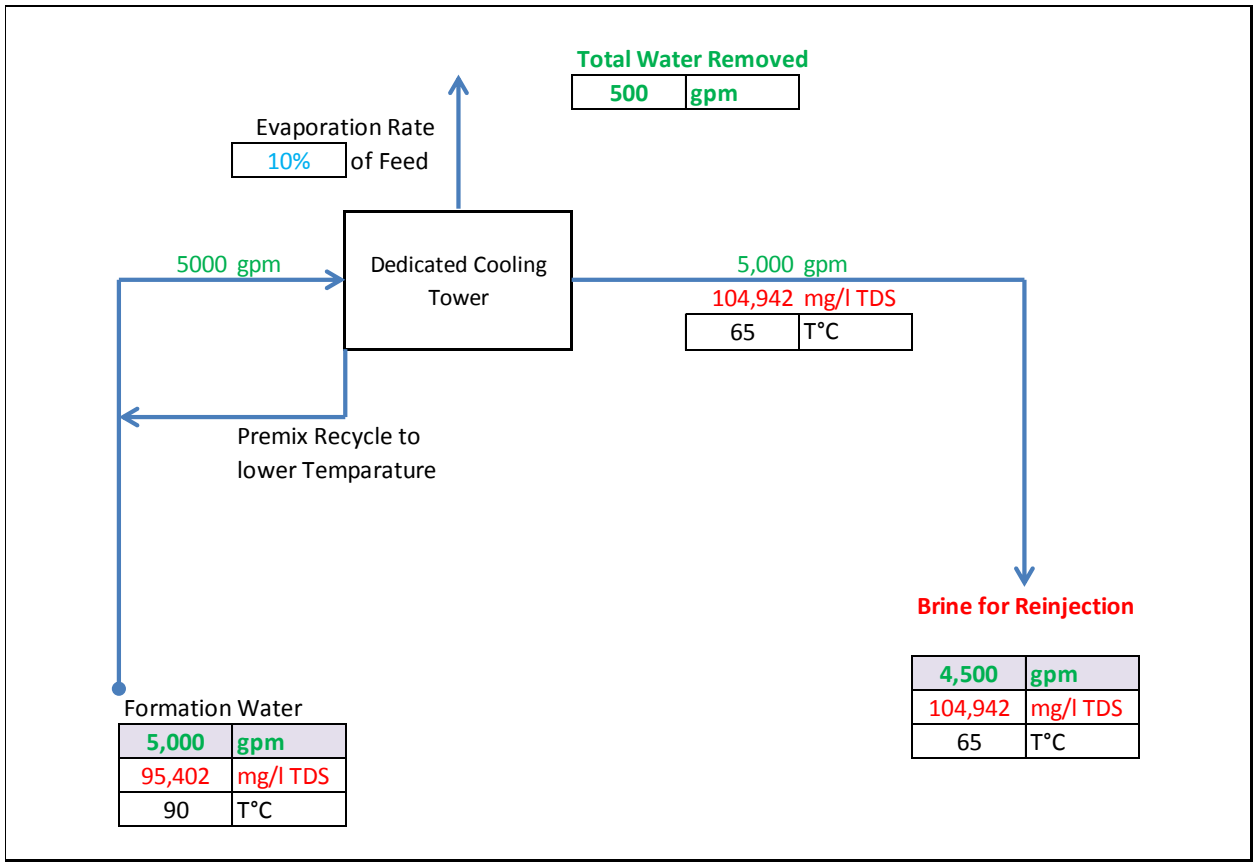

Figure 22: Option 1A – Dedicated Direct Contact Cooling Tower + Brine Reinjection

Option 1B: Direct Contact Chamber

Option 1B, pictured in **Figure 23**, employs a direct Contact Flash chamber to vaporize 500 gpm of formation water under vacuum conditions. The flashed steam is then condensed by direct contact with the power plant cooling water, which is thereby beneficially diluted by 500 gpm of pure water as it is returned to the plant's cooling loop. The direct contact with the cooling water is essentially a barometric condenser and serves to create the vacuum necessary for the flashing to take place. The added heat load will have to be removed by the cooling tower.

The reason why Option 1B (and 1C) flash off less formation water than the cooling tower of Option 1A is that the contact air helps the evaporation process.

Option 1B: Advantages

The advantages of this approach include:

- As described for Option 1A, this approach is also simple and low tech. The equipment involved is relatively inexpensive and cheap to operate.
- The only equipment involved for Option 1B is a flash contact chamber; cooling water can be sourced from the associated power plant.
- During the cool winter and transition months, when the cooling tower load is low, the condensed produced water will provide the benefit of a clean cooling tower makeup water, thereby reducing the plant makeup water needs and reduce the cooling tower blowdown rate. During the warm summer months, the added hot condensate will, however, need to be dissipated by the cooling tower, resulting in a net zero gain.
- The direct contact flash chamber operation is a low-risk process, assuming a constant feed temperature of 90°C. It uses existing and proven technologies.

Option 1B: Disadvantages

There are several major disadvantages that counter the benefits of this and the other Option 1 scenarios. These include:

- The large produced water feed, which is required to satisfy the thermodynamic requirement to flash off 500 gpm of water, translates into a relatively large production well that is capable of delivering about 6,250 gpm.
- Because the flash chamber removes only about 8% of the produced water, the residual brine that must be reinjected into the formation amounts to about 5,750 gpm. Both of these large production and reinjection demands translate into a high capital investment.
- The process adds heat to the power plant's cooling system at a rate of approximately 250 MMBTU/h or 21,000 cooling tower tonnes. This heat rejection will add the equivalent of 1 cell to a mechanical draft cooling tower system.
- The same issues as described in the disadvantages for Option 1A with regard to a potential formation water temperature decline apply here as well.
- The H_2S and other contaminant issue in this scenario will be similar to that described for Option 1A.

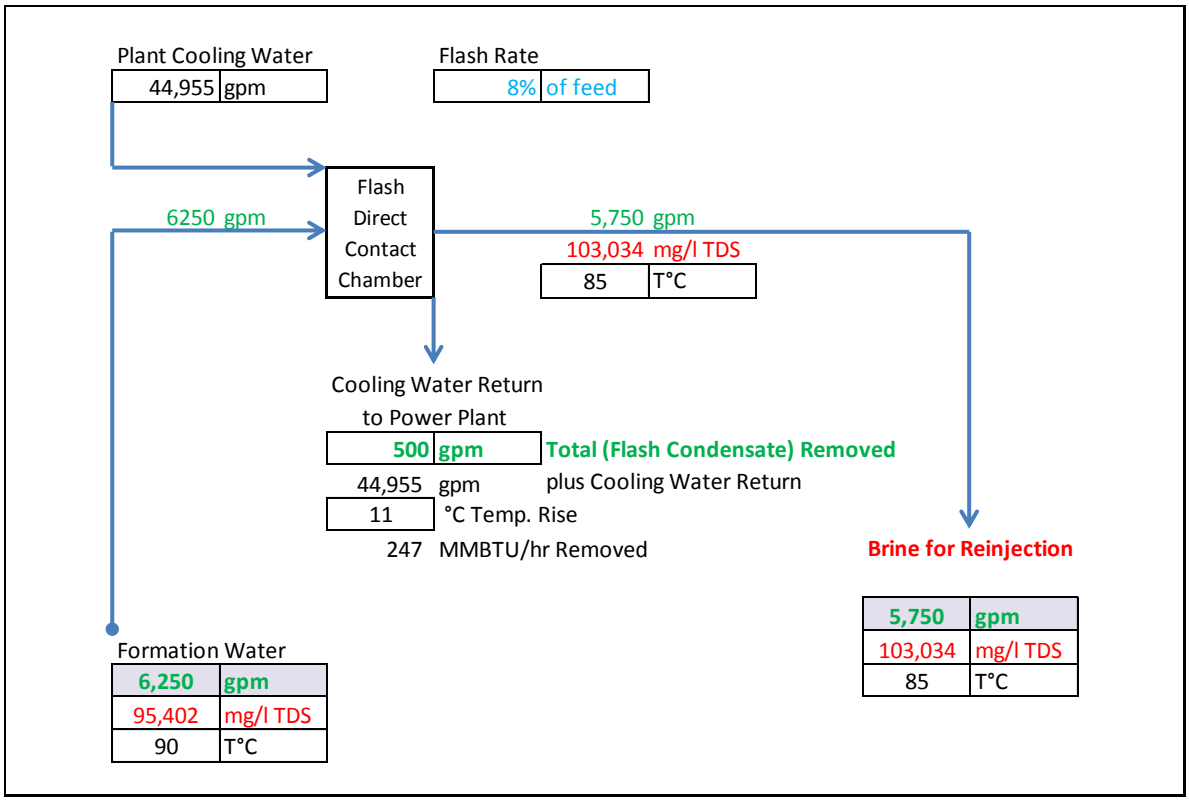

Figure 23: Option 1B – Direct Contact Flash Chamber + Brine Reinjection

Option 1C: Flash Contact Chamber Plus Surface Condenser

Option 1C uses an approach similar to the other Options 1, except that the flashed water is condensed and captured. Again, using a large produced water flow, 500 gpm of water is flashed off and then recaptured via a surface condenser. The difference between Option 1C and Option 1B is that the surface condenser captures the condensate as a separate, high-quality stream for beneficial use. Heat rejection for condensation would be provided by the power plant's cooling water, adding roughly 250 to 275 MMbtu/hr to the plant's cooling load. The condensation process would be carried out under a vacuum condition, which would be provided via a vacuum pump or a steam ejector. The surface condenser would be large and the formation water feed and brine disposal demands high. The flow schematic of Option 1C is presented in **Figure 24**.

Option 1C: Advantages

The advantages of this approach for the removal formation water include:

- As described for Options 1A and 1B, the Option 1C approach is also simple and low tech. The equipment involved is relatively inexpensive and cheap to operate.
- The equipment involved is a flash contact chamber and surface condenser.
- The process will generate 500 gpm of almost pure water for beneficial use.
- The flash chamber surface condenser system is low risk by using existing and proven technologies.

Option 1C: Disadvantages

The major disadvantages are similar to those stated of Option 1B and include:

- The same large formation water and reinjection demands stated for Option 1B.
- This option will have the same heat rejection demand on the power plant's cooling system as described in Option 1B.
- The same issues with regard to a potential produced water temperature decline, as described in the disadvantages for Option 1A and 1B, apply here as well.
- The H_2S and other contaminant issues in this scenario will be similar to those described for Option 1A and 1B.

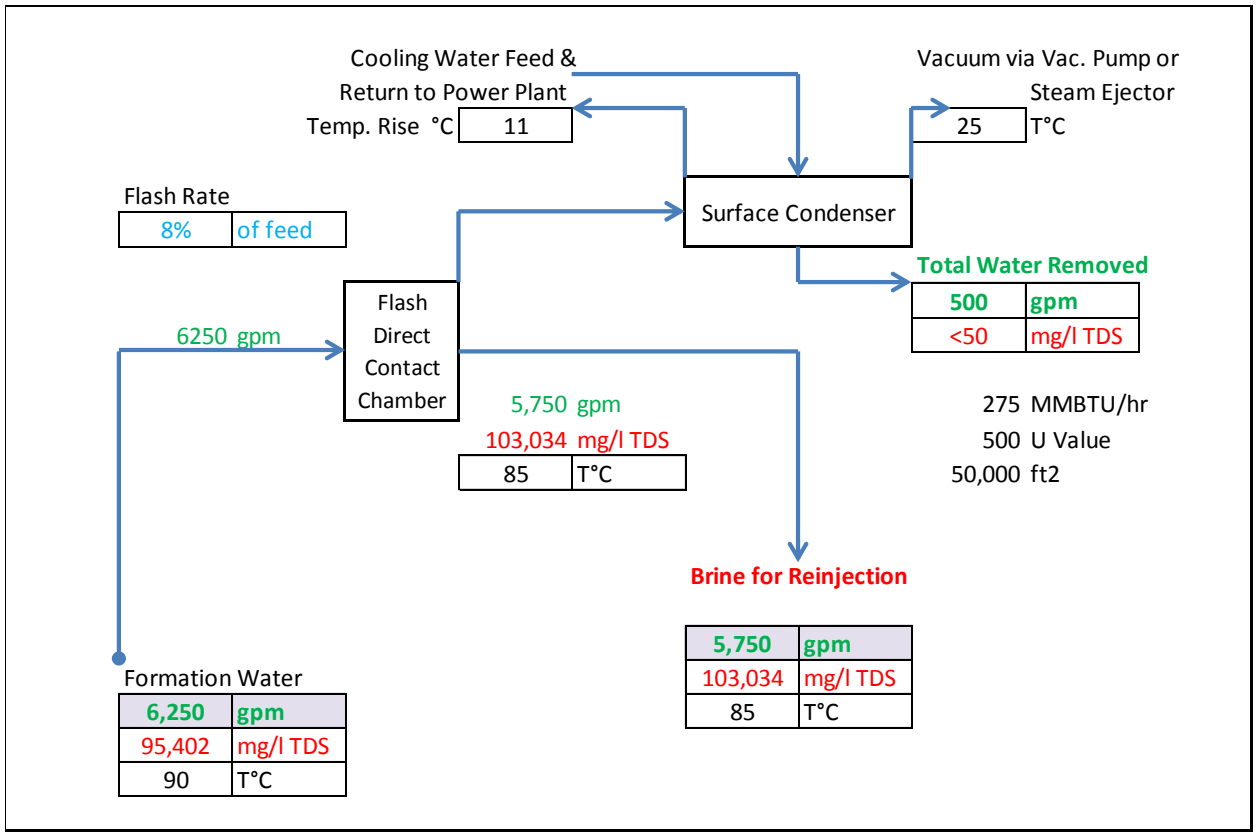

Figure 24: Option 1C – Flash Contact Chamber Plus Surface Condenser + Brine Reinjection

Option 2: Membrane Separation Processes:

As pointed out above, the maximum operating temperature of conventional membranes is 35°C. High-temperature membranes are available, but their use for desalination has been used mainly in R&D and demonstration projects.

As such, this study focused on the use of membrane separation processes that are within the current membrane-operating envelope, especially because the operating pressures required by the high feed water salinity may negatively impact the use of high-temperature membranes. Demonstration testing to verify this latter assertion, should however, be conducted as a part of the Phase II testing.

Because of the brief holdup time within the membrane elements, the processing can usually be done with a certain amount of supersaturation of calcium carbonate and calcium sulfate. Precipitation of these and other salts within the membrane passage may, however, require one or more scale inhibitors.

At 50% recovery scale inhibitors are very likely to be successful. The maximum recovery achievable without softening will need resolution in pilot studies once steady state conditions are reached with the formation water withdrawal. Current scale inhibitors for membrane systems can reach 3 to 4 times normal saturation levels for calcium sulfate and calcium carbonate. Levels at 2 times silica saturation are also achievable so higher recovery may not be scale limited.

Option 2: Formation Water Flash Tank Cooler + Nanofiltration Only

A nanofiltration system allows passage of monovalent ions, impeding the passage of multivalent ions to a much greater extent. Most of this effect is directed at the anions, so sulfate rejection may be very high while chloride is only poorly rejected. This results in a balancing of the osmotic pressure difference across the membrane and allows operation at TDS levels normally above the reverse osmosis capacity since only the osmotic pressure difference (salinity gradient) across the membrane is important.

In this option, we also capture a small flash portion as high quality condensate from the formation water cooling. This reduces the capacity needs of the membrane system. It should be noted, that if formation water temperature declines over time the capacity of the membrane system will need to increase to offset the reduced flash condensate available.

Option 2: Advantages and Disadvantages

This option has the advantage of simplicity. It also recovers some 80 gpm of high purity water captured in the cooling process, which reduces the capacity requirement of the Nanofiltration system (**Figure 25**).

The primary disadvantage is that the NF permeate is of a high TDS. While it will have limited hardness, the product water will have almost 2-3 times the NaCl concentration of seawater. Conceivably this water could be used in saline cooling towers, however, these are expensive in terms of both CAPEX and OPEX.

It is also possible that undesirable volatiles, potentially present in the formation water, such as hydrogen sulfide, will be captured and quite possibly concentrated in the flash condensate. If this happens, a stripping process, rejecting the volatiles to the air may also be required.

This option was considered primarily to look at the simplest membrane application.

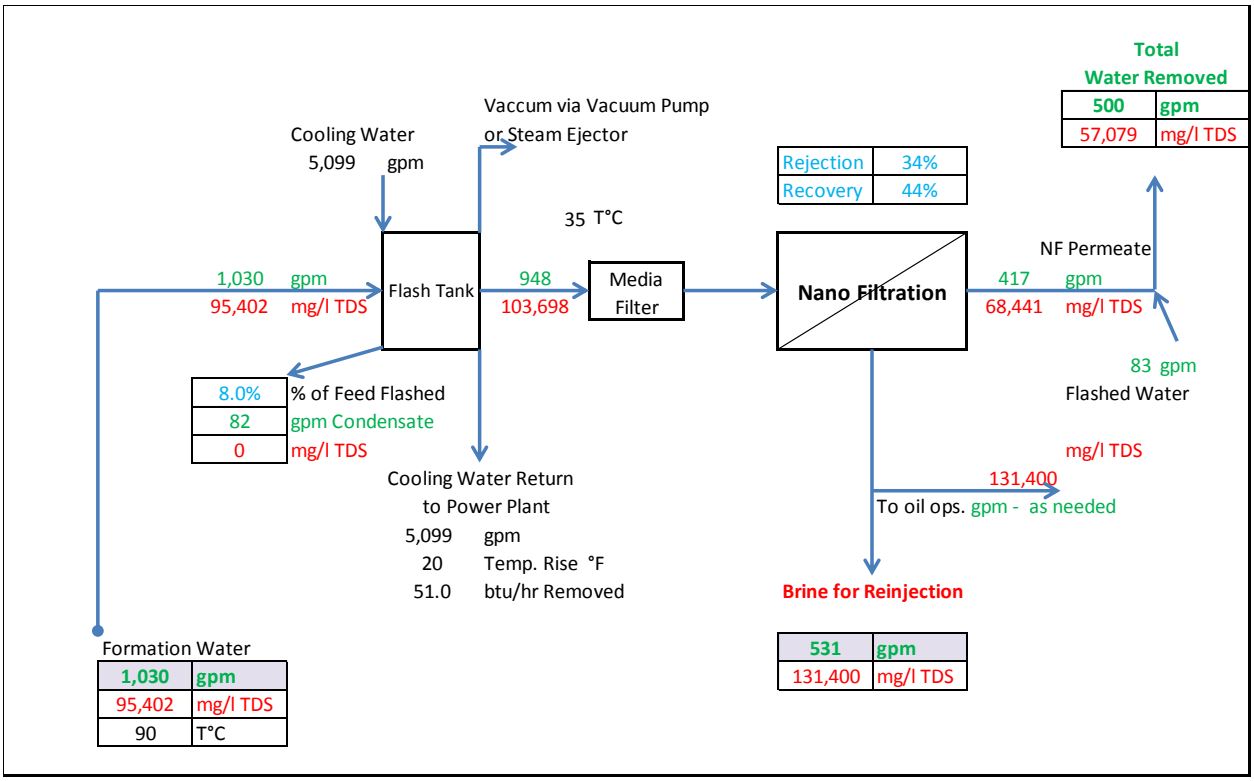

Figure 25: Option 2 - Formation Water Heat Exchanger + Nanofiltration

Option 3: Formation Water Cooler + Nanofiltration+ Reverse Osmosis:

Options 3 (A and B) are essentially the same as Option 2, but with a reverse osmosis system added to purify the NF permeate to make the final product water more suitable for beneficial use in the associated power plant (**Figure 26**). This very soft RO permeate could be ideal for use as cooling tower makeup.

Option 3A and 3B: Advantages and Disadvantages

Both of these options have the advantage of providing high quality permeate. They have, however, the major disadvantage high overall costs when the formation water and reinjection well costs are included. Membranes will be significantly less costly to operate than evaporators. However, this operating cost differential is unlikely to make up for the high cost of formation water pump up and return.

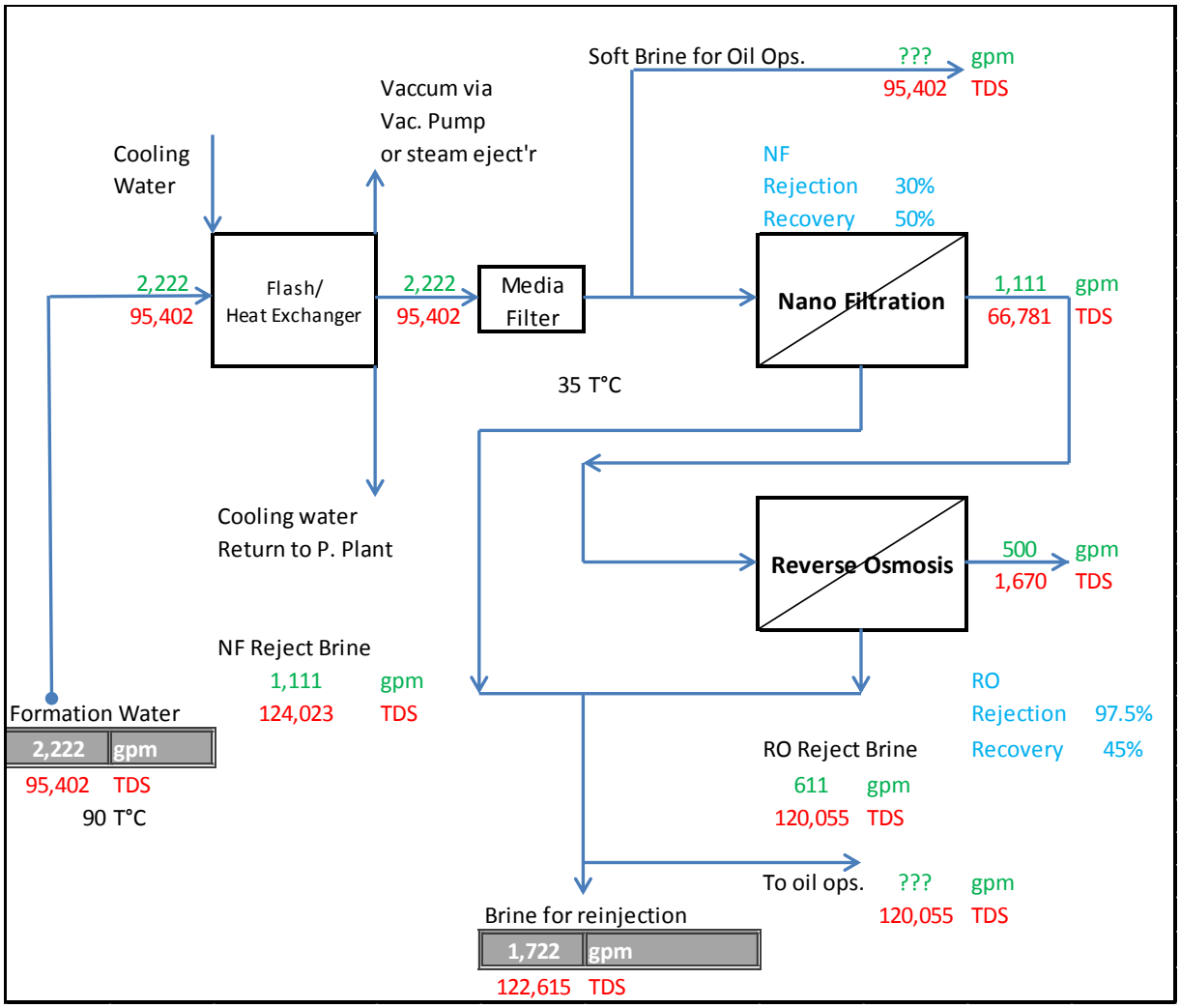

Figure 26: Option 3A - Formation Water Cooler + Nanofilter + Reverse Osmosis

Option 3B: Warm Lime Softening + Nanofiltration+ Reverse Osmosis

Option 3B is the same as Option 3A but with warm lime softening pretreatment added. This is the same as 3 with warm lime softening added. This is also the membrane option with the greatest likelihood of long term operation with few problems. Lime softeners in front of membrane systems have proven to be very effective pretreatment methods (**Figure 27**).

The produced water temperature increases the performance of the lime softening system, particularly in regards end point hardness and silica, as well as in the sludge settling characteristics.

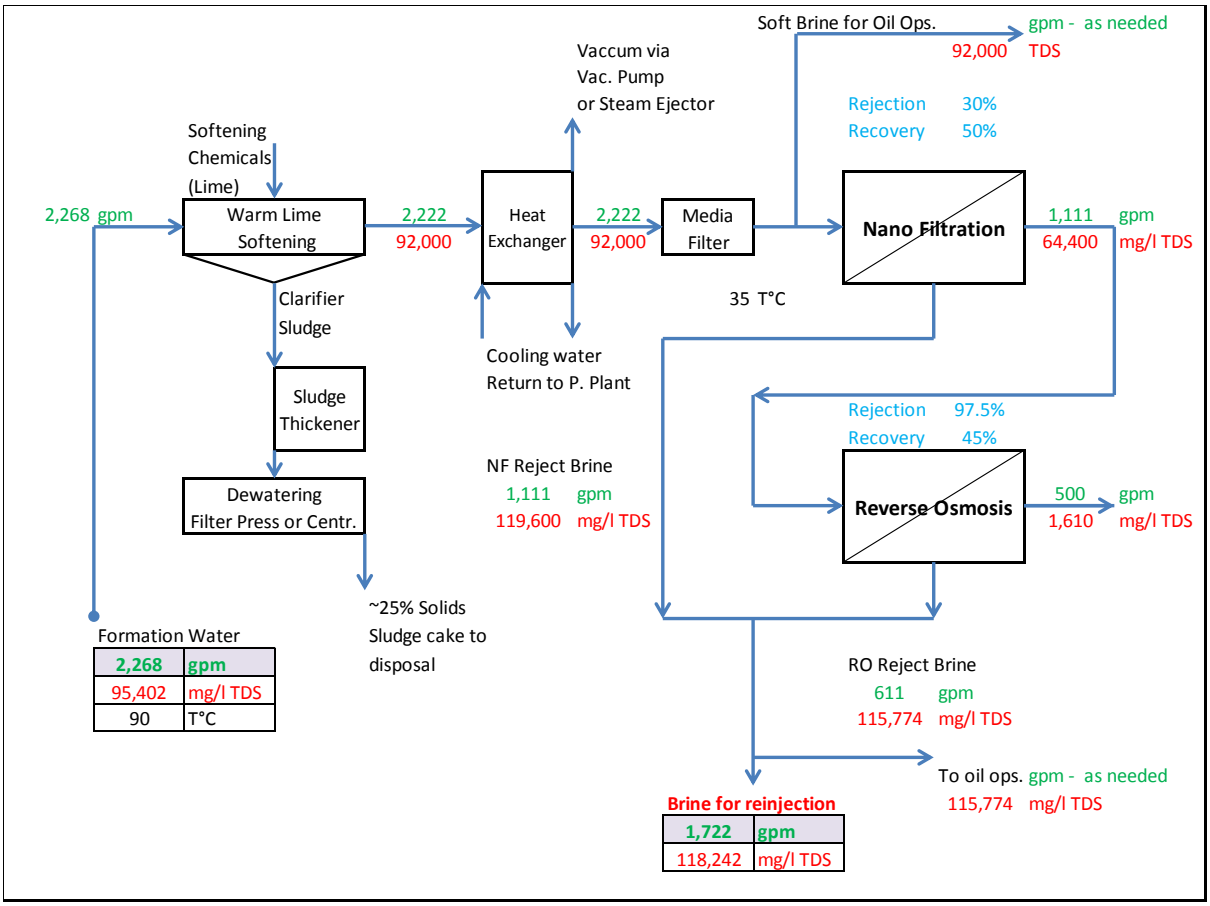

Figure 27: Option 3B - Warm Lime Softener + Formation Water Cooler + Nanofilter + Reverse Osmosis

Evaporation Systems

Option 4A: Softener + Mechanical Vapor Recompression Evaporator

Evaporation using a mechanical recompression cycle is the most common process applied in power plant and other industries to deal with high-salinity wastewaters. MVR Evaporators in their Brine Concentrator manifestation are ubiquitously used in these industries. Furthermore, in EOR and SAGD applications, MRV Evaporators are commonly used to concentrate produced waters rich in sodium chloride. Because of the evaporator's ability to process high-salinity water, its application to extract the 500 gpm of formation water is considered a most favorable approach, requiring considerably less formation water feed and much less brine residual for reinjection.

Cooling of the formation water is not required, and the latent feed water heat will be helpful in the overall energy balance. To concentrate the formation water to the highest degree possible in the MVR Evaporation system, the feed water will require prior softening to remove the calcium, alkalinity, and silica, which would otherwise scale the evaporator. Addition of lime to the softener will not only precipitate the bicarbonate as calcium carbonate but will also reduce the hardness sufficiently to prevent calcium sulfate scaling. The precipitation process, which will co-precipitate magnesium, will reduce the silica content to a level at which silica scaling will not be an issue in the evaporator or in the reinjected brine concentrate.

This scenario proposes to use of warm lime softening (WLS), which not only eliminates the need to reduce the feed temperature, but typically also causes the softening reactions to proceed more quickly and efficiently. A determination will be made during the Phase II pilot testing to determine whether sufficient silica is removed from the high TDS formation water to ensure that silica scaling does not occur in the reinjection process. Should the silica removal in the WLS be questionable, dolomitic lime can be substituted for lime to add additional magnesium for higher silica removal.

The idea of adding a flash tank to flash off about 8% of the formation water, as described in Option 2A, may be considered as a trade-off to reducing the evaporator size. It is unclear, however, how much economic benefit would be realized by adding equipment and complexity to the treatment system. This alternative can be further investigated for all of the evaporator options. A process sketch of this MVR Evaporator treatment approach is shown in **Figure 28** below.

Advantages of the MVR Evaporator Option

The main advantages of using this evaporative technique include the following:

- It is a well-proven, off-the-shelf technology.
- Of all the previously described scenarios, it has the lowest formation water feed and the lowest brine reinjection.
- The process produces 500 gpm of high-quality distillate with a TDS of <10 mg/l of inorganic salts. This water may be used for the power plant's boiler makeup ion exchange system.
- The unsaturated and clean brine concentrate residual may be well suited for drilling and facing operations.

Disadvantages of the MVR Evaporator Option

- The main disadvantage of the evaporator approach is that the formation water must be softened before the evaporation step. Softening adds process complexity and leaves a residual sludge/filter cake that must be disposed of. Most power plant sludges are either deposited in on-site landfills or are hauled off to conventional landfills. The nature of this sludge residual would have to be tested for toxicity to see whether it can also meet the standards set for disposal in a conventional landfill.
- Evaporators are complex systems of high-alloy construction to prevent corrosion. Their operating costs are also relatively high, mainly due to the energy consumption of the vapor compressor, which is the heart of the system. As such, the CAPEX and OPEX for the MVR Evaporator on a stand-alone basis are relatively high. These costs are, however, mitigated by the small feed water and reinjection demand (high overall water recovery), so that the total project and operations costs are favorable.
- The influence of some of the formation water constituents, such as boron, will have to be further investigated. (While in a non-precipitating evaporator boron does not pose a processing problem, boron, depending on operating pH, does volatilize over with the distillate resulting in a contamination issue.)

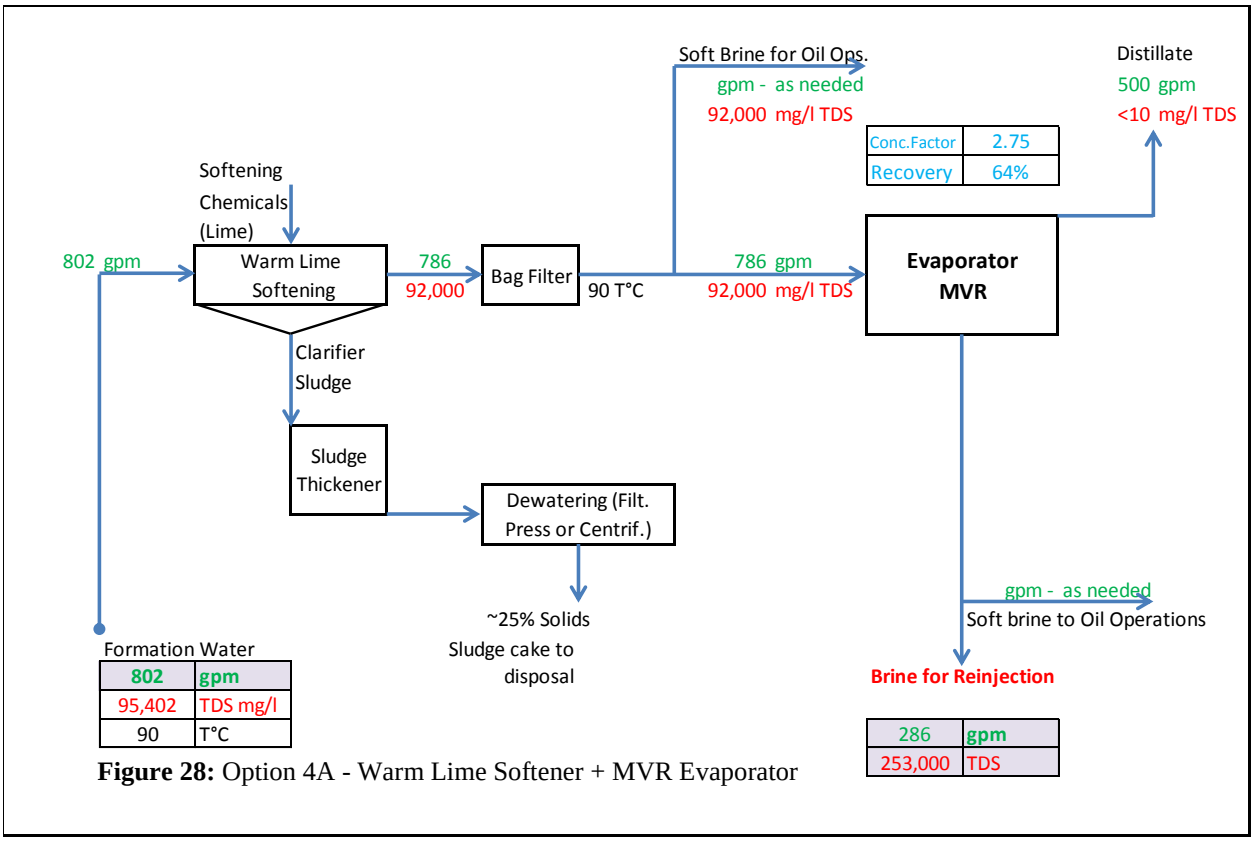

Figure 28: Option 4A - Warm Lime Softener + MVR Evaporator

Option 4B: Multiple Effect (MED) Evaporator

The interest in using a multiple effect in place of a MVR Evaporator is in its potential to use the formation water's latent heat as an essentially free driving source to power the evaporation process. If enough energy could be delivered by the formation water to evaporate 500 gpm of brine, then the goal would be achieved.

Sufficient formation water would be fed to the first effect of the MED system to flash off enough steam to feed the remaining effects. The steam would then be passed on to the next effect to create the cascading steam generation/condensation process for all of the vapor bodies in series. The steam generated in the final effect would be condensed in a water-cooled condenser. A small portion of the brine residual from the flash chamber (1st effect) would be passed on to the next and subsequent effects in a cascading manner. The final MED blowdown is then mixed with the residual from the flash chamber and reinjected into the formation.

Because the energy of formation water, based on feed and discharge temperature differential, yields only 105 BTU per pound (190 – 85 BTU) and the GOR of a 6-effect system (realistic maximum number of effects) is about 4 to 5.5, it would take about 8,530 gpm of feed water to make the system work, leaving 8,030 gpm for reinjection. The mass and energy balance of this approach is shown in **Figure 29**.

Based on the high formation and reinjection water demand, the costs for the wells, plus the CAPEX of the large MED system, this option is unattractive and was, therefore, not considered competitive with the MRV Evaporator. It is, therefore, not pursued beyond this initial evaluation stage.

One advantage of the MED vs. the MVR approach is that softening would not be required because of the low extraction rate per pass through the system. This advantage would, however, not be sufficient to economically justify this option. Use of outside steam to supply additional energy for either the MED would reduce the large feed and blowdown rates, but such a steam supplement would negate the energy advantages envisioned for this approach and would still make the MVR Evaporator a more economical and simple choice.

It should be noted that Multi Stage Flash (MSF) evaporation was also considered, but this technology, which would also rely on the formation water's latent heat driving force, would suffer from the same disadvantages as the MED approach.

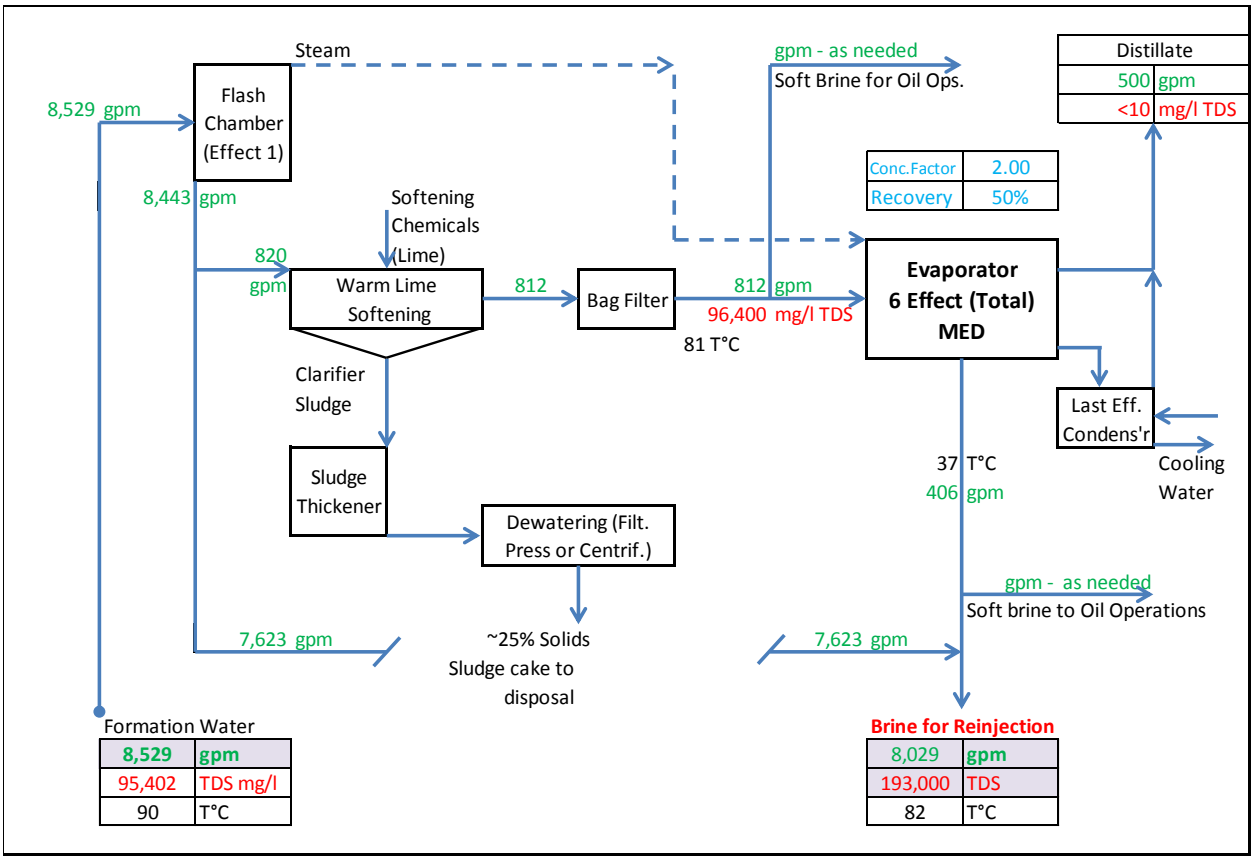

Figure 29: Option 4B - Warm Lime Softener + MED Evaporator

Option 5: Softener + Evaporator + Crystallizer

Option 5 adds a crystallizer to Option 4A to further concentrate and crystallize the evaporator blowdown. This approach embodies all of the aspects and benefits of the MVR Evaporator scenario and provides a means to take the total process residual to dryness, leaving a salt cake for disposal. The flow schematic of this scenario is shown in **Figure 30**.

The crystallizer power cycle would also be mechanical vapor compression, which provides energy savings for such a large system. Because of the large feed rate and the high salinity and crystal concentration of the process slurry involved, it would be preferable to have the crystallizer system consist of 2 parallel units, each of 50% or 60% capacity. Doing so provides redundancy and assures continuous processing even if one unit is in need for maintenance or repair. As is the case with MVR Evaporators, MVR crystallizers are common in the power plant industry and are used as the final step in ZLD operations. They have been in successful service in power plants for more than 30 years. Similar to the evaporator distillate, the crystallizer produces high-quality water, typically guaranteed to be <50 mg/l TDS.

Dewatering of the crystal slurry in a system of this size would be done using a centrifuge, probably in a 2 x 50% or 2 x 100% configuration, which would leave a moist salt residual ready for on- or off-site disposal. Due to the high salt content of the formation water, the salt production by the crystallizer will be about 250 tonnes/d (on a dry basis). It is estimated that this translates to a landfill airspace requirement of about 2 to 4 acres per year, 25 feet deep.

Alternatives are currently being developed that allow the crystallizer slurry (no dewatering system needed) to be mixed with reagents to stabilize the otherwise soluble salts so that they become nearly impervious to water intrusion and leaching. One of the major reagent components could be the power plant's generated fly ash. Because our application will be located in an arid region, however, the stabilization of residuals will not be further considered.

Advantages of the MVR Evaporator and Crystallizer

In addition to those cited for the MVR Evaporator, main advantages of adding a crystallizer include:

- The crystallizer technology is well proven and offers off-the-shelf readiness.
- The combination results in the lowest formation water feed requirement of all the options listed.
- There is no brine residual that requires disposal via reinjection.
- The combination produces 500 gpm of high-quality distillate with a TDS of <25 mg/l inorganic salt content. This water may be used for the power plant's boiler makeup ion exchange system.

Disadvantages of the MVR Evaporator and Crystallizer

In addition to those cited for the MVR Evaporator, main disadvantages of adding a crystallizer include:

- The addition of a crystallizer adds process complexity. Crystallizers are more difficult to run and require more operator and maintenance attention than evaporators.
- Because of the high salt concentration being processed, crystallizer metallurgy faces a high corrosion potential compared to that experienced in an evaporator and, thereby, makes the crystallizer significantly more expensive.
- The dewatering of the salt slurry is often associated with high operations and maintenance efforts.
- Crystallizers are high in OPEX and CAPEX.
- The salt cake residual must be disposed of in a landfill, either on- or off-site.

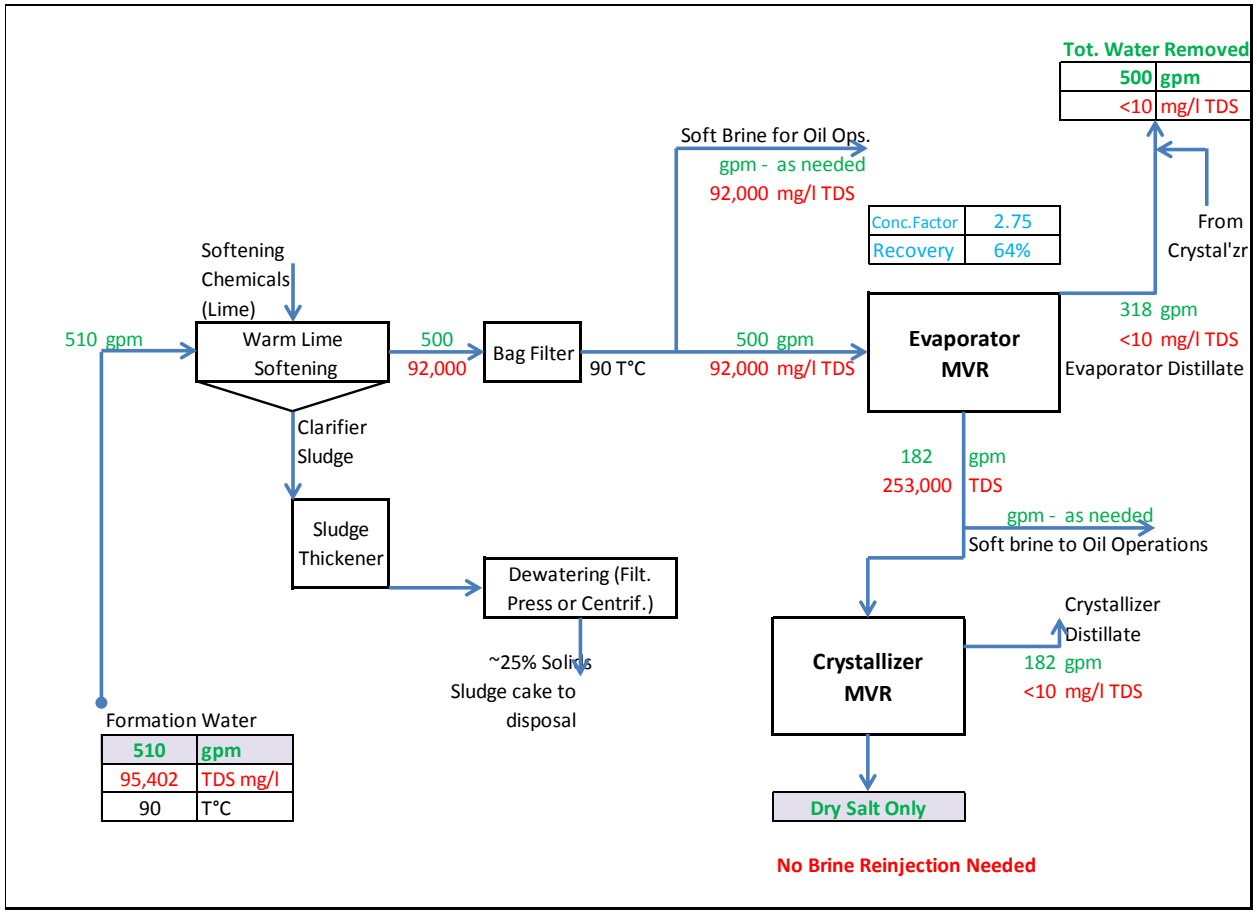

Figure 30: Option 5 - Warm Lime Softener + Evaporator + Crystallizer

Option 6: Membrane Distillation (MD)

We evaluated the applicability of the MD process to our requirements. With the formation water at 90°C, one may assume a potential temperature differential of (90°C - 30°C) = 60°C (108°F) could be available for evaporation.

MD operates essentially as a multi-effect evaporator, meaning that the steam/vapor generated in the first effect is used to evaporate more water in the second effect, and so on. The formation water is hot enough to not require additional heating. The thermal performance of MD systems is not highly efficient thermodynamically, however. We made some speculative assumptions as to performance by calculating various configurations. The highest reported GOR for MD systems with similar feed and exit temperatures ranges from 4 to 11. It must be noted that the details of the 11 GOR system are unavailable and likely do not include any "waste heat" inputs. In this application we anticipate at 50% recovery (i.e., a concentration factor of 2) a Boiling Point Rise (BPR) of about 3.5°C (6°F). This BPR is additive between each effect, so a maximum number of effects is probably limited to 6 or less. A 6-effect system, with no external heat addition, could conceivably operate with somewhat more than 50% recovery, leaving the brine concentrate residual at approximately 30°C (86°F).

A GOR of say five means essentially that 1 kg of the initially generated steam can be used to generate a total of 5 kg of steam (condensate). In a membrane distillation system using the formation water brine, we first need to get the 1 kg of steam. In terms of our required 500 gpm, the system will need to first produce the equivalent of about 94 gpm of steam at as high a temperature as possible, say at least 80 - 81°C (176°F – 178°F). This can be accomplished in a flash evaporator, but will require approximately 8,500 gpm of brine. **Figure 31** illustrates a possible configuration with a sample heat and material balance. The 80.6°C brine return could also be flashed to steam, using more cooling tower water.

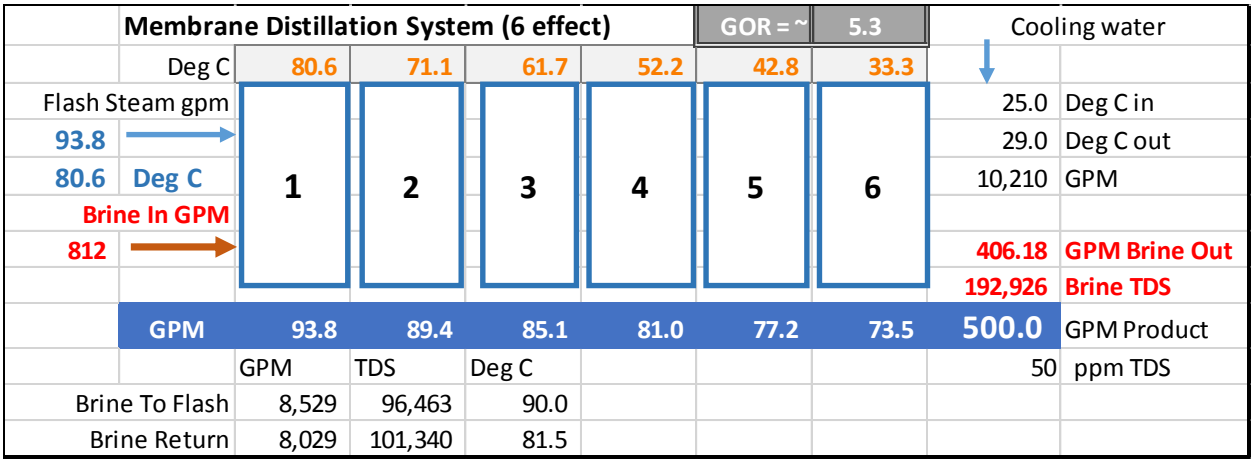

Figure 31: Membrane Distillation Thermal Balance

The treatment system highlighting the overall MD process is shown in **Figure 32**. It should be noted that the flow and mass balance is identical as that for Option 4B, the Multiple Effect Evaporator process except that, based on the MD supplier claims, no feed softening would be required. The MED could potentially have better thermal performance, although at much greater capital cost than an MD system.

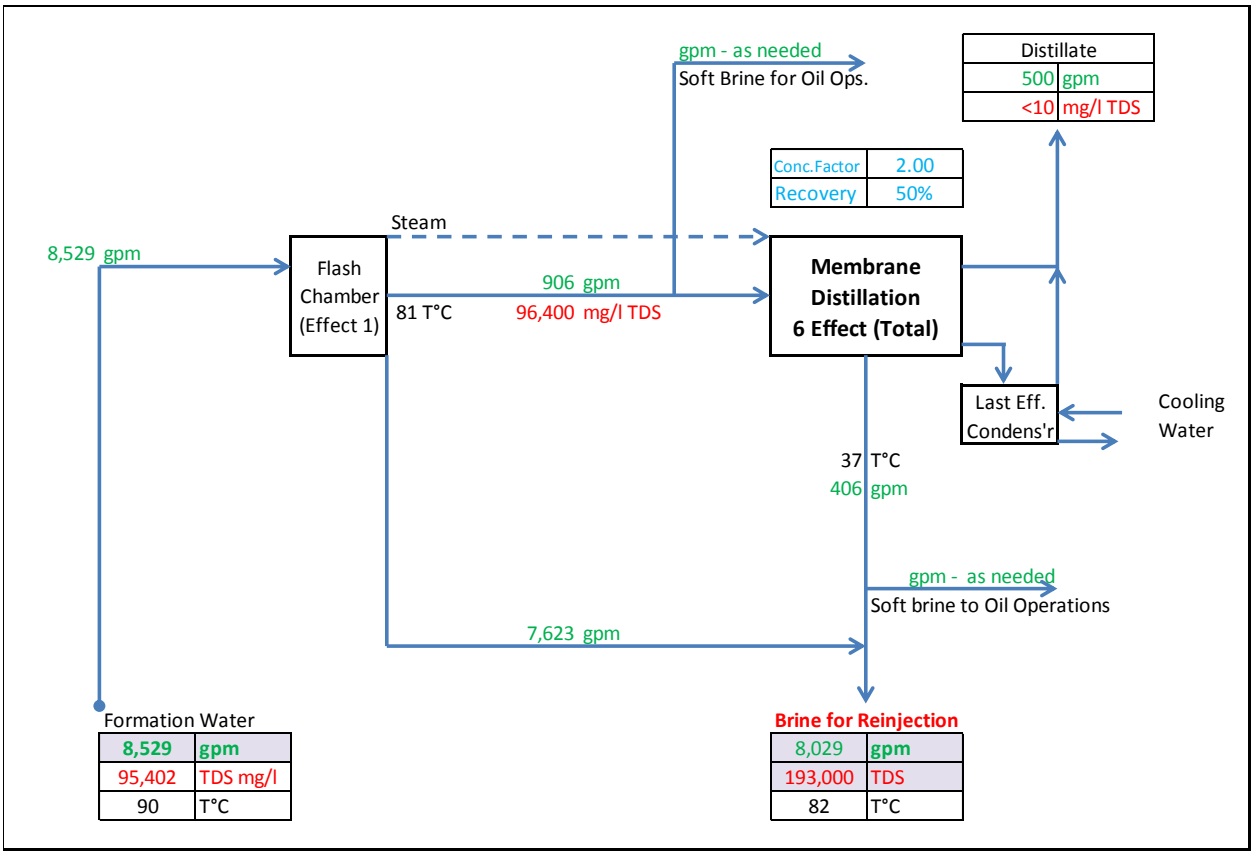

Figure 32: Option 6 – Membrane Distillation

Steam Driven MED and MD Systems

To reduce the formation water and reinjection demand, both the MED and MD systems could utilize low-pressure steam as the prime thermal driver instead of flashing the formation water. Conceivably, if located close to the station boiler and turbines, a steam takeoff from the feed preheaters could be used. The required rate would be about 60,000 lbs/hr of 12-15 psia steam. The total formation water requirement is then set by the recovery of the system, which we had set at 50% for the MD.

The thermal and mass balance of using supplementary plant steam is illustrated in **Figure 33**. As previously noted, the MED and MD processes share the same thermodynamic platform and differ only in the physical process of distillate generation.

Unless the supplementary steam is truly waste or low-value steam, this approach will most likely not be competitive with the MVR Evaporator process. Taking steam from the feed preheaters or from the turbine exhaust will reduce the energy conversion efficiency in the turbine and lead to a higher heat rate in the power station.

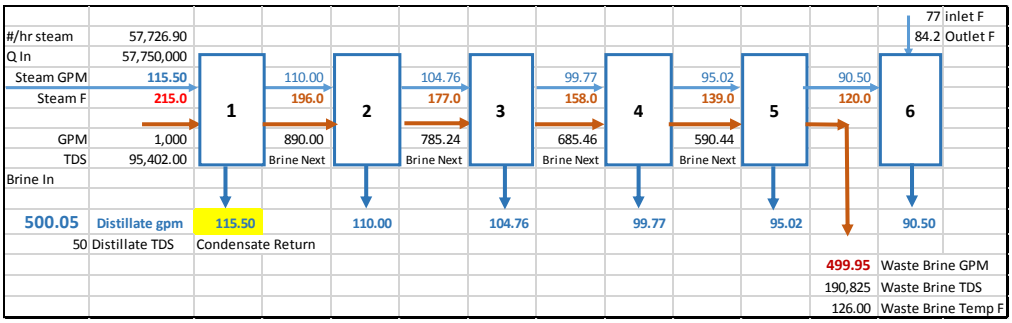

Figure 33: Steam Driven MED and MD Systems

MD Discussion

MD is an interesting option. Although in reality it is an evaporative process, the membrane provides some advantages to traditional multi effect distillation (MED) processes. The membranes are hydrophobic and allow only vapor to pass through, automatically rejecting salts. This apparently conveys some antiscaling and antifouling properties to the process not seen with heat transfer surfaces or conventional membranes which pass water. In addition, because this is a thermal process, the boiling point rise, rather than osmotic pressure is important. Higher BPR can be overcome by simply using a bigger temperature differential.

We have seen above that using formation water as the MD (or MED) heat source requires substantial formation water flow rates, making the economics of the MD plant rather poor in comparison to MVR and conventional membranes. However, if the MD system could be supplied with low grade waste heat, then the economics change substantially as the CAPEX of a MD plant should be significantly less than an equivalent MVR system. With waste heat, the OPEX of the MD will also be less than conventional membranes or MVR systems.

Waste heat could conceivably be provided by turbine exhaust steam from one of the power station turbines, or from a purpose built steam turbine. Consider that our 500 gpm requirement could be met with a single, nominal 25 MW steam turbine exhaust, at say about 50°C to 54°C (120 °F to 130 °F), using a single effect MD system or a 10 - 15 nominal MW turbine exhaust with a 2 effect MD system. The turbine exhaust needs to be set for non-condensing operation at about 2 psia. This means that the overall efficiency of the turbine, compared to a typical turbine condensing at 1 psia, is reduced. An example of this turbine performance is shown in **Table 6**.

Table 6: Nominal Turbine Performance

Nominal 12 MW Turbine		
Shaft Power	MW	10.4
Exit Temperature	F / C	126 / 52.2
Steam Flow	Lb/hr	135,000 (270 gpm)
Steam Exit Enthalpy	Btu/lb	1,111.7
Heat rate (nominal)	Btu/kWh	12.773
MD System, 2 effects	gpm	500
Cooling required	MMBtu/hr	135 / 11,250 tonnes

The advantage of this approach is that some 10-12 MW of additional power is generated. The 52 °C (126 °F) exit temperature provides for about 22°C (40°F) for 2 effects. If necessary, the turbine could be specified at higher exit temperature.

The MD process can be confirmed at various temperature and recovery ranges during the pilot testing phase, and the economics of using waste heat can be further refined during this phase. Testing of at least a 2 effect system should be demonstrated and the maximum achievable recovery verified.

Electro Coagulation (EC)

Electro Coagulation (EC) may be considered as a potential process to replace or to supplement the softening and or metals removal and turbidity reduction step in any of the above-described options requiring softening pretreatment.

EC consists of a series of cells, immersed in the process water, that are subjected to an electric current. This action destabilizes suspended, emulsified, or dissolved components by adding metal salts that neutralize and cause agglomeration of the charged colloids in the water. These same additives are typically added to chemical softening or clarification processes in the form of solid or dissolved metal salts.

The EC sacrificial electrodes cause charged coagulants to be introduced into the water. Additionally, minute hydrogen gas bubbles are formed at the electrodes that help in the separation process. The charged particulates serve to coagulate and supposedly introduce chemical changes to the impurities, thereby aiding in the agglomeration and separation. The minute gas bubbles act as an induced gas floating device (IGF) and help in the separation of the pollutants from the liquid bulk. Once formed, the separated material must still be removed in a clarifier or by other means, including multimedia filtration or ultra-filtration.

The EC's sacrificial electrodes can be in the form of parallel plates or of other configurations, and be made of various metals that are selected to optimize the removal process. The two most common electrode materials are iron and aluminum. Metal ions split off and are sacrificed into the liquid medium in accordance with Faraday's Law and form metal oxides. The electrodes are, therefore, part of the consumables of the EC treatment. There is not much hard EC data available, but the evidence is that some of the industries claims are true. Side-by-side pictures of

samples show a very murky feed water transformed after treatment into a pristine water of very low turbidity.

The reason for inclusion in this technology review is that, depending on performance, EC may be able to be used in place of or as a supplement to the front-end formation water treatment for processes, such as membrane separation. Testing, however, will be needed to confirm or demonstrate that the scale tendencies in a downstream process can be reduced using this technology.

SCADA Operations During Pilot Testing

It is apparent that the nation as a whole could benefit from creating reliable, ultra-secure methods of accessing data remotely from SCADA systems. Currently SCADA systems at sensitive installations are generally disconnected from direct internet access, meaning that remote access to real time data, and especially control functions are, of necessity, via private network connections. These are expensive and may not always be private.

As a consequence, developers are working to create a means to access SCADA systems with inherently safe methods, using both hardware and software. As part of the pilot testing platform, we suggest to provide a platform for vendors to demonstrate and test such methods with the SCADA control systems, which can then be used at the test sites.

To provide this test platform a prototypical SCADA system can be created with separate PLC's and MMI software, which mimics the actual systems in near real time.

G. Economic Evaluations and Comparisons

Presentation of Economics of Options:

To judge the merits of the various RSU treatment options described in the previous section, their economic impact on the overall project picture must be included in the evaluation. The analysis must address not only the capital and operating costs of the treatment systems, but must also include the supporting structure, as the cost of the formation and reinjection wells may be significant, if not overwhelming. A summary of well parameters and costs are listed in **Table 7**. The economics of the overall treatment system picture is presented in **Table 8** and will be discussed later.

In costing the formation and injection wells, it is assumed that the maximum capacity for both the formation water and the reinjection wells is 150 gpm per individual well. The capacity of either will, therefore, be costed in 150 gpm increments, i.e., the total capacity needed (in gpm) divided by 150. The total number of wells column in **Table 8** encompasses the formation and reinjection wells.

A comparison of the CAPEX of the formation water treatment systems alone without the influence of the wells is presented in **Table 9**. This provides a perspective in case the installation costs for the wells can somehow be reduced by use of existing wells or other means.

Table 7: Assumption of Well Costs

Parameter	Variable	Units	Comment
Maximum Formation Well Capacity	150	*gpm*	per well
Maximum Reinjection Well Capacity	150	*gpm*	per well
CAPEX per Well (Formation or Reinjection)	$3,000,000	*$*	per well
Formation Well Draw Depth	5,000	*ft*	
Reinjection Pressure	500	*bar*	
Total Formation Water Removal Rate	500	*gpm*	
Operating Days per Year	350	*d/yr*	
Electric Power Costs	$0.10	*$/kWh*	

Table 8: Economic Comparison of Various Treatment Options

Assump-tions:	Max Well Capacity (each well)	*150*	*gpm*			
	CAPEX for each well	*3,000,000*	*$*			
	Form Well Draw Depth	*5,000*	*ft*			
	Reinjection Pressure	500	psi			
	Form. H2O Removed	500	gpm			
	Power Cost	$0.10	$/kWh			
Option	**Teatment Process**	**Form. H20**	**Injection**	Total	Total Installed	NPV
		Well	Well	No of	CAPEX	20 years
		gpm	*gpm*	Wells		10% Interest
By Order of Presentation						
1A	Dedicated Cooling Tower	5,000	4,500	63	$196,000,000	$212,870,000
1B	Direct Contact Flash	6,250	5,750	80	$244,000,000	$263,130,000
1C	Flash Evap w/Surface Cond'nsr	6,250	5,750	80	$244,000,000	$263,130,000
2	Nanofiltration (NF) Only	1,000	500	10	$39,985,574	$49,550,000
3	NF + RO	2,268	1,722	27	$105,161,298	$126,970,000
4A	MVR Evaporator	802	286	7	$52,599,040	$66,680,000
4B	MED Evaporator - no outside E	8,529	8,029	110	$364,185,330	$383,170,000
5	MVR Evaporator + Crystallizer	510	0	3	$78,859,200	$97,760,000
6	Mem. Distillation - no outside E	8,529	8,029	110	$343,040,000	$362,030,000
Sort Options by NPV						
2	Nanofiltration (NF) Only	1,000	500	10	$39,985,574	$49,550,000
4A	MVR Evaporator	802	286	7	$52,599,040	$66,680,000
5	MVR Evaporator + Crystallizer	510	0	3	$78,859,200	$97,760,000
3	NF + RO	2,268	1,722	27	$105,161,298	$126,970,000
1A	Dedicated Cooling Tower	5,000	4,500	63	$196,000,000	$212,870,000
1B	Direct Contact Flash	6,250	5,750	80	$244,000,000	$263,130,000
1C	Flash Evap w/Surface Cond'nsr	6,250	5,750	80	$244,000,000	$263,130,000
6	Mem. Distillation - no outside E	8,529	8,029	110	$343,040,000	$362,030,000
4B	MED Evaporator - no outside E	8,529	8,029	110	$364,185,330	$383,170,000
Sort by Total Installed CAPEX (Well + WTS)						
2	Nanofiltration (NF) Only	1,000	500	10	$39,985,574	$49,550,000
4A	MVR Evaporator	802	286	7	$52,599,040	$66,680,000
5	MVR Evaporator + Crystallizer	510	0	3	$78,859,200	$97,760,000
3	NF + RO	2,268	1,722	27	$105,161,298	$126,970,000
1A	Dedicated Cooling Tower	5,000	4,500	63	$196,000,000	$212,870,000
1B	Direct Contact Flash	6,250	5,750	80	$244,000,000	$263,130,000
1C	Flash Evap w/Surface Cond'nsr	6,250	5,750	80	$244,000,000	$263,130,000
6	Mem. Distillation - no outside E	8,529	8,029	110	$343,040,000	$362,030,000
4B	MED Evaporator - no outside E	8,529	8,029	110	$364,185,330	$383,170,000

Table 9: Estimated CAPEX of the Installed Water Treatment Systems

Assump-tions:	Max Well Capacity (each well)	*150*
	CAPEX for each well	*3,000,000*
	Form Well Draw Depth	*5,000*
	Reinjection Pressure	500
	Form. H2O Removed	500
	Power Cost	$0.10
Option	**Teatment Process**	WTS Installed CAPEX
Sort by WTS CAPEX		
1B	Direct Contact Flash	$4,000,000
1C	Flash Evap w/Surface Cond'nsr	$4,000,000
1A	Dedicated Cooling Tower	$6,000,000
2	Nanofiltration (NF) Only	$9,985,574
6	Mem. Distillation - no outside E	$11,880,000
3	NF + RO	$25,361,298
4A	MVR Evaporator	$30,839,040
4B	MED Evaporator - no outside E	$33,025,330
5	MVR Evaporator + Crystallizer	$68,659,200

H. Discussion of Economic and Technical Aspects

Options 1 through 6, discussed above, each have their advantages and disadvantages, some from a technical and recovered water perspective and others from an economic perspective. The selection of the best water treatment and beneficial use scenario(s) must be found in a combination of both where the technical requirements are satisfied at the lowest overall cost. The technical merits and detriments of the various options are summarized in **Table 10**, which also lists the CAPEX and Net Present Value (NPV) estimated for each technology approach. OPEX is not included (except in the NPV calculation), because it seems to play a subordinate role in the overall economic picture. The same cost values were previously presented in detail in **Table 8**. They are included in **Table 10** for reference and clarity.

This overview paints a relatively clear picture of the technologies that should be considered prime candidates that merit further consideration.

Table 10: Technical and Economic Summary of Options 1 through 6

1C	Dedicated Cooling Tower CAPEX: $196MM NPV: $213MM	Simplest of all processes. Low risk. Easy to operate and maintain	High formation water and reinjection requirement. No net gain in water recovery
1B	Direct Contact Flash CAPEX: $244MM NPV: $263MM	Simple process. Low risk. Easy to operate and maintain. Net positive water gain during cold months	High formation water and reinjection requirement
1C	Flash Evap with Surface Condenser CAPEX: $244MM NPV: $263MM	Simple process. Low risk. Easy to operate and maintain. Net positive water gain of high-quality water	High formation water and reinjection requirement
2	Nanofiltration Only CAPEX: $42MM NPV: $52MM	Relatively simple process. Low energy demand. No presoftening required. For conventional membranes, formation waters is cooled. Use of high-temperature membranes may be possible. Moderate formation water and reinjection requirement	Results in a high-salinity permeate, only of interest if there is a demand for a softened, but high TDS brine, such as in drilling operations
3	Nanofilter + Reverse Osmosis CAPEX: $127MM NPV: $149MM	Relatively simple process. Low energy demand. Presoftening may be required. For conventional membranes, formation water is cooled. Use of high-temperature membranes may be possible. Results in relatively high-quality permeate, soft, and low turbidity	Higher formation water and reinjection requirement than NF alone
4A	MVR Evaporator CAPEX: $51MM NPV: $65MM	Low formation water and reinjection demand. Proven technology. Low risk. Produces high-quality distillate (≤10 mg/L)l No need to cool formation water	Needs front-end warm lime softening. More expensive technology in both OPEX and CAPEX compared with membrane processes. Formation water needs to be softened
4B	MED Evaporator with no energy supplement CAPEX: $364MM NPV: $383MM	Proven technology. May be able to utilize formation water heat to reduce energy demand	Needs front-end warm lime softening. Subject to the amount of supplementary steam used. May have large feed and reinjection demand. More complicated to operate than the MVR version
5	MVR Evaporator + Crystallizer CAPEX: $79MM NPV: $98MM	Lowest formation water and no reinjection demand. Proven technology. Low risk. Produces high-quality distillate (≤25 mg/). Crystallizers can be difficult to operate	The evaporator-crystallizer combination is expensive technology in both OPEX and CAPEX. Formation water needs to be softened. Approximately 260 m3/d of salt must be disposed of
6	Membrane Distillation CAPEX: $343MM NPV: $361MM	Uses multiple flash bodies. Less susceptible to scaling, may not need front end softening. Uses formation water for energy source	Unproven technology on this scale. May need softening of concentrate prior to reinjection. Otherwise, same negatives as the MED evaporator

Discussion of Economics:

Based on the given assumptions, a review of the cost summaries presented in **Table 8** shows that the formation water and brine reinjection flow volume demand has a significant impact on the CAPEX and NPV of the total installation. With the exception of Option 2 -- i.e., the scenario using only pretreatment followed by NF -- the processes with the least feed water and reinjection demand are the ones showing the most favorable economics.

Options 1: Although all three scenarios in Option 1 have the immense benefit of providing a simple, low-tech, and low-risk approach to removing the requisite amount for formation water, their high formation water and reinjection requirement translates into unacceptably high capital costs. The 3 versions of Option 1 should, therefore, not be further pursued.

Option 2: Given that Option 2 produces a very saline NF permeate as product water, which most likely has no beneficial use and would become a burden for ultimate disposal, this option is discounted.

Option 3: This option, which features the addition of RO, using the NF as a necessary pretreatment, results in an acceptable water quality that would be of beneficial use within the power plant or other. The relatively low CAPEX makes this option of interest, but it does require a high volume of formation water and brine reinjection, which results in a high total CAPEX and NPV. Although these costs are high, this membrane technology ranks third in the overall cost evaluation. For this reason, it may have enough merit to remain under consideration.

Option 4A: This option, which treats the formation water using an MVR Evaporator, appears to be the most technically advantageous of all the options and has the lowest overall CAPEX and NPV. This option is considered to be the best available approach to removing and treating the requisite amount of formation water: it consists of all technologies that have been proven in similar application, it produces the highest quality water for beneficial use, and it results in the smallest process waste residuals. The evaporator concentrate may also lend itself to lithium and possibly boron recovery.

Option 4B: The MED system, which is also an evaporation process, is less favorable unless there is an excess of low-value steam available from the associated power plant. In a version where the formation water's latent heat is used as the energy source, this option is too costly owing to its high feed water and brine disposal requirement. If supplemental steam were used, this demand would decrease, possibly even to the level required for the MVR Evaporator scenario. Use of waste or low-value steam has been discussed in power plant applications for many years but has never progressed beyond the conceptual paper stage. There are currently no MED Evaporator systems used for power plant wastewater treatment in the U.S. For the sum of these reasons, this option is not recommended.

Option 5: A crystallizer is used in conjunction with a MVR Evaporator. The big advantage offered by this approach is that it requires the least amount of formation water and has no brine to reinject. There is, however, a large amount of salt residual that must be disposed of. Compared to the MVR Evaporator only scenario, the addition of crystallizer to the process of Option 4A significant increases the capital and operating costs. Experience in the power industry and EOR

operations has shown that waste brine disposal via deep well injection, when possible and as proposed in Option 4A, is the preferred choice. Although landfill deposition of crystallizer salts is a common occurrence in power plant applications, the amount of salt generated and requiring disposal in this RSU application is significantly larger by comparison and may, aside from the costs, be a burdensome operation. Even though Option 5 consists of all proven technologies and its CAPEX and NPV rank closely behind the cheapest acceptable option, the use of a crystallizer should remain under consideration. The slurry concentrate, recirculating within the crystallizer, may also lend itself well for the recovery of lithium and possibly boron.

Option 6: This Membrane Distillation option is similar to the MED Evaporator system of Option 4B and has essentially the same advantages and disadvantages, as well as similar costs. The potential use of waste or low-value steam, described for the MED, applies here as well. The one distinction that sets it apart from the MED is that MD systems appear to be less susceptible to scaling, so that a front-end softener may not be required. If, however, auxiliary steam were to be used to minimize the formation and reinjection flows, then the MD concentrate may have to be conditioned via softening prior to reinjection. Because MD is not as proven a technology as MED in similar applications, further testing would be required to qualify it as a potential process candidate.

Because the capital costs for the formation and reinjection wells are so dominant compared with the water treatment system costs (see **Table 8**), the economic model assumptions were modified to determine a hypothetical well cost that would level the playing field for the water treatment systems. Using the economic model, it was found that the three Option 1 scenarios would be approximately equal to Option 4A (MRV Evaporator) if the formation and reinjection well costs were reduced to $400,000 per 150 gpm well. Such a low well cost number is obviously not realistic.

I. Recommended Technologies (Three Scenarios)

Based on the technical and economic factors enumerated above it is recommended that three main technologies be pursued for application in the RSU formation water treatment program. The pros and cons of all the options and the reason for selecting the three technology approaches have been illustrated.

The recommended process trains are in order of preference:

1. Option 4A: Softening pretreatment followed by evaporation in an MVR Evaporator.
2. Option 5: The same as Option 4A, but with a crystallizer added to evaporate the evaporator blowdown to dryness.
3. Option 3: Although not economically as favorable as the first two choices, this technology offers a backup and would be of more interest if the formation water and reinjection costs were found to be lower than assumed in this study.

Because Phase II of this project consists of an active demonstration program where technologies will be tested, it is recommended that some of the other technologies be included in the test program evaluation but at a lower level of effort. Such work could be in the form of laboratory or bench scale testing.

IX. ROCKY MOUNTAIN BRINE TREATMENT TEST CENTER

A. Overview

The high-temperature, high-salinity, and general "difficult to treat" characteristics of the Madison formation water will require bench and pilot demonstration testing even for what would otherwise be off-the-shelf technologies. In addition to the three selected treatment approaches, other up-and-coming technologies should also be investigated for this application. It is recommended that some of this testing be done off-site for cost and logistic reasons, while others, such as the membrane separation processes, which require large formation water volumes, be done on-site.

The formation water characteristics are unique, and it is recommended that any real demonstrations be done on the actual water. Preliminary check-out and proof-of-concept work may be accomplished using synthetic formation water if the actual water is not available in time, as will most likely be the case at the beginning of Phase II.

As discussed in the previous sections, there are a number of candidate technologies that can be considered to treat the requisite formation water and make it suitable for beneficial use. Most of these methodologies have some pretreatment requirement to meet the processing goal.

B. Pilot Testing Approach

The demonstration of the different technologies will be done on- and off-site, depending on the mobility and cost of installation for the pilot test equipment, as well as on the formation water and brine disposal volume needs. On-site vs. off-site staffing requirements and staffing costs are another factor to be considered.

Because the produced water may not be available early in the project, we anticipate that some of the initial check-out, fine tuning, and proof-of-concept work at the beginning of Phase II will be done at off-site laboratories using synthetic formation water. This work will then be followed by using the limited amounts of actual formation water that should be available from the monitoring well, which is scheduled to be installed at the beginning of Phase II.

C. Technology Selection for Pilot Testing

The main technologies recommended for pilot testing and demonstration are:

1. Evaporation
2. Crystallization of evaporator concentrate
3. Nanofiltration using conventional temperature membranes
4. Nanofiltration followed by Reverse Osmosis using conventional temperature membranes

In addition to the above, the following pretreatment processes will also be bench and pilot tested, as they are anticipated to be an integral part of the overall treatment scheme:

1. Flash evaporation and formation water cooling
2. Lime softening for hardness, alkalinity, and silica reduction
3. Hot lime softening for hardness, alkalinity, and silica reduction
4. Electro Coagulation as a possible substitute for the softening process

Other technologies that should be investigated via bench testing but not necessarily pilot tested include:

1. Use of high-temperature Nanofiltration membranes
2. Use of high-temperature Reverse Osmosis membranes
3. Membrane Distillation

Not-yet-identified treatment processes can also be tested if such processes are later identified and show merit.

D. Bench and Pilot Testing Venues

Analytical Laboratory:

Formation and process water streams will be chemically analyzed on a regular basis throughout the Phase II testing interval. This work will be done at an analytical laboratory using industry standard procedures. It is anticipated that some, if not all, of this work will be done at the University of Wyoming's analytical laboratory with some samples sent to an accredited laboratory for verification.

Off-site Bench Testing and Analytical Laboratories:

It is envisioned that much of the preliminary work will be done at the University of Wyoming's Center of Excellence in Produced Water Management (CEPWM) Laboratories, which is currently headed by Jonathan A. Brant, P.E., Ph.D. Other venues will also be considered.

The University of Wyoming facility has the equipment necessary to conduct softening bench testing as well as membrane separation processing. Their current Ultra- and Nanofilter and Reverse Osmosis test unit can be used for both ambient and high-temperature processing. The latter will require some modifications of its components to make it suitable for high-temperature operations.

The glassware or bench test evaluations of flash evaporation / cooling of the hot formation water can also be carried out at this facility, most likely in conjunction with the University's analytical laboratory.

On-site Pilot Testing:

On-site testing should be done for those technologies that require a relatively high volume of formation water feed and/or need the formation water to be in an "as is" condition as it exits the well. The latter can be important to some processes, such as flashing or softening, where prior

exposure to the atmosphere and/or cooling may change the nature and concentrations of some of the components.

Technologies that require large volumes of feed are mainly the membrane separation processes like Ultra- and Nanofiltration and Reverse Osmosis. This Rocky Mountain Brine Treatment Test Center will offer the opportunity to pilot test the above and other processes on-site using "fresh" formation water.

Off-site Pilot Testing:

Off-site pilot testing is recommended for those technologies that do not require high and ongoing volumes of formation water and utilize equipment that would be costly to transport to and install at the RSU test site. The specific technologies in this category are the evaporation and crystallization processes.

Evaporator Pilot Testing

Although it is possible to ship a pilot-sized evaporator to a site, most evaporator testing of this type is conducted at laboratories operated by the main evaporator vendors.

The heart of MVR and multi-effect falling film evaporator systems are the long vertical tubes where the evaporation takes place and most of the potential processing issues, i.e., scaling and plugging occurs. A full-scale evaporator may have 1,800 or more 2-inch diameter by 60+ ft long tubes through which many thousands of gallons per minute of brine circulate as a thin falling film.

An evaporator test unit can mimic this process accurately using 1 to 3 shorter tubes featuring a falling film brine flow equal to that of a full-scale system. The amount of brine required is, therefore, relatively small, amounting to only a few gallons per hour of makeup. The total volume of feed water for testing will be 150 to 400 gpd, which can easily be trucked to the off-site facility.

Scaling or other problems typically manifest themselves relatively quickly so that a test duration of approximately three weeks should be sufficient to validate the process. Chemical analysis of the feed, distillate, and concentrate streams is part of the test procedure. Depending on the constituents, vent condensing with subsequent chemical analyses may also be conducted. Monitoring of the heat transfer value experienced will also provide important data for a full-scale design can be based.

Demonstration of the vapor recompression cycle is not considered to be necessary, as this simple thermodynamic process is based on evaporator heat transfer and boiling point rise. Both of these parameters will be part of the test data. The process demonstration and collected data will be applicable to both the MVR and MED evaporation processes. The potential of extracting such constituents as lithium and/or boron from the brine concentrate can be pursued as part of the evaporator testing.

Crystallizer Testing

The validity of crystallizer testing is typically conducted on a bench and glassware scale. The high TDS brine feed, from either evaporator concentrate generated from prior evaporator testing or from boiling down formation water to the evaporator blowdown concentration, is then further concentrated in a glassware apparatus, usually a rotary flask, to crystallize the salts to dryness. All three crystallizer process streams, i.e., the distillate, crystalline solids, and residual liquor, are subjected to detailed chemical analyses. Several test runs, often performed in parallel, are usually required to assure the test results.

Supplementary to evaluating the evaporator concentrate, the crystals formed during the crystallization testing may be subjected to redissolution to investigate to potential recovery of components for beneficial use, most likely limited to lithium and boron.

E. ROCKY MOUNTAIN BRINE TREATMENT TEST CENTER

It is envisioned that the site will have only limited access to utility connections from Jim Bridger Station, located approximately 1.2 miles away. As such, the BEST facility at the RSU – which we are calling the Rocky Mountain Brine Treatment Test Center (Rocky Mountain BTTC) will be self-sufficient, with only an electric power connection to Jim Bridger power station. Other utilities, such as service water and waste disposal, will be in the form of tanker trucks or other mobile means.

The schedule calls for a two-year testing period (BP3) for Phase II. Much of this time will be spent in developing the formation water and reinjection wells so that the actual formation water at full-flow capacity will most likely not be available until the latter part of 2017 or early 2018. As such, the test center will be designed and built in anticipation of the produced water availability for long-term testing. Upon completion of Phase II, the permanent support platform can remain active and be used for follow-on testing for this or future testing of other projects.

Basic Concept:

The Rocky Mountain BTTC will be built to accommodate various treatment processes of interest, either on a stand-alone basis or as one that is integrated with one or all of the pretreatment systems.

Aside from its high temperature and salinity, the formation water also exhibits a high hardness level and is saturated in some key components. Some treatment processes of interest may require either a reduction in brine temperature and/or softening and silica removal or meet yet undefined pretreatment requirements.

The envisioned Rocky Mountain TTC concept is that the facility will consist of a:

- Permanent pilot testing support system
- Support platforms for various technologies to be pilot tested

This arrangement will provide pretreatment of the produced water. The water can thus be supplied "as received", cooled, softened, and multimedia filtered as needed. Pretreatment can consist of none, some, or all of the above in series.

Permanent Pilot Test Support Platform:

The permanent pilot test support system is intended to provide pretreatment for Phase II testing. The installation support structure will, however, also be available for any future pilot testing at the RSU study site.

As shown in the block flow schematic of the envisioned pilot facility, displayed in **Figure 34**, the layout features a permanent platform where the water is preconditioned for the potential needs of downstream technologies and a platform where various technologies can be pilot or bench tested. The permanent platform consists of the following major components:

- Formation water feed/holding tank
- Dedicated cooling tower to supply cooling water to the formation water heat exchanger
- Formation water heat exchanger
- Conventional chemical softener/clarifier
- Chemical feed system for the softener or other
- Small sludge holding tank for clarifier purge
- Multimedia filter
- Wastewater storage tank
- Forwarding and recirculation pumps for each component as needed
- Piping that connects each unit operation
- Bypass piping around each unit operation
- Piping connections to allow treated or untreated formation water to be shipped off site
- Instrumentation and control system as needed
- Control room
- PLC and HMI
- Chemistry laboratory for field analyses

In addition to the above, the permanent Rocky Mountain BTTC will provide:

- Electric power
- MCC
- Service water
- Liquid waste disposal
- Spill containment
- Low-point wastewater and drainage sump
- Sanitary facilities
- Access roads

The formation water, which will be sourced as a slip stream from the extraction/reinjection loop of the main RSU test site, will be piped to the Rocky Mountain BTTC, where it will be housed in a feed storage tank. The piping arrangement will be provided so that the hot formation water can be routed either directly to any of the various treatment processes or to the formation water

cooler, which is at the beginning of the process train. Process flow connects will also exist to connect and bypass any one of the pretreatment systems.

Rocky Mountain BTTC Platform Utilities:

The Rocky Mountain BTTC utilities will be as follows:

- Power: 3P/480 V at least 200 KW
- Service Water: The service water, supplied by water tanks, may be pumped directly from the tankers to avoid stagnation and potential biological growth issues
- Wastewater Disposal: Drains and miscellaneous process spills will be collected in a low-point sump, which is then pumped to either to the Wastewater Collection Tank or to a waste hauler for disposal
- Wastewater Collection Tank: All process wastewater will be routed to this tank and then pumped to or trucked for blending with the reinjectate
- Plant air: An air compressor will furnish plant air. If instrument air is required, it will have to be filtered as part of the individual process skid

Pilot Test Center Site Layout and Preparation:

The test center layout will have an area of about 0.2 to 0.3 acres. It will be leveled and graveled, with access roads around its perimeter. The layout of the pilot test facility, as presently envisioned, is shown in **Figure 34**.

Concrete pads will be poured to support structures and equipment, including tanks, sumps, and testing pads as needed. Because of the extreme weather conditions at the site, test equipment and processes will be housed in shipping containers to the highest degree possible. The heated containers will obviate the need for freeze protection within these housings.

A control room and small field laboratory will be housed in a dedicated container, as will the MCC and other support items. All will be part of the permanent platform. It is expected that the technologies to be pilot tested will be brought on-site and housed in shipping containers so that only the placement and the hookups of process flow piping and utilities to make the treatment operation functional will be required. There will be space to test several technologies in parallel, subject only to the feed water needs. Process flow hookups between unit operations will be via flexible, quick-connect hoses. Where exposed to the environment, these hoses will be equipped with freeze protection.

The formation water supply to the feed water tank will be a slipstream of approximately 20 gpm taken from the formation – reinjection well loop. Depending on distance, the flow connection will be either hard or flexible piping, which will be trenched or elevated and heat traced. The site will be surrounded by access roads to provide convenient access to all equipment.

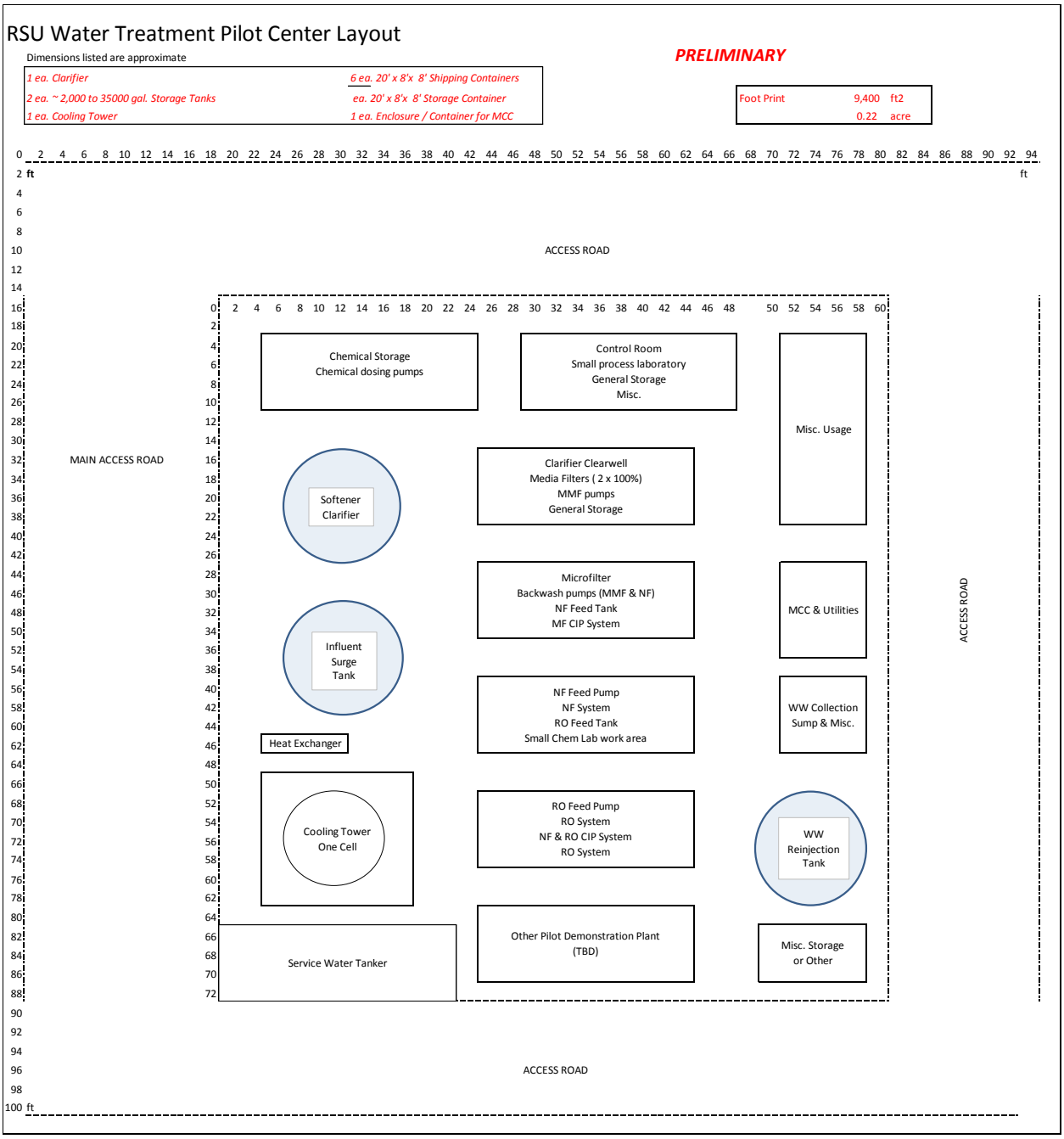

Figure 34: Rocky Mountain BTTC Layout

Pilot Test Support Platform Integration:

Permanent Pilot Test Platform

The block flow schematic displayed in **Figure 35** illustrates the general arrangement and integration of the permanent platform with the technology portion of the facility. As can be seen, the various processes of the permanent system can provide "as is", cooled, and/or softened and/or filtered water to any one of the technology pilot tests.

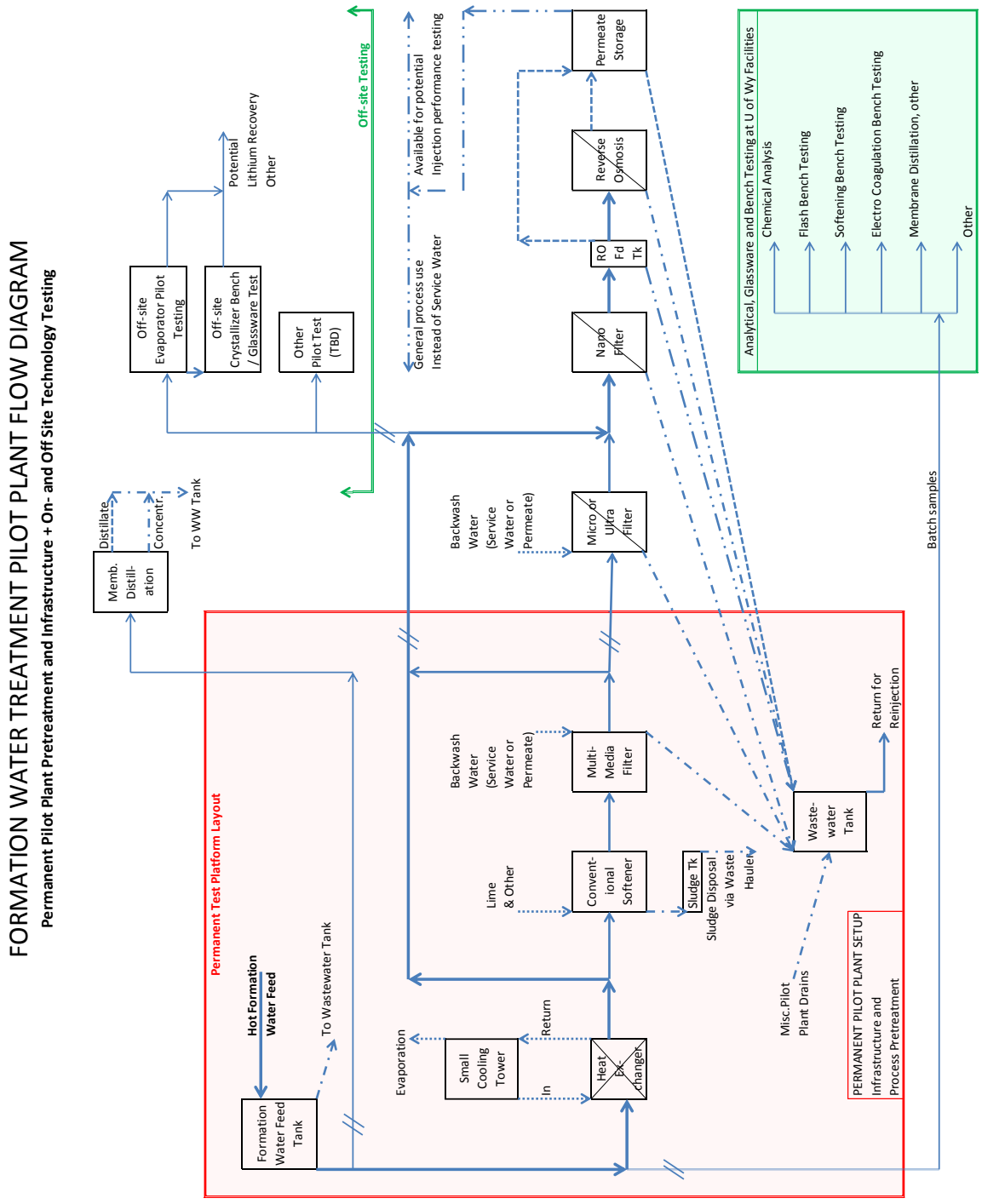

Figure 35: Flow Schematic of the Rocky Mountain BTTC

The Formation Water Feed Tank acts as a surge tank for the hot, incoming formation water. It will be sized at 3000 to 4000 gallons so that it will provide a minimum storage time of about four hours if the clarifier is operated at full capacity.

The formation water cooler is in the form of a flat plate heat exchanger, as the water is expected to be clean and particulate free. Scaling may be an issue as the water cools, although most components will become more soluble as the water is cooled. Cooling water is supplied via a single cell, dedicated cooling tower. The tower is provided because cooling water from Jim Bridger Station will not be available. Air cooling in this climate would be cost prohibitive.

The conventional softener clarifier has a capacity of 20 gpm. Hardness and silica will be reduced using lime addition. Depending on the softening performance of this high TDS water, dolomitic lime may be needed to achieve the required silica reduction, which will be determined during the softener bench testing. The reason for using a conventional rather than a warm lime softener is that use of the latter may be too complicated in a pilot testing situation, especially if operated during the cold winter months. The operating temperature is anticipated to be 35°C to 40°C and just below the RO and NF membrane temperature limitation.

Sludge from the clarifier will be blown down periodically to a small sludge holding tank or directly to a waste hauler. As the sludge volumes will be relatively small, use of a dewatering system was thought to be too labor intensive for the pilot test. A standard multimedia filter (MMF) is provided to filter out entrained clarate particles. The system is provided in a 2 x 100% configuration to allow on-line backwashing using a clean water source. The backwash will be directed to the wastewater storage tank. The pretreatment platform will have a piping arrangement that will allow the routing of process streams either in series or to bypass any one of the unit operations.

Technology Pilot Test Platform

The technologies currently identified for pilot testing are:

1. Evaporation
2. Crystallization
3. Membrane Separation
4. Membrane Distillation

For the evaporation and crystallization, the pretreatment platform will be used to soften and filter the cooled formation water, which will then be trucked to the off-site evaporator testing facility located at one of the evaporator vendors. Depending on the evaporator pilot test unit feed capacity, multiple truckloads may have to be dispatch, probably in one week intervals. The crystallization work will be done with the same water, using either evaporator concentrate or softened water that is boiled down in the vendor's laboratory.

Membrane separation will be done on-site and will consist of several runs. It is anticipated that the test sequence will initially consist of two runs using softened and unsoftened water followed by Nanofiltration only. This will allow the Nanofilter performance to be evaluated without worrying about the RO and determine if softening will be required.

A Micro or Ultrafilter will also be recommended for testing. Past experience has shown in power plant applications that the reverse osmosis performance is greatly enhanced when Micro- or Ultrafilters are used ahead of the RO. The performance increase is manifested by providing much longer run times between cleaning (CIP) of the RO membranes allowing more wastewater to be processed over time. The need for a MF or UF pretreatment will be part of the membrane system evaluation.

Once the NF processing performance has been successfully established, the testing will continue by adding the RO to the process string. It is anticipated that run duration so several weeks will be required for each of the membrane process evaluations. While most treatment systems typically prefer to operate continuously, membranes systems are more forgiving so that they can be shut down, possibly daily, assuming the proper precautions in the form of flushing and preserving the membranes ae practiced prior to shut down. Restart of the membrane system is easy and quick. Shutting down and restarting the clarifier is trickier and would require a longer startup times. Membrane Distillation can also be evaluated on site assuming that the unit can provide its own steam energy source. It is assumed that a vendor would be interested in showing such a system's performance in treating the formation water. Testing could be done using "as is", cooled and/or softened feed water. The size of such a test unit has not yet been determined.

X. GEOCHEMICAL MODELING OF FLUID EXTRACTION AND REINJECTION

A. Overview

An important issue having to do with managing the produced formation waters is mineral scaling. Fluids removed from the subsurface will be saturated with minerals present in the formation. The analysis of the saturation states of fluids from both the Weber and Madison formations (Quillinan and McLaughlin, 2013) indicates that both formation waters are slightly supersaturated with calcite and dolomite. The Weber formation is also saturated with anhydrite (CaSO4), whereas the Madison appears to be slightly undersaturated with anhydrite. Fluids obtained from wells are notoriously difficult to sample without some effects brought about by sampling, such as gas loss or mineral precipitation during transit. The observed supersaturation of carbonates could be due to reactions of the fluids with rock chips during ascent (see below), some loss of carbon dioxide, or error in pH measurement, all of which affect the calculated mineral saturation state. It is probably acceptable from these data to conclude that the Weber formation fluids are saturated with calcite and anhydrite, and that the Madison formation fluid is saturated with carbonate (it is dominantly a carbonate formation containing calcite and dolomite) and is a bit undersaturated with anhydrite. This knowledge is important because changes in temperature, degassing, and desalination of the fluids will all cause one or more of the solids to become supersaturated and precipitate, which will negatively impact fluid processing and add to the treatment cost

It was observed (Quillinan and McLaughlin, 2013) that the hydrogen sulfide contents of the well fluids significantly increased over time (**Table 11**) and that the sulfate contents decreased,

probably indicating some “souring” of the fluid due to microbial sulfate reduction. For now, we will ignore this effect in our modeling, but note that if sulfate reduction continued through the production phase it could lead to iron sulfide and other metal sulfide scaling, and of course would necessitate methods to avoid hydrogen sulfide emissions.

Species	mM	Species	mM	Species	mM
HCO3-	54	SiO2(aq)	2.19	Br-	1.8
Ca++	42	Na+	1255	Al+++	.07
Cl-	1505	Sr++	0.6	Ba++	.034
F-	0.2	SO4--	19.59	NH4+	2.9
Mg++	8.3	Fe++	0.6	Li+	13.65
K+	100	Mn++	0.15	pH = 6.43	

Table 11: Fluid composition in millimolal of Madison Formation brine from Energy Lab analysis of Dec. 3, 2012 used in GWB modeling

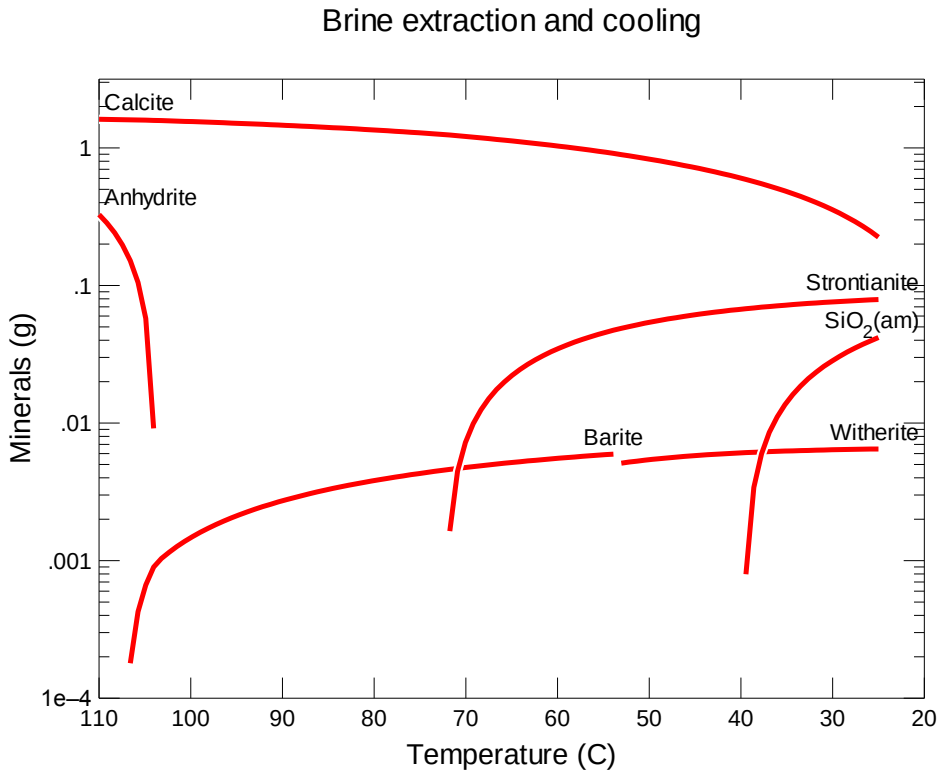

Figure 36: Simulation of cooling of Madison Formation brine. Composition of system is held constant. Mineral precipitation and dissolution is allowed. Results show that calcite is present initially at 95 C (the formation temperature) but dissolves as fluid cools. Anhydrite is always undersaturated. Several barium and strontium minerals are predicted to form in small amounts (Barite-BaSO4; Witherite-BaCO3, and Strontianite-SrCO3). Amorphous silica is also predicted to form below about 40°C

Results of geochemical modeling of brine extraction, brine processing (desalination), and brine concentrate reinjection are provided below. In each case we identify potential problem areas

having to do with mineral scaling. For brine reinjection, we identify compositional limits on brines such that mineral precipitation is predicted to not occur in the formation which could potentially cause loss of permeability.

The calculations were carried out using the GWB software package (Bethke, 1996) using a new high-temperature Pitzer data base (thermo_da0ypfR2.dat) developed by the DOE Yucca Mountain Project for modeling salt-water interactions at nuclear waste repositories. The "Pitzer" model for electrolyte solutions provides more accurate calculations of mineral solubilities and ion activities in concentrated solutions (Pitzer, 1977) than the more commonly used Debye-Hückel model.

B. Extraction of Formation Fluids

The host formation temperature is 92-95^{o}C (Quillinan and McLaughlin, 2013). Cooling the formation water to ambient will cause some minerals to get more soluble (calcite and anhydrite) and others to get less soluble (silica and most silicates). **Figure 36** above shows the calculated mineral saturations as the fluid hosted by the Madison Limestone is brought up the well bore and cools. We use the December 3, 2012 analysis of the Madison formation fluid in our modeling calculations because the Madison is the most likely formation for CO_2 storage, and the December 3, 2012 analysis is thought to be the most representative.

The simulations show that calcite is supersaturated in the fluid but that as the fluid cools the calcite will partially dissolve. This suggests the possibility that suspended limestone rock chips carried along with the fluid would partially dissolve and might be responsible for the observed calculated supersaturation of calcite at 100^{o}C. Anhydrite is calculated to be undersaturated at 95^{o}C and, along with calcite, is not expected to be a scale former during brine withdrawal. Some other phases are predicted to precipitate during cooling including barite, witherite, celestite, and amorphous silica. Although small in total mass, they could lead to scaling of the well and also of surface storage tanks. Fortunately, previous work has shown that barite is reluctant to precipitate and often will remain in solution even at supersaturation levels of 100 or more. Also, silica generally is not a problem unless the concentration is above about 140 ppm, based on experience in geothermal fluids. Our highest measured value is 127 ppm, about at the limit of where silica can be a problem. Silica anti-scalants are available that could be used if needed.

We conclude that producing the formation fluids is not likely to lead to problems involving mineral scaling. The fluids will be at or near saturation in several minerals, but not at high enough levels to get over known kinetic inhibitions to precipitation.

C. Treatment of Formation Fluids

It is in the treatment step that mineral precipitation is likely to be a problem. Desalination involves removing water and, therefore, makes a more concentrated residual brine. If the brine

starts out near saturation, it will inevitably become supersaturated as desalination proceeds. **Figure 37** shows a simulation that removes water from the Madison brine at 25°C. We assume here that only water is removed from the brine. The calculation shows that calcite (CaCO3), strontianite (SrCO3), witherite (BaCO3) and silica are predicted to form as water is first removed. Of these, silica is probably the most problematic as it is more difficult both to control and to remove. Calcite, strontianite, and witherite are all carbonates and can be controlled by acidifying the fluid to prevent their formation, or adding antiscalants designed to allow them to remain supersaturated in the solution. In addition, they are relatively easy to remove using acid. In contrast silica is more difficult to control and remove once it has formed. Antiscalants are available for silica but are used much less frequently. Silica is a more difficult scaling issue in the water treatment industry and is likely to be a concern for us moving forward.

As water removal continues, some additional minerals are predicted to form, starting with fluorite (CaF_2) at about 50% recovery, followed by anhydrite ($CaSO_4$) and finally halite (NaCl). At 50% recovery, the salinity is twice the starting salinity (18 wt %) so is beyond treatment using membranes. Thermal methods would be needed to further desalinate such fluids.

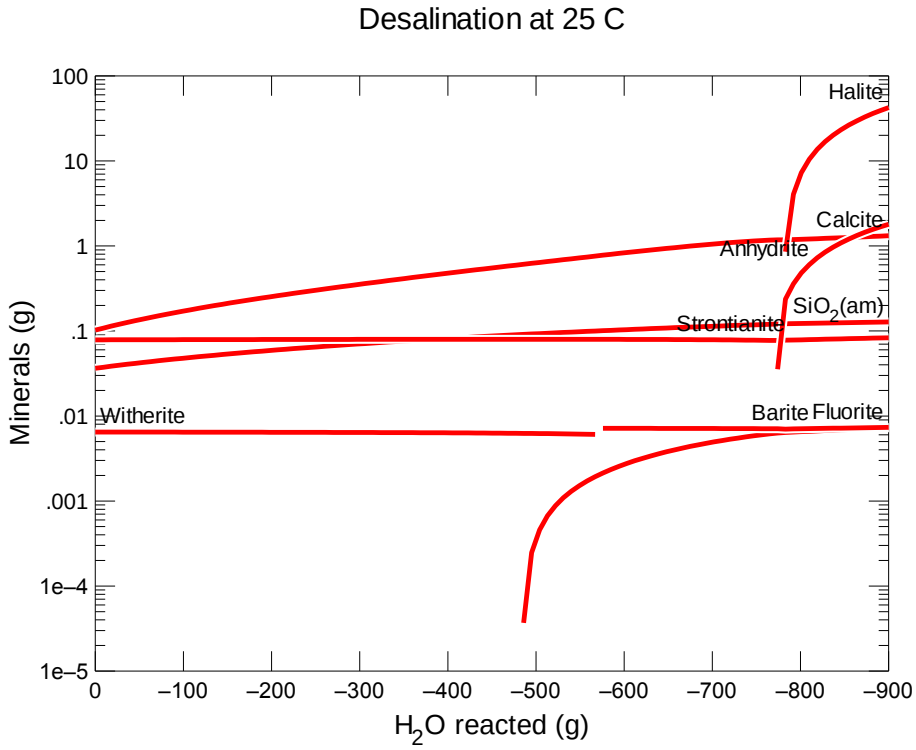

Figure 37: Simulation of removing water from Madison brine. X-axis shows grams of water removed from initial 1000g mass. Y-axis shows masses of minerals predicted to precipitate. 900 grams of water removal (far right side of diagram) corresponds to 90% water recovery.

An actual reverse osmosis system allows some salt passage into the permeate, which should be accounted for in the simulation. However, salt rejection for most reverse osmosis membranes is on the order of 98% or greater. Allowing for 2% salt passage would not be discernable in **Figure 37**.

D. Reinjection of Concentrates

It is clear that mineral scaling will be an issue for the treatment process. One way to avoid some of the problem is to use a pre-treatment method to remove some of the more insoluble components (such as calcium and silica) to avoid later scaling. Two of the commonly used methods to do this are lime softening and nanofiltration. Both selectively remove the most insoluble elements and allow the pre-treated fluid to be desalinated to a greater water recovery without scale formation. If silica needs further lowering, as may be the case for the Madison Formation brines (see below), magnesium hydroxide can be added to the lime to allow formation of less soluble magnesium silicates. The lime softening process can be tuned using pH and magnesium additives to meet most reinjection specifications.

Table 12: Calculated compositions of fluids derived from Madison brine that would be at or below saturation with all minerals at 95ºC, and therefore would not be likely to give rise to mineral scaling during reinjection. Calculated for three values of water recovery at an assumed pH of 6

Species	20% recovery		50% recovery		90% recovery	
	mM	*mg/kg*	*mM*	*mg/kg*	*mM*	*mg/kg*
Calcium	9.3	338	8.1	278	1.1	31
Magnesium	6.6	146	5.4	114	.73	12.7
Sulfate	24.5	2130	40	3230	63.2	4340
Bicarbonate	20	1100	20	1120	166	7260
Strontium	0.08	6.2	0.12	8.9	0.02	1.8
Barium	.001	0.2	.004	0.5	0.02	2.2
Silica	1.35	34	.59	28	.55	25

mg/kg = milligrams of species per kg solution

Table 12 shows the composition of fluids derived from the brine obtained from the Madison Formation that could be safely reinjected into any formation at 95ºC. They were determined by taking Madison formation fluid, recovering the indicated amount of pure water (20, 50 or 90%) while allowing mineral precipitation, and then heating the fluid back to 95ºC again while allowing mineral equilibration.

The resulting composition at 95°C is at saturation or is undersaturated with all known minerals. The composition provides a target for removal of insoluble species (hardness) during the softening or nanofiltration process. We assume in the calculation that the pH of the injected fluid is 6.0. The results are meant to provide an approximate indication of how much hardness and silica can be allowed for a reinjected brine at a given recovery. The reason for the compositional difference at the different recoveries is the salinity and also the sequence of mineral precipitates that form and are removed in the simulation. The results need to be adjusted for pH as well as possible reactions with existing brines in the subsurface, both of which are case dependent. The predicted mineral precipitates during reinjection of Madison processed brines at three different water recoveries (20, 50, and 90%) is presented in **Figure 38**.

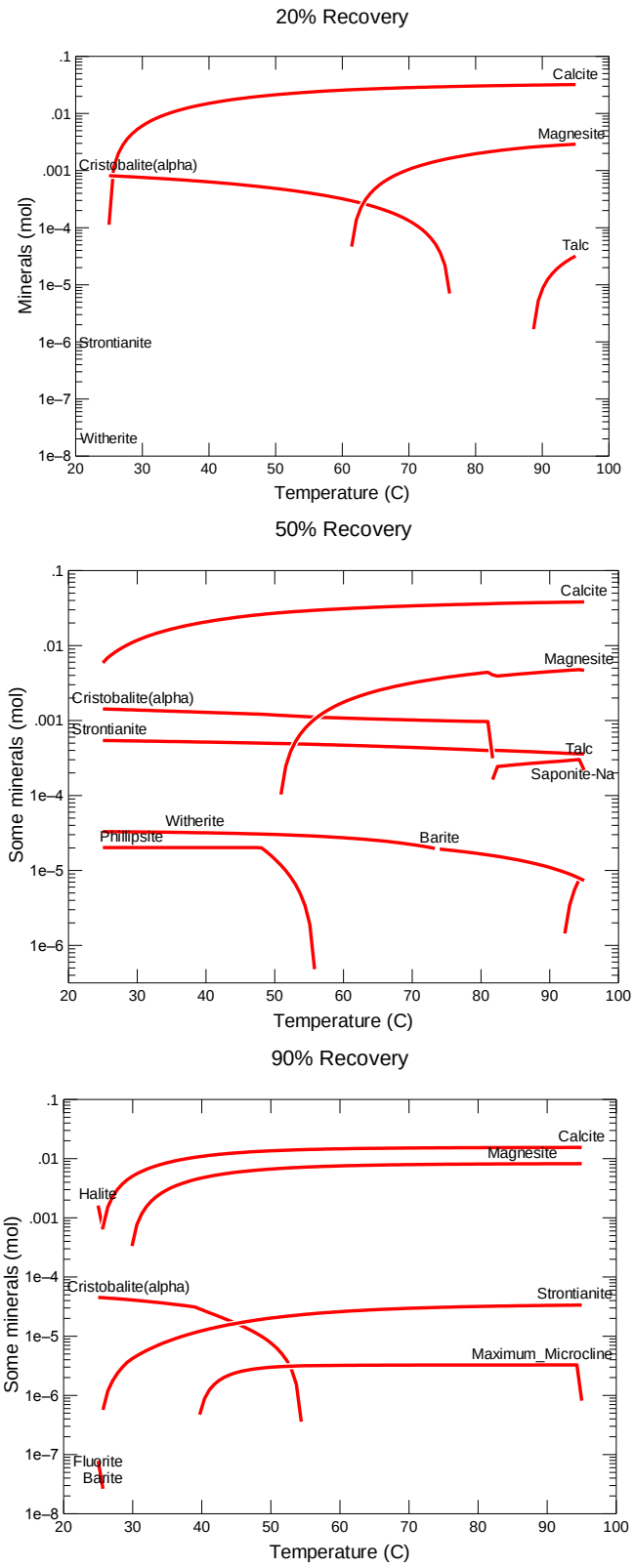

Figure 38: Predicted mineral precipitates during reinjection of Madison processed brines at three different water recoveries (20, 50, and 90%)

XI. BENEFICIAL USES OF DISPLACED AND TREATED BRINE

A. Analysis of Potential Economic Benefits from Mineral Recovery

Overview of mineral recovery:

The Madison brine contains several dissolved species which, if separated as marketable products, could offset costs associated with brine treatment. **Table 13** gives the estimated market value of possible by-products from the Madison Formation fluid based on their concentrations in the formation water. The market value of the product provides a method for sorting species based on potential cost offset, and also allows us to eliminate some species as having too small a value for further consideration. The market value is given in terms of the amount of the component in one cubic meter of formation fluid.

Table 13: Values of marketable species present in Madison brines.

Product	Species in fluid	Current Market value ($/kg)	Species mg/L (Madison)	kg/m^3 in fluid	Market value of product ($ per m^3 of formation fluid
$(NH_4)_2CO_3$	NH_3 + carbonate	1.00	47.4 (NH_3)	0.268	0.27
$B(OH)_3$	**Boron**	**1.50**	**101**	**0.578**	**0.87**
NaBr	Bromine	0.25	140	0.180	0.05
Cu	Copper	4.40	1.35	0.001	0.01
CaF_2	Calcium + Fluoride	0.30	2.8 (F^-)	0.012	0.00
Li_2CO_3	**Lithium**	**10.00**	**91.6**	**0.488**	**4.88**
MnO_2	Manganese	1.50	7.8	0.012	0.02
$MgSO_4{\cdot}7H_2O$	Magnesium + Sulfate	0.10	195 (Mg)	1.977	0.20
KCl	**Potassium**	**0.45**	**3780**	**7.210**	**3.24**
SiO_2	Silica	1.50	127	0.127	0.19
S	H_2S	0.30	81.9	0.082	0.02
			Total market value of products ($/m^3 fluid) =		**$ 9.74**

To provide a baseline for these values, a useful comparison is the cost of desalination of seawater using reverse osmosis. The cost of producing a cubic meter (one metric ton) of fresh water from two cubic meters of sea water is currently about $1. Since the Madison Formation waters are almost three times more concentrated than sea water, the treatment cost is likely to be at least triple that of sea water. Therefore, to significantly off-set this cost, the value of the extracted co-product should be at least a significant fraction of $3. As a rule of thumb at this point, we might only consider extracted products with a value of at least $1 per cubic meter of brine (30% of the minimum estimated treatment cost) to have a noticeable impact on overall treatment costs. Of those products listed in **Table 13**, only lithium and potassium are in this range, and boron high enough to also be considered.

The market value of the product includes costs associated with extraction, processing and transportation. These costs are generally a substantial fraction of the market price, and of course would not off-set costs for brine treatment, but would be additional costs. We can use lithium to get an idea of what fraction of the market price is profit vs. production cost. The lowest cost producer of lithium in the world is Sociedad Química y Minera (SQM), which produces a ton of lithium carbonate (the most common lithium commodity) for about $1500/ton (Hill, 2015). Other producers with less favorable ores or brines produce lithium carbonate in the range of $2000 to $5000/tonne. (The estimated cost of production for the Simbol Materials process used to extract lithium from Salton Sea geothermal brines was $4500/ton, which was not low enough to encourage commercialization.) Market prices for lithium carbonate have ranged from around $2000 to recently over $10,000 per ton, but have generally been around $4000-6000/ton over the last decade. These data suggest that the cost of production of lithium carbonate as a fraction of the market price is on the order of one half for a typical producer. This suggests our price off-set for lithium might be around half of the market value of the product, assuming we can extract the product with the same efficiency as the current commercial producers. Clearly the price offset will vary considerably from product to product, with the low value products such as potash and boric acid having lower markup. But for assessing the economic value of mineral co-production, we might start with the optimistic assumption that the off-set will be as high as half of the total market value of the product.

From **Table 13** we see that the total value of all by-products sums to about $10 per cubic meter of brine. It is of interest to compare this value with the overall costs of carbon sequestration. Because of the density difference of our brine (1.05 kg/L) and liquefied carbon dioxide (~0.75 kg/L depending on storage depth) we assume that about 1.5 tonne of brine must be removed per ton of carbon dioxide to achieve volume for volume replacement. In that case the total value of extracted minerals is about $15 per tonne of carbon dioxide, and half of that (our assumed off-set) is $7.50 per tonne. This value is small but still potentially significant compared to the current estimated cost of carbon sequestration of $50 or more per ton of carbon dioxide, and especially the DOE long-term goal of $25 per tonne of carbon dioxide. The value of the by-products could potentially pay for a major fraction of the treatment cost. A more precise estimate for the value of extracted minerals is a task for Phase II of this project.

Co-extraction from a CCUS site also benefits from cost savings associated with sharing of infrastructure. Carbon storage will involve well drilling and construction of surface facilities to transport carbon dioxide and brines. Mineral extraction can take advantage of those investments and therefore will share in their costs. Whereas 100% of the costs associated with drilling wells, pumping brines, and constructing evaporation ponds associated with lithium production in the salt flats of South America are mining costs, the costs associated with lithium production from brines extracted as part of carbon sequestration are shared by both CCUS and mineral co-production.

Recovery of lithium, potassium, and boron from Madison formation waters:

In this section we compare current extraction technologies for the three candidate by-products with the set of brine treatment technologies discussed previously, with the goal of identifying those treatment technologies that produce fluids favorable for mineral extraction. For example,

thermal processing to produce a dry salt by-product will generate fluids highly enriched with lithium and potassium which may be modified at little additional cost to carry out selective extraction of lithium and potassium salts. In this section we survey how the variety of treatment technologies described above map onto known extraction technologies such that economic benefits may be derived.

Lithium:

Current lithium production and market

Most of the lithium produced in the world today is extracted from lithium-containing brines in South America, Tibet, Nevada and a few other locations (Garrett, 2004). Extraction from these shallow salt-saturated brines (at most a few hundred meters deep) is inexpensive compared to hard rock mining of lithium-rich ores such as pegmatites containing lithium-rich spodumene, and lithium-enriched clays (hectorite). Lithium contents of the brines can be as high as 1000 ppm Li. Hard-rock ores generally have between 0.5 and 2 weight percent lithium.

Lithium extraction technologies exist for both brine and hard-rock ores. Extraction from brines is very simple due to the extremely high solubility of lithium chloride. The brines are simply evaporated away. Other less soluble minerals such as halite (NaCl) and sylvite (KCl) precipitate, gradually increasing the concentration of residual lithium. This is generally carried out using solar evaporation ponds in dry climates with high evaporation rates. Once the concentration of lithium reaches about 5000 ppm, the lithium can be selectively extracted by adding sodium carbonate (soda ash) to the brine which selectively precipitates relatively pure lithium carbonate, which is much less soluble than sodium carbonate. Currently lithium carbonate is the main lithium commodity, although the battery market prefers lithium hydroxide and new lithium producers appear to be targeting $LiOH{\cdot}H_2O$ as their main product[1].

Extraction of lithium from mineral sources is more complex than that for brines, and generally involves flotation followed by dissolution of the lithium mineral concentrate in sulfuric acid. As with the brine process, the final step is to add sodium carbonate to selectively precipitate lithium carbonate, often from a lithium sulfate solution rather than lithium chloride because the mineral has been dissolved using sulfuric acid.

For both types of ores (brines and minerals), a variety of methods are used to remove species such as calcium, magnesium, sulfate, boron and others that interfere with the process and may end up as contaminants in the product, or cause precipitation of lithium-containing phases such that lithium extraction recovery is reduced. Ion exchange resins, pH adjustment, temperature swings, and other methods are used to minimize the effects of these contaminants.

[1] Almost all of the soda ash used to produce lithium carbonate in South America originates in mines in the Green River Formation in Wyoming. Transport of approximately equal tonnages of carbonate solids go in both directions, to and from South America and North America. It is therefore ironic that the first step in preparing the lithium for use in lithium batteries is to remove the carbonate by reacting with lime to make lithium hydroxide. Direct production of lithium hydroxide from a lithium chloride solution would be much more efficient in terms of overall carbon footprint.

Of particular interest to us are lithium-enriched brines in deep aquifers such as at the Salton Sea geothermal system (200-300 ppm Li) and the Smackover Formation in Arkansas (350-400 ppm Li, 2-5 km depth). Although these fluids have been targeted for extraction, as of now there are no commercial facilities in operation suggesting extraction methods remain too expensive (Evans, 2010).

The current market for lithium is about 37,000 ton Li per year. If we assume a CCUS project is developed at the RSU study site that captures all of the carbon dioxide from the Jim Bridger power station, we would need to extract and treat about 60,000 m^3 per day of brine assuming the volume of removed brine equals the volume needed for carbon dioxide storage. Over one year that volume of brine would contain about 2000 tonnes of lithium, or roughly 5% of the world's market. This is enough to be strategically important as a U.S. producer but not so much so that it strongly affects the global supply.

Extraction of lithium from Madison brines

Lithium extraction would clearly benefit from a water treatment process that produces concentrated brine as well as one which has removed contaminants such as calcium and magnesium that form insoluble carbonates and interfere with lithium carbonate precipitation. Of the processes under consideration, the option that combines softening and mechanical vapor recompression (Options 4A and 5) appears to be very well suited for co-production of lithium. In this process, the brine is first softened to remove calcium, magnesium and silica using lime, and then concentrated to the desired recovery using the MVR thermal cycle. About a 50X concentration would be needed to reach the target of 5000 ppm Li to allow extraction as lithium carbonate. At that point soda ash would be added and a crystallizer used to produce and separate the lithium carbonate product. The remaining brine would then be ready for disposal back into the formation (Option 4A) or evaporated to dryness and disposed of in a landfill (Option 5). To get to 50X concentration would require drawing off the slurry concentrate periodically and using a crystallizer to extract and dewater the solids before continuing the process.

The NF-RO process also could be used to feed a lithium extraction crystallizer. Both the NF-RO process (Option 3A) and the lime softening-NF-RO process (Option 3B) would produce a concentrated brine from which hardness (Ca and Mg) has been removed and would be suitable for further concentration to produce a lithium chloride brine. Because of the relatively large volume of brine from the NF-Ro process, a lithium selective ion exchanger (such as manganese spinel or aluminate described below) would be needed as an additional lithium concentration step. Both treatment processes Option 3 and Option 4 are also favorable for potash production, discussed in the next section.

Note that both of these possible treatment processes for lithium recovery may be negatively impacted by the boron present, and boron removal may need to be carried out prior to lithium extraction. This is commonly done using a solvent extraction step prior to soda ash addition. Boron is common in the South American brines and is generally separated and sold as an additional revenue stream.

Methods that extract lithium directly from less concentrated solutions also should be considered. Ion exchangers can be used at much lower lithium feed concentrations than the 5000 ppm needed for lithium carbonate precipitation. Besides conventional cation exchange resins based on polystyrene and polyacrylates, there are also specialty ion exchangers that could operate in a passive way to extract lithium either before desalination, or prior to brine concentrate reinjection. The most successful are based on a manganese spinel phase that is selective for lithium (Feng et al., 1992). Exchangers of this type could be used, for example, to extract lithium from an NF/RO concentrate at much lower salinity (lower recovery) than brines produced using MVR. The disadvantage is that the brines would probably need to be held in a large tank or pond to provide sufficient residence time for selective extraction. Highly selective ion exchangers tend to have slow uptake kinetics.

Another selective ion exchange substance that might be useful for lithium extraction is the aluminate layered double hydroxide (Burba and Bauman, 1990). Reacting aluminum hydroxide (gibbsite) with lithium salt solutions produces a layered structure where lithium occupies the vacant octahedral sites in the gibbsite structure. Chloride ions are held between the octahedral sheets to balance charge (opposite of clays where the interlayer sites contain cations). Because of its small ionic size, lithium is very selectively incorporated into the octahedral sites in the structure, while other ions are not taken up in significant amounts. This material is particularly attractive because lithium is removed by the exchanger only from highly saline solutions near halite saturation (probably because the lithium is less strongly hydrated). If the lithium loaded material is then placed in dilute water, it gives up lithium chloride. So unlike conventional ion exchangers, the loading-unloading cycle for lithium aluminate needs no chemicals, such as acids or bases, to regenerate the solid. The potential disadvantages are the need for relatively high temperature for uptake (90-100^{o}C), the need for the lithium feed to be in salt-saturated brines, the relative small capacity for this ion exchanger (if it is loaded or unloaded beyond certain concentration limits the structure is destroyed), and handling difficulties. The material has a texture like that of wet clay. It needs to be pelletized into some sort of solid that can be used in ion exchange columns for practical use.

The aluminate material might be useful for extracting lithium from a Madison brine that is at halite saturation (5X concentration) but not the 50X concentration needed for lithium carbonate precipitation. The aluminate could eliminate the need for further concentration of the feed, and instead the lithium product obtained from the LiCl solution removed from the aluminate in pure water. Because there is no carbonate phase necessary to extract the lithium, the LiCl solution could be directly reacted with caustic to make lithium hydroxide for batteries.

Extraction of potassium from Madison brines:

The potash market is very large compared to lithium. In 2012 the market was 51 million tonnes, or about 1000 times larger than the lithium market. Almost 90% of potash (KCl) is used to make fertilizers for agricultural use. The main commodity for potash is potassium chloride from which the other products (K_2SO_4, KNO_3, KH2PO4) are made (Garrett, 1996). As with lithium, the amount of potassium that could be extracted from Madison brine is small relative to the market. About 80,000 ton per year would be produced at the RSU study site (using the same assumptions as were made for lithium recovery). This is less than 0.2% of the global potash trade.
Most potassium is mined from evaporate deposits where it commonly occurs in an almost pure

mixture of KCl (sylvite) with halite (NaCl). It thus is inexpensive to mine and process. In most evaporate sequences found in nature, halite (NaCl) and sylvite (KCl) co-precipitate from solution during evaporation. There is very little solid solution of sodium and potassium between the two phases so that they both exist in near pure form, and the mixture commonly referred to as "sylvanite". A very inexpensive flotation technology exists for separation of halite from sylvite in sylvanite ores that is used to separate the valuable KCl from the nearly worthless NaCl.

A with lithium recovery, potash (KCl) removal from the Madison brine could be carried out as part of the MVR process. As the fluid is concentrated (water removed) it will reach halite saturation at about 5X concentration and sylvite saturation at about 15X concentration. As water removal continues past 15X concentration, halite and sylvite will continue to precipitate. The process would be stopped at about 50X concentration where lithium is now sufficiently concentrated for it to be extracted by soda ash addition. The sylvanite solid mixture would be separated from the brine and the potash recovered using the conventional flotation process. The brine would be used for lithium extraction via soda ash addition, and then either returned to the formation, or evaporated to dryness and disposed of in a landfill. As with lithium recovery, a crystallizer would need to be added to the MVR system to reach the necessary concentration factors.

The potassium extraction process would benefit from upstream removal of less soluble calcium and magnesium phases. Lime softening or nanofiltration could be used. The processes of Options 3 and 4 include both an upstream softening step and concentration of the fluid to high levels, and would integrate well with potassium and lithium recovery. Because of the low value of potash relative to lithium, it seems unlikely that passive extraction using ion exchangers on less concentrated solutions of potassium would be cost effective.

Extraction of boron from Madison brines:

As with potash, most of the world's boron is mined from evaporite deposits of boron-containing minerals. These include mainly borax (Na2B4O7.10H2O), kernite (Na2B4O7, 4H2O, colemanite (Ca2B6O11.5H2O), and sassonite (B(OH)3) (Garrett, 1998). Unlike evaporates that form from evaporation of ocean waters, boron deposits apparently form from evaporation of carbonate-rich waters and are derived from terrestrial water-rock reactions that lead to waters with high carbonate to calcium ratio (Drever, 1982). Most deposits are thought to contain additional boron derived from a geothermal source such as boron-rich hot springs.

Most of the mined boron is used in glass and ceramics, polymers, and for agricultural uses. The current market size is about 4,000,000 tonnes per year as boron. Extraction of all the boron in the Madison (assuming a full-scale CCUS site that sequesters all of the carbon dioxide from the Jim Bridger plant) would be around 2000 ton per year. Because these evaporate deposits are large in volume and fairly pure, boron is relatively inexpensive to produce (~$1.50/kg, see **Table 13**).

Much of the mining and processing of boron ores has to do with re-precipitation of boron-containing phases that is not relevant for extracting boron from brines. However, a process involving solvent extraction of boron removed from lithium brines is of interest. Boron present during precipitation of lithium carbonate will end up as an impurity in the lithium carbonate and

must be removed prior to soda ash addition. The boron can be removed using solvent extraction employing a mixture of a polyol (e.g., iso-octanol) and kerosene that will preferentially take up boron from the salt solution. This process could be used to remove boron prior to soda ash addition for concentrated Madison brines produced using MVR. Although the value of the boron would probably not be significant, it must be removed to make market-grade lithium carbonate. A purified boron product should therefore be considered as it may have value in local markets.

Summary:

The value of the mineral components in Madison brines is significant relative to the costs of processing the brines were they to be removed for carbon dioxide storage. Several of the proposed treatment methods suggested for processing the Madison brines lend themselves well to extraction of both lithium and potassium. The favored method is that of mechanical vapor recompression (MVR) which is fed with hot lime softened brine. Both lithium and potassium could be extracted from such a process using known technologies. In addition, some recently developed lithium ion exchangers may also be used for lithium removal although the process costs are more difficult to estimate because of the lack of commercial operations utilizing these technologies.

In Phase II of this project we will use compositional data from pilot testing of the brine treatment technologies to better evaluate the potential economic benefits of mineral coproduction using the technologies we have identified from existing lithium, potassium and boron mining operations.

B. Beneficial Use of Treated Formation Water

This subtask takes an in-depth look at water use in the Greater Green River Basin (GGRB). The primary purpose is to identify areas of consumptive use that could benefit from an additional water source. In this case the additional water is sourced from brine produced and treated at the RSU.

A preliminary study by CMI suggested that the RSU is geologically and geographically well-suited for CO_2 injection. (Surdam and Jiao. 2007). Subsequent work -- including high quality numerical simulations and realistic 3-D reservoir modeling -- confirmed these findings and identified pressure management as the greatest remaining obstacle to injection (Surdam, 2013). CMI proposed to overcome this challenge by producing groundwater in a 1:1 ratio with injected CO_2. The groundwater in the targeted RSU aquifers can exceed 75,000 mg/l, so any produced fluids must be treated and/or used in brine-tolerant applications. (Quillinan and McLaughlin, 2013)

CMI's solution requires that 80 million barrels of groundwater brine be produced per year, assuming an average annual injection of 15 million ton of CO_2. Over 75 years this would total 6 billion barrels of brine to be treated and sent to groundwater consumers in the GGRB. This study addresses the consumptive use opportunities for such water produced in tandem with CO_2 injection in the RSU.

Water security in the Colorado River Basin:

The Colorado River supplies water for some of the fastest growing urban and industrial areas in the western United States, but in recent decades water demand has outstripped supply. For the earliest years on record (1903-1934) the Colorado River flowed at an average rate of 22,000 ft^3/s into the Gulf of California. However subsequent development and use of Colorado River water reduced this rate to less than 4,000 ft^3/s. (J.C. Kammerer 1990.) Of the water volume lost before reaching the Gulf, 64% is used for irrigation and 32% is lost to evaporation. These factors have combined to result in a salinity exceeding 40% at the river's mouth. (Benke, Arthur C.; Cushing, Colbert E. (2005). Rivers of North America.)

The Green River, which is proximal to the RSU study site, is the single largest tributary to the Colorado River and well placed to alleviate the stressed Colorado River system. The Green River contributed an average of 6,026.25 ft^3/s to the Colorado River in 2013 (the most recent year on record). This contribution could be increased by offering consumers in the GGRB an alternative to using Green River water, leaving more water in the river for consumption downstream.
The following sections consider GGRB customers whose needs could tolerate a treated brine such as that produced in tandem with injection of CO_2 in the RSU.

Local Water Use:

Water use in the GGBR can be broken into three main categories: (1) agricultural; (2) domestic/municipal; and (3) industrial.

Agriculture Uses

Agricultural water use -- primarily for irrigation and to lesser degree watering livestock -- accounts for the vast majority of water consumption in the Greater Green River Basin. The total irrigated area in the Greater Green River Basin is estimated at 334,500 acres (Leonard Rice Engineers, Inc. 2009). **Figure 39** (modified from WWC Engineering et al., 2007) illustrates the area of lands irrigated with either surface water or groundwater in the Greater Green River Basin, and their proximity to the RSU study site.

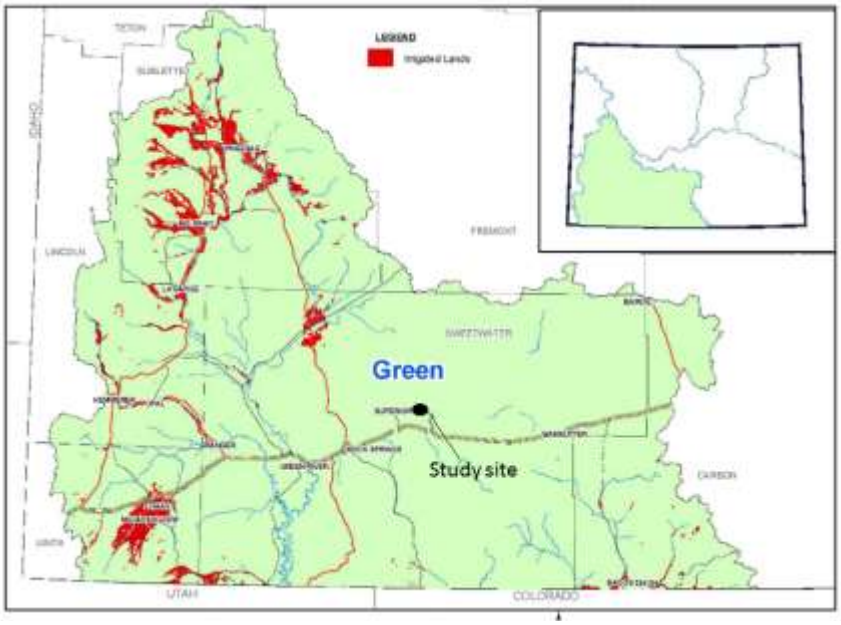

Figure 39: Irrigated lands in the Wyoming Greater Green River Basin

Water quality parameters:

Irrigation waters are generally limited in terms of two parameters: salinity and sodicity. Salinity is measured in terms of Total Dissolved Solids (TDS) whereas sodicity is measured as the Sodium Adsorption Ratio (SAR). Different plants have varying tolerance for salinity but in general, high salinity can affect germination and the emergence and growth of

seedling plants. SAR is another important measure of the suitability of water for irrigation. Irrigation with waters that are high in sodium relative to calcium and magnesium can degrade soil quality. Over time, the application of high SAR water to clay-rich soils will disperse clay particles causing swelling soils and reduced soil porosity, water infiltration, and root penetration (Hanson et al., 1999). The potential impacts of high SAR are less severe when the water is of higher salinity because a higher electrolyte concentration in soil solution reduces the effect of sodium-induced swelling of clays and associated changes in soil structure (Hoffman et al., 1990).

$$SAR = \frac{Na^{+}}{\sqrt{\frac{Ca^{2+} + Mg^{2+}}{2}}}$$

The Wyoming Department of Environmental Quality (WDEQ) provides water quality standards for beneficial use of groundwater for agriculture (Class II), and livestock (Class III; WDEQ, 2005). To meet Class II or Class III standards a water must not exceed threshold concentrations for a variety of analytes. Among these, waters meeting agriculture standards must have SAR of ≤ 8 and a TDS ≤ 2,000 mg/L, while waters meeting livestock standards may have up to 5,000 mg/L TDS (WDEQ, 2005).

Constituent	Recommended maximum contaminant level (mg/L)
Aluminum (Al)	5.0
Arsenic (As)	0.10
Beryllium (Be)	0.10
Boron (B)	0.75
Cadmium (Cd)	0.01
Chromium (Cr)	0.10
Cobalt (Co)	0.05
Copper (Cu)	0.20
Fluoride (Fl)	1.0
Iron (Fe)	5.0
Lead (Pb)	5.0
Lithium (li)	2.5
Manganese (Mn)	0.20
Molybdenum (Mo)	0.01
Nickel (Ni)	0.20
Selenium (Se)	0.02
Vanadium (V)	0.10
Zinc (Zn)	2.0

[1] Adapted from Rowe and Abdel-Magid, 1995

Table 14: Recommended MCL's for long term agricultrural use

In addition to salinity and sodicity a number of other constituents in irrigation water can be toxic to plants and/or harmful to the soil structure. **Table 14** provides recommendations for some additional constituents on the maximum contaminant levels for long term use.

The 334,500 irrigated acres within the Greater Green River Basin are entirely comprised of grass hay and alfalfa. Leonard Rice Engineers, Inc. (2009) estimate that greater than 96% of irrigation within the water district containing the RSU study site is grass hay and/or pasture, with just less than 4% devoted to alfalfa.

Previous work calculated consumptive irrigation requirements (CIR) for the GGRB (Leonard Rice Engineers, INC., 2009; and WWC Engineering et al., 2010). CIR is defined by the amount of water over and above the effective precipitation that is required from a surface or groundwater source to fully meet crop consumptive use. These studies report an average of an 11% shortfall in CIR over the entire GGRB.

Municipal and Domestic Uses

Municipal and domestic uses are a relatively small in the GGRB but are an important part of the overall water use. Municipal water uses are satisfied by public water supply systems, which are served by surface water, groundwater, or combinations thereof.

The nearest municipalities to the RSU study site include the small towns of Superior, Rock Springs, and Green River. Superior -- the nearest town to the RSU study site -- obtains water from wells completed in the Ericson Sandstone. The towns of Rock Springs and Green River belong to the Green River/Rock Springs/Sweetwater County Joint Powers Water Board, which supplies of 75% of the municipal water in the GGRB (from groundwater wells and the Green River). Peak demand for the Joint Powers Board is approximately 70.58 acre feet per day and current capacity exceeds 97 acre feet per day, indicating the sufficient supply is available for current and future municipal use. Rural domestic water use is reported to be sourced from domestic groundwater wells. Total municipal and domestic groundwater use in the Green River Basin (surface and groundwater) is 9,489 acre feet per year.

Industrial Uses

The majority of industrial water use goes to electrical power generation. Trona mining and processing make up the next most significant group. Other users such as coal, oil, gas, and uranium producers consume less than 1% of the total industrial water use in the GGRB (**Table 15; Figure 40**).

Table 15: Industrial water use in the Greater Green River Basin and the distance to the RSU study site

Facility Name	Water use (acre feet)[1]	Percentage	Distance to RSU Study Site (miles)
Jim Bridger Power Plant	28,560	50.3%	1.5
Naughton Power Plant	11,114	19.6%	93
Tronox	7,362	13.0%	53
Tata Chemicals	3,788	6.7%	50
Chiner	2,994	5.3%	46
Solvay Chemicals INC	2,234	3.9%	52
Church and Dwight	160	0.3%	50
Simplot Phosphates	605	1.1%	21

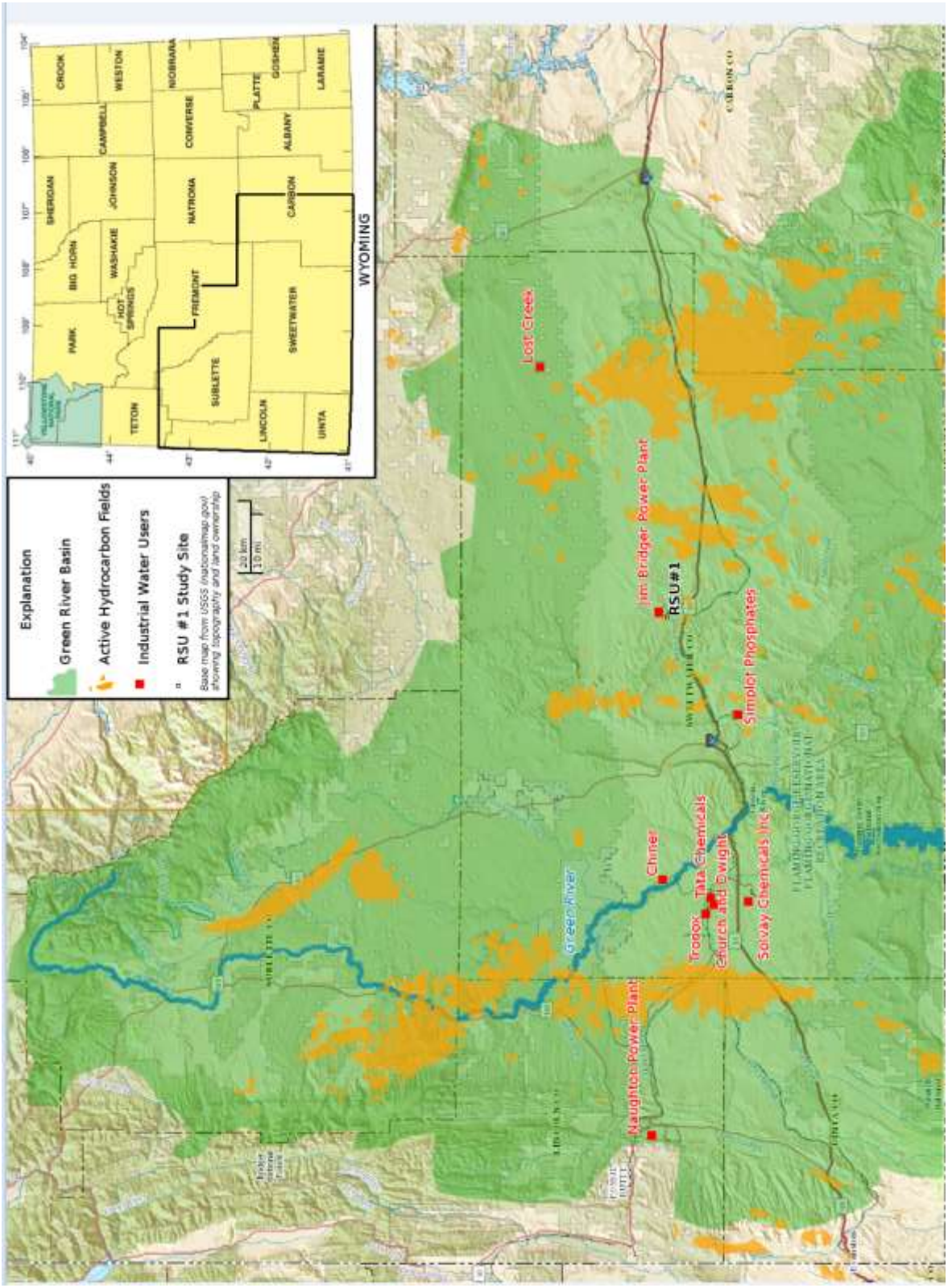

Figure 40: Location of industrial water users in the GGRB in relation to the RSU study site.

Electric Power Generation

Power plants are the largest industrial water users in the Green River Basin, accounting for approximately 70% of industrial water use. The Jim Bridger and Naughton power stations, both owned and operated by PacifiCorp, were estimated to consume approximately 47,800 acre-feet of surface water per year in 2010. Both power plants enjoy the security of storage water: PacifiCorp maintains a contract for storage water from Fontenelle Reservoir for use at the Jim Bridger power station during times of severe drought and also owns Viva Naughton Reservoir, which serves as the primary supply for the Naughton power station. In both plants, water is used to produce steam for power production and also is used in the cooling processes. The majority of the water is evaporated in the cooling towers or lost through evaporation ponds. Minor water volumes are used for dust abatement, plant washdown and domestic purposes.

Cooling water management plans balance the costs of additives, versus make-up water. This balance is adjusted by controlling the number of cycles in the cooling tower. The number of cycles describes how much the water has been concentrated by evaporation in the tower. Higher cycles require more additives, but less make-up water. Lower cycles require more make-up water, but fewer additives. High purity, potable, make-up water is conducive to high cycles. Lower quality make-up water can still be used at high cycles with the proper additives, or if it is low hardness. Make-up water up to 3,000 TDS as $CaCO_3$ can be economically managed with additives (Keister, 2001). Even higher TDS make-up water can be used if it is softened before use (Keister, 2001). Some considered techniques for water treatment the RSU study site are expected to produce soft water, which could be used as cooling tower make-up water with minimal additives.

Soda Ash Production and Other Chemical Products

The soda ash industry consumes over 29% of the industrial water used in the GGRB. The four producers of soda ash in the GGRB are Tronox, Tata Chemical, CINER Resources Corporation, and Solvay Minerals, Inc. These four companies draw water from the Green River and refine raw trona mineral into soda ash by dissolving raw trona mineral to remove impurities. All of the producers, with the exception of Solvay Minerals, Inc., have on-site power generation facilities, which consume additional amounts of water. Water is also used for dust abatement and domestic supplies. All of the water at these four facilities is discharged through cooling towers or evaporated from holding ponds.

Church and Dwight purchases soda ash from the Tata chemical plant to produce baking soda and powdered laundry detergent. Church and Dwight use approximately 160 acre feet of water from the Green River. Simplot Phosphates produces chemical fertilizer and obtains its water from the Green River/Rock Springs/Sweetwater County Joint Powers Board. In 2000 the facility used approximately 560 acre-feet of water.

Other Industrial Users (<1%)

Coal Mining. Most coal-bearing formations are highly porous and saturated with water. This makes most coal mines net water producers. However, some water is consumed for dust abatement, and pile-spray-down. These applications are especially critical because coal dust ignites easily and poses a serious fire hazard at coal mines in the GGRB.

Uranium mining. All active uranium mines in the United States, use the In Situ Recovery (ISR) method. (EIA, 2015) This method can recycle about 95% of the water used in the mining process. (Cameco, 2016) The remaining 5% is sourced from agricultural wells, domestic supplies, and rivers. This make-up water must be treated with oxygen and bicarbonate before entering the mining loop. However, if a water source already enriched in bicarbonate were available for use the water would not require treatment. Some treatment options for water produced from CCUS at the RSU study site are expected to result in water enriched in bicarbonate which would be ideal for this use.

Water is also used in the ISR process to recharge uranium-selective resin-bead columns. These columns are used to remove the uranium from the mine water and must be periodically recharged by passing salt water over them (Uranium Energy Corp, 2015). Depending on the chosen treatment options reject brine from the RSU may have appropriate chemistry and salinity for this use. If so, the nearest uranium processing plant is Lost Creek, operated by Ur-Energy, approximately 50 miles east-north-east of the RSU study site (Ur-Energy, 2015).

Oil and Gas. The most recent USGS assessment using a geology-based methodology of the southwestern Wyoming province estimated 84.6 trillion cubic feet of undiscovered natural gas, 131 million barrels of undiscovered oil, and 2.6 billion barrels of undiscovered total natural gas liquids. (Kirschbaum et al., 2002). A follow-up report concludes that "Southwestern Wyoming will continue to be one of the largest sources of natural gas in the United States." (Biewick, 2009). As oil and gas exploration continues in the region, new opportunities for reuse of waste products will become available, such as using waste brine to formulate drilling fluid. Significant opportunities for beneficial use of brines as drilling fluid exist because 80% of all drilled wells use a water-based drilling fluid (Spears and Associates, 2004). In standard drill-rig operation, the density of the fluid is increased by saturating it with salts such as calcium chloride and altering the pH to avoid clay swelling. (Schlumberger, 2016). By starting with a brine already containing some or all of the necessary salts a company could reduce the cost of formulating and mixing a drilling fluid from fresh water.

Another beneficial use for the water is as an enhanced oil recovery agent after appropriate treatment. The degree of treatment is substantially less than required for agricultural or domestic use. If successful, the treated water would become a commodity capable of providing a revenue stream to help offset pumping and treatment costs. The use of saline water with modified chemistry to increase oil recovery has been shown to work in several fields cases. (Seccombe et al. 2008, Vledder et al. 2010). This option is particularly attractive in older fields that are already undergoing waterflood enhancement. There are several of these types of oil fields in the area of the RSU that could be screened to determine if they are good candidates.

Summary of Beneficial Use:

Production of brine in tandem with CO_2 injection will remove the last major technical obstacle to CCUS in the RSU. Rather than being a waste-product, this brine can be treated and put to beneficial use in a variety of local industries. These industries benefit from a low cost alternative to drawing Green River water. This alternative water source in turn allows more water to remain in the Green River, increasing supply in the Colorado River system which is presently stretched

to capacity. A valuable opportunity exists to test CCUS techniques, reduce operating costs in a variety of industries, and also conserve water in the arid west.

XII. LIFE CYCLE ANALYSIS OF TREATMENT, MANAGEMENT STRATEGIES, AND GAP ANALYSIS FOR EXTRACTED WATER AND TREATMENT PRODUCTS AT THE RSU

A. Definition and Scope

Life cycle analysis (LCA) (**Figure 41**) was first developed to define environmental impacts of manufacturing processes. The method also has utility in defining the lifetimes of many different products or materials, the cycles and processes that will be used to create and alter these products, and the creation and disposition of wastes associated with these processes. This analysis will address processes expected, and possible cost risks that are found, in the different choices for processing, handling, and waste disposal for the handled material (extracted water from a CO_2 storage site) and the separated liquids or solids from that water. For this prefeasibility study (Phase I) the scope is simplified and qualitative; and will be expanded to a full-scale, quantitative LCA during the Phase II portion of the project when specific treatment systems will be tested. Phase I defined key components, products, and issues related to water extraction, treatment, disposition, and waste handling and disposal, including a high-level cost analysis and basic definition of cost-associated risks. We also identify knowledge gaps found during this analysis.

In this case, the primary material to be handled and processed is produced water from the RSU. Although Phase II will likely focus only on the Madison limestone formation, we present an LCA that considers both the Madison and Weber formations. The Weber water contains approximately 100,000 to 120,000 mg/L of TDS, while the Madison contains approximately 70,000 to 90,000 mg/L TDS in the form of various dissolved minerals, predominantly sodium chloride but also including divalent ions, sulfate, bicarbonate, and some valuable constituents including lithium.

The principal goal of the extraction is CO_2 storage management and plume pressure management in the injection formation. Extracted water may be a valuable resource in the region and may be useful as a water supply. Separation of fresh water from the saline water stream reduces the volume of wastewater that needs to be stored, managed, and disposed. Separation also creates a waste brine or solids stream that must be disposed, or utilized in other processes. Extraction, treatment, storage, pumping, and disposal of water can be an expensive undertaking. For example, Class I well disposal costs in the Rock Springs area is estimated at nearly $4/bbl of water (calculated from current commercial services). Understanding the cumulative effect on the system processes and costs across the end-to-end CCUS/pressure management/water treatment process will help best define treatments and will clarify appropriate and cost- effective handling, storage, and disposal methods.

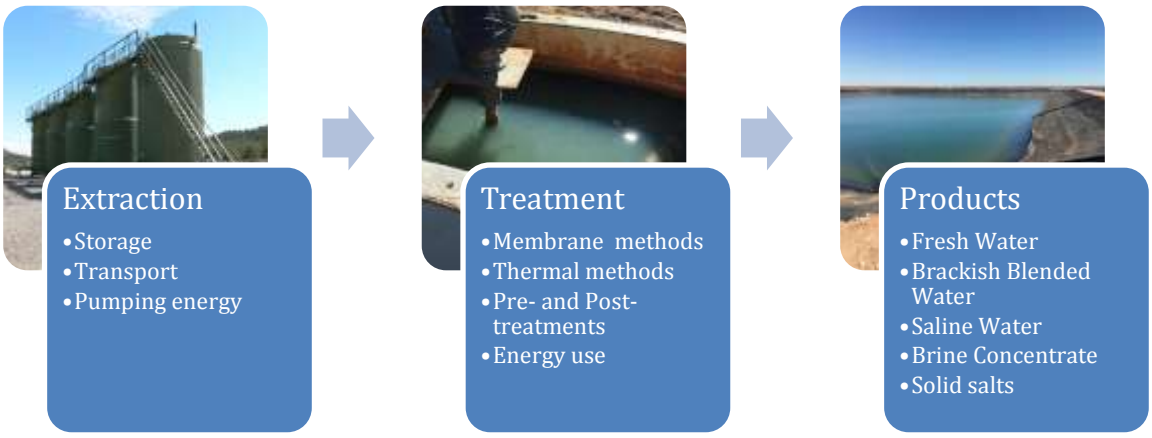

Figure 41: Life Cycle Analysis flow diagram.

B. Lifecycle Inventory and Processes

Processing/Treatment:

Potential use scenarios

The Phase I LCA focuses on extracted water from the Weber or Madison formations. **Table 16** shows average major ion values for primary constituents of interest as well as source temperature. Full water chemistry data are available in the *Appendices*.

Table 16: Selected major ions and physical properties of Madison and Weber extracted water.

Constituent or Parameter	Average Weber	Average Madison	Constituent or Parameter	Average Weber	Average Madison
Alkalinity, Total as $CaCO_3$ (mg/L)	1769.50	1,263	Dissolved inorganic carbon (mg/L)	465	539.5
Carbonate as CO_3 (mg/L)	ND	ND	Dissolved organic carbon (mg/L)	3.7	2.7
Bicarbonate as HCO_3 (mg/L)	1,677	2,073	Total organic carbon (mg/L)	3.7	2.75
Calcium (mg/L)	659	1,367	Total recoverable phenolics (mg/L)	0.385	0.375
Chloride (mg/L)	60,043	51,397	Sulfide (mg/L)	60.02	55

Constituent or Parameter	Average Weber	Average Madison	Constituent or Parameter	Average Weber	Average Madison
Fluoride (mg/L)	8.67	6	Sulfide as hydrogen sulfide (mg/L)	63.52	58
Magnesium (mg/L)	40.67	174	Chemical oxygen demand (mg/L)	5770	2495
Nitrogen, Ammonia as N (mg/L)	22.17	27	pH	7.04	6.6
Nitrogen, Nitrate+Nitrite as N (mg/L)	0.10	0.10	Total dissolved solids @ 180 C (mg/L)	105985	86642
Nitrogen, Nitrite as N (mg/L)	ND	ND	BOD (mg/L)	286.85	142.1
Phosphate	ND	ND	Sodium adsorption ratio (SAR)	388.5	191.5
Potassium (mg/L)	1,925.00	3,995	TDS calc. inorganic	113,880	89,789
Silicon (mg/L)	35.60	48	TDS measured	105,985	86,642
Sodium (mg/L)	42,469.00	31,783	TDS with HCO3 added	107,662	88,715
Strontium (mg/L)	20.00	59	Iron (mg/L)	15.75	13.61
Sulfate (mg/L)	9,316.67	2,300	Lithium (mg/L)	64.27	96.17
			Boron (mg/L)	66.45	98.1

Chemical properties, temperature, and flow rates will affect both the treatment processes to be chosen, as well as the potential use scenarios evaluated under the Beneficial Use section which describes three major user categories in the region of the storage site, including agriculture, municipal/domestic, and industrial. **Table 17** lists several specific potential users, and the quality of water that might be useful for the particular use shown, by type of water product.

Table 17: Potential uses and users of extracted water by water type, and water quality limits/criteria for each use.

Product	Use	Company/Industry/User	Key Criteria
Fresh Water	Source Supply	Jim Bridger Power Plant	Green River quality
		Naughton Power Plant	
		Tronox Mining	
		TCNA (TATA) Chemicals	
		Chiner	
		Solvay Chemicals Inc.	
		Church and Dwight	
		Simplot Phosphates	
	Rangeland restoration	Federal, state, or private landowners	Salinity SAR Metals
	Agriculture	Private landowners	Salinity SAR Metals
	Oil and Gas operations-fresh water	Private Companies	Process-specific criteria or local fresh ground water quality
	Green River Base Flow	State or Federal	Green River Quality
	Water Rights swaps	Private or Federal	Green River Quality
	Tax Credits, interstate transfers, or other beneficial uses	State	Green River Quality or use specific
	Aquifer Storage and Recovery (ASR)	State or Federal	Local ground water quality
Brackish Water-including blended waters	Process water or solution mining operations	Tronox	Site dependent
		Simplot Phosphates	Site dependent
Saline Water (may include as-is extracted water, "clean brine", or brine concentrates)	Process water	Chemical Companies	Process dependent
	Chemical Feedstocks (minerals, ions, acids, bases, etc.)	Chemical Companies	Process dependent
	Road application-deicing	State or Private Companies	NPDES or state land application criteria
	Oil and Gas operations-drilling	Private Companies	Hydraulic Fracturing or drilling water requirements. May include boron, TSS, TDS, microbes, pH
	Oil and Gas operations-weighted brine ("10 pound brine")	Private Companies	Salinity Microbes
	Refinery operations-process water	Private Companies	Salinity

Notes: TDS=total dissolved solids; TSS=total suspended solids; NPDES=National Pollutant Discharge Elimination System; SAR=sodium absorption ratio.

Of the liquid products that may be created, fresh water is the most widely useable for a variety of purposes. Regional industries depend strongly on the Green River for fresh water supplies. This high-quality water source is a benchmark for supply quality for fresh water that could be separated from the extracted water. Total dissolved solids in the Green River is approximately 250 mg/L in the Rock Springs area (http://waterplan.state.wy.us/basins/green/issues.html).

Industries are unlikely to purchase or use water of lesser quality unless there is a specific process demand, or if no negative effects can be demonstrated on their processes. However, the Green River Basin is a part of the Colorado River system. As discussed above, this river system is over-allocated, and, thus, additions of fresh water to the baseflow of the river may have environmental and other benefits for downstream users. Fresh water may be useable as a means of swapping or supplementing junior water rights, for example. The longer the fresh water supply can be maintained, the more valuable the input will be to water rights accounting in the river system. Finally, aquifer storage and recovery (ASR) may be a feasible means to store fresh water for future uses. Regional ground water quality and aquifer storage locations and capacities will need to be considered as well as permitting, local hydrology, and injection well design and construction.

Environmental and Process Limitations

Water extracted from the Rock Springs site will be handled as righted water under the permit requirements of the Wyoming State Engineers Office. Environmental or other limitations to the uses listed above include discharge regulations such as those found in National Pollutant Discharge Elimination System (NPDES) permits or state discharge and handling permits and the water rights permitting framework. Handling and disposal of waste products falls under Wyoming environmental waste disposal mechanisms and permits. The greater the extraction of useful product volumes, the less waste disposal is needed. Permits for other uses or discharges (e.g., ASR) will need to be obtained as appropriate from the appropriate Wyoming state agencies, and possibly Federal agencies.

There are three different scenarios for extracted water handling that are relevant to this analysis.

1. The initial water extraction for the Phase II BEST project pilot studies will be from an unaltered injection formation. A small water volume (up to thousands of gallons) will be extracted shortly after drilling the injection, monitoring, and/or production wells during BP2. Initial extraction will be representative of formation water quality.
2. At the beginning of BP3 water provided from the Jim Bridger power station will be injected into the storage reservoir at a rate of approximately 100 gpm (injection rate will vary though the two years of injection). Once water is being extracted at the production well (up to 50 gpm anticipated), the Jim Bridger water will be mixed with the extracted brine, including a treated stream of water. The extracted water may contain some previously injected water; thus the water chemistry of the extracted water may change during the two years of Budget Period 3. This water may or may not represent formation water chemistry for treatment purposes.
3. A higher design rate representative of a full-scale CCUS project will be developed from test results in Phase II. The brine extraction rate for a CCUS project is estimated to be

500 gpm (C. Haussman personal communication, 2/25/16). This water will be representative of the original formation, possibly with some remaining Jim Bridger water.

Because there is potential for variations in the different phases of test waters extracted, care must be taken to evaluate the most appropriate scenarios for each phase of testing. Ultimately, this LCA will take the results of the Phase II test, with the assumption of the original formation chemistry, and apply those results to a long-term plan for extraction and water treatment at the site beyond Phase II.

Goals of Treatment/Processes (treatment targets to support uses)

Treatment processes will be targeted to meet specific goals for useful products in the region. As shown in **Table 17**, four different types of water may be produced from the treatments:

(1) Depending upon treatments selected and identified local needs-fresh;
(2) A brackish blend (fresh + added saline water);
(3) Saline (as-extracted, or as "clean/softened brine"); and
(4) "Weighted" brine concentrate.

Additional products may include solids or specific minerals separated from brine concentrates or pretreatments. **Table 18** lists the solid products that may be recovered from extracted brine and possible uses for these products.

Table 18: Solid products and product uses from extracted brine and brine concentrates.

Product	User	Criteria
Road salt	States, local govt., private companies	Metals, water content
Salt for chemical processes	Private companies	Metals, water content
Lithium salts	Private companies	Concentration in source water, other metal impurities
Potassium	Private companies	Metals content of brine/salts
Magnesium	Private companies	Metals content of brine/salts

*Note that for **Tables 17** and **18**, potential uses and users are identified. Actual presence of a market and transportation feasibility will be verified in Phase II (BP2).*

Transportation and Storage Scenarios

A simple transport and storage model is shown in **Figure 42**. Distances X1, X2, and X3 correspond to distances between the extracted water source and the treatment plant, the treatment plant to the point of use of the finished water product, and from the treatment plant to the point of waste disposal (primarily, liquid waste concentrate). Transportation methods will include truck transportation (sole transport method for Phase II) or pipelines (temporary or permanent, used for analysis of a full scale project). Storage methods depend upon permit requirements, volumes to be stored, handling requirements, and the length of time of storage needed (permit dependent), and include either tanks or ponds. Solid waste transport may fall under distance leg X3 with transport being performed by truck. Modeling (CO_2-PENS WTM) will evaluate the feasibility of transportation of treated water to various points of use on a cost basis (Sullivan Graham, Chu et al. 2015).

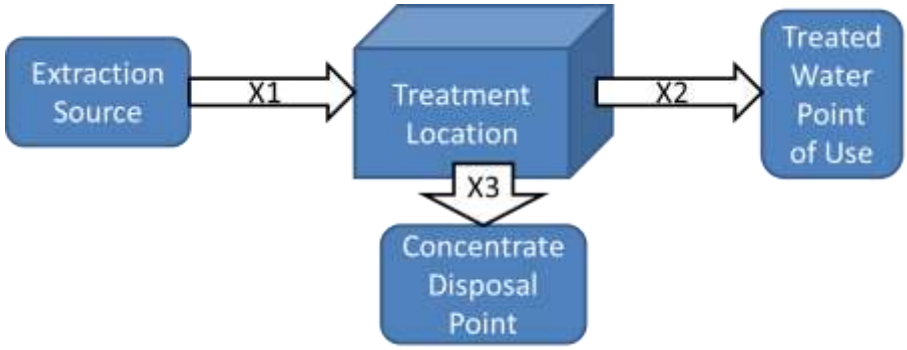

Figure 42: Simple transportation model

Product Life:

Clean water

One scenario for product life is that for treatment of extracted water with a resulting fresh water finished product (TDS of 250 mg/L or less). Fresh water has the greatest number of options for use. This option requires the most extensive treatment process to reduce the dissolved solids to compete with Green River water quality criteria. Consistency of flow volumes and quantity of production will be important for potential users and may be a potential system goal or target. The larger the flow stream, and the more consistent and long-lived the production operation, the less risk occurs for the user. If risks to the Green River water supply exist (e.g., drought, junior water rights suspensions, calls on allocations) then the presence of an alternate fresh water supply will be an advantage to local fresh water users. Transportation to potential users may be a limiting factor for fresh water and will impact costs.

C. Blended water:

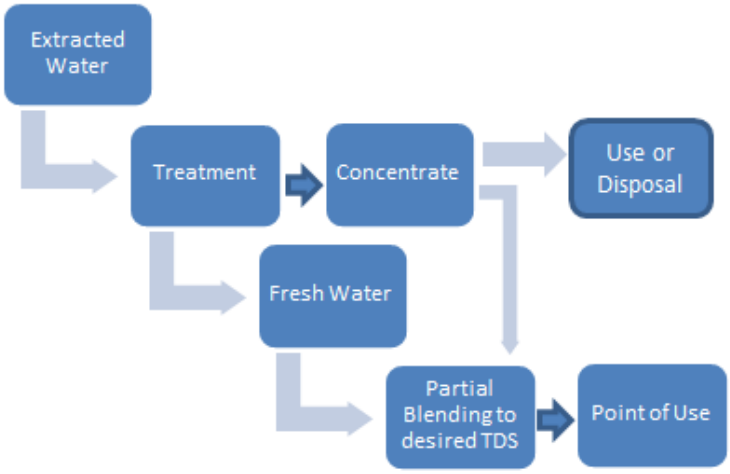

Brackish or blended water (brine plus fresh) that meets criteria for specific uses may be a product option for this treatment facility. This water may vary from 1,000-10,000 mg/L TDS or greater. Brackish water may be a product of a less-complete salt removal process (e.g. hot membrane system) or a product of blending of very clean RO or thermal product water with untreated saline water influent. This option is dependent upon finding a user who may be able to utilize brackish water instead of fresh water in their operations. For example, potash mining can use brackish water for solution mining operations. Other local mining or chemical operations may be able to use blended brackish water as a substitute for fresh water from the Green River or ground waters. Brackish water may be an option for thermoelectric cooling. Because local users frequently source fresh process water from the Green River, the substitution of brackish water will require evaluation of their system processes and acceptance of perceived lower-quality water. However, an alternate water source may create advantages in times of fresh water shortages or limits on river withdrawals.

Brine Products

Clean brine: "Clean brine" implies brine that has had most of the TDS and divalent scale-forming mineral components removed (softened). Oil and gas operations can use this brine readily in hydraulic fracturing and some drilling operations, where the brine is a useful substitute for local fresh or brackish ground water or surface water, particularly in times of drought or other shortage situations. Large quantities of brine >1-10 million gallons are usually needed for hydraulic fracturing operations over short periods of time (days).

"Ten Pound" brine: Ten pound or "weighted brine" is a product used in drilling and completion operations by oil and gas companies. Weighted brine is used to increase drilling fluid density to control high down-well gas pressures in boreholes during drilling and completions, and to minimize dissolution when drilling through salt strata. It is a valuable product that is derived from RO or thermal brine concentrates.

Road application brine: Brine may be useful as a deicing or road application product in winter months. Local market conditions will dictate the feasibility of use of this product.

Brine as a chemical feedstock: Brines have applications for the chemical industry as a feedstock for chemical production. About 45% of salt produced in the U.S. is utilized in the chemical industry (USGS, 2000; http://minerals.usgs.gov/minerals/pubs/commodity/salt/salt00.pdf). Acid and base production utilizes brines as do other chemical processes. Shipping of brine offsite may be a limiting cost factor and competition with other brine or salt producers may reduce the value of this product.

Concentrate reject

Rejected concentrate from ultrafiltration, nanofiltration, and reverse osmosis membrane filtration may be useful as a brine product (see "ten-pound brine", above), may need further treatment (e.g., via a crystallizer to extract additional water) and will need to be disposed if a product market is not found. Primary disposal options include evaporation ponds, freeze-thaw ponds, and reinjection via Class II wells (RCRA-exempt oil and gas wastes) or Class I (non-exempt hazardous and other wastes) wells. For the Phase II pilot testing, disposal will occur via the injection well that is a proxy for CO_2 disposal wells. For a full-scale site operation, Class I well disposal, and possibly Class II disposal, is the most feasible option based on the known regulatory framework for the extracted water. For the larger volumes of concentrate reject to be produced from a full-scale operation, a cost-benefit and permit analysis will be needed to determine the most feasible disposal options. A cost of $\$23/m^3$ was quoted at the time of this report from a local Class I well disposal facility. Exploring other, less costly methods of disposing (or eliminating) brine concentrate is a goal of this study.

Solid Products

Brine solids: Concentrated solids from thermal treatment or zero-liquid-discharge (crystallizer) processes will require disposition if created in the treatment process. These solids will be composed primarily of sodium chloride by weight. Determination of hazardous constituent concentrations or the presence of TENORM (technologically-enhanced naturally-occurring radioactive material) should be evaluated as required by the disposal facility or permit. Water content should be evaluated by paint filter testing prior to disposal if required by the disposal facility or permit.

Other solid wastes that will be generated include lime solids, coagulated solids, and spent filters. These are discussed below.

System Energy:

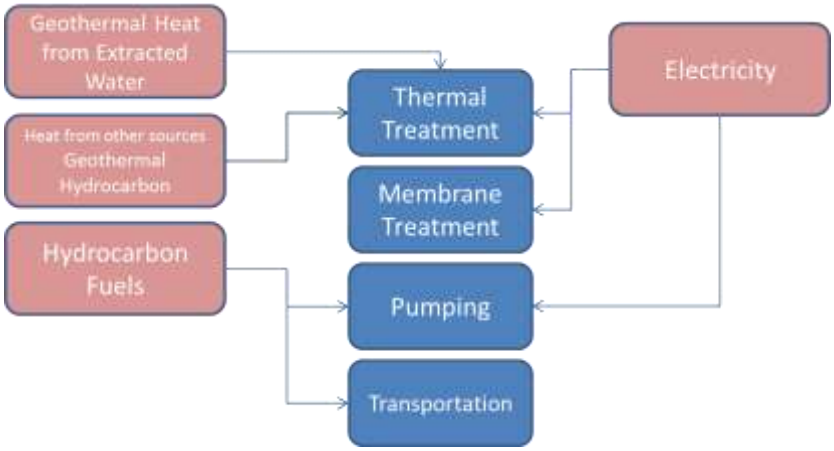

Figure 43: Potential energy sources for site operations.

Figure 43 shows sources of energy for different uses at the site. Energy could be derived from offsite generated electricity, heat from the extracted water, heat from other sources (e.g., hydrocarbon combustion, local power plant heat) or hydrocarbon fuels (gas, diesel). **Figure 44** shows where these energy sources will be used, either for process, transport, or material subsystems. A site objective is therefore to reduce/avert the use of CO_2-emitting energy sources whenever possible. For example, there is opportunity for energy recovery from gravity flow, and pressure recovery from membrane treatment systems with proper system design. This is one of the advantages of a field demonstration site, where opportunities for low/no carbon energy will present themselves as operations are developed.

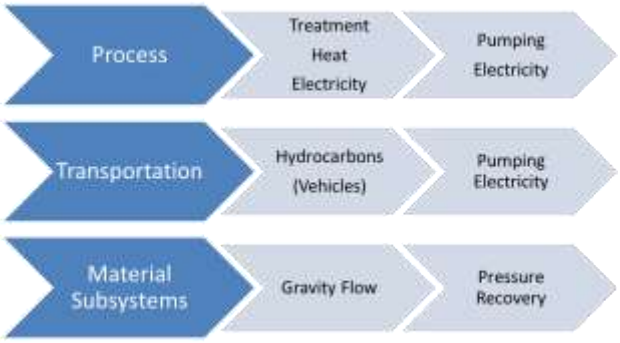

Figure 44: Process, transportation, and material subsystem energy uses.

Electrical energy is the primary form of energy that will be used for extracted water treatment at the site. The local cost of electricity $0.0651 per kWh. Energy recovery devices should be utilized for membrane treatment systems to increase energy efficiency. If possible, waste (geothermal) heat may be extracted from the source water for use in thermal treatments or pretreatment processes. Waste heat may also be useful as a means of heating local buildings or site systems. Heat derived from hydrocarbon sources may need to be used in thermal processes but should be avoided. Energy will also be used in transportation. Truck transportation will use diesel or gasoline fuels, while pumping (for system use and pipeline head gains) will use

electrical energy, or possibly hydrocarbon fuel for small onsite pumps or generators. Beyond Phase II, transportation distances, and thus energy use for transport, should be minimized. Whenever possible, gravity flow should be used in pipeline and storage designs for maximum energy efficiency. Otherwise, water and product transportation costs can greatly increase (by a factor of 2 or more) the costs of treatment.

Emissions (air):

Direct air emissions may come from the extracted water. Very low quantities of volatile organic compounds (VOCs) were detected in the Weber and Madison waters (*Appendices*). Detectable levels of H_2S were found in the extracted Madison water. Open ponds or tanks for extracted water storage may result in volatile air emissions. Aerated or mixing processes may also release volatiles.

No VOC emission limits are expected to be exceeded in the Phase II study based on the analyzed water quality and the design extraction rate of up to 50 gpm. However, this scenario should be re-evaluated for the larger quantities of water that are expected to be handled beyond a Phase II test. Potential emissions of H_2S should be monitored during site operations and pumping (included in a site health and safety plan) and evaluated with respect to Wyoming permit requirements and OSHA requirements.

Indirect air emissions will come from generation of electricity used at the site. SOx and NOx components of fossil-fuel-fired power plants are the primary components of these types of emissions. Particulate and metals emissions (e.g. mercury) may also be emitted. The detailed Phase II LCA, including selected water treatment technologies during BP 2, will evaluate the amounts of generated electricity to be used at the site, based on selected technologies that are tested, and the potential emissions from that generation.

Processes that result in overspray or drift of the treated water should also be evaluated to prevent deposition of salts onto land surfaces. This may include cooling towers, evaporation ponds, or other spray/aerosol emitting processes. Combustion emissions from hydrocarbon sources (vehicles, generators, pumps) should be minimized whenever possible in onsite operations.

Reuse potential of products:

Onsite reuse potential exists for some water products, such as:

Fresh Water: reuse of treated fresh water may occur for operations requiring washdown, flushing, dust control, etc. The limitations of permitted uses may need to be considered. For example, if use results in “discharge to navigable waters”, an NPDES permit may be required.
Cooling water: treated fresh, brackish, or untreated saline water may be useable as cooling water for certain treatment processes. Reuse of site-supplied water is preferable to importing offsite fresh water.

Waste Management/End of Product Life:

Waterborne Waste:
Waterborne wastes primarily will consist of concentrate reject from treatment and other separations processes. Waterborne wastes that exceed reinjection volumes in the Phase II effort (expected to be negligible) will be disposed via a Class I well reinjection process and permit. For long-term site operations beyond Phase II, an appropriate mechanism for disposal of waterborne wastes will need to be identified. Volumes expected in Phase II will likely be ~15 gpm or less.

Solid Wastes:

Lime Solids: If hot or warm lime softening is chosen as a pretreatment for mineral scale reduction, then lime solids disposal will be needed. Lime can often be used as a soil amendment and applied to land surfaces; it may also be disposed in solid waste landfills. Determination of hazardous constituents may be needed if there is concern that metals or radioactive constituents have adsorbed or become concentrated in the lime. Determination of hazardous constituent concentrations or the presence of TENORM (technologically-enhanced naturally-occurring radioactive material) should be evaluated as required by the disposal facility or permit.

Coagulated solids: If coagulants are used to flocculate divalent or mineral constituents, then solids will be generated from this process. Coagulated solids should be disposed in appropriate solid waste landfills. Determination of hazardous waste exemption may need to be performed to meet disposal criteria. Determination of hazardous constituent concentrations or the presence of TENORM (technologically-enhanced naturally-occurring radioactive material) should be evaluated as required by the disposal facility or permit.

Brine solids: Concentrated solids from thermal treatment or zero-liquid-discharge (crystallizer) processes will require disposition if created in the treatment process and are determined to be wastes, rather than salable byproducts. These solids will be composed primarily of sodium chloride by weight. Determination of hazardous constituent concentrations or the presence of TENORM (technologically-enhanced naturally-occurring radioactive material) should be evaluated as required by the disposal facility or permit. Water content should be evaluated by paint filter testing prior to disposal if required by the disposal facility or permit.

Spent filters: Filtration processes will lead to the accumulation of spent filters. Most spent filters can be disposed in municipal solid waste landfills. Evaluation of the filters for hazardous or TENORM constituents should be performed per state regulations or landfill requirements.

Post-Consumer products and packaging: Should be recycled and reused locally, and minimized as much as possible.

Fugitive or accidental releases: must be avoided to meet permit requirements and safe operating procedures. Containment structures and secondary containment should be used to prevent spills of saline extracted waters and salt water products and byproducts during processing, transfers, and pumping. Leak detection systems should be installed for ponds and

storage facilities within secondary containment and to permit specifications. Transfers of solid materials should be protected from spills, airborne dust generation, and tip-over situations. Cleanup of spilled solid materials should follow site permit or best operating practices. Fugitive air emissions are discussed above.

D. Life Cycle Analysis for Expected Treatment Scenarios

Several water treatment options were developed for evaluation in Phase I (discussed above). Options 1A through 1C are variations on a simple flash evaporation system, and create the lowest amounts of product fresh water, and the largest amount of brine for reinjection. They are the simplest systems by design and can handle the largest amounts of influent water. Options 2 and 3 are membrane-based treatment systems that create larger amounts of fresh water product, but also are more complex, with more possible waste streams created. Options 4 and 5 are thermal treatment options that can handle a lower amount of influent volume, create less treated fresh water than Options 2 and 3 (although creating a larger fraction of $Q_{fresh\ out}/Q_{in}$), and a lower volume of brine waste, or no liquid waste in the case of Option 5 (Zero liquid discharge).

Table 19 shows the input and output energy sources, emissions, waste streams, and product streams for each option. Waste and product volumes, costs, and carbon footprint will be assigned in detail in Phase II. Additional treatment methods developed by outside projects may also be analyzed in Phase II if they are demonstrated at the BEST site.

Table 19: Breakdown of energy, inputs, and outputs by water treatment option.

Option	Energy In kWh	Energy Out kWh	Chemical Inputs Kg/d	Air Emissions kg/d	Waste streams m^3/d; kg/d	Product streams m^3/d; kg/d
1a-Flash Evaporation	E_{fm} E_{sys}	E_{inj}	--	CO_2 Nox+Sox	$Brine_{reinj}$	FW
1b-Cooling Tower Evaporation	E_{fm} E_{sys} E_{hc}	E_{inj}	Scale Inh. pH adjust	CO_2 Nox+Sox	$Brine_{reinj}$	FW
1c-Flash Evaporation w/condenser	E_{fm} E_{sys} E_{vac} E_{hc}	E_{inj}	Scale Inh. pH adjust	CO_2 Nox+Sox	$Brine_{reinj}$	FW
2-Softening+ NF	E_{fm} E_{sys} E_{vac} E_{hc}	E_{inj}	Scale Inh. Lime pH adjust	CO_2 Nox+Sox	$Brine_{reinj}$ Filter cake Dewater Media filters Backwash chemicals Waste membranes	FW Soft Brine
3-Softening+ NF + RO	E_{fm} E_{sys} E_{vac}	E_{inj}	Scale Inh. Lime pH adjust	CO_2 Nox+Sox	$Brine_{reinj}$ Filter cake Dewater	FW Soft Brine

	E_{hc}				Media filters Backwash chemicals Waste membranes	
4-Softening+ Evaporator	E_{fm} E_{sys} E_{vac} E_{hc}	E_{inj}	Scale Inh. LimepH adjust	CO_2 Nox+Sox	$Brine_{reinj}$ Filter cake Dewater Media filters	FW Soft Brine
5-Softening+ Evaporator+ Crystallizer	E_{fm} E_{sys} E_{vac} E_{hc}	E_{inj}	Scale Inh. LimepH adjust	CO_2 Nox+Sox	$Brine_{reinj}$ Filter cake Dewater Bag filters Dry salt?	FW Soft Brine Dry salt?

Note: NF= nanofiltration; RO=reverse osmosis; E_{fm}=electricity for formation pumping; E_{inj}=electricity for injection pumping; E_{sys}=electricity for pumping through system; E_{hc}=electricity for all purposes from onsite hydrocarbon-fueled generator; E_{vac}=electricity for vacuum pump; $Brine_{reinj}$=reinjected brine, pH adjust refers to either acid or base additions.

Impact/Risk/Cost Assessment (high level):

Assessed scenarios

We used the CO_2-PENS Water Treatment Model (WTM) to assess cost risks for selected scenarios for the Phase I assessment. The WTM was developed using the GoldSim© platform (Sullivan Graham, Chu et al. 2014). GoldSim© is used to develop analysis models that perform multi-realization, probabilistic simulations. A FORTRAN code captures the logic of treatment process selection and is linked within GoldSim©. GoldSim© utilizes custom data elements for input of user-specified parameters including stochastic distributions. The WTM captures all decision points; both stochastic range and constant data input values.

During a preliminary system design phase, site-specific information may not be available and so literature data must be used to assess treatment train processes and costs. Note that all cost values shown are in US$. All model values and results are for cubic meters (m^3) of water unless otherwise stated. In this study, modeling assumptions are based on U.S. infrastructure, water management, and regulatory systems. This is a "one-way" analysis, in that the reciprocal effects of time-related reservoir responses to CO_2 injection and pressure-front variations, as well as changes in water chemistry over time, are not considered to have an effect on brine production and treatment systems (Ziemkiewicz et al, IJGGC in review).

We selected two scenarios for modeling based on the options outlined in Sec. VIII. We used Option 2, (Softening+Nanofiltration); and Option 5 (Softening+Evaporator+Crystallizer). These options reflect either membrane treatment or thermal treatment and incorporate two different kinds of waste disposal (brine reinjection/evaporation and zero-liquid discharge). We varied transportation distance based on variable distances to possible fresh water users, and varied flow rates by ±20%. Most other criteria were the same for each choice, see **Table 20** for parameters. We ran 500 realizations for each scenario, sufficient to perform an importance analysis with the results.

Table 20: List of known Constant Values for simulations:

Flow Rate Q in to system	500 gpm = 2725 m3 /day
Disposal method	Class I well or evaporation pond
Water Type	NOT produced water
Storage	Yes. Tanks and ponds both okay as appropriate to flow rates.
Location	west of 100th meridian Not near ocean
Organic Pretreatment	No
Scaling mineral calculations	Yes, use chemistry criteria provided
Formation:	Madison Fm.
Power cost:	0.10 per kWh
Energy Recovery:	No
NF reject rate (goal)	50%
Transportation distance from extraction well to treatment location (X1)	1 km
Transportation distance from treatment location to disposal location (X3)	1 km

Factors to test in simulation:
Transportation distances from treatment location to Point-of-use location (X2): three options:

1) 1.6 km (to Jim Bridger Plant);
2) 80 km (to River or chemical plant)
3) 150 km (to Naughton power plant or agricultural location)

Test flow rate effects:

1) Flow rate at 500 gpm
2) Flow rate at 500 gpm +20%
3) Flow rate at 500 gpm -20%

Table 21 shows the results from the three different transportation distance options, calculated with a flow rate of 500 gpm (Q_{in}); and two scenarios using the shortest transportation distance but including a 20% increase or decrease in influent flow rate. The model converges on a final treated volume based on calculated recovery rates for each treatment method (NF or Thermal). Costs shown are based on a Class I well disposal for the separated brine concentrate, but at a literature-based cost rate that is much lower than the local quoted disposal rate (Sullivan Graham, Chu et al. 2015).

Table 21: Results for WTM with variation in transportation distance and flow rate.

Scenarios	NF Class I well total cost (mean) $/m^3	Thermal Class I well total cost (mean) $/m^3	Final treated volume (mean) m^3, NF	Final treated volume (mean) m^3, Thermal
X2=1.6km, 2725 m^3/d	1.68	2.00	1569 (57.6%)	1757 (64.5%)
X2=80 km, 2725 m^3/d	3.44	3.76	1569 (57.6%)	1757 (64.5%)
X2=150km, 2725 m^3/d	5.00	5.32	1569 (57.6%)	1757 (64.5%)
X2=1.6 km, 3270 m^3/d	1.67	1.99	1883 (57.6%)	2108 (64.5%)
X2=1.6 km, 2180 m^3/d	1.70	2.02	1255 (57.6%)	1405 (64.5%)

Note: NF=Nanofiltration

Variance analysis to detect risks

When sufficient realizations (usually >100) are simulated in the WTM model, the variance of different input aspects can be analyzed to detect which inputs are most likely to affect total costs. **Figure 44** below, shows the importance analysis for the different input variables in each of the two cases. Because inputs for some variables are the same, and are relatively constrained, for the two cases (e.g., the input chemistry is the same so antiscalent dosing is the same for each option) there is little difference in variance between the two scenarios and within each case between the different disposal methods. We plotted the results based on disposal method because different disposal methods often include large cost variances, although that is not seen in this analysis. Transportation clearly contains the largest cost variance for both scenarios-based on the range of input distances. Costs to transport will vary greatly, and may be quite large, if a distant user requires transport of product water for long distances (here, up to 150 km). The second largest source of cost variance is the influent flow rate. We deliberately included a ±20% range in flow rate because it is still unknown what variation may occur during carbon storage and water extraction operations. This variance affects the costs much less than that seen from transportation-clearly transportation costs will have a greater influence on total costs. This means that we have added a goal to minimize transportation distances as part of our water treatment objectives.

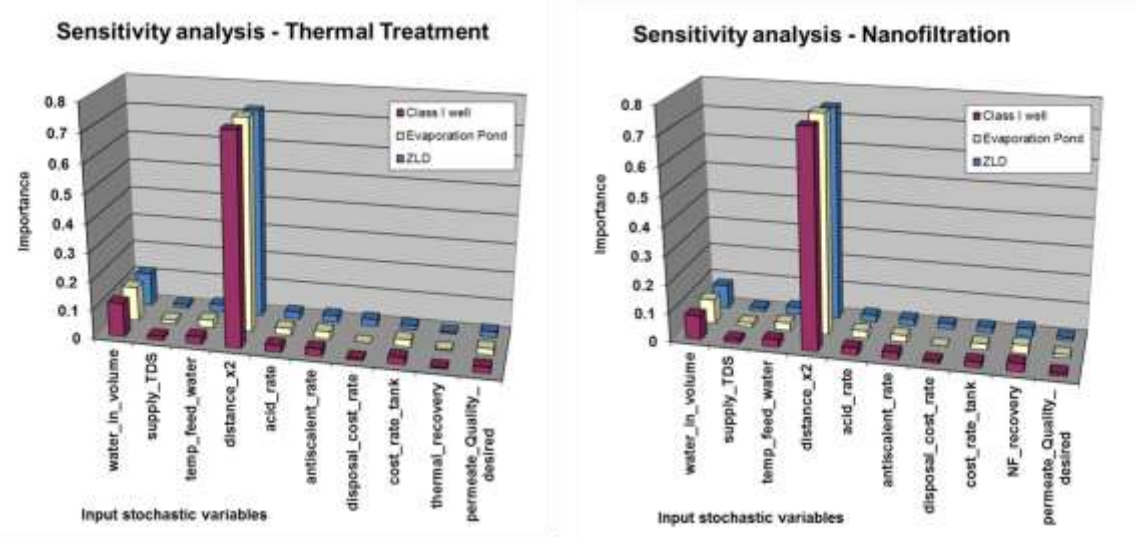

Figure 44: Importance analysis of input variables on system results for (left) thermal treatment, and (right) nanofiltration membrane treatment, shown with three disposal options.

Variance that is not captured in this model scenario include variance in pretreatment costs (e.g. for warm lime softening instead of acid/antiscalent addition), and variance in concentrate disposal costs. Warm lime softening costs were calculated based on capital cost information from C. Haussman (personal communication 2/25/2016) and O&M cost information from (Doran and Leong 1998), updated through inflation indexing to 2015 costs. These are inexact costs based on estimates and yielded a cost of 0.73$/m^3. This is above the model calculated pretreatment cost based on the water chemistry inputs, 0.35-0.62 $/m^3. These costs need to be validated using local O&M costs at 2016 rates. Until then the variance from pretreatment may be predicted to be larger than actual variance. The goal of minimizing mineral scale potential of the reject water/brine may need to be adjusted based on brine fate in the total system if the costs remain high after further analysis.

Our current model yields a set of mean final costs (including treatment cost) using Class I well disposal (without storage and transport) from 1.67-5.32 $/m^3. This is one order of magnitude lower than a local quote for Class I well brine disposal of 23.88 $/m^3, not including transportation and storage (T&S) costs (S. Quillinan, personal communication, 03/03/2016). The current model uses a literature-based Class I well disposal cost rate range from 0.02 to 0.25 $/m^3 (not including T&S). This indicates that the local cost of brine disposal will add large variance to the treatment costs, and that a goal of minimized or eliminated brine disposal volumes will be very important to reduce overall treatment costs. Phase II will incorporate final disposal cost quotes into the model for comparative analysis. **Figure 45** shows an example of a model run that incorporates both a higher range of pretreatment (including lime softening estimates) and Class I disposal (including the local site estimate). The importance of Class I disposal is magnified, while influent volume variation, feed water temperature, and X2 transportation distance are the next most sensitive factors.

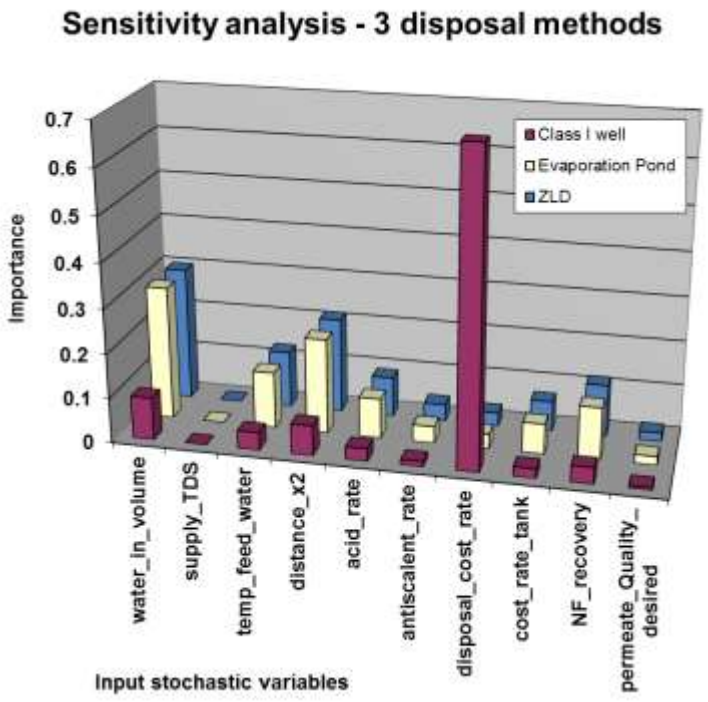

Figure 45: High-variance Class I disposal and pretreatment cost analysis.

In summary, analysis of costs and cost variance in the system reveals that there is a need for science-based data collection for several steps in the treatment train, and that optimization of processes and costs via system testing will yield better, cheaper, and more efficient total system designs and improved overall system goal setting.

LCA inputs to overall system objectives

The development of successful field site operations relies on sound engineering principles for a successful CCUS/pressure management/water treatment strategy, and also in developing areas where scientific observation and experiments can improve operational efficiencies, costs, and methods. The LCA points out places where improvements can be made relative to specific site objectives.

Figure 46 shows objectives for three pillars of site operations: CCUS, pressure management, and water treatment. Some of the objectives are part of primary site objectives, while some arise from LCA analysis. Many link across pillars and are bidirectional. Some relate specifically to engineering design parameters or cost factors, and some are directly related to the environmental footprint of the site. Optimizing all of these objectives is challenging and will be part of the scientific analysis of site operations in Phase II.

Within the LCA, we identified a number of knowledge gaps that will be filled during Phase II research. These include:

- Real user markets and user-specific criteria (quality, volume, flow rate) for various water products created.
- A framework for water rights for fresh water created
- Feasibility assessment for Aquifer Storage and Recovery (ASR) (requirements, costs, etc.)
- Real user markets for solid products including metals
- Feasible minerals/metals separation processes and economics
- Alternative brine concentrate disposal options (other than deep well injection).
- Solid product transportation and disposal costs
- Optimization strategy for energy uses (this is a goal for Phase II)
- Detailed air emissions evaluation
- Impacts of real transportation and disposal costs on end-to-end system costs
- Validation of onsite pretreatment and well disposal costs and possible cost variations.

Site-specific information to be gathered during Phase II testing will resolve these gaps.

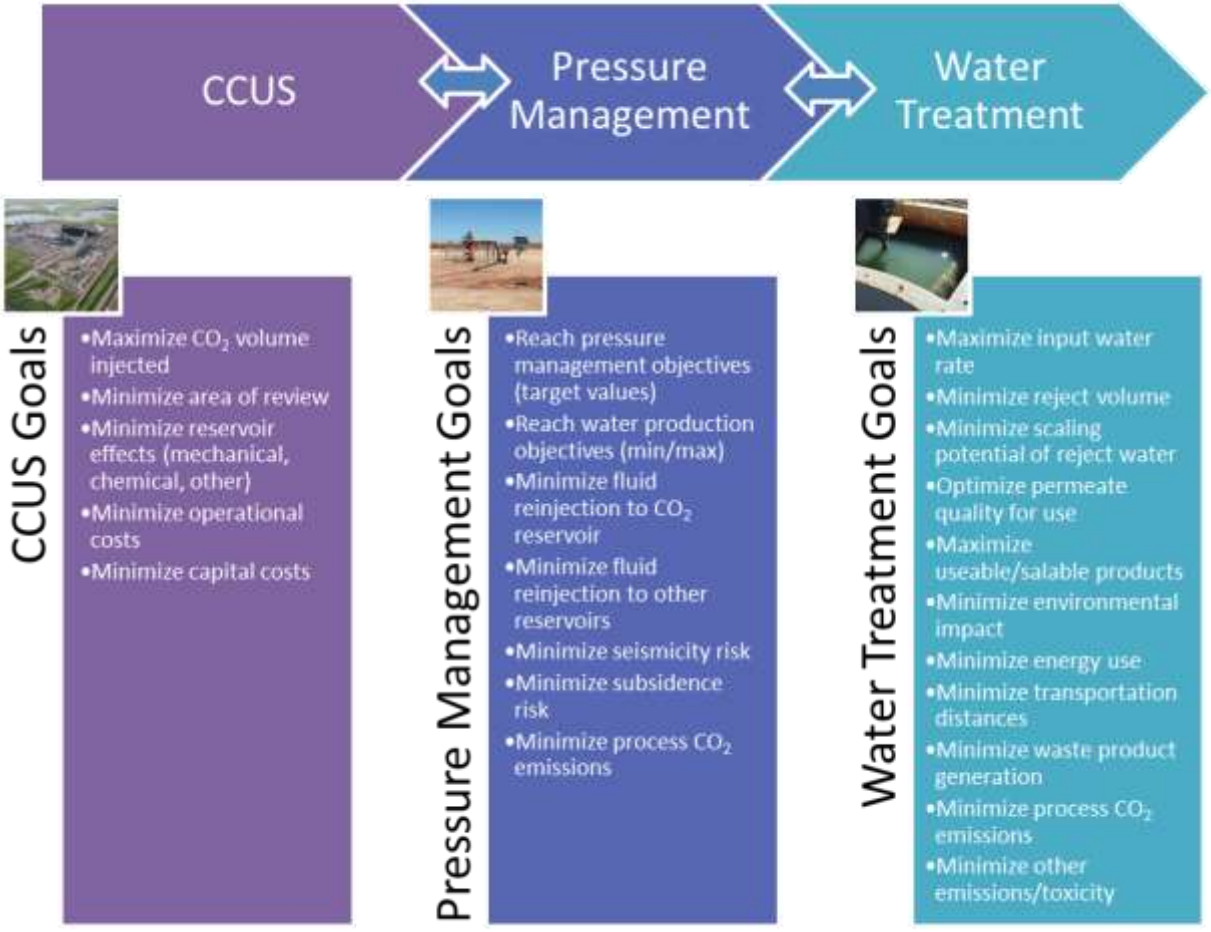

Figure 46: Linked CCUS-pressure management-water treatment objectives.

E. Conclusions

From the LCA and importance analysis in this Phase I stage, we found that minimizing transportation distances, brine disposal costs (via volume reduction) and pretreatment costs will be important parts of cost control. Influent flow rate to the treatment system may also create increased cost variance. Market forces will dictate the potential for use of some products from water treatment. Maximizing the extraction of fresh water from the brine stream will greatly reduce disposal costs (and transportation costs), unless a market is found for "clean brine" products. Minimizing the use of hydrocarbon fuels, and optimizing energy uses in site operations is expected to reduce the carbon footprint. A full understanding of the effects and impacts of these processes on the overall system life cycle can be achieved with ongoing LCA, cost measurement, and site-specific analysis during Phase II testing.

XIII. GEOLOGICAL MODELING, INJECTION SIMULATIONS, AND STORAGE PERFORMANCE ASSESSMENTS

A. Reservoir Condition

In this task, we incorporated updates to the geologic framework model into an FEHM model. The 3-D geologic framework model has been updated with newly available data from the interpretation of the 3-D seismic survey, well logs, and cores (Surdam, 2014; chapters 6 and 7). These data informed stratigraphic interfaces between materials, heterogeneous porosities, and permeabilities within formations. The updated FEHM model includes the Jim Bridger Fault, located approximately 7,500 feet northeast of RSU #1, and Fault #1 located approximately 2500 feet southwest of the RSU #1 test well. Other faults have been identified with less certainty and can be included in the model as well.

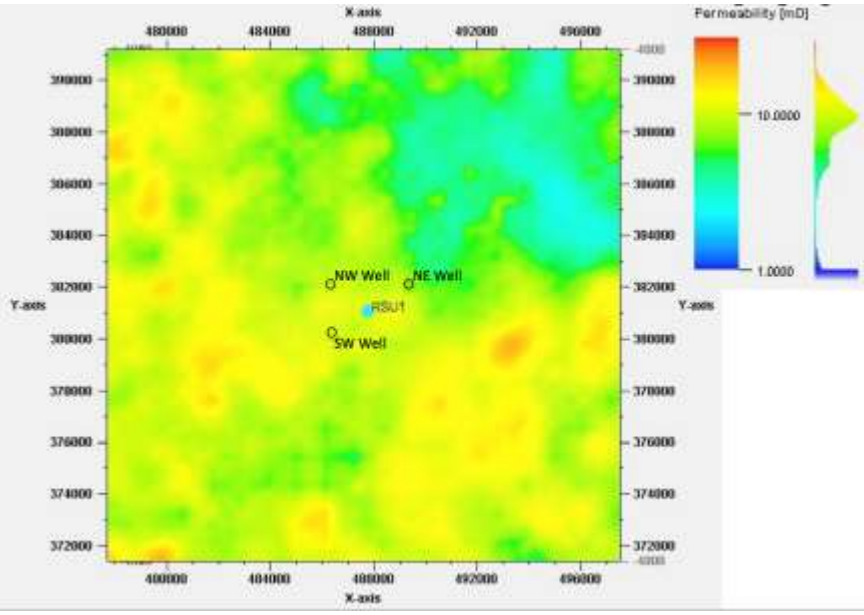

Figure 47: Permeabilities derived from the Jim Bridger 3-D seismic survey. Axis units are in feet and are in the SPCS27-4903 coordinate system. The approximate location of RSU #1 test well and 3

potential wells locations (NW, SW, and NE wells) are identified.

Seismically derived porosities were used to derive permeabilities, presented in **Figure 47**. Refer to Surdam (2013) chapter 9 for details of the derivation of the porosity/permeability relationships. We interpolated these porosities and permeabilities for the Lower Madison formation into the FEHM model. On the basis of well logs and seismic surveys, the Upper Madison Formation is considered to be a potential upper seal on the Lower Madison and is modeled with low uniform permeability (1×10^{-18} m^2; 0.001 mD), as are the other formations. In **Figure 48**, the distinct difference between porosities/permeabilities in the Upper and Lower Madison formations derived from well logs in the RSU#1 test well are apparent (Surdam, 2013; chapter 9).

The approximate locations of the RSU#1 study site and 3 potential well locations (NW, NE, and SW wells) are identified in **Figure 47**. The potential well locations are around 1000 feet to the northwest (NW Well), northeast (NE Well), and southwest (SW well) of RSU#1.

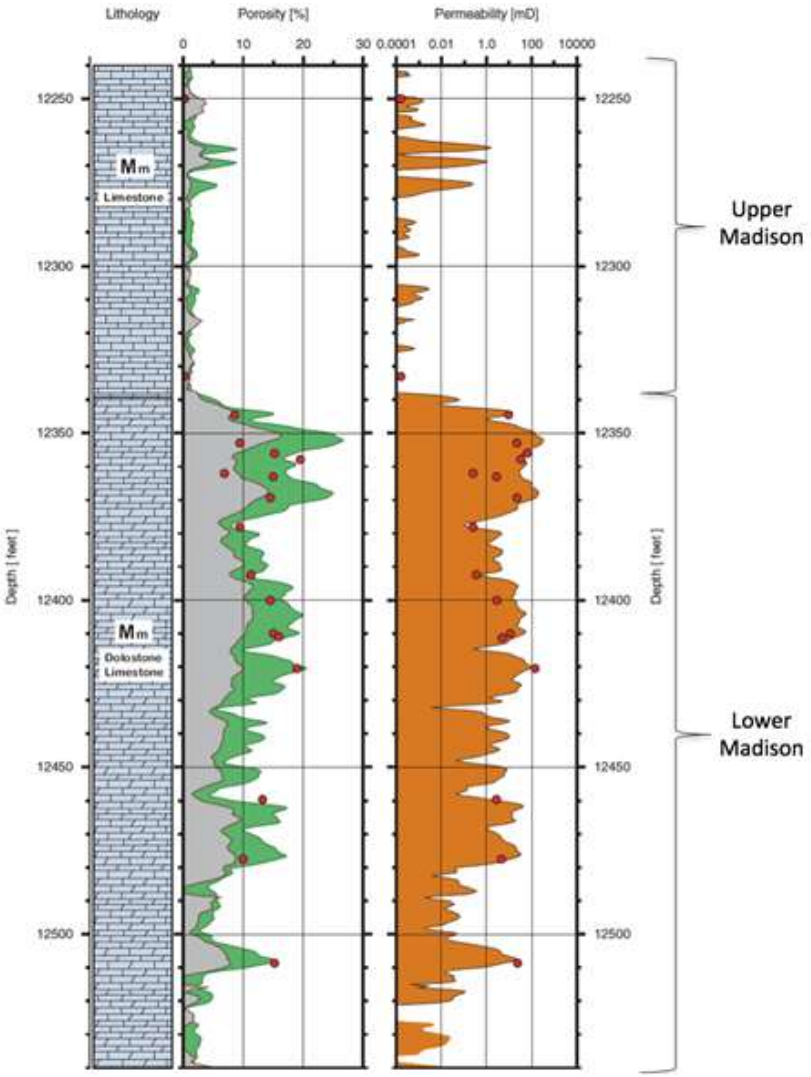

Figure 48: Open-hole logs and core data in the Madison Formation in the RSU #1 test well. Tracks from left to right are (1) lithology, (2) density (green) and sonic (gray) porosity with total porosities from core (red dots), (3) permeability from logs (orange) overlaid with core measurements (red dots). The approximate delineation between Upper and Lower Madison

formations is indicated on the right. Modified from **Figure 9.3** in Surdam (2013).

B. Computational Mesh and Simulation Setup

We generated an FEHM mesh laterally centered on the RSU #1 test well with approximate lateral extents of 6 by 6 km and from depths below the surface from 2.8 to 4.3 km. The mesh conforms to formation interfaces between the Darby, Lower Madison, Upper Madison, Amsden, and Weber formations, although distinct porosities and permeabilities are only applied to the Madison layers. The mesh refinement along the Madison is presented in **Figure 49**, where the vertical resolution is variable, around 9.4 m in the Upper Madison and 8.7 m in the Lower Madison. The uniform lateral resolution of the mesh is 67 m.

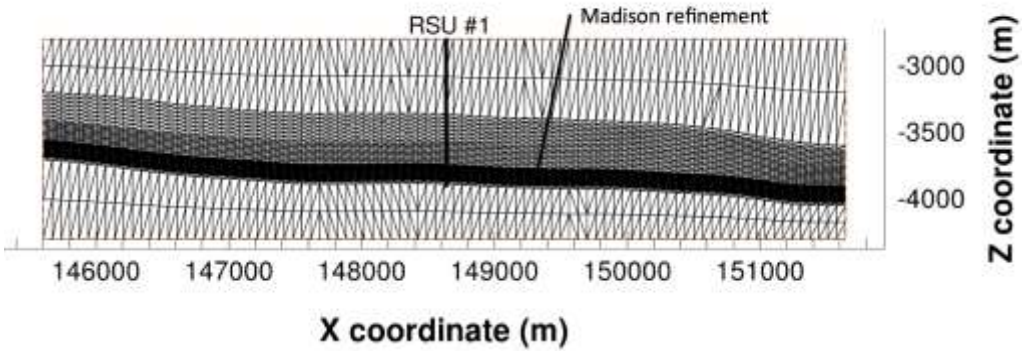

Figure 49: Vertical cross-section through RSU #1 of nodal connectivity of the FEHM mesh. Increased mesh refinement along the Madison formation is apparent. X-axis is in the SPCS27-4903 coordinate system and Z-axis is depth below surface.

Vertical cross-sections of the base case porosities and permeabilities in the FEHM model are plotted in **Figure 50**, where background porosities are 0.01 and permeabilities are 1×10^{-18} m^2 (0.001 mD). Vertical cross-sections of initialized hydrostatic pressures and geothermal temperature gradient are plotted in **Figure 51**. The hydrostatic pressure gradient is 9.73 kPa/m and surface pressure is atmospheric (101.325 kPa). The geothermal gradient is 25.5°C/km and the surface temperature is 4.4°C.

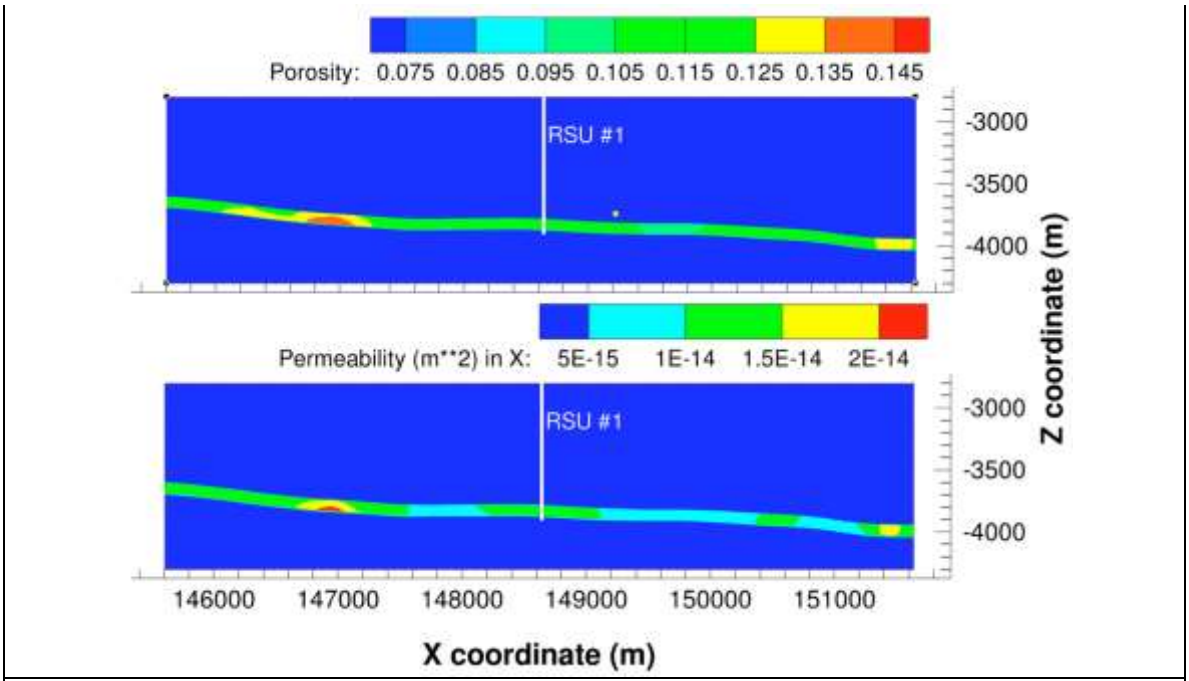

Figure 50: Vertical cross-sections of porosities and permeabilities interpolated into the Lower Madison in the FEHM model. Background porosities and permeabilities (blue regions outside of the Lower Madison) are 0.01 and 1×10^{-18} m^2, respectively. X-axis is in the SPCS27-4903 coordinate system and Z-axis is depth below surface.

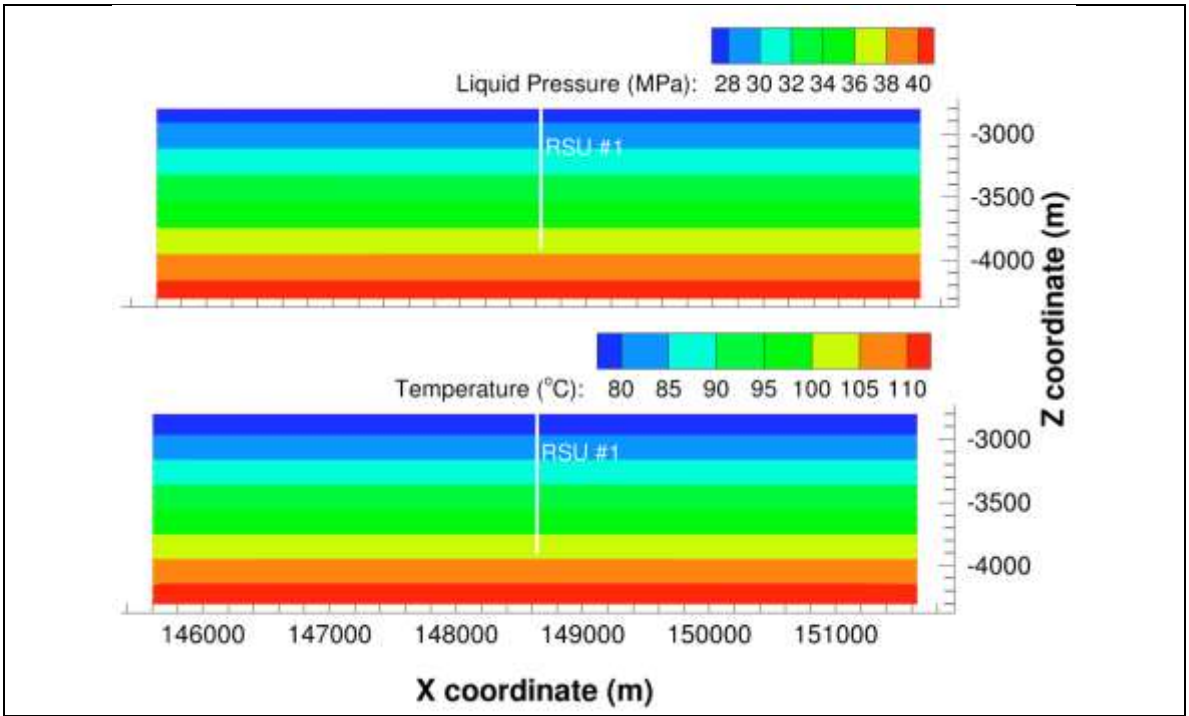

Figure 50B: Vertical cross-sections of initial pressures and temperatures for the FEHM model. X-axis is in the SPCS27-4903 coordinate system and Z-axis is depth below surface.

The Jim Bridger Fault and Fault #1 lineaments defined on the FEHM mesh are indicated in plan view in **Figure 51**. We incorporate sealing faults by assigning zero porosity to nodes (blue nodes in **Figure 51**). Since the Jim Bridger Fault extends beyond the model domain, nodes to its northeast are assigned zero porosity as well. FEHM solves the heat equation for zero porosity nodes, but removes the nodes from flow solutions. For scenarios when a fault is not sealing, we use the seismically derived porosities and permeabilities for those nodes. Reservoir compartmentalization scenarios are investigated below by modeling various combinations of the Jim Bridger Fault and Fault #1 either acting as sealing faults or not.

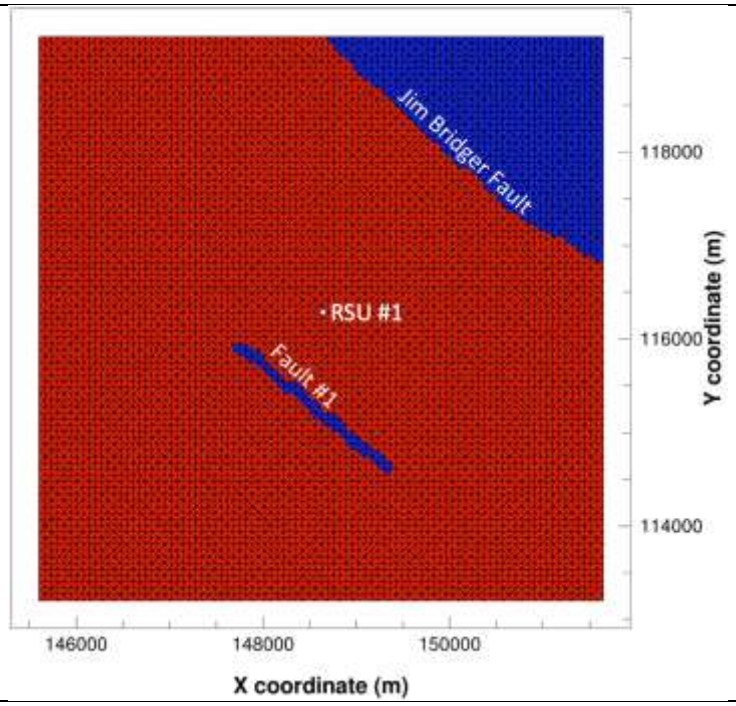

Figure 51: Location of Jim Bridger Fault and Fault #1 in FEHM model delineated by red and blue regions. We identify sealing faults by assigning zero porosity to cells (blue cells). Lateral nodal connectivity of the FEHM mesh is represented as black lines. Axes are in the SPCS27-4903 coordinate system.

There are significant uncertainties at the RSU site including heterogeneous permeabilities and porosities, number and location of faults, sealing capacities of faults, integrity of caprock, etc. There are also many decisions that need to be made in order to design a brine extraction storage test including injection regime, production regime, well locations, tracer selection, etc. Models provide a relatively inexpensive and efficient means of investigating the potential outcome of alternative test designs and the effect of uncertainties on these outcomes.

C. Simulation Results with Step-Rate Injections

We simulated multiple injection-production scenarios, including pulse rate injection, constant rate injection, step rate injection, pulse rate production, constant rate production and constant pressure production.

Based on the simulation results, we propose to use a novel approach with combination of pulse tests and interference tests for the Phase II field test. Interference and pulse tests in combination with pressure transient analysis have been used for reservoir characterization (Lee, 1982; Kamal, 1983) and utilize characteristics of pressure response resulting from imposed injection or withdrawal. Interference tests are used to determine whether two or more wells in same formation (reservoir) are in pressure communication and if there is communication, use the results to estimate interwell reservoir properties. An interference test is performed by either injecting or producing from a well and observing pressure response in the observation well. The magnitude and timing of the deviation in pressure change at the observation well can be used to assess reservoir characteristics and infer how the pressure change in the reservoir is affected by not only reservoir characteristics but also imposed injection or production conditions. Similarly, the pulse tests are used to determine pressure communication between well pairs as well as interwell formation properties. The pulse tests use a series of injection or production pulses consisting of injection (or production) from for an active well then shutting it in and repeated in a regular pattern. The pressure response in an observation well is recorded during the pulse sequence. Similar to interference tests, the pressure response can be used to determine pressure response characteristics of a reservoir. We have performed simulations of a hypothetical injection/production schedule as shown in **Figure 52** with an objective to simulate potential reservoir response.

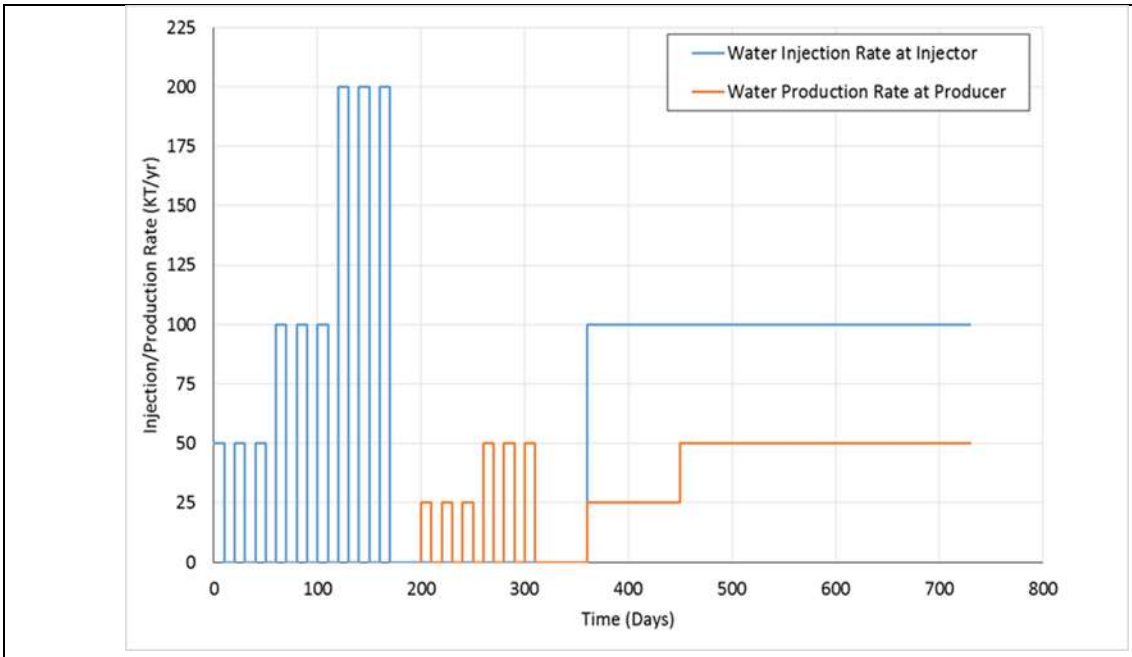

Figure 52: Example injection/production rates for combined pulse/interference tests.

The injection/production schedule has two parts with two different objectives. The first part of the schedule (lasting one year) includes multi-rate injection/production pulse tests. The pulse tests consist of multi-rate injection pulses followed by multi-rate production pulses. The injection pulses begin with pulses at an injection rate of 50 KT/Yr (1.5844 kg/s) followed by pulses at 100 KT/Yr (3.1688 kg/s) and 200 KT/Yr (6.3376 kg/s). Three pulses are applied at each injection rate with each pulse consisting of 10 days of injection followed by a 10-day, no pump shut-in period. The third injection rate pulse is limited to the maximum injection rate limit for proposed injection well design. To maximize relevance to commercial operations, the chosen proposed injection rates are comparable to industrial scale injections with vertical wells. Following the third set of injection pulse tests, the injector is shut-in for a period of 30 days prior to production pulses. Note that during the injection pulse test period the production well is not producing.

During the production pulse phase, water is produced through the production well using a similar multi-rate, pulse production approach. The production pulses begin at a production rate of 25 KT/yr and step up to 50 KT/yr. Note that during the time the production pulses are applied there is no injection taking place. The combined injection/production pulse tests are designed to provide a range of data:

1. Pressure transient data during the build-up and decline phases can be used to characterize the Madison formation including reservoir compartmentalization as well as effective permeability of Madison and the sealing layer above it.
2. Information on pressure increase due to variation in injection rates during injection pulse tests will be used to assess how the scale of injection affects pressure change and reservoir response time. Similarly, the characteristics of pressure decline data during the no-pump periods can be used to assess how pressure decline rate and magnitude of decline is affected by injection rates as well as in-situ pressure including pressure build-up.
3. Pressure decline data due to variation in production rates during production pulse tests can similarly be used to assess how the magnitude of production rate affects the magnitude of pressure decline and the lag time between beginning production and reservoir pressure decline.

While the injection/production schedule is simple, its novelty is in the use of multiple rates which makes the approach very powerful in providing a range of valuable information including how scale of injection and production affects reservoir response. The pulses are designed to last longer than the traditional pulse tests (days rather than hours) in order to characterize a larger reservoir volume.

We have performed flow simulations of the pulse tests using a pair of wells with the injection well and a monitoring/production well placed 1000’ away in the north-west direction from the injector as shown in Figure 47. **Figure 53A** shows results of the predicted pressure change in the monitoring well during injection pulse tests and **Figure 53B** shows the predicted pressure change in the injection well during production pulse tests.

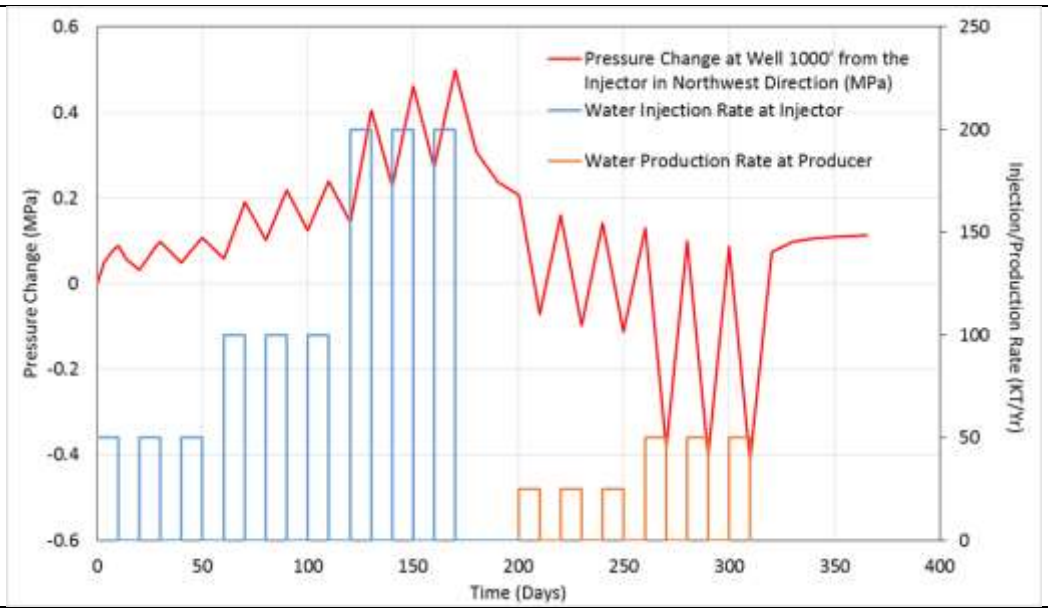

Figure 53A: Predicted change in pressure at the monitoring/production well 1000' apart from the injection well in north-west direction.

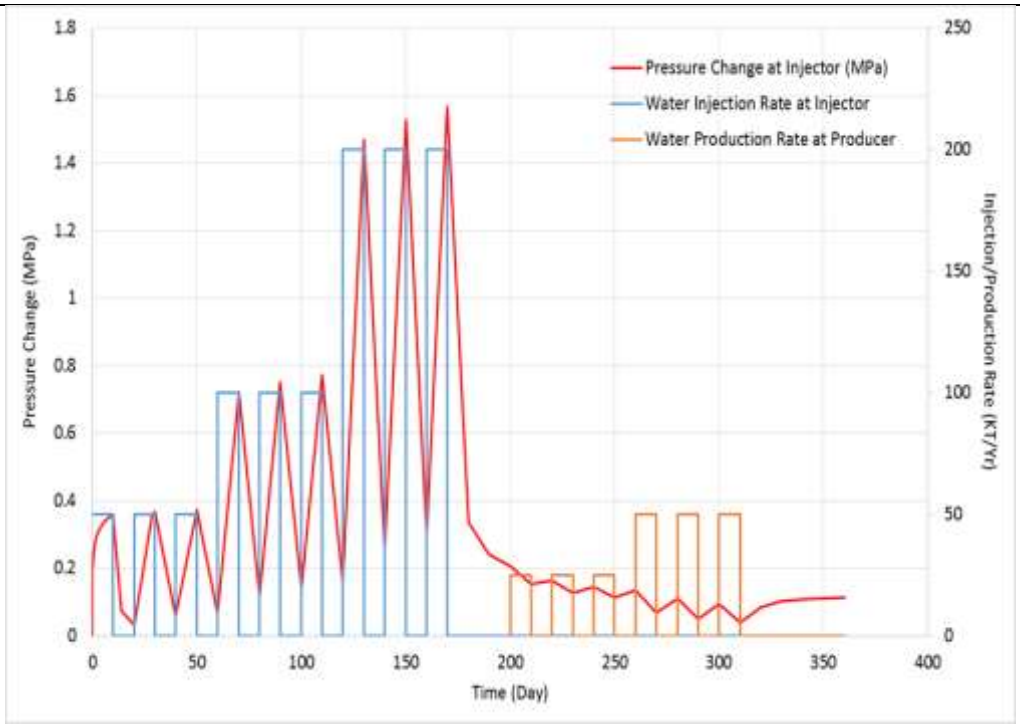

Figure 53B: Predicted change in pressure at the injector well.

Figures 53A and **53B**: demonstrate interesting trends. The magnitude of overpressure increases proportionally to the injection and production rates. The lag time (time to peak change in overpressure) follows the pulse cycle time (10 days) indicating that the reservoir boundaries are

not felt by the amount of injection (or production). These predictions are based on the assumption that only the Jim Bridger fault is sealing and the reservoir extends to 3 km from the injector. The field test observations (including peak overpressure magnitudes and lag time) will help with identifying the reservoir domain as well as the location of Jim Bridger fault and whether it is sealing or not.

The second phase of the injection/production schedule is focused on demonstrating effectiveness of brine production to manage pressure. This phase is initiated after a 30-day, no-pump period after the final production pulse test and lasts for almost a year. The objective of this phase is to understand how brine production alleviates reservoir pressure as well as to characterize the effect of production rate and duration on pressure management. As demonstrated in **Figure 52**, the injection begins at 100 KT/yr and is maintained at this rate for the entire year. At the same time, the production well is produced at 25 KT/yr for 3 months. After 3 months the production rate is increased to 50 KT/yr and is maintained at this rate for the remainder of the year. To assess the effect of brine production on reservoir pressure we performed numerical simulations to compare the pressure change at multiple locations in the reservoir with and without brine production. **Figure 54A** shows the effect of brine production on pressure change at the injection and production wells.

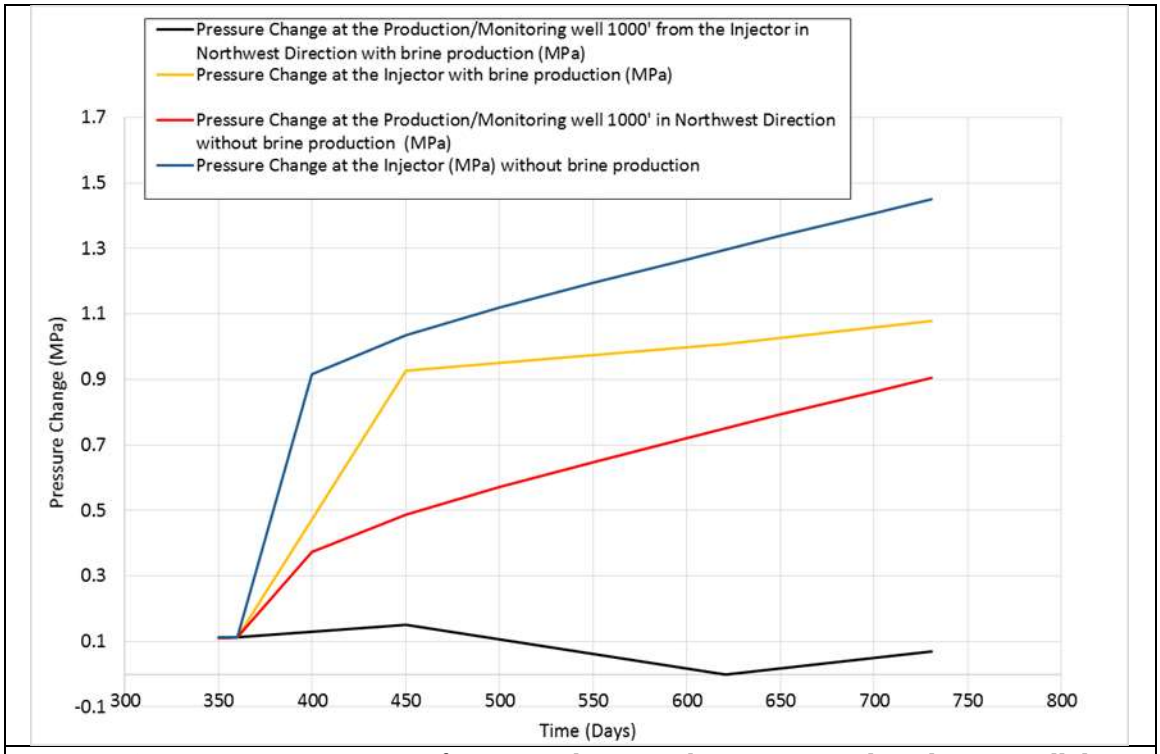

Figure 54A: Comparison of pressure change at the injection and production well due to brine production. The figure shows predicted response with and without brine production.

Figures 54B and 55A demonstrate how brine production reduces pressure within the reservoir domain. **Figure 54B** compares pressure changes at two locations 1000' from the injector with and without brine production, while **Figure 55A** compares the plume of pressure change at the end of simultaneous injection/production test through one year of continuous brine production. **Figures 54B** and **55A** demonstrate the spatial nature of production on pressure reduction demonstrating the effect of reservoir heterogeneity on pressure response. Additionally, **Figures 54A** & **54B** also demonstrate the effect of imposed production conditions on pressure reduction. Note that although the results in **Figures 54A** & **54B** are shown starting with Day 350, they are continuation of simulations of injections/production pulse tests.

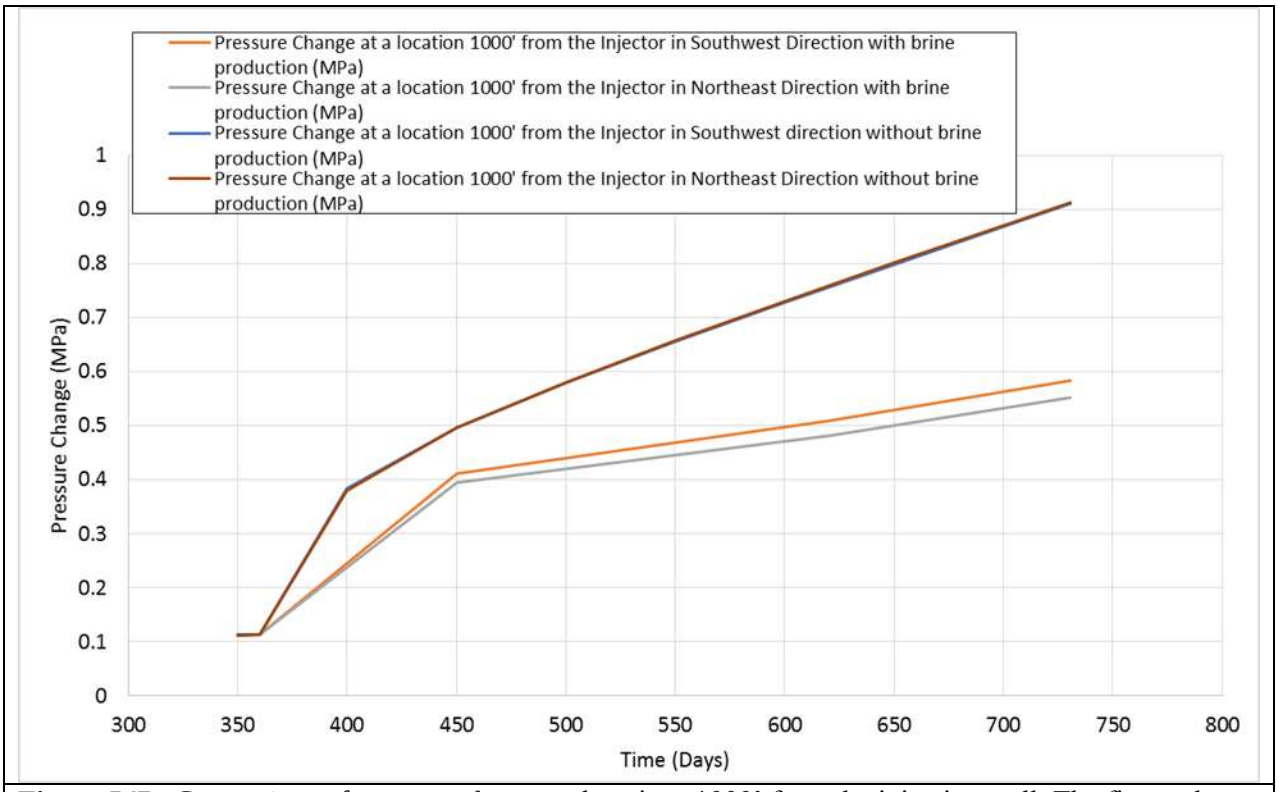

Figure 54B: Comparison of pressure change at locations 1000' from the injection well. The figure shows predicted response with and without brine production.

The results presented in **Figures 53 - 55A** are for a set of simulations which assumed the production well located at 1000' in the northwest direction from the injector. We characterized the effect of production well location on the predicted pressure change by varying the location of the production well from northwest to northeast, southeast and southwest. **Figure 55B** shows the predicted pressure change after 1 year of simultaneous injection/production for the four different production well locations. Results in **Figures 53A – 55B** show that the injection/production schedule with rates as shown in **Figure 53** can lead to a pressure change of the order of 1 MPa, which can be detected with downhole pressure monitors that have sensitivity of 0.001 MPa (as the ones that will be deployed during our Phase II experiment).

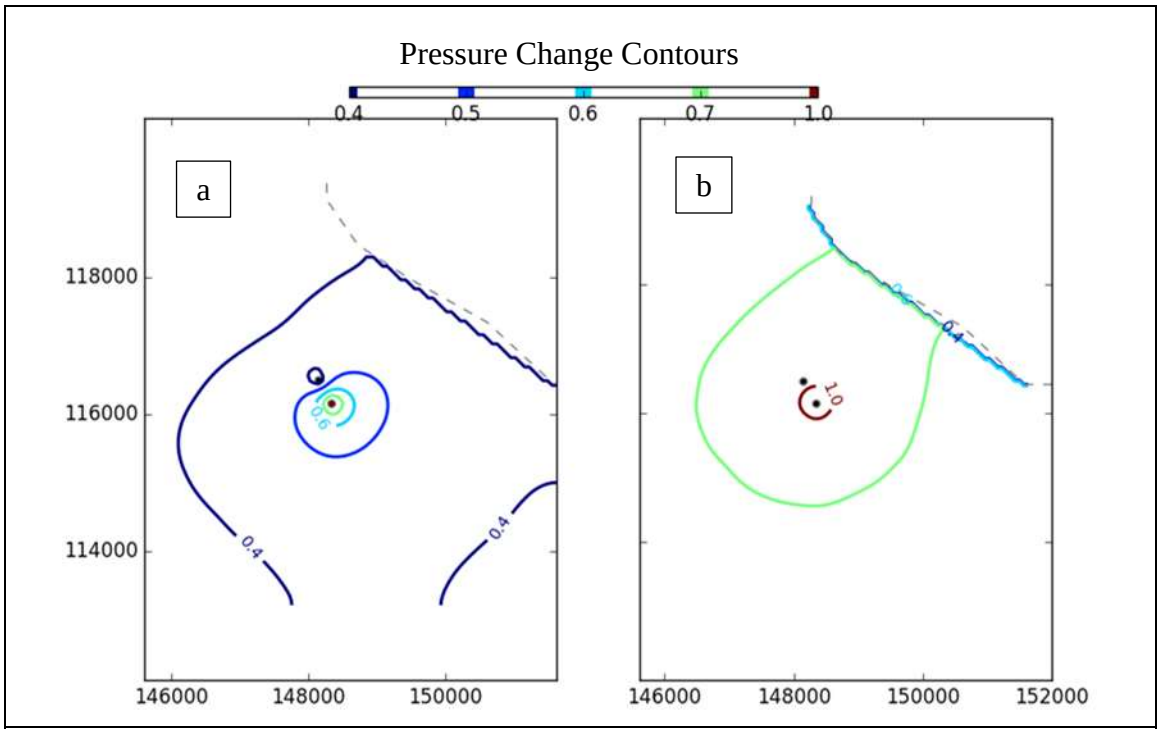

Figure 55A: Comparison of differential pressure plume with brine production (a) and without brine production (b). The figure shows contours of pressure change at the end of the simultaneous injection/production phase.

As stated earlier, we simulated a range of injection production scenarios with the reservoir model for RSU. In **Figures 56A, 56B, 56C, and 56D**, we present FEHM simulated overpressure contours from a step-rate injection regime at RSU #1 with producers located at the NE and SW wells (refer to Figure 47). The step-rate injection regime in these simulations is 50 kt/year for 90 days, then 75 kt/year for 90 days, then 100 kt/year for 180 days, and finally 200 kt/year for 360 days. Refer to **Figure 58** for a graphical representation of the step-rate injection regime. **Figures 56A, 56B, 56C, and 56D** are associated with 4 reservoir compartmentalization scenarios: no sealing faults present; Fault #1 is a sealing fault; Jim Bridger Fault is a sealing fault, and both Fault #1 and Jim Bridger Fault are sealing faults, respectively. In these figures, time increases from left to right and columns are associated with different pressure management scenarios, including no production, a single well producing (NW, NW, or SE) or a combination of NW and SW wells or NE and SE well producing. Scenarios indicating no production at a well are actually set to produce at 2 MPa overpressure, but since overpressure at the producers rarely reaches 2 MPa, this is practically equivalent to not producing at the well. Production at wells is modeled by extracting fluid from the model to maintain hydrostatic pressure (0 MPa overpressure). Therefore, the top rows of plots in these Figures are associated with practically no pressure management.

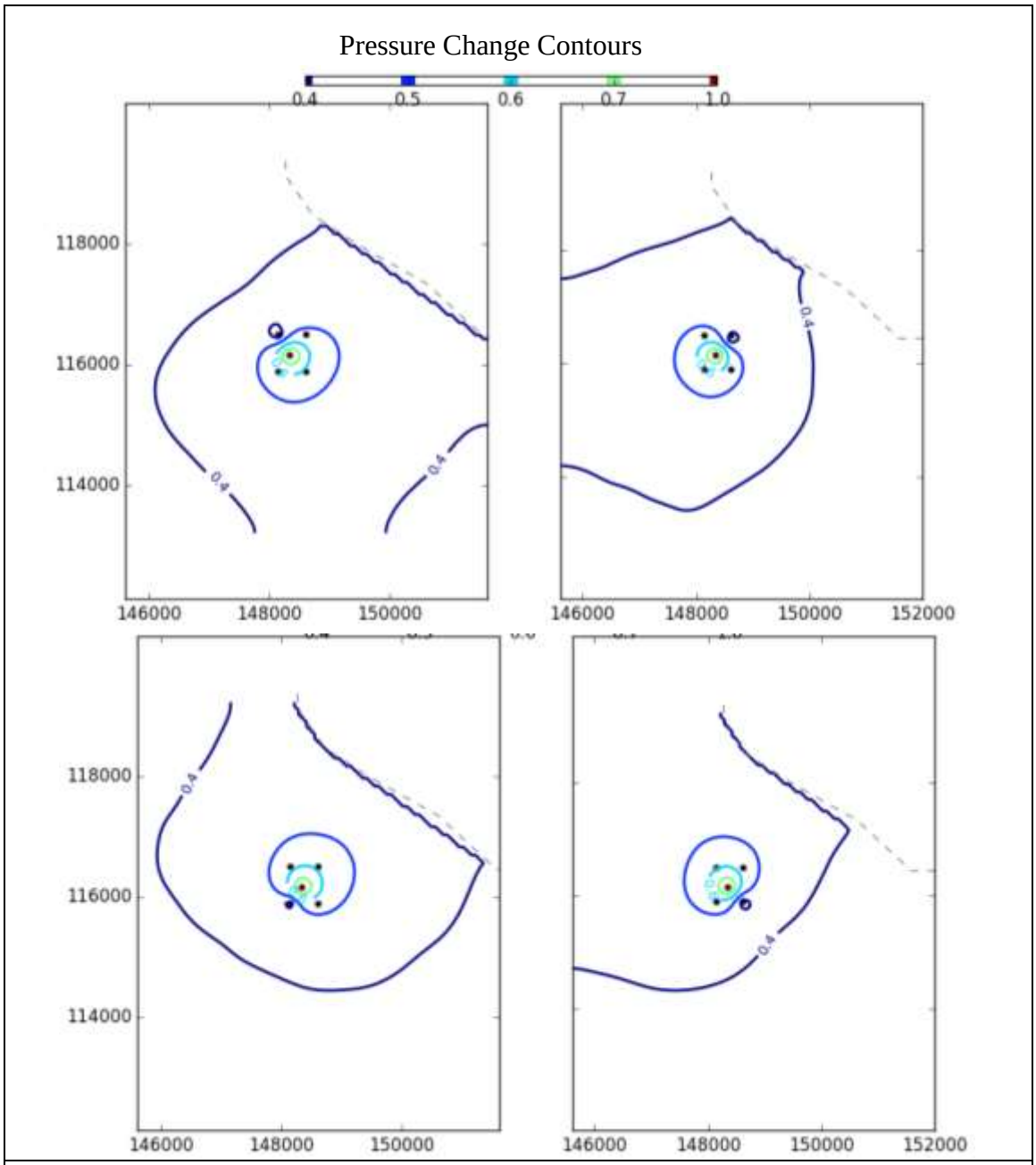

Figure 55B: The effect of production well location on overpressure plume in the reservoir. The figures show the predicted overpressure contours at the end of the simultaneous injection/production phase.

The impacts of the pressure management strategies are apparent in many of the plots. For example, in **Figure 56A (and 55B)**, the ability to control the shape of the overpressure plume by various combinations of production wells is apparent. Overpressure cones of depression at production wells are easily identified in the overpressure contours. The ability to direct the overpressure plume away from a single producer is apparent in the 2nd to 4th rows. The reduction in overpressure from the scenario without production (top row) to including a single production

well (2^{nd} to 4^{th} row) to including two production wells (5^{th} and 6^{th} rows) is easily identified by the contour color changes across these row.

This plotting scheme is replicated in **Figures 56B, 56C, and 56D**, where various reservoir compartmentalization scenarios are investigated. In these figures, overpressure contours are affected by the existence of the sealing faults. In these cases, overpressure contours stack up on fault boundaries over time adding complexity to the overpressure plume. The effect of reservoir compartmentalization on pressure management strategies can be investigated in these plots. For example, comparisons of pressure contours along Fault #1 and the Jim Bridger Fault for alternative production wells scenarios are easily made in these figures.

In **Figure 57**, we combine the last columns of **Figures 56A, 56B, 56C, and 56D** (overpressure contours at year 2) to allow reservoir compartmentalization inter-comparisons in the same figure. This indicates that reservoir compartmentalization will have a significant effect on overpressures throughout the reservoir and represents a major source of uncertainty for pressure management design.

Figures 56A, 56B, 56C, 56D, and57 are information rich representations of general spatial and temporal characteristics of alternative compartmentalization scenarios and pressure management strategies. A multitude of questions concerning reservoir scale field test design can be drawn from careful inspection and comparison of these figures.

We provide a more detailed inspection of simulation results at point locations in **Figures 58, and 59**. Production flow rates at the SW, NE, and NW wells are plotted in **Figure 58**. The stepped injection rate is plotted as a dashed line for reference. Based on this analysis, the production rate is only incrementally impacted by reservoir compartmentalization, with the largest production rates associated with both faults acting as sealing faults in general, although in most cases, there is little difference. The lack of sensitivity of production rate to reservoir compartmentalization is likely due to the close proximity of the producers to the injection well (1000 ft). For CO_2 injection, producers would be located farther away from the injector to avoid CO_2 breakthrough at the producer, and may be more significantly impacted by reservoir compartmentalization.

Figure 59 presents similar information, dividing the production flow rates by the injection flow rate to produce production/injection ratios. This analysis indicates that if two wells are producing at hydrostatic pressure, the simulated ratio is below 0.4 (last two rows). However, if only one well is producing at hydrostatic, the ratio is around 0.55 depending on the compartmentalization scenario (top three rows). Therefore, to maintain hydrostatic pressure at a point around 1000 feet from the injector would require a production rate of around half of the injection rate. To maintain hydrostatic pressure at two locations around 1000 feet from the injector would require a production rate of up to 80 % (40 % at each producer) of the injection rate.

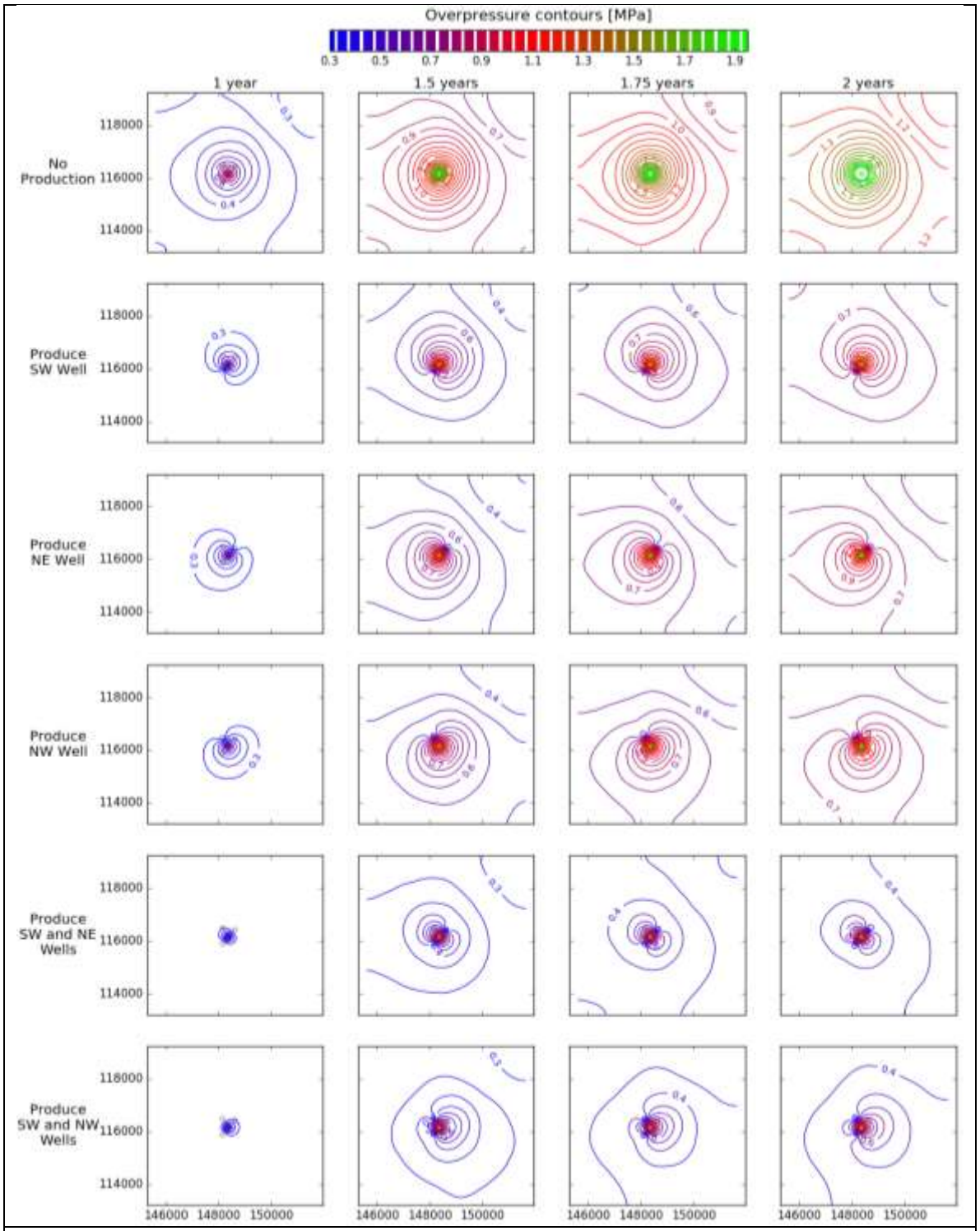

Figure 56A: Overpressure contours without sealing faults present (boundaries are no flow). Contour interval is 0.5 MPa. The matrix of plots present different times (columns) and different pressure management production scenarios (rows). Open circles indicate well locations. Axes are in the SPCS27-4903 coordinate system in meters.

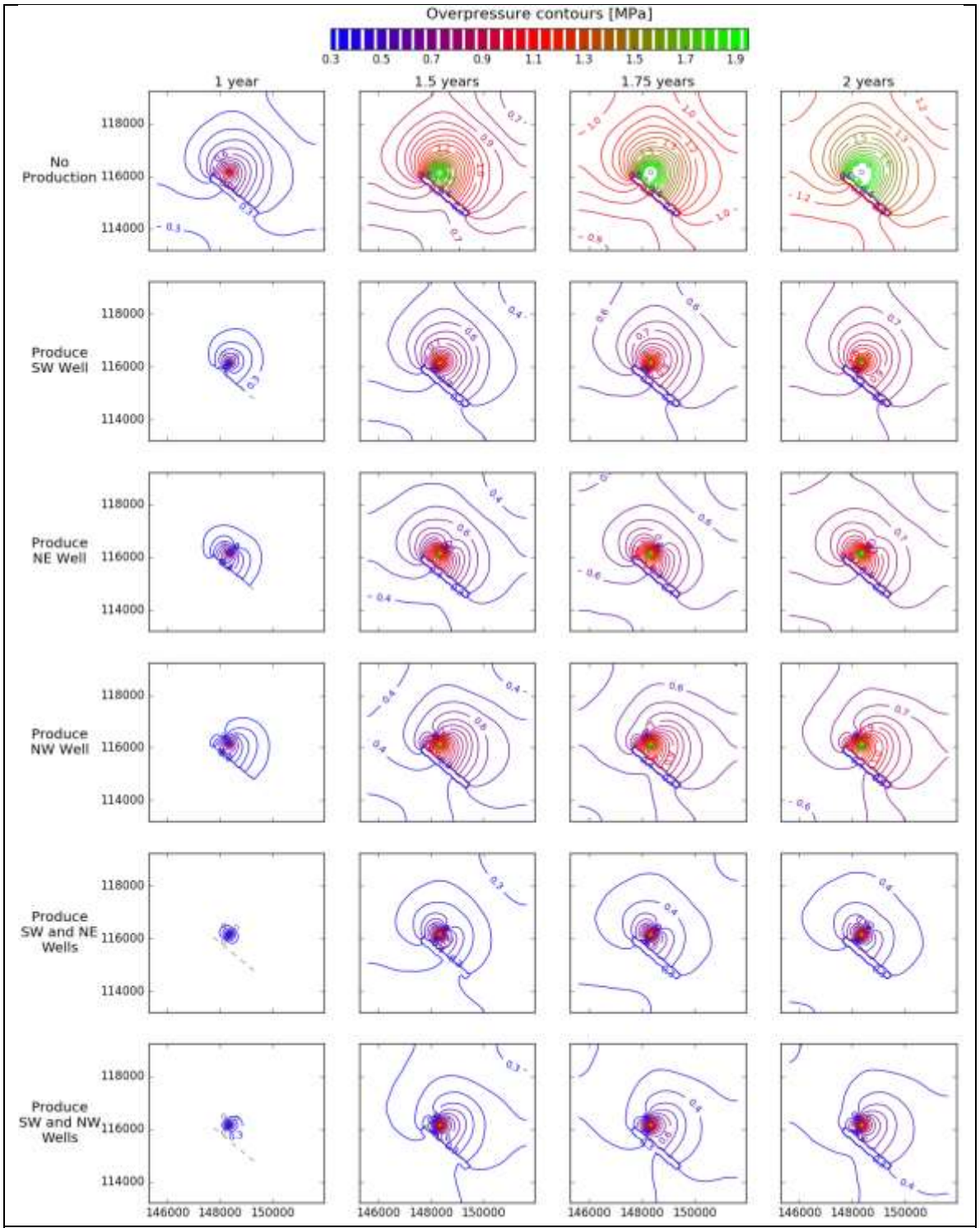

Figure 56B: Overpressure contours in MPa with Fault #1 as a sealing fault. Contour interval is 0.5 MPa. The matrix of plots present different times (columns) and different pressure management production scenarios (rows). A dashed line indicates Fault #1 and open circles indicate well locations. Axes are in the SPCS27-4903 coordinate system in meters.

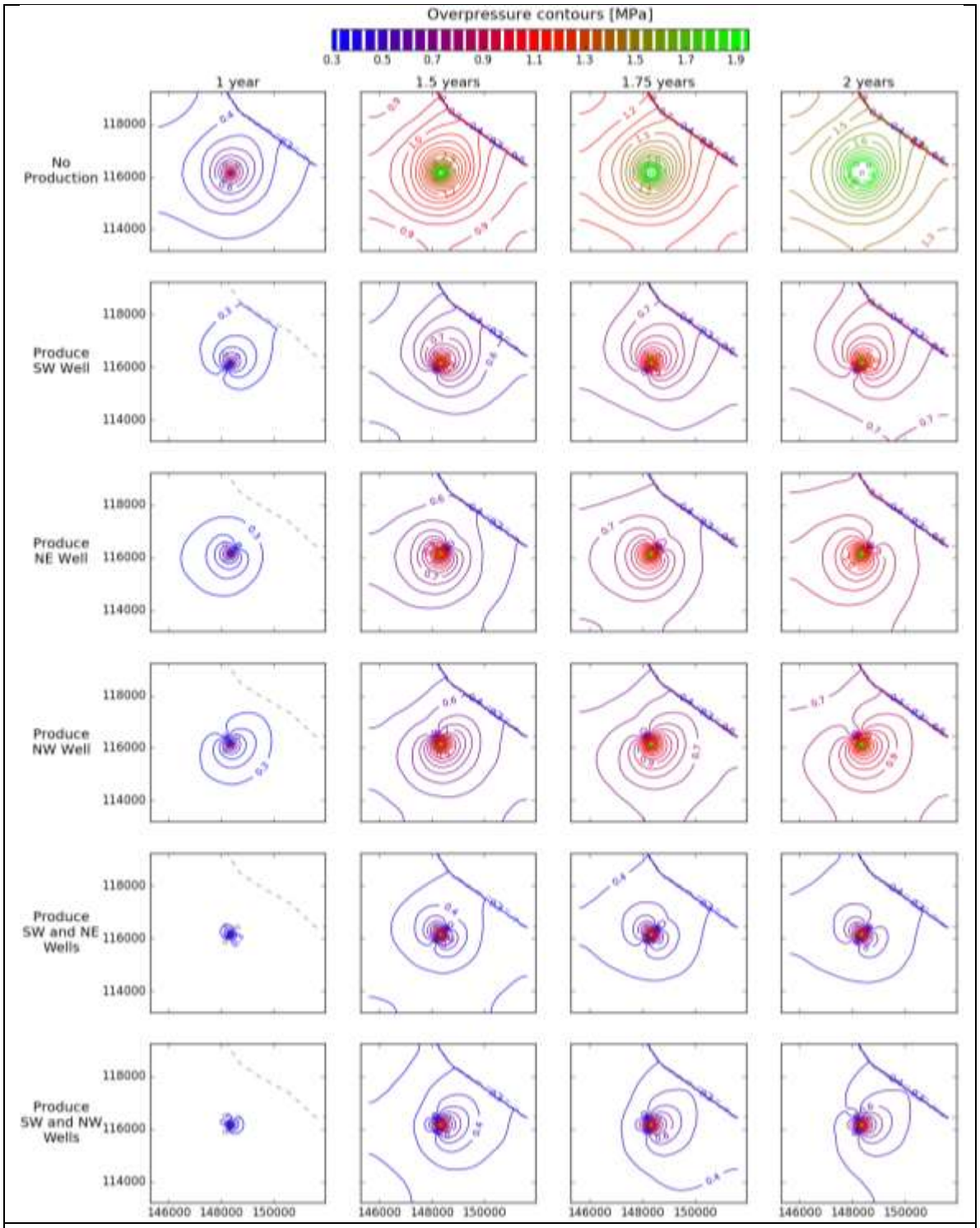

Figure 56C: Overpressure contours in MPa with Jim Bridger Fault as a sealing fault. Contour interval is 0.5 MPa. The matrix of plots present different times (columns) and different pressure management production scenarios (rows). A dashed line indicates the Jim Bridger Fault and open circles indicate well locations. Axes are in the SPCS27-4903 coordinate system in meters.

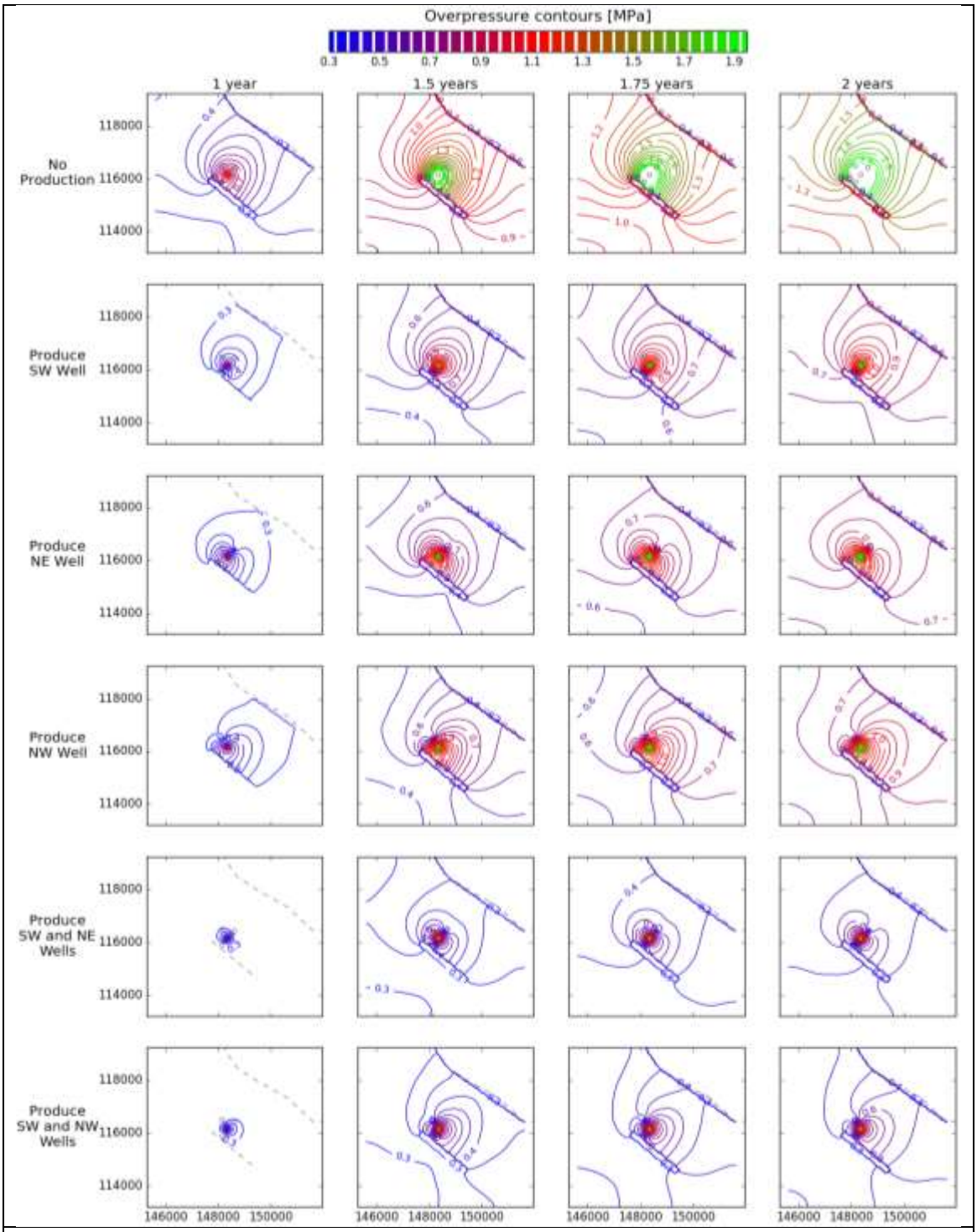

Figure 56D: Overpressure contours in MPa with Fault #1 and Jim Bridger Fault as sealing faults. Contour interval is 0.5 MPa. The matrix of plots present different times (columns) and different pressure management production scenarios (rows). Dashed lines indicate Fault #1 and the Jim Bridger Fault and open circles indicate well locations. Axes are in the SPCS27-4903 coordinate system in meters.

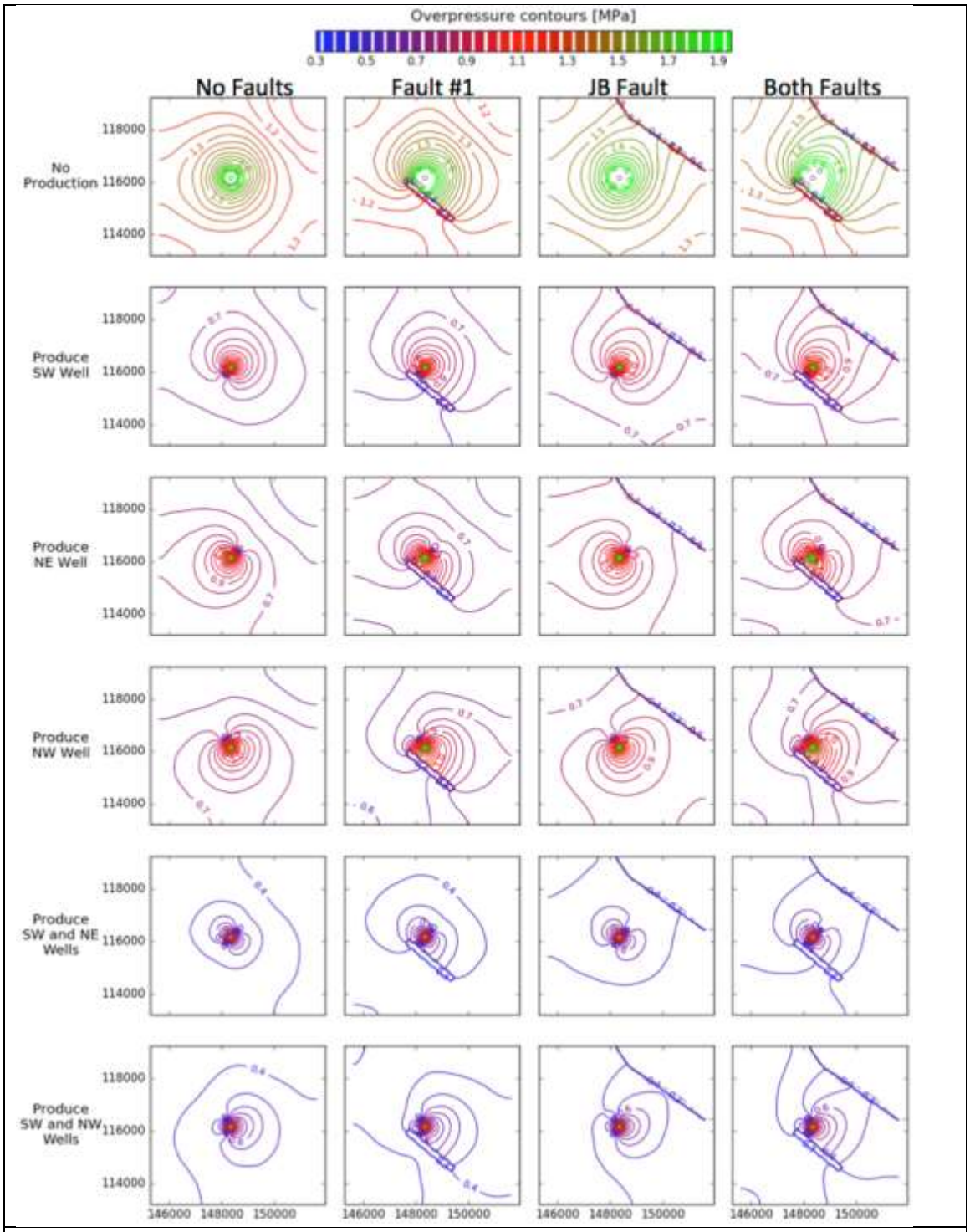

Figure 57: Overpressure contours at 2 years. Contour interval is 0.5 MPa. The matrix of plots present different reservoir compartmentalization scenarios (columns) and different pressure management production scenarios (rows). Dashed lines indicate Fault #1 and the Jim Bridger Fault and open circles indicate well locations. Axes are in the SPCS27-4903 coordinate system in meters.

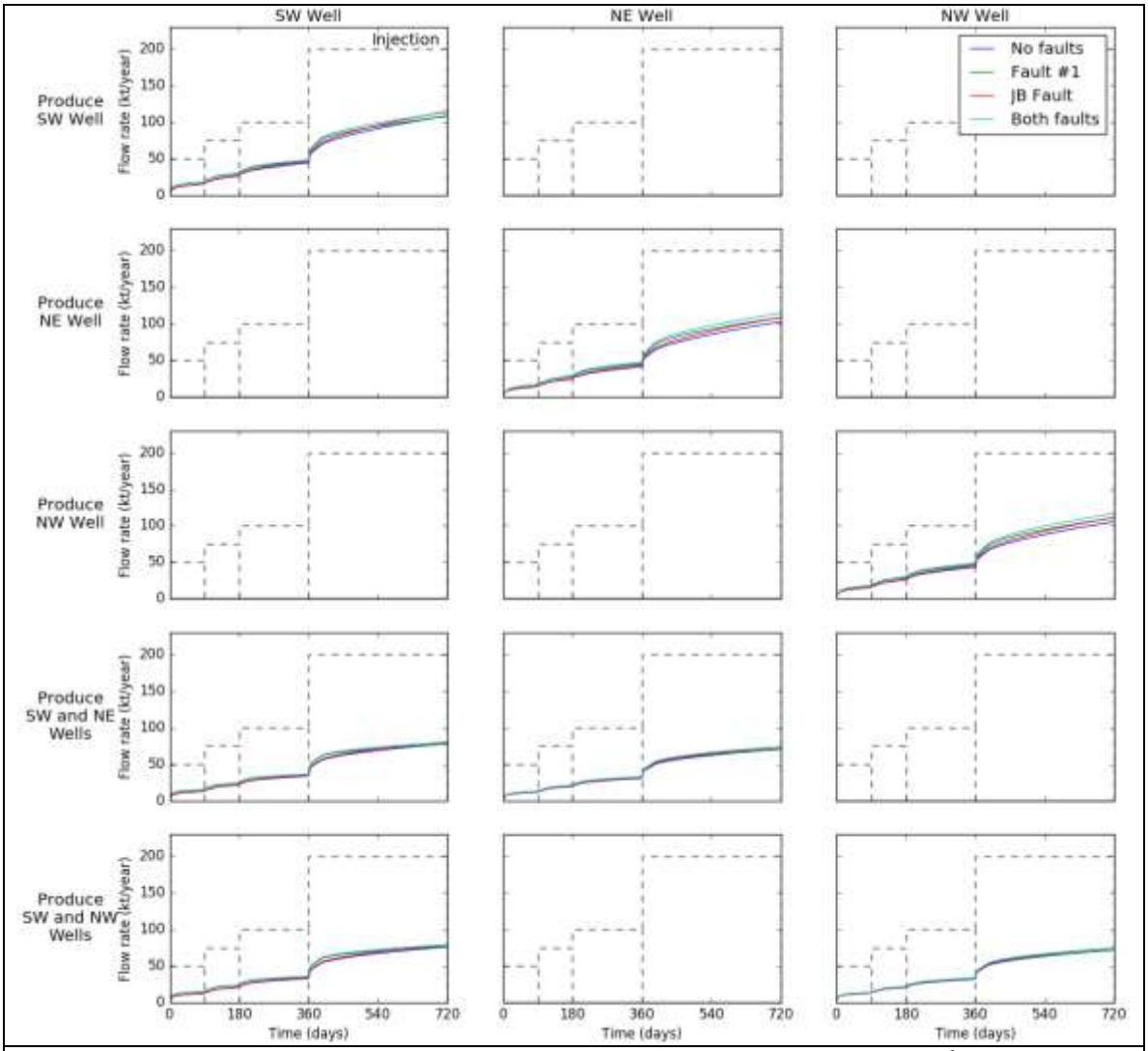

Figure 58. Production flow rate time series at SW Well (1st column), NE Well (2nd column), and NW Well (3rd column). Stepped injection flow rates are plotted as dashed lines for reference. Rows contain different pressure management scenarios. The colored lines in each plot indicate different reservoir compartmentalization scenarios, including no sealing faults present, Fault #1 is sealing, Jim Bridger (JB) Fault is sealing, and both faults are sealing.

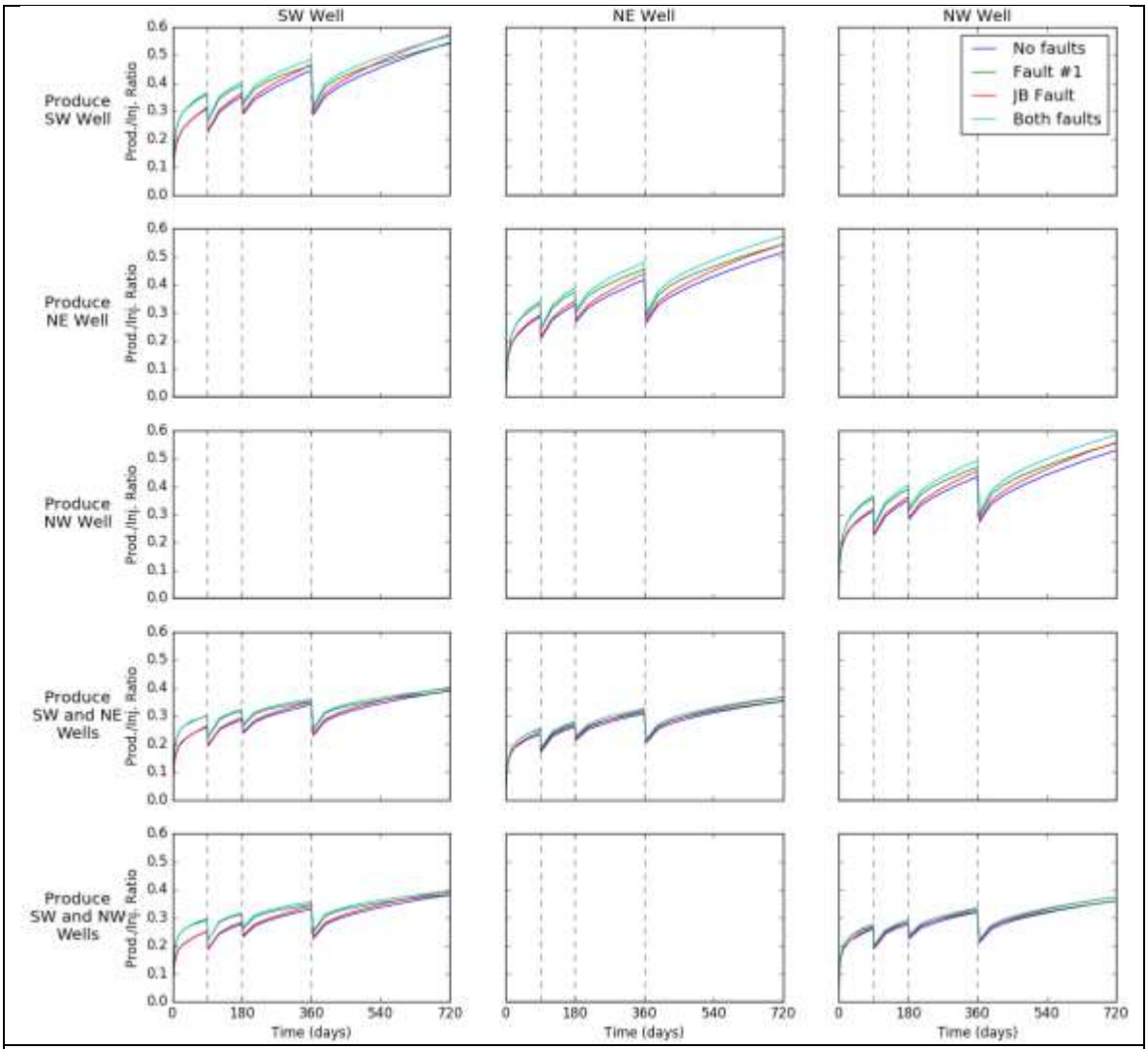

Figure 59. Production versus injection ratio time series for the northeast (NE) and southwest (SW) wells. Vertical gray dashed lines indicate times of injection rate step changes. Columns contain different pressure management scenarios indicating the overpressure to begin producing at the NE and SW wells. The colored lines in each plot indicate different reservoir compartmentalization scenarios, including no sealing faults present, Fault #1 is sealing, Jim Bridger (JB) Fault is sealing, and both faults are sealing.

Direct monitoring of pressures at the injection, producer, and monitoring wells will be important observations made during the test. **Figure 60** presents simulated overpressures at the injector, NE, SW, NW wells, and the maximum simulated overpressure along the Jim Bridger Fault.

The lack of overpressure when the producers are active (producing enough brine to remain at hydrostatic, 0 MPa overpressure) is apparent in many of the plots. The effect of reservoir compartmentalization leads to the largest pressure occurring when both faults are sealing and the lowest pressures when no faults are sealing, in general, which is apparent by noting the ordering of colored lines in each plot. Based on the first row of plots, we expect that overpressures will

not reach 2 MPa at the production wells until nearly 2 years if none of the wells are producing. The point at which 2 MPa is reached is easily identified for the SW Well as the overpressure curve flattens at this level for the Fault #1 and both faults scenarios (first row, 3rd column).

If one well is producing, the other wells reach overpressures slightly greater than 1 MPa. SW Well has higher overpressures when Fault #1 is sealing due to its proximity to this fault, reaching closer to 1.5 MPa. If two wells are producing, the other well reaches an overpressure of around 0.75 MPa. Overpressure at the Jim Bridger Fault reaches 1.5 MPa if no production occurs and both faults are sealing. This is reduced to around 0.75 MPa if one well is producing and around 0.5 MPa if two wells are producing. The combination of producing wells does not appear to have a significant affect on the overpressure at the Jim Bridger Fault.

The effect of alternative pressure management strategies can be investigated by comparing plots along columns, with practically no pressure management on the top and two wells producing on the bottom two rows.

D. Pressure Management Decision Analysis

The modeling analyses above provide comparisons of overpressures and production rates between pressure management strategies and compartmentalization scenarios. Analyzing these simulations is a relatively inexpensive and efficient means to inform field test design decisions. In this section, we describe a formal approach to use these simulations to quantify the robustness of alternative test design decisions given uncertainties and lack of information concerning the conditions in the reservoir (i.e., Madison formation and other stratigraphic layers).

A large amount of data collection and analyses have been performed at the Rock Springs Uplift site (Surdam, 2013). These data and analyses are extremely informative in characterizing conditions in the reservoir. However, this still constitutes direct data collection from a single well at the depths of interest (RSU #1) and indirect measurements of properties from geophysical surveys. There still remains significant uncertainty and lack of information concerning lateral porosities and permeabilities away from RSU #1 and locations of faults and their sealing capacities. In order to make robust test design decisions, these uncertainties and gaps in information will have to be considered.

In this section, we describe a formal approach to quantify the robustness of alternate test design decisions. The approach utilizes concepts from information gap theory (Ben-Haim, 2006; Harp and Vesselinov, 2013). The main outcome of the analysis is a metric of robustness, where robustness quantifies the ability to be incorrect in our characterization of the reservoir and still meet design criteria.

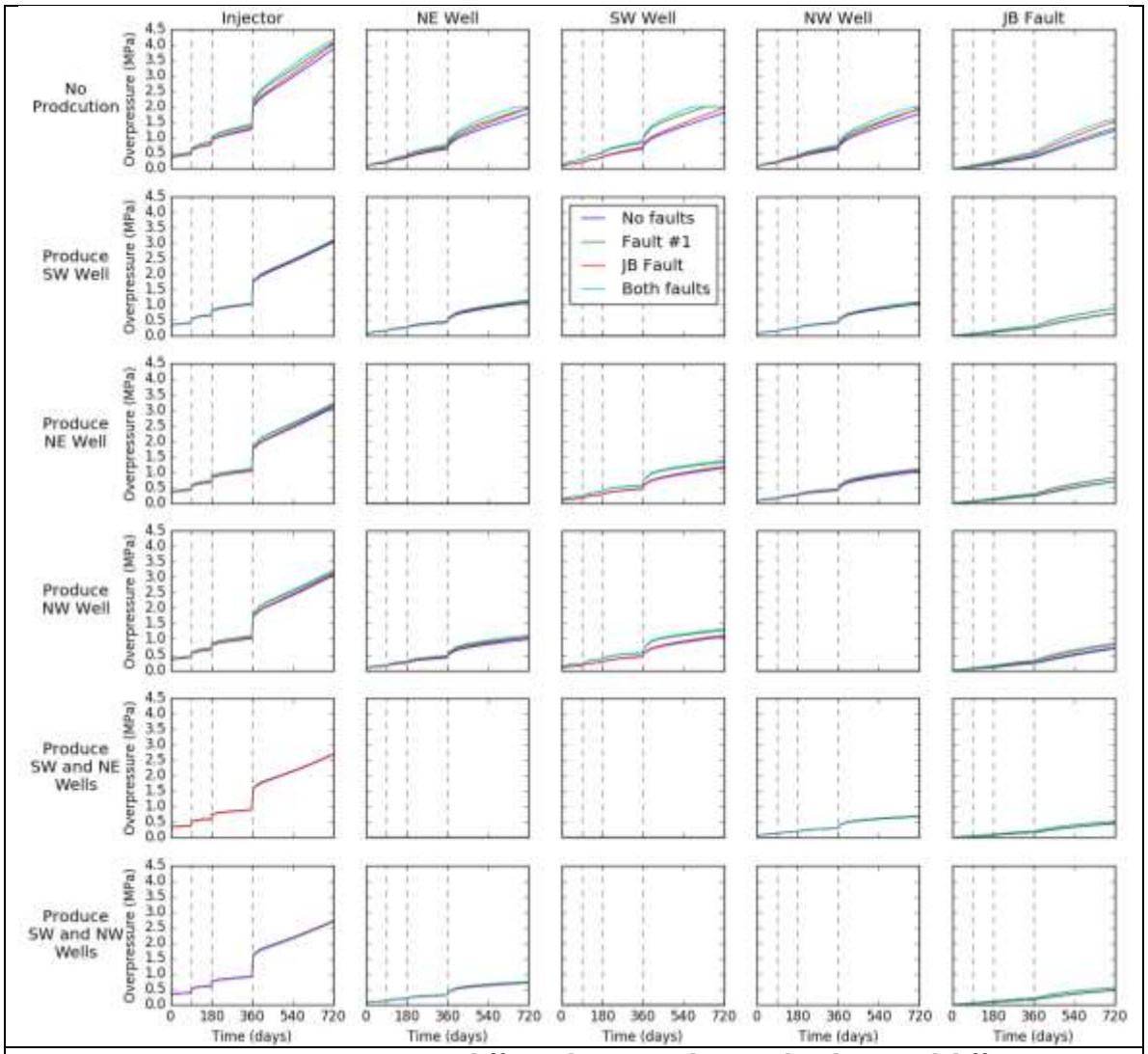

Figure 60: Overpressure time series at different locations along each column and different pressure management strategies along each row. The colored lines in each plot indicate different reservoir compartmentalization scenarios, including no sealing faults present, Fault #1 is sealing, Jim Bridger (JB) Fault is sealing, and both faults are sealing.

The extensive analyses in Surdam (2013) provide us with reasonable nominal model parameters to characterize the reservoir. For example, the analysis of well logs, core, and 3D seismic survey provide nominal heterogeneous permeabilities. These nominal properties provide the best estimate of the reservoir permeability field, and are currently the most reasonable estimates to use in making test design decisions. However, there remains significant uncertainty and lack of information concerning the permeability field.

A probabilistic characterization of permeability uncertainty in this case is ill defined as the only source of this type of information is from the 3D seismic survey, an indirect source of information with a high degree of interpretation. A probabilistic (Bayesian) decision analysis

would require the specification of prior probabilistic distributions of parameters (e.g., parameters defining the spatial distribution of permeabilities), which is not warranted here. A robust Bayesian analysis, exploring the sensitivity of alternative priors, would help build confidence in Bayesian decision analysis; but would require a set of Bayesian analyses, each with significant computational cost.

We describe a non-probabilistic approach to quantifying the robustness of alternative decisions using concepts from information gap theory. The approach is different than optimization strategies in that the robustness of alternative decisions is evaluated as opposed to searching for the optimal solution. The downside of optimal solutions is that they often have no robustness. In the search for the optimal solution (i.e., the solution that meets design specifications, reduces costs, saves time, etc.), a solution is identified that is on the verge of failing if our characterization of the system is incorrect. The alternate approach of quantifying decision robustness guides decision makers in the evaluation of the risk of failure of alternate decisions.

We focus on the uncertainty associated with the seismically derived permeabilities of the Lower Madison Formation. A permeability modifier that translates the Lower Madison permeabilities by a specified order of magnitude parameterizes this uncertainty as

$$k_{LMm}^{mod}(\mathbf{x}) = f_k k_{LMm}(\mathbf{x}) \text{ , (1)}$$

where k is permeability, f_k is the order of magnitude modifier, and $\mathbf{x}$ defines vector locations within the Lower Madison Formation.

We define an uncertainty model as nested sets of values of f_k that expand from its nominal value. The nominal value of f_k is zero, since this is the case where Lower Madison permeabilities are not modified from the seismically derived values. Therefore, we can define an uncertainty model as

$$U(h) = \{f_k : |f_k| \leq h\}, h \geq 0, \text{ (2)}$$

where h defines the boundary of the nested sets around $f_k = 0$, often referred to as the horizon of uncertainty in information gap theory. It should be apparent that U is a set-based uncertainty model without bounds (i.e., h has no upper bound), as opposed to probabilistic, distribution-based uncertainty models. The uncertainty model U allows us to explore the implications of deviations from nominal without requiring probabilistic assumptions.

The performance criterion for the test design is to not exceed a critical overpressure that would lead to a seismic event at the Jim Bridger Fault:

$$\mathrm{d}p_{JBF} = \max\left(\mathrm{d}p\left(\mathbf{x}_{JBF}\right)\right) \leq \mathrm{d}p_{crt}, \text{ (3)}$$

where dp is overpressure (pressure above hydrostatic), $\mathbf{x}_{JBF}$ are vector locations along the Jim Bridger Fault, and dp_{crt} is the overpressure criterion at the Jim Bridger Fault. It is assumed that the Jim Bridger Fault is a sealing fault and that Fault #1 is not, or does not exist.

The alternative decisions to select from are the location of the producer or producers ($\mathbf{x}_p$) and the overpressure at which the producer will start producing and maintain thereafter ($\mathrm{d}p_p$).

We define robustness as the amount that Lower Madison permeabilities can be modified and the overpressure criterion at the Jim Bridger Fault is not exceeded. Using equations (2) and (3), we describe this mathematically as

$$\hat{h}(\mathbf{x}_p, \mathrm{d}p_p, \mathrm{d}p_{crt}) = \max\left\{h: \left(\max_{f_k \in U(h)} \mathrm{d}p_{JBF}\right) \leq \mathrm{d}p_{crt}\right\} \quad (4)$$

Since the overpressure criterion at the Jim Bridger Fault ($\mathrm{d}p_{crt}$) is also unknown or uncertain, and may be a factor that ultimately needs to be "decided", it is included as an input to the robustness, $\hat{h}$.

The plots along the top in **Figure 61** contain maximum overpressures along the Jim Bridger Fault after 2 years ($\mathrm{d}p_{JBF}$) given the step-rate injection regime presented Figure 58 plotted as a function of the order-of-magnitude modification to the Lower Madison Formation permeabilities (f_k). In Figure 61, the left column is associated with producing at the NE Well only, while the right column is associated with producing at both the NE and SW Wells. Producing at both the NE and SW wells leads to the greatest reduction in Jim Bridger Fault overpressures for smaller values of overpressure production threshold, $\mathrm{d}p_p$ (compare the difference in the blue curves in the left and right plots in the top row of **Figure 61** versus the lack of difference in the turquoise curves). This is due to the lag time in starting to produce in these cases while pressure builds.

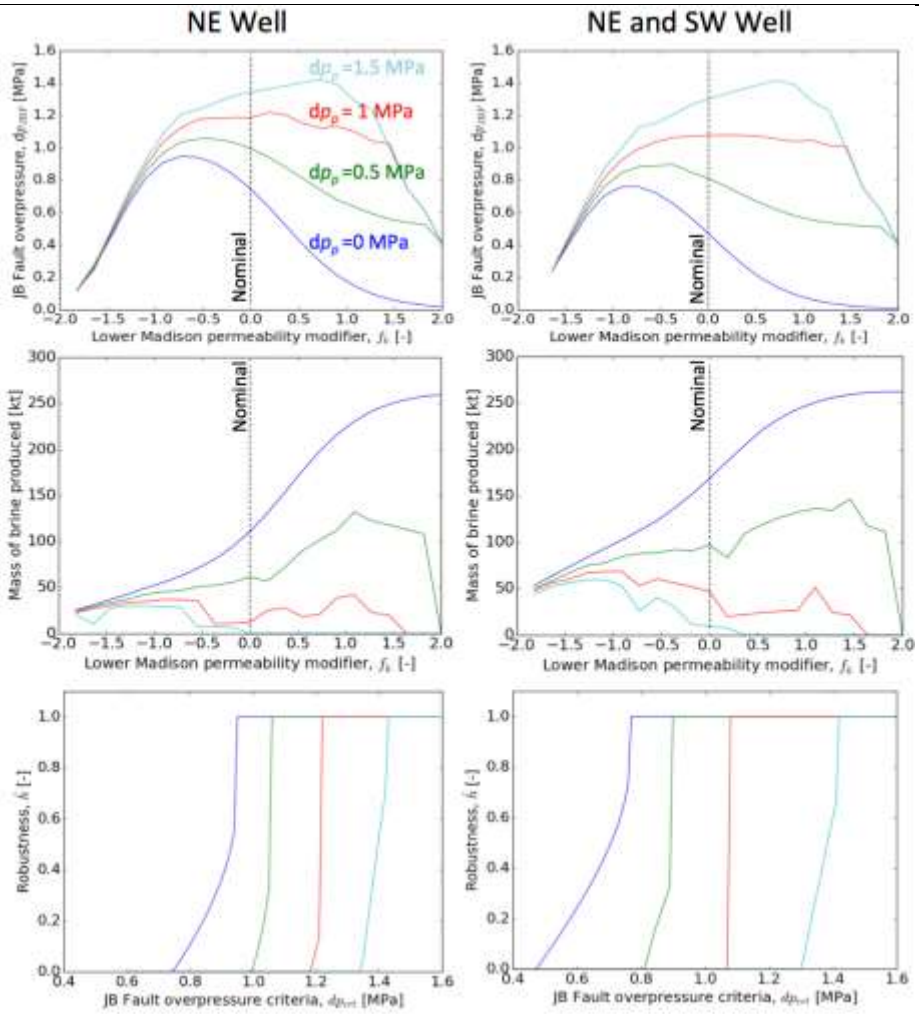

Figure 61: Decision analysis comparing robustness of producing at 0, 0.5, 1, and 1.5 MPa overpressure (colored lines) at the NE Well only (left column) and the producing at the NE and SW Wells (right column). On the top row are plots of maximum overpressure at 2 years at the Jim Bridger (JB) Fault versus the order of magnitude modification to the Lower Madison permeabilities. The middle row contains plots of the mass of brine produced as a function of permeability modifier. Vertical dashed lines identify the nominal permeability modifier in the 1st and 2nd rows of plots. The bottom row of plots contains robustness curves for alternative decision versus overpressure criteria at the Jim Bridger Fault.

Overpressures at the Jim Bridger Fault trend towards zero for extremely large positive or negative permeability modifications from nominal. As permeabilities decrease, overpressures are restricted closer to the RSU #1 fault, and do not reach the Jim Bridger Fault. While, as permeabilities increase, overpressures easily distribute uniformly throughout the reservoir.

It is also interesting to note that for dp_p equal to 0 and 0.5 MPa (blue and green curves), overpressures increase as permeabilities are decreased from nominal, while for 1 MPa (red curve), overpressures are nearly flat around nominal, and for 1.5 MPa (turquoise curve), overpressures increase with increasing permeabilities. The reversal in sensitivity is due to a lack

of production at higher production overpressure thresholds, as apparent in the middle row of plots in **Figure 61**, which contain the mass of brine produced as a function of modification to permeability (turquoise curve goes to zero at higher values of f_k).

The mass of brine produced is a surrogate for the cost of alternative test designs. Increased mass of brine produced is expected to be associated with higher costs due to treatment and disposal. At nominal, producing the NE Well at hydrostatic overpressure results in producing around 100 kt of brine (blue curve, center-left plot), while producing both the NE and SW Wells results in producing around 170 kt of brine (blue curve, center-right plot). This provides an indication of the potential additional cost associated with producing brine at two wells as opposed to one.

It is also important to note that the uncertainty in the Lower Madison permeability leads to significant variation in the amount of brine produced. For example, in the case of producing only at the NE Well, underestimating the permeability by an order of magnitude ($f_k = 1$ in the left middle plot of **Figure 61**) results in more than two times the brine production. Similarly, underestimating the permeability by an order of magnitude ($f_k = -1$) results in around half the brine production. Similar, albeit less dramatic effects are seen in the right middle plot of **Figure 61** when producing the NE and SW wells.

The top plots of Figure 15 provide the necessary information to quantify the robustness of alternative decisions via equation (4) plotted in the bottom plots in **Figure 61**. In these plots, it is apparent, not surprisingly, that producing at both the NE and SW wells is more robust than only producing at the NE well. Of course producing at two wells will lead to greater expense, as discussed above. Quantifying the gains in robustness for more expensive options is a logical approach to decision making.

Robustness is truncated at a 1 order of magnitude modification to Lower Madison permeabilities ($f_k = 1$). This is not an inherent boundary for robustness (equation (4)), but has been imposed here as a *de facto* maximum robustness to facilitate comparisons between alternative decisions.

Robustness is plotted as a function of the overpressure criteria at the Jim Bridger Fault since an appropriate value is uncertain. Plotting robustness in this way allows the evaluation of pressure management strategies given more or less conservative overpressure criteria. For example, if only the NE Well is produced, non-zero robustness is achieved only if we can accept that an appropriate overpressure criterion for the Jim Bridger Fault is at least 0.75 MPa (blue curve, left-bottom plot). This requires that the well be produced at hydrostatic. Maximum robustness is attainable in this case only if we can consider 0.95 MPa as a safe overpressure at the fault. Alternatively, if both wells are produced, more conservative fault overpressure criteria can be considered. For example, if both wells are produced at hydrostatic (blue curve, right-bottom plot), non-zero robustness can be achieved if we accept a fault overpressure criterion of greater than around 0.5 MPa and maximum robustness is achievable if we accept a fault overpressure criterion of around 0.75 MPa. For either producing at the NE well or both wells, decisions to produce at higher overpressures require accepting less conservative fault overpressure criteria.

The plots in **Figure 61** provide a logical approach to making robust decisions when encountered with non-probabilistic uncertainty. Uncertainty models for other gaps in information can be included in the analysis; for example, an uncertainty model for the sealing capacity of the Jim Bridger Fault can be included in the analysis. Other additional decisions can be evaluated, including other producer configurations or alternative injection/production regimes.

Data from field tests would refine the FEHM model, improving our characterization of the reservoir and increasing simulation accuracy. These enhancements to the FEHM model would allow refinement to subsequent decision analyses. While the field test will inject water into the reservoir, the information will lead to refinements and improvements to CO_2 injection simulations at the site. The decision analysis described here can be applied to pressure management decisions for CO_2 injection as well.

In addition to the step-rate injection coupled with constant-pressure production scenario described earlier, we also simulated scenarios with step-rate injection coupled with constant-rate production at rates 25 KT/yr and 50 KT/yr and constant-rate injection at 100 KT/yr and 200 KT/yr coupled with constant-pressure and constant-rate production. The results of these simulations are not presented here though the overall trends in these scenarios are similar to the ones shown through the results presented here. Finally, we also performed simulations of CO_2 injections to compare the differences between the predicted overpressure due to CO_2 as injecting fluid and water as injecting fluid. We will use similar approach during Phase II to demonstrate how the field test results with brine can be extended to CO_2 injections at RSU and other similar sites. Results of other injection/production scenarios with water and CO_2 will be submitted as part of the Phase I final report.

XIV. GEOMECHANICAL IMPACT ASSESSMENT

A. Laboratory Characterization of Geomechanical Properties of Reservoir Rock and Caprock

In Phase I we began to conduct triaxial coreflood experiments to investigate the impact of injection-induced stress changes on the mechanical stability and permeability of the RSU reservoir and caprock. Fourteen samples were provided to LANL for testing as shown in **Table 22**. These were provided as 1"-diameter core with lengths from 1-3".

Table 22: Samples sent to Los Alamos National Laboratory.

Sample	Depth	Formation
RSU-05	10,607.3	Dinwoody
RSU-13	10,638.1	Dinwoody
RSU-122	10,649.1	Dinwoody
RSU-125	10,671.8	Dinwoody
RSU-127	11,197.7	Weber
RSU-183	11,786.0	Weber

Sample	Depth	Formation
RSU-195	12,215.6	Amsden
RSU-199	12,224.6	Amsden
RSU-205	12,255.9	Upper Madison
RSU-212	12,323.8	Upper Madison
RSU-218	12,349.9	Madison
RSU-224	12,381.9	Madison
RSU-104	12,414.5	Madison
RSU-107	12,421.5	Madison
RSU-117	12,513.5	Madison

First we summarize the measured geomechanical properties of the core that were obtained using triaxial techniques by Core Laboratories of Houston, Texas. These are presented in **Figures 62, 63 and 64**, which show the Poisson's Ratio, Young's Modulus, and Mechanical Strength as a function of sample depth. As is typical, each of the rock formations shows quite significant scatter in the rock properties. The Young's modulus and compressive strength of the Weber is significantly greater than the Madison. The one sample of the Amsden shows a uniquely high compressive strength.

Figure 65 shows the compressive strength of the samples as a function of the confining stress used in the test. **Figure 66** isolates the strength results for the Weber and Madison Formations. These show that the Madison is a weaker formation with little change in strength with confining pressure. The strength of the Weber, however, increases significantly with confining pressure.

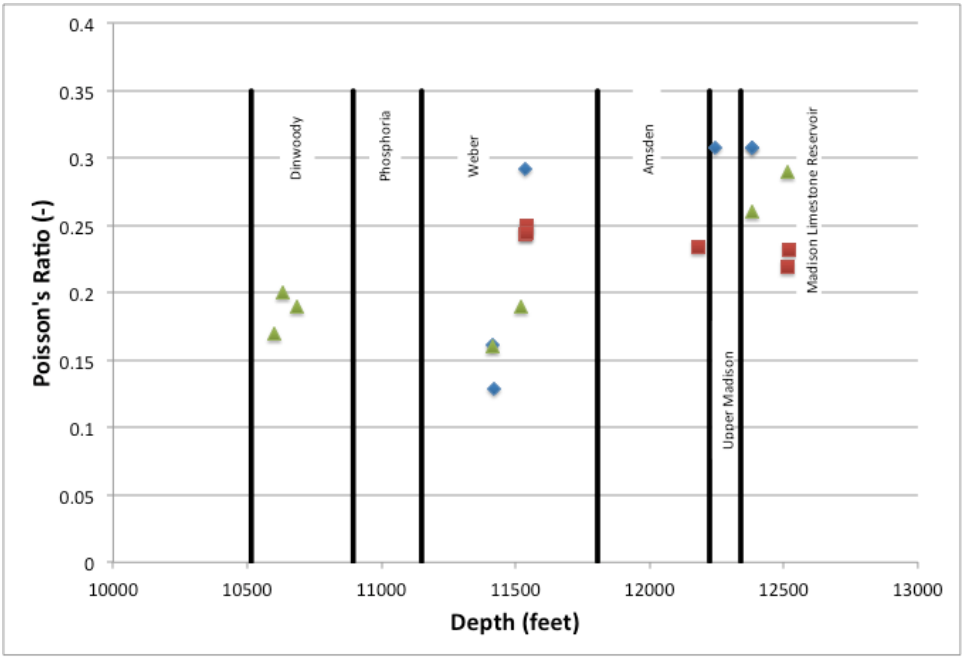

Figure 62: Poisson's ratio as a function of depth for RSU samples. The three different symbols represent different measurement series from Core Laboratories.

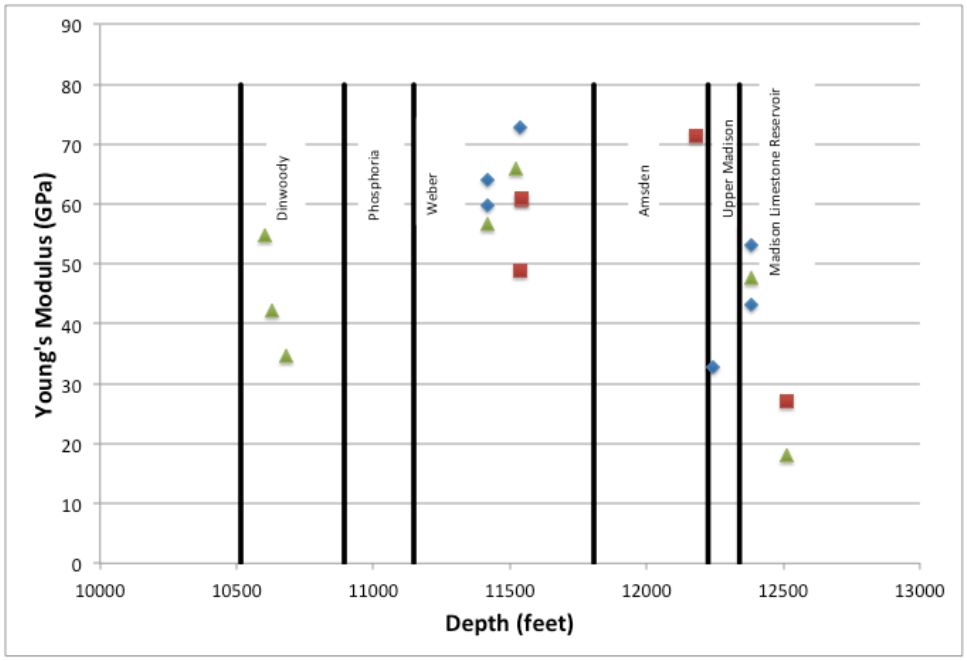

Figure 63: Young's modulus as a function of depth for RSU samples. The three different symbols represent different measurement series from Core Laboratories.

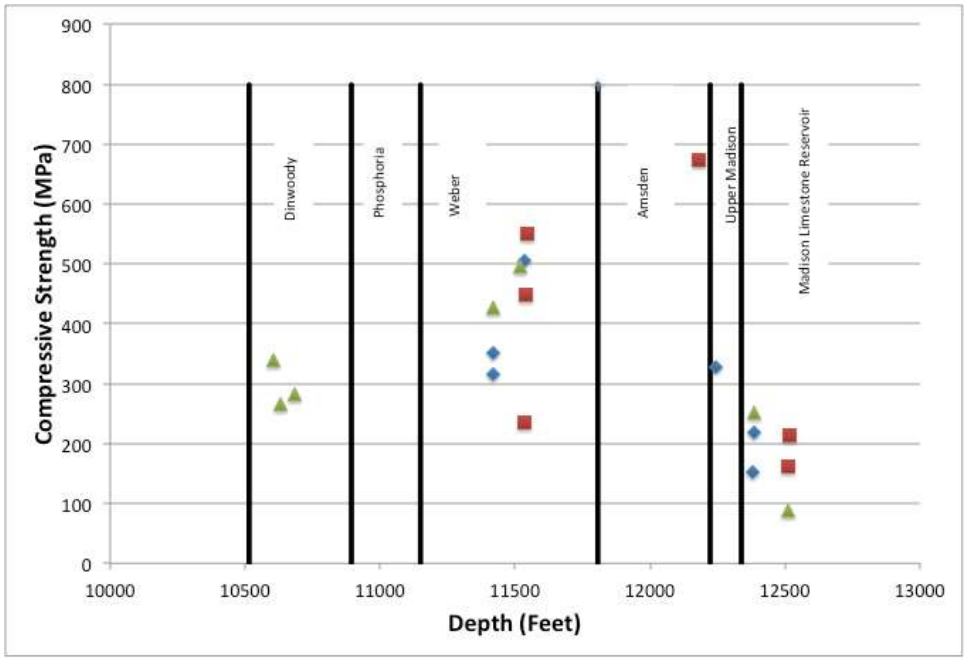

Figure 64: Compressive strength as a function of depth for RSU samples. The three different symbols represent different measurement series from Core Laboratories.

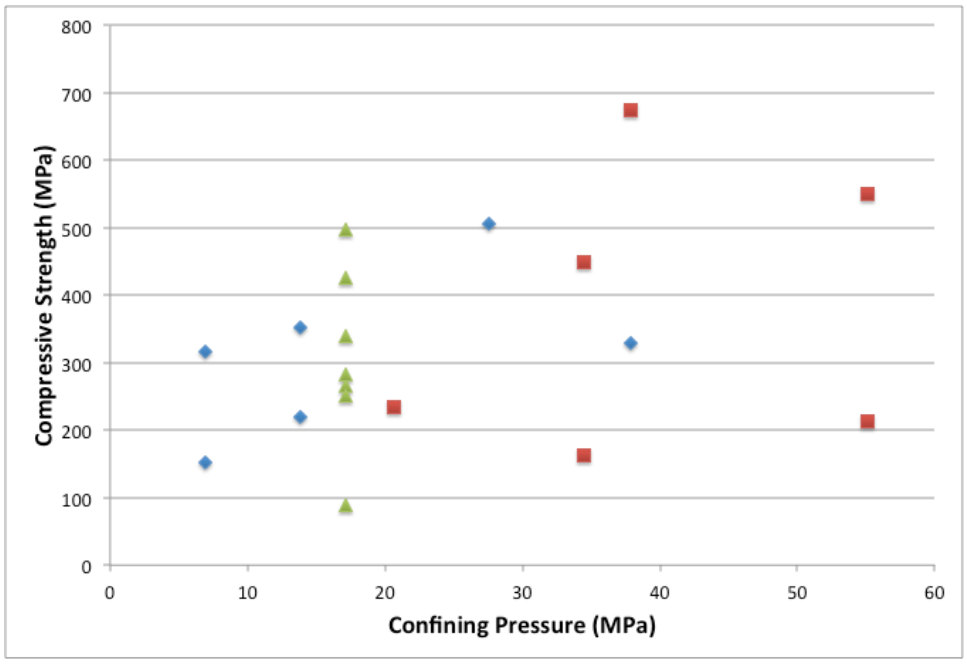

Figure 65: Compressive strength as a function of confining strength. There is a significant range of compressive strengths but there is a slight tendency toward increasing strength with increasing confining pressure. The three different symbols represent different measurement series from Core Laboratories.

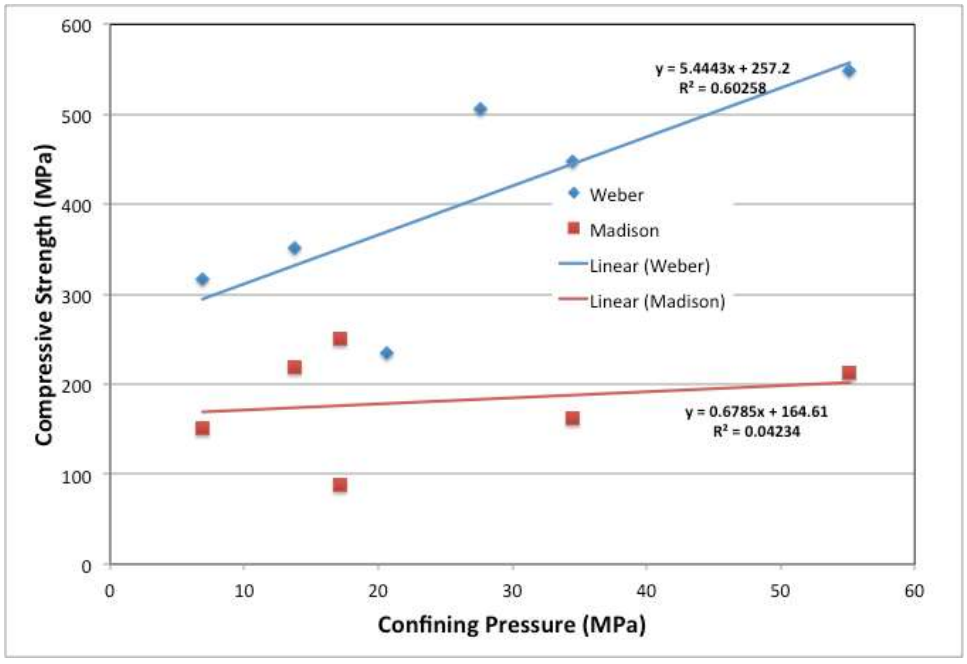

Figure 66: Compressive strength as a function of confining strength for the Weber and Madison Formations. The Weber is much stronger than the Madison (cf., **Figure 64**). The Madison has no distinct trend in strength versus confining pressure, while the Weber becomes much stronger with increasing confining pressure.

Background:

The experimental program is designed to determine the mechanical response of the reservoir and caprock samples to fluid injection. The most significant potential response is the creation or activation of fractures by increased pore pressure. In this project, we focus on determining changes in permeability resulting from fracture of core as input to understanding the permeability of the Weber and Madison reservoirs and the caprock leakage potential of the Dinwoody and Amsden/Upper Madison caprock seals. We also record acoustic emission data to provide insight into potential microseismic events.

In order to design the experiments, we consulted the 2013 University of Wyoming Master's thesis of Luke Shafer: "Assessing injection zone fracture permeability through the identification of critically stressed fractures at the Rock Springs Uplift CO_2 sequestration site, SW Wyoming". The thesis analyzes stress conditions within the reservoir and provides very useful results for analyzing the potential for injection-induced rock failure at RSU. The results from Shafer's report for the Madison Formation are summarized in **Table 23**.

The conditions for the Madison (vertical stress = 92 MPa, horizontal stress = 57 MPa) exceed the capabilities of direct simulation in our triaxial device. However, we can simulate the effective stresses: $\sigma' = S - P_p$, where S is the total stress and P_p is the pore pressure. Thus we chose the "zero pore-pressure" option shown in **Table 23**, which uses a horizontal stress of 24 MPa with zero pore pressure to simulate the effective normal stress on an optimally oriented fracture.

Table 23: Summary of critical stress calculations for the Madison formation from Luke Shafer's thesis.

Data from Luke Shafer's Thesis				
Total Vertical Stress	92.2518888	MPa	13380	psi
Total Maximum Horizontal Stress	73.084456	MPa	10600	psi
Total Minimum Horizontal Stress	56.8128224	MPa	8240	psi
Pore Pressure	37.0938088	MPa	5380	psi
Biot Coefficient	0.835			
Poisson's Ratio	0.25			
Internal Friction Coefficient	0.624			
Fracture Friction Coefficient	0.6			
Sliding Friction Coefficient	0.7			
Assumed Friction Coefficient	0.624			
Intermediate Values				
Assumed Friction Angle	0.557879891	rad	31.96416323	deg
Effective Vertical Stress	61.27855845	MPa	8887.7	psi
Effective Maximum Horizontal Stress	42.11112565	MPa	6107.7	psi
Effective Minimum Horizontal Stress	25.83949205	MPa	3747.7	psi
S	43.55902525	MPa	6317.7	psi
T	17.7195332	MPa	2570	psi
Optimum Oriented Critical Fracture				
Orientation to Min. Horizontal Stress	0.506458218	rad	29.01791839	deg
Effective Normal Stress on Fracture	34.17850403	MPa	4957.170958	psi
Shear Stress on Fracture	15.03288657	MPa	2180.335003	psi
Shear Stress for Fracture	21.32738652	MPa	3093.274678	psi
Effective Normal Stress for Fracture	24.09116437	MPa	3494.126608	psi
Pore Pressure Change for Fracture	12.08064631	MPa	1752.148923	psi
Critical Effective Vert. Stress for Fracture	51.19121879	MPa	7424.65565	psi
Critical Effective Max. Horiz. Stress for Fracture	32.02378599	MPa	4644.65565	psi
Critical Effective Min. Horiz. Stress for Fracture	15.75215239	MPa	2284.65565	psi
Critical Pore Pressure for Fracture	49.17445511	MPa	7132.148923	psi
Conditions for Triaxial Direct-Shear Experiment				
Zero-Pore Pressure Option				
Confining Stress	24.09116437	MPa	3494.126608	psi
Pore Pressure	0	MPa	0	psi
Failure by Pressure Increase				
Confining Stress	34.17850403	MPa	4957.170958	psi
Pore Pressure (Final)	12.08064631	MPa	1752.148923	psi
Full Reservoir Conditions				
Confining Stress	56.8128224	MPa	8240	psi
Pore Pressure (Final)	49.17445511	MPa	7132.148923	psi

A Mohr-Coulomb failure analysis for a pre-existing (cohesionless) fracture in the Madison based on **Table 23** is shown in **Figure 67**. The yellow circle shows the undisturbed stress conditions for the Madison, while the green circle represents the shift of the Mohr-Coulomb circle due to increased pore-pressure and the resulting reduction of the effective normal stress. The circle intersects the failure criteria at an effective normal stress of 24 MPa.

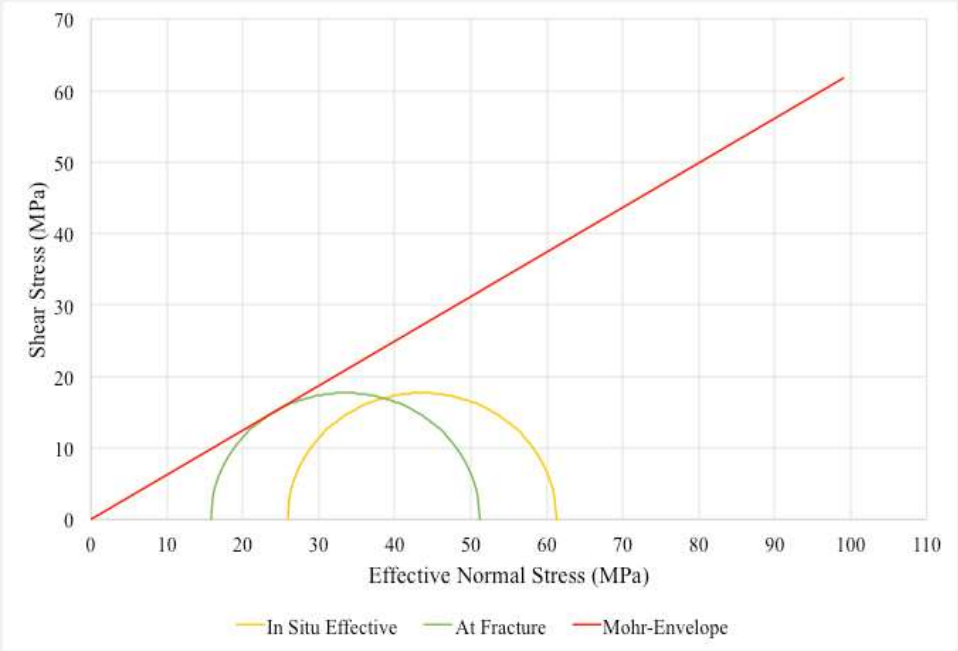

Figure 67: Mohr-Coulomb failure analysis for a pre-existing fracture in the Madison Formation based on **Table 23**. The failure envelope is based on the "assumed friction angle" in Table 2.

Shafer's thesis shows ample evidence for pre-existing fractures as shown in **Figure 68**. A conservative assumption for these fractures is that some are optimally oriented and are cohesionless. This allows application of the failure criteria in **Figure 67**.

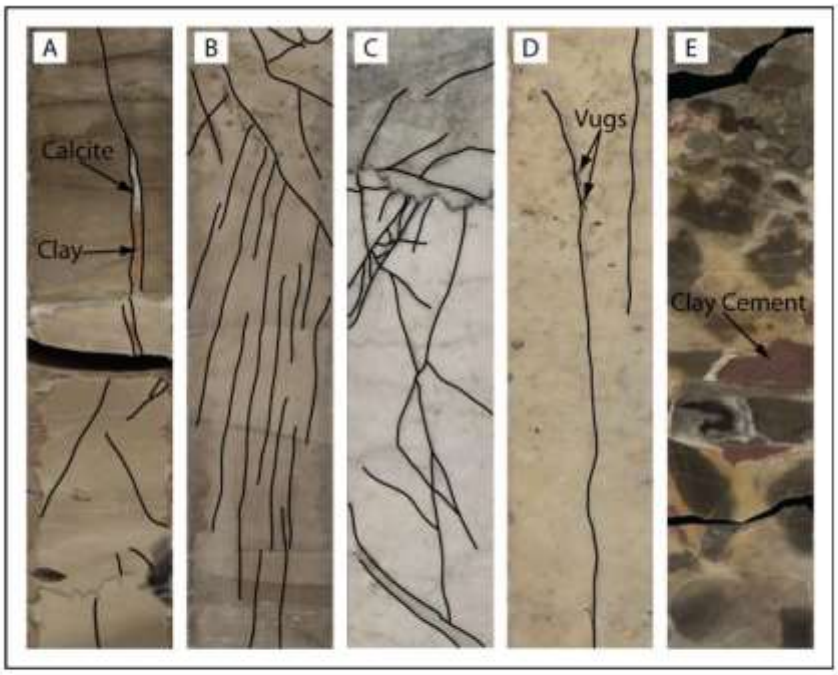

Figure 3.6: Examples of class one fractures in the Madison. (A) Sub-vertical fracture termination at a horizontal stylolite and filled with both calcite and lithified clay material (red-brown material above stylolite). (B) Parallel small aperture fractures, filled with material that did not effervesce in HCl. (C) Brecciated interval in Madison zone B, with clasts cemented by calcite, and apparently terminating at a stylolite. (D) Sub-vertical fractures which are mostly filled with calcite, but vugs have developed on several observed fractures. (E) Brecciated interval, cemented with lithified clay and calcite.

Figure 68: Figure 3.6 of Luke Shafer's master's thesis showing natural fractures in the Madison Formation.

Experimental Procedure:

Our experimental approach is to conduct direct-shear triaxial coreflood experiments using a sample configuration illustrated in Figure 69. We have shown that the direct-shear approach allows creation of through-going fractures that facilitate direct measurement of permeability under *in situ* stress conditions (Carey, J. W., Lei, Z., Rougier, E., Mori, H., and Viswanathan, H. S. (2015). Fracture-permeability behavior of shale. Journal of Unconventional Oil and Gas Resources, 11:27–43).

Our procedure for characterizing the potential activation of existing fractures is as follows:

1. Prepare sample in triaxial system
2. Pressurize the Madison specimen to 24 MPa with isotropic stress and without pore-pressure
    a. Conduct several permeability measurements in steps along the way to 24 MPa to assess the effect of stress on permeability
3. Apply deviatoric stress to the specimen until it fractures. Estimated deviatoric stress is 15MPa
4. Return specimen to isotropic conditions (24 MPa) and measure permeability of damaged rock

5. Test the stress necessary to reactivate the fracture system by increasing the deviatoric load until the specimen begins to slide
    a. Calculate sliding friction coefficient
    b. Measure permeability as a function of displacement along the fracture
6. Complement the tests in #5 by measuring the increase in pore pressure necessary to initiate reactivated sliding along the failed fracture plane
    a. Calculate sliding friction coefficient
    b. Measure permeability as a function of displacement along the fracture
7. Record acoustic emission data to assess microseismic response of formation damage and fracture reactivation.

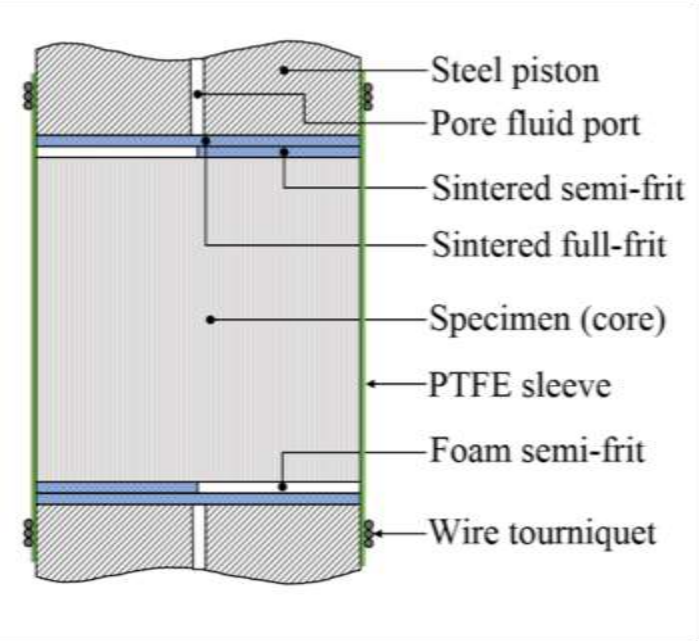

Figure 69: Direct-shear configuration for the triaxial experiment. Application of a vertical stress results in the formation of a concentrated shear stress along the centerline of the sample as the foam semi-frit deforms. Fractures will form that connect the upper and lower pistonnes allowing measurement of permeability.

The results of these experiments are designed to provide several key pieces of information for geomechanical analyses:

1. Direct-shear strength at reservoir effective-stress conditions
2. Permeability of newly generated fractures
3. The friction coefficient for reactivation of existing fractures
4. The permeability of reactivated fractures as a function of continued displacement
5. The stress necessary to reactivate fractures
6. The pore pressure necessary to reactivate fractures in combination with a deviatoric load
7. Microseismic (acoustic emission) activity during fracture damage and displacement

Experimental Results:

During Phase I, we chose a Madison Formation sample from depth 12, 421' (**Table 23**). We followed the procedure described above. Unfortunately, our experiment did not proceed as planned. **Figure 70** shows the experiment up until the point of failure. The plot shows permeability measurements collected at a low confining pressure (500 kPa; 5 bars) and at 6 MPa and 12 MPa as we proceeded toward the target value of 24 MPa isotropic pressure. The steps in the red curve are ladders of differing constant flow rates that we used to measure permeability and assess hysteresis. As the pressure increased above 20 MPa (not shown) the confining pressure membrane (PTFE sleeve of **Figure 69**) ruptured and hydraulic oil entered the sample and the pore-pressure system of the triaxial device. We had to then stop the experiment.

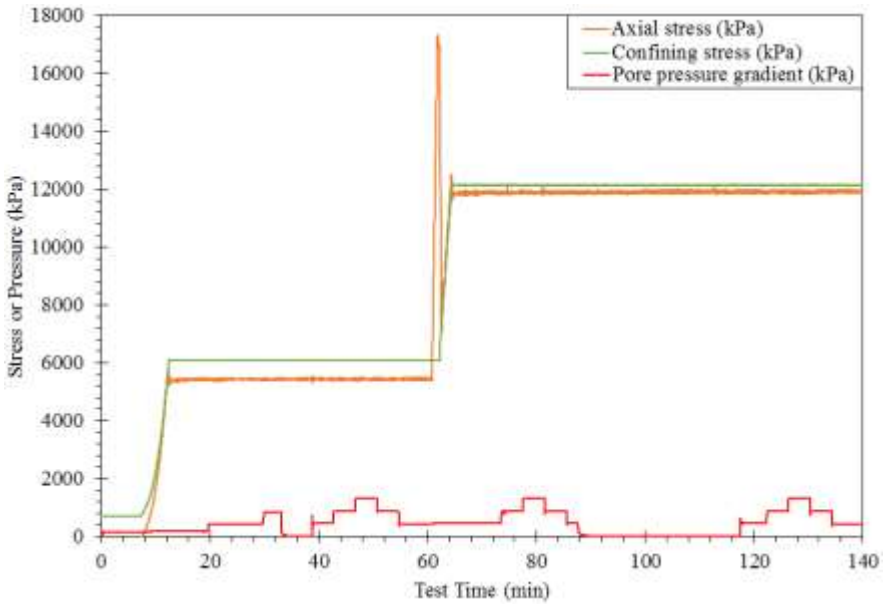

Figure 70: Experimental history for Madison Formation sample 12,421'.

The permeability data we collected are shown in **Figures 71** and **72**. The permeability values were about 9 mD under unstressed conditions and declined to about 6 mD with increasing confining pressure.

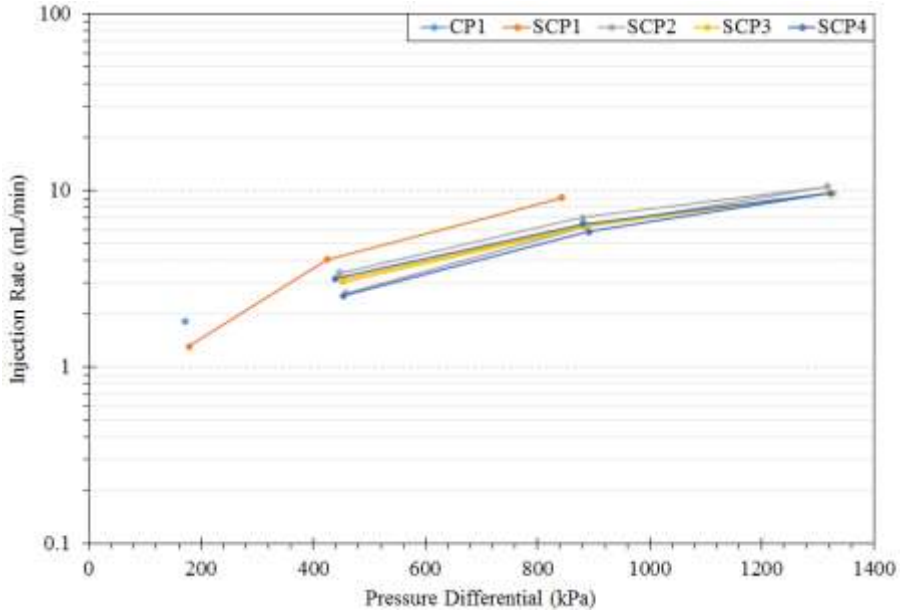

Figure 71: Pressure-flow data for the Madison Formation specimen from 12,421' as a function of injection rate and pressure-drop across the sample. The first measurement (SCP1) was anomalous with respect to subsequent values.

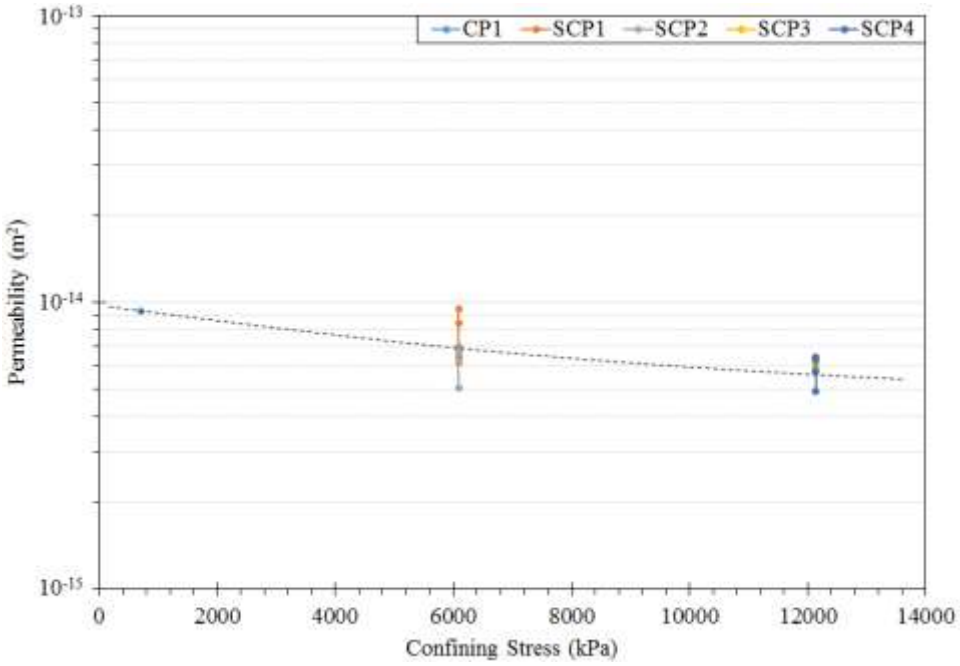

Figure 72: Permeability data for the Madison Formation specimen from 12,421' as a function of confining stress. Permeability drops slightly with increasing confining pressure.

Conclusions:

We summarized the existing geomechanical data for RSU samples and assessed the critical stress conditions necessary for fracture-reactivation. Using these results, we developed an experimental approach to the measurement of key fracture-permeability relations governing the development of permeability in damaged RSU rock units. In particular, the approach will allow assessing the stress conditions necessary to reactivate fractures and the consequences of potentially enhanced permeability along these reactivated fractures. The experimental method also collects acoustic emission data to inform understanding of potential microseismicity associated with injection-induced fracture damage.

Unfortunately, we were able to conduct just a single experiment during Phase I and the experiment was not completely successful. We did obtain useful permeability data as a function of applied stress for the Madison. We plan to continue with the work during the remainder of Phase I and show the very interesting fracture-reactivation characteristics of RSU rock units.

B. Assessment of Geomechanical Risks and Calculations of Risk Minimization Through Brine Production

The geomechanical risks of injection on reservoir and caprock was investigated through stress modeling, stress-change calculations using a couple stress, pore-pressure and flow calculation code that models stress changes in the rock. Several scenarios were run for the injection zone to help assess the potential for induced seismicity. These same injection scenarios were used as a starting point for modeling a production well to be brought on line to reduce and manage the reservoir pressure.

The probability for reducing identified geomechanical risk through brine production was done in addition to the stress modeling. A ground motion prediction equation (GMPE) model was run for the suggested injection site at Rock Spring Uplift (RSU). Scenario induced events were modeled with hypocenters originating at the RSU injection well. Peak ground acceleration was then calculated from a proxy model for the shear wave velocity in the upper 30 meters of the RSU site. The proxy model was based on the topographic slope and geology at the site (Wills and Silva, 1998; Wills et al., 2000).

Stress Modeling:

We have completed the work related to development of a geologic framework model (GFM) for RSU study site to estimate the state-of-stress and changes in the in-situ stress due to fluid injection (**Figure 73**).

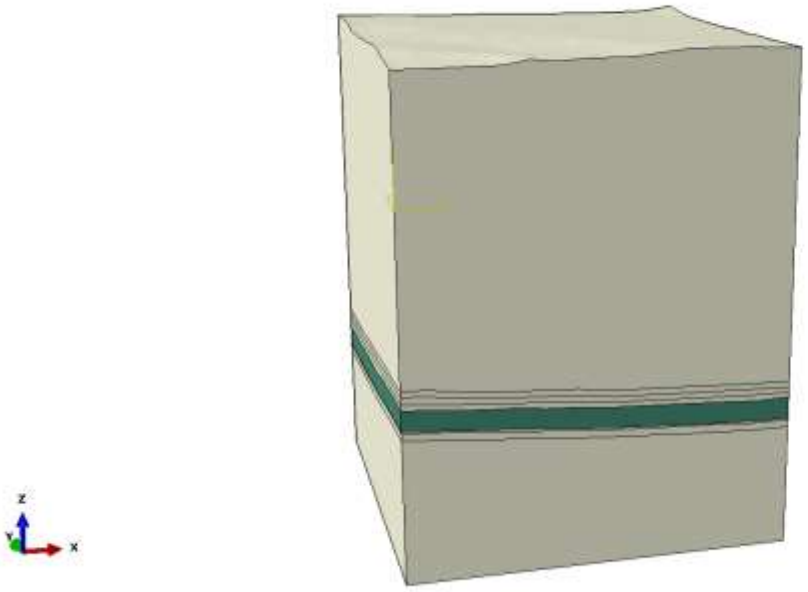

Figure 73: Geologic Framework Model for the Rock Spring Uplift study area. The location of Madison Formation is shown in green.

These calculations are performed using ABAQUS toolkit. **Figure 74** is the initiation of the GFM with topographic loading and the applied geostatic and tectonic stresses.

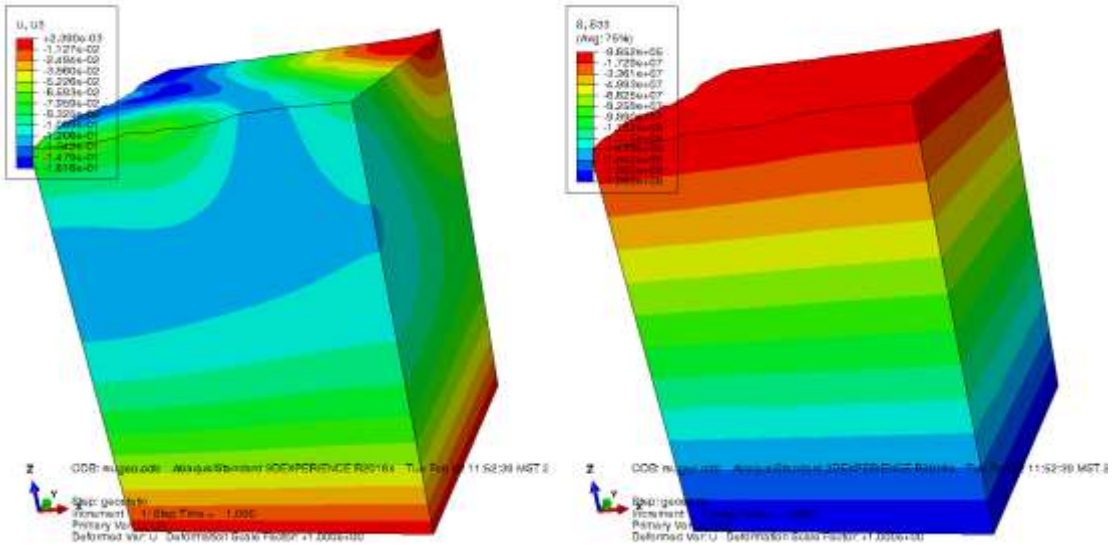

Figure 74: ABAQUS model after applying the lithostatic and tectonic stresses. The Madison carbonate sequence has a vertical stress between 130 MPa and 150 MPa.

The Madison carbonate sequence experiences between 130 and 150 MPa in vertical stress.

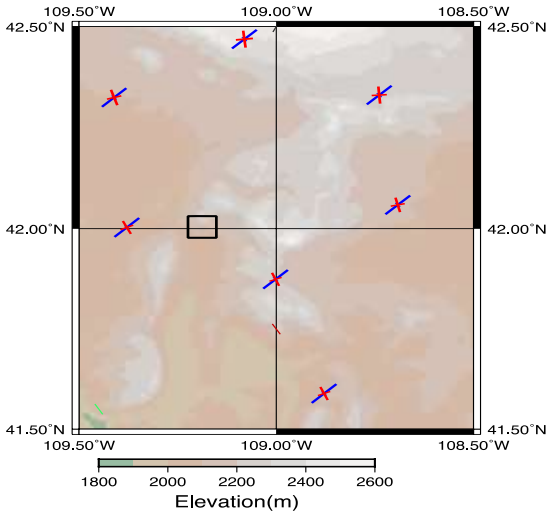

Figure 75: The shaded topography and regional tectonic stress in the area. The study area is the black box centered at 42.00° North. Blue lines are compressive stress, 17 MPa at N43°E. This calculated value agrees with recent stress measurements made at depth.

The tectonic stress in the region was calculated form previous work (Coblentz and Karlstrom, 2011; Humphreys and Coblentz, 2007) and is shown in **Figure 75**.

A fault has been inferred in the Northeast corner of the RSU study site. Its orientation places it approximately orthogonal to the maximum tectonic stress. **Figure 76** is a map of the study area with the inferred fault and its relation to the injection well and the Jim Bridger power station. In order to estimate the injection effects of this fault, the ABAQUS mesh was adapted to represent the fault and the fault was modeled as a no-flow and free-flow boundary. The following graphics are stress difference maps of two injection rates, 100,000 ton/year and 200,000 tonnes/year of water in the Madison formation. Additionally, we modeled the Madison with three uniform permeabilities: 1 mD, 10 mD and 100 mD.

Results of these calculations will be used to estimate induced seismicity risks during the fluid injection field test.

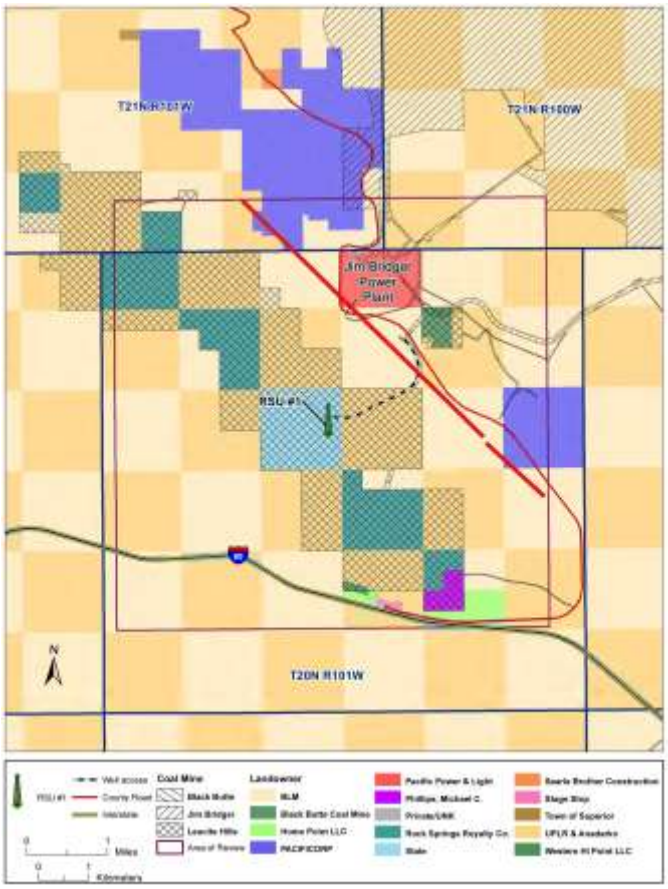

Figure 76: The Rock Springs Uplift study area (magenta outline) with the inferred fault (thick solid straight line) relative to the RSU# 1 injection well and Jim Bridger Power Plant.

Figure 77 is a map view of the proposed injector well and producer wells modeled in this study. The mottled green background represents the measured interval velocity in meters per second of a surface in the Madison Formation. The inferred fault shows up as an introduction of high velocity material in the Northeast corner of the region. We modeled the two injection rates at the 'First Well injector' and following the 1-year injection, we modeled identical extraction rates in the at the production/monitoring well location. Both injection and production were done at the center of the Madison formation and water was the injected and produced fluid.

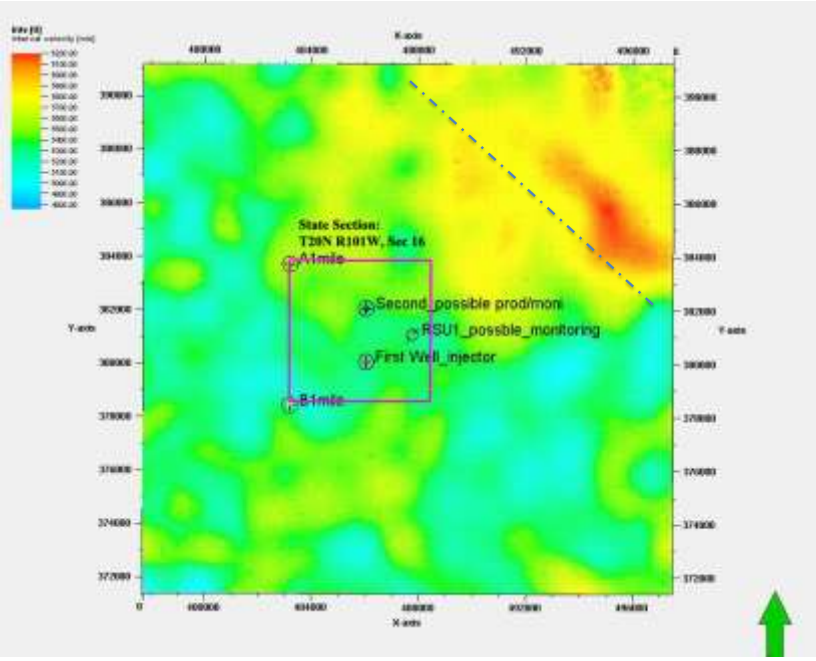

Figure 77: Map view of the RSU study site. The modeled injector and producer wells are shown. The inferred fault location is shown as the dashed blue line.

The Madison formation was initiated with a mean pore pressure of approximately 36 MPa. There is significant topology in the formation itself (see **Figure 73**) so the pore pressure is linearly interpolated from the top surface to the bottom surface of the formation. We then examined the model from a consistent surface that tracks near the mid-plane of the Madison Formation. The following figures show the residual stress in the model after first injecting water at 100,000 and 200,000 tonnes/yr for ten years in a 1 mD permeability formation. We calculate the residual pressure field by subtracting the initial pressure stress condition from the final calculation after ten years. We then search through the entire Madison Formation elements and find peak positive (compression) and negative (expansion) stress and map it to the plane in the figure. **Figure 78** is the residual pressure along the center of the Madison formation at 100,000 and 200,000 tonnes/yr after 10 years. The peak residual pressure stress is 7.02 MPa at 100,000 tonnes/yr and 14.05 MPa at 200,000 tonnes/yr. Some mesh dependency can be seen where the finite element mesh was refined for the region around the fault.

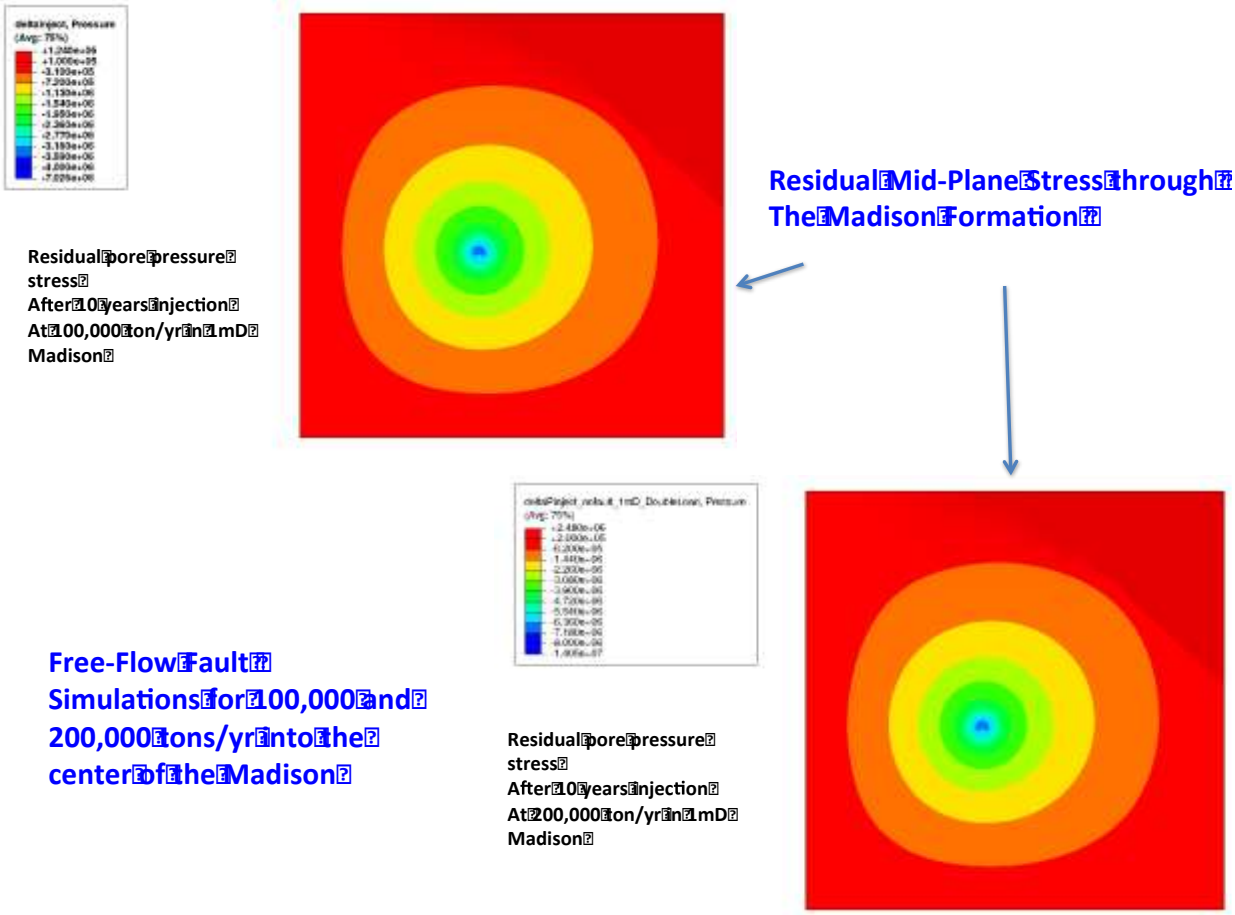

Figure78: The residual total pressure along the center of the Madison formation at 100,000 and 200,000 tonnes/yr after 10 years injection. The peak residual pressure stress is 7.02 MPa at 100,000 tonnes/yr and 14.05 MPa at 200,000 tonnes/yr.

Figure 79 is the residual total pressure along the center of the Madison formation at 100,000 and 200,000 tonnes/yr after 10 years of extraction after injection. The peak residual expansive pressure stress is 0.604 MPa at 100,000 tonnes/yr and 1.209 MPa at 200,000 tonnes/yr.

The extraction of the water shows that the residual stress can be significantly reduced from a well at a different location. Multiple extraction wells would improve the ability to tailor the reservoir pressure and keep pore pressures manageable.

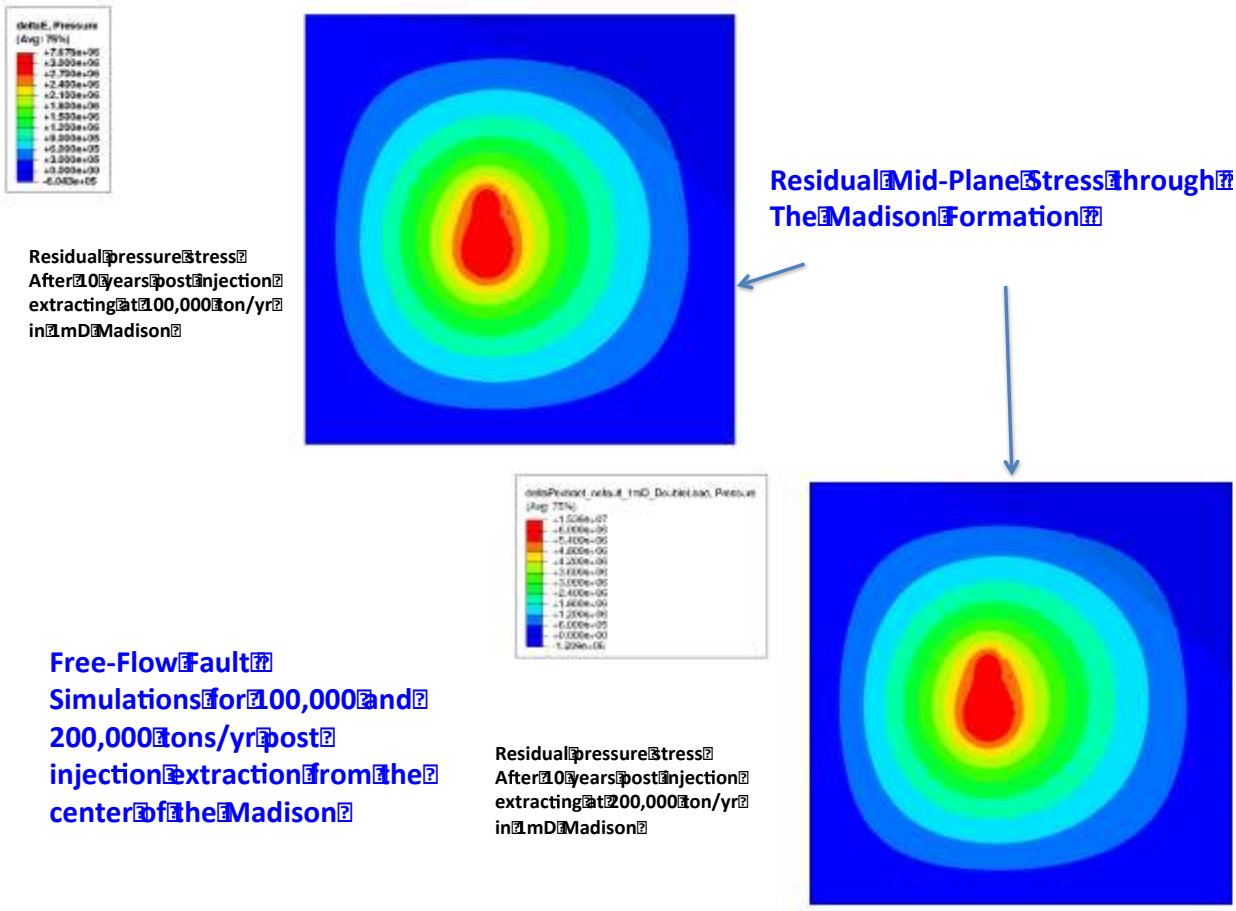

Figure79: The residual total pressure along the center of the Madison formation at 100,000 and 200,000 tonnes/yr after 10 years extraction. The peak residual expansive pressure stress is 0.604 MPa at 100,000 tonnes/yr and 1.209 MPa at 200,000 tonnes/yr.

The mesh was then modified to define the fault as a no-flow boundary. This was done to determine if the additional pore pressure from injection could reach the fault and change the effective stress along the fault. One possible outcome of injection is the triggering of slip along pre-existing faults. As stated before, the fault in in a tectonically compressive environment of approximately 17 MPa normal to the fault.

Figure 80 shows the residual total pressure along the center of the Madison formation at 100,000 and 200,000 tonnes/yr after 10 years' injection. The peak residual pressure stress is 7.102 MPa at 100,000 tonnes/yr and 14.20 MPa at 200,000 tonnes/yr. The fault can be seen as the no-flow boundary in the upper right corner of the model. At this permeability, the peak expansive stress is still centered at the injector well and the effect of the fault is a 0.1 MPa positive change in the pressure.

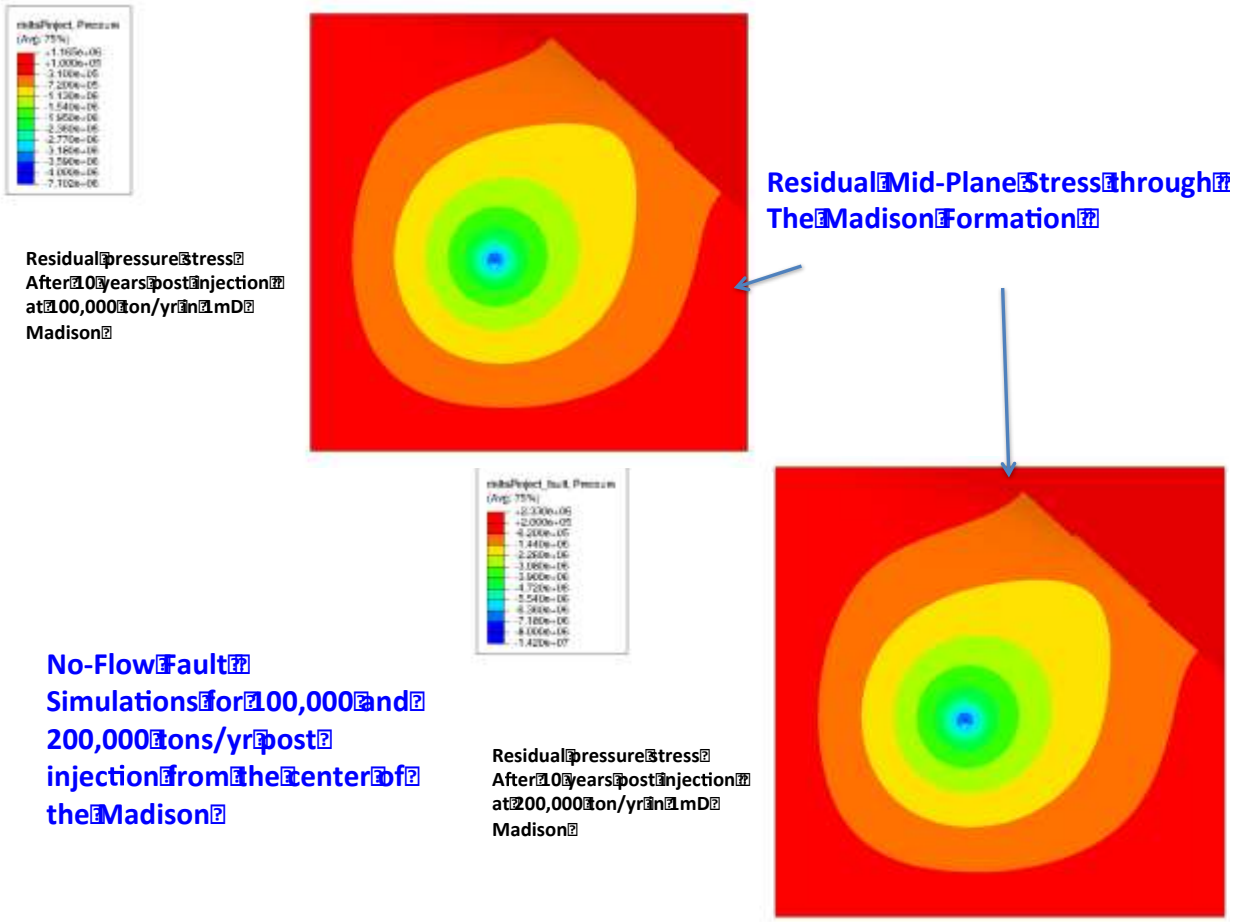

Figure 80: The residual total pressure along the center of the Madison formation at 100,000 and 200,000 tonnes/yr after 10 years injection. The peak residual pressure stress is 7.102 MPa at 100,000 tonnes/yr and 14.20 MPa at 200,000 tonnes/yr.

Figure 81 shows the residual total pressure along the center of the Madison formation at 100,000 and 200,000 tonnes/yr after 10 years of extraction post injection. The peak residual expansive pressure stress is 0.478 MPa at 100,000 tonnes/yr and 0.956 MPa at 200,000 tonnes/yr. The fault can be seen as the no-flow boundary in the upper right corner of the model. Because of the fault, the extractor well has a smaller volume to pull water from and this results in a reduction of the peak expansive pressure by 0.2 to 0.3 MPa.

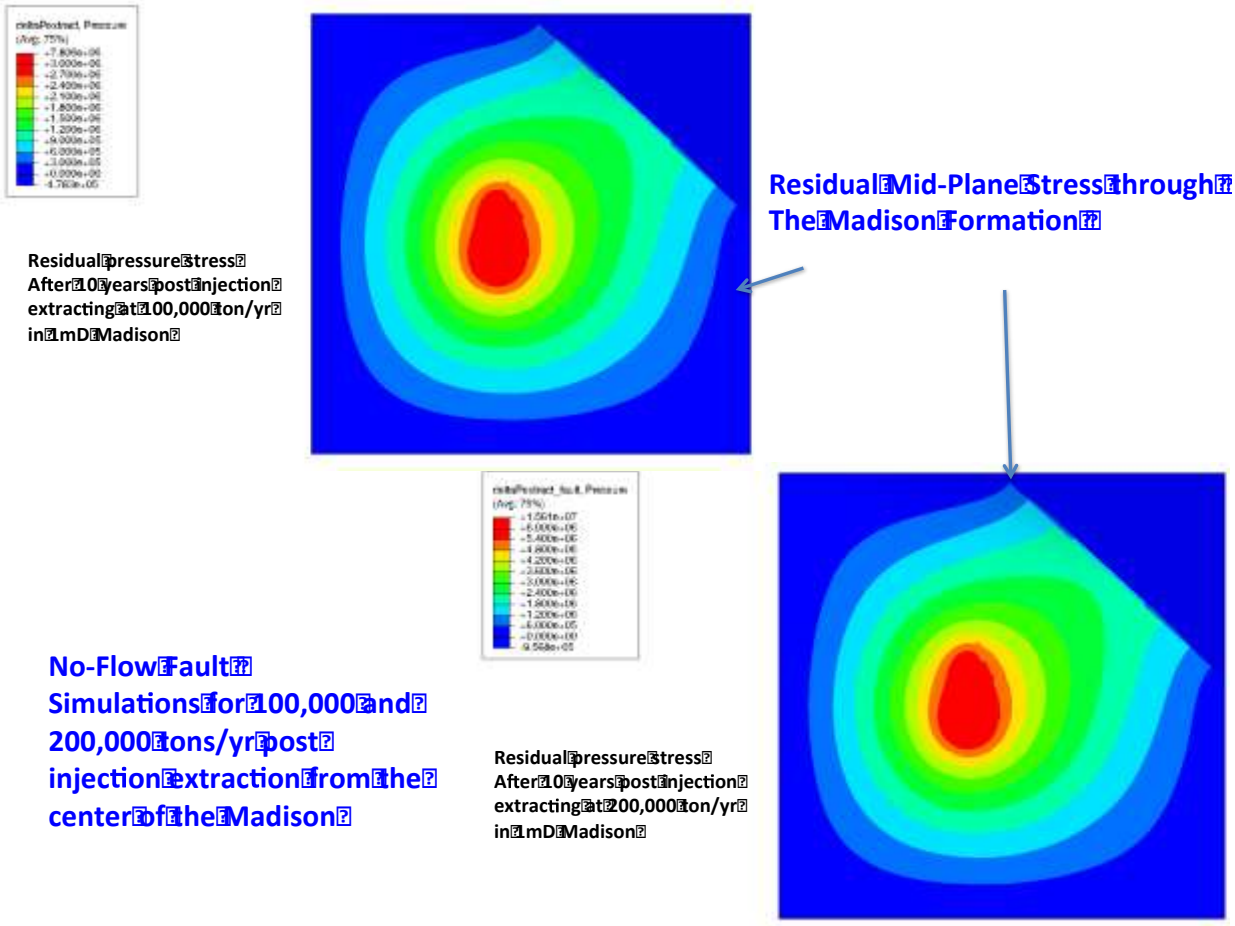

Figure 81: The residual total pressure along the center of the Madison formation at 100,000 and 200,000 tonnes/yr after 10 years extraction. The peak residual expansive pressure stress is 0.478 MPa at 100,000 tonnes/yr and 0.956 MPa at 200,000 tonnes/yr.

We did similar calculations for the Madison Formation at 10 mD and 100 mD permeability and found lower residual stress fields. The stress scaled linearly in both of these cases which is logical because of the Darcy flow assumptions. The problem should be revisited with the more complex permeability structure created by the researcher at University of Wyoming.
Using the 1 mD case as a conservative case (i.e. maximum delta stress) the peak stress modeled during injection may get close to the tensile strength of the Madison. The Madison Formation has a linear compressive strength relationship with confining stress,

Strength = 0.6785x + 164.61 (MPa)

This gives a potential strength in compression of 260 MPa. The minimum strength in compression is 164.61 MPa at zero confining stress. Typical earth material is about 1/10 as strong in tension as in compression about 16 MPa in the case of the Madison. This is why the expansion stress during the 200,000 tonnes/yr injection rate may come close to the yield strength of the formation.

However, it appears that the stresses in this most extreme case modeled are not near the tectonic stress on the modeled fault. The maximum stress on the fault after 200,000 tonnes/yr in 10 years is between 2.2 and 1.4 MPa far below the tectonic stress of 17 MPa (see **Figure 80**). For this reason, it is not probable that the injection process will trigger a tectonic event.

Ground Motion Prediction Modeling:

At the higher injection rate, there is a potential to induce some low magnitude seismicity near the injection point. This has been observed at enhanced geothermal sites (EGS) where induced seismicity has been correlated with injection. Stone et al, (in prep) have developed a ground motion prediction equation (GMPE) based on data measure from 9 different EGS and geothermal sites.

Details on the induced earthquake ground motion evaluation

Hypothetical median ground motion for induced moment magnitude earthquakes of magnitude 2 and 4 were developed for the study region. The median predicted ground motion is 5% damped 10-Hz horizontal spectral acceleration. The hypothetical induced earthquakes were placed at an approximate model injection depth of 3.5 km (and considering the 2100 m relief in topography), at the center of the study region. Ground motion predictions were based on the empirical study of global induced earthquakes by Douglas et al (2013).

Figure 82 is the topography in the region around the RSU study site. The ground motions for each grid point in the study area were corrected for site conditions based on a topographic slope proxy of shallow shear-wave velocity (Vs30). The topographic slope proxy of Wald and Allen (2007) was used to infer an average Vs30 for each of the over 4000 sites.

The digital topographic map of was used for the proxy evaluation. The full aleatory sigma for the ground motion prediction is available so that the complete predicted distribution of ground motion can be used if necessary.

Figure 83 is the shear wave velocity in the upper 30m (Vs30) in the RSU study site derived from the topographic slope. The range in velocity is from 300 to 1000 m/s. Local site response is typically dominated by the upper shear wave velocity. The predicted ground motion from an induced event can be calculated using the magnitude, distance and local response in order to estimate the hazards from the induced earthquake.

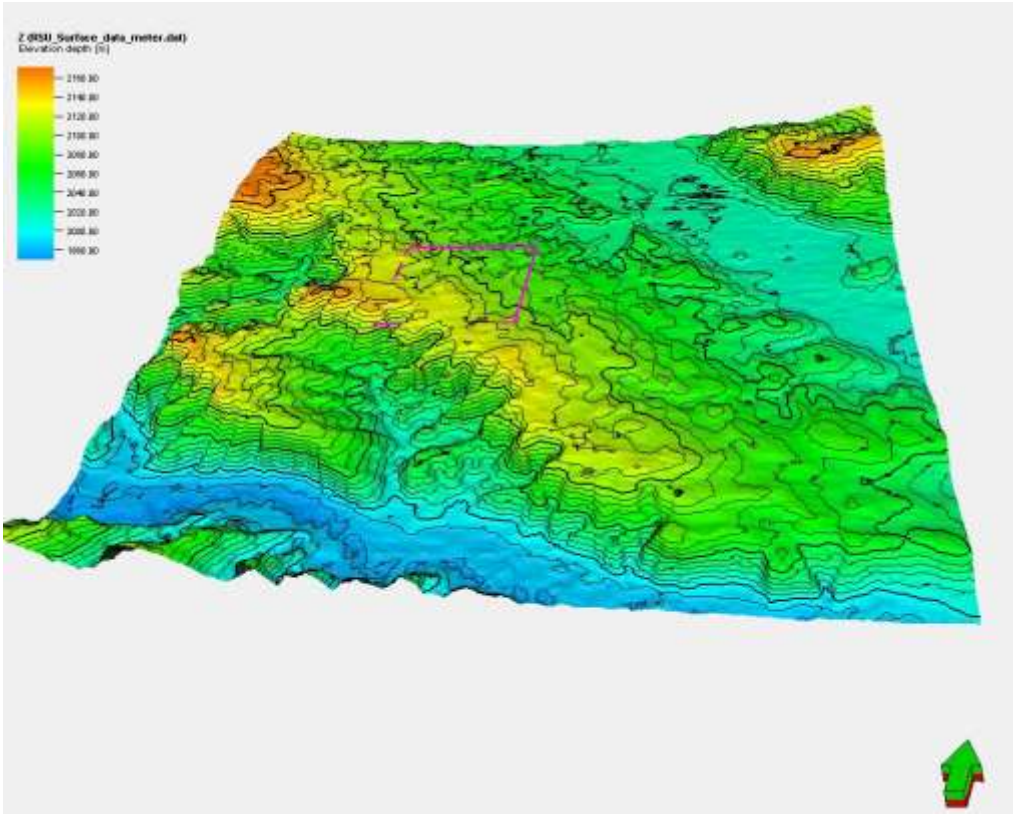

Figure 82: Topography in the region near the Rock Springs Uplift. The RSU study site is the magenta box outline. It is a 6 km by 6 km square.

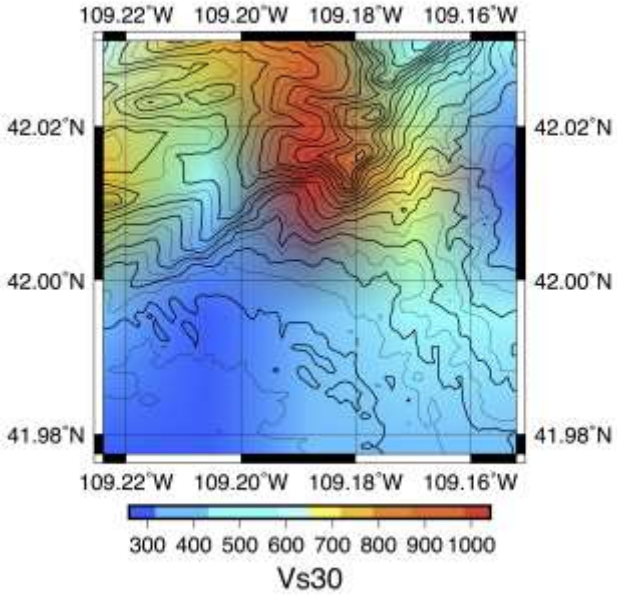

Figure 83: Shaded Vs30 map in m/s for the RSU study site using the topographic slope proxy

Using the Vs30 and depth to the events, peak ground acceleration (PGA) can be calculated. **Figure 84** is the PGA calculated for a magnitude 4.0 induced event at the RSU study site.

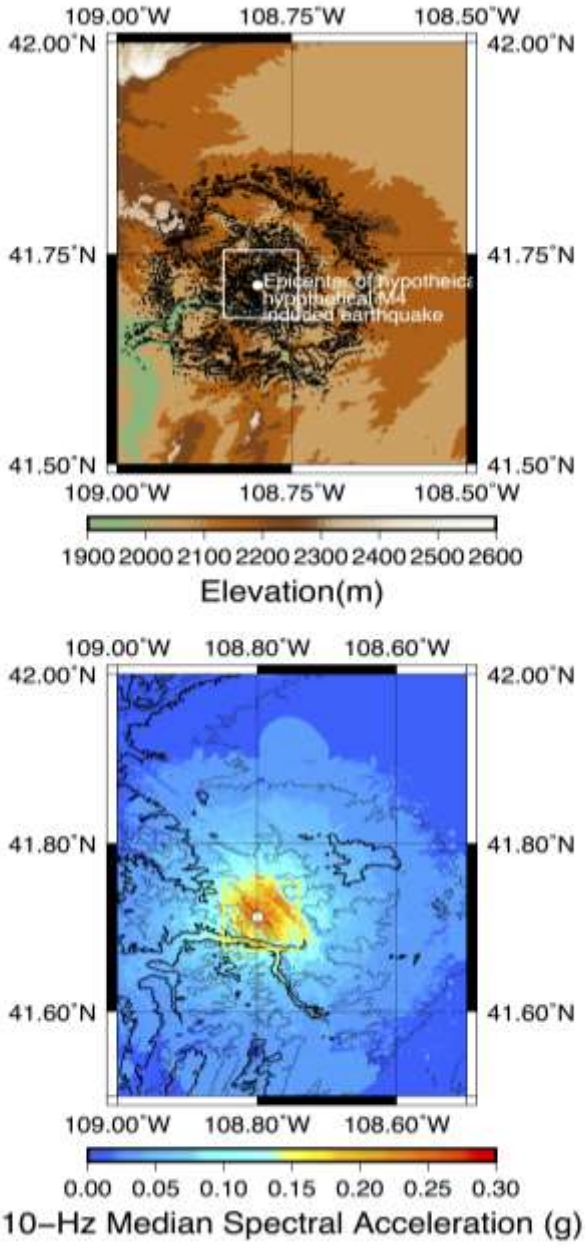

Figure 84: Upper plot shows the shaded topographic relief map with the contoured 10 Hz Median spectral acceleration calculated for an induced M 4.0 earthquake. The lower plot is the shaded relief map of the 10 Hz Median spectral acceleration calculated for an induced M 4.0 earthquake with the topographic contour superimposed.

The peak acceleration, approximately, 0.4 g, is seen at some distance from the earthquake epicenter. This is because of the lower shear wave velocities estimated on the flatter relief. **Figure 85** is the PGA calculated for a magnitude 2.0 induced event at the RSU study site.

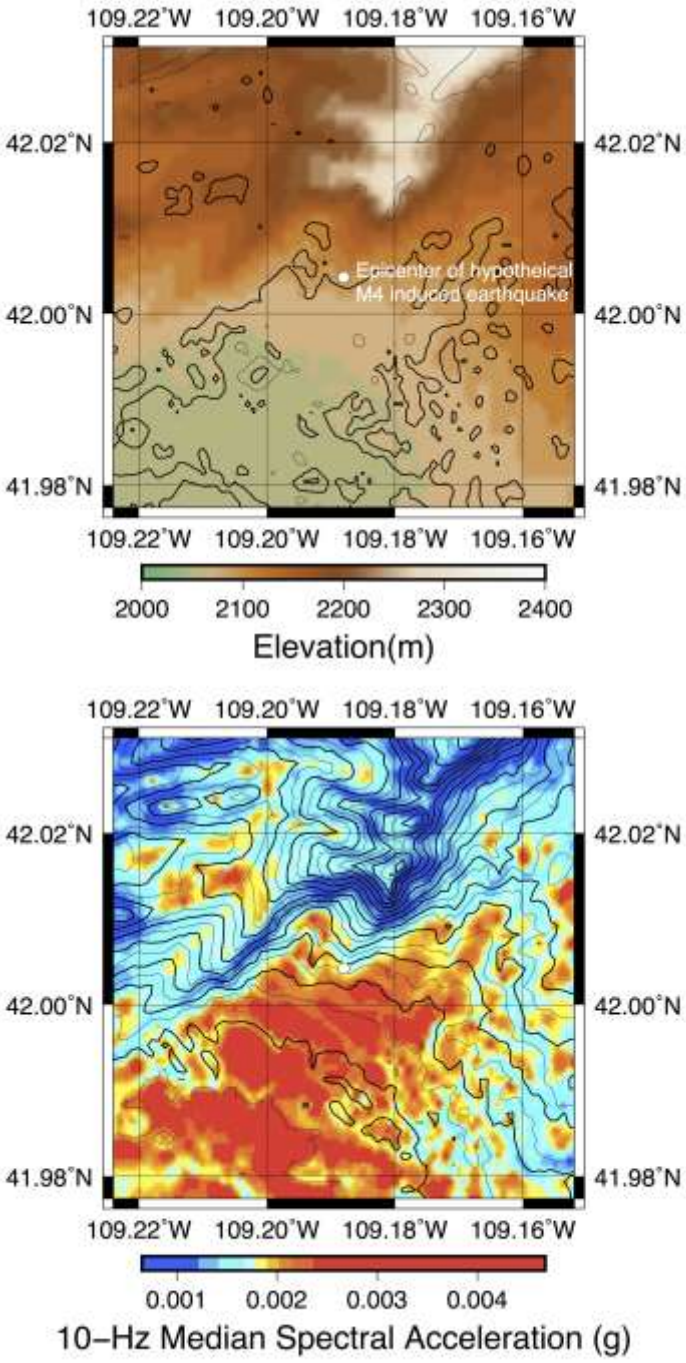

Figure 85: Upper plot shows the shaded topographic relief map with the contoured 10 Hz Median spectral acceleration calculated for an induced M 2.0 earthquake. The lower plot is the shaded relief map of the 10 Hz Median spectral acceleration calculated for an induced M 2.0 earthquake with the topographic contour superimposed.

The peak acceleration, approximately, 0.004 g, is distributed around the earthquake epicenter but is still located on the flatter relief.

Conclusions:

The coupled stress and flow modeling reveal that the stresses in this most extreme case modeled are not near the tectonic stress on the modeled fault. The maximum stress on the fault after 200,000 tonnes/yr in 10 years is between 2.2 and 1.4 MPa (see Figure 80) far below the tectonic stress of 17 MPa. For this reason, it is not probable that the injection process will trigger a tectonic event.

The modeling further shows that production can keep the reservoir stress below the failure stress of the caprock or formation. A strategic plan of a production well should be able to pressure manage the reservoir.

Additionally, the ground motion potential of induced seismicity at the RSU study site has been evaluated. A ground motion prediction equation model, developed for injection induced seismicity, was used to estimate the ground motion from a M4.0 and M2.0 induced event at injection depth. The 10 Hz median spectral acceleration was calculated for these events and the sensitivity to the Vs30 model was demonstrated. The peak ground motion from the M 4.0 event was approximately 0.4 g, 2 km from the epicenter. Better estimates can be done with actual measurements of the upper shear-wave velocity and background seismicity.

All the tools are in place for being able to reduce the uncertainty of the ground motion if actual background events are measured at the site or induced during injection.

XV. IDENTIFY AND DEVELOP GEOPHYSICAL MONITORING METHODOLOGIES TO TRACK DIFFERENTIAL PRESSURE MIGRATION

This task provided input for optimal design and deployment of geophysical monitoring technologies during field test (active and passive seismic). It is crucial to design time-lapse seismic surveys and a passive seismic monitoring network to ensure that most significant information of fluid-injection-induced reservoir changes can be recorded. To reliably design cost-effective time-lapse seismic surveys and an optimal passive seismic monitoring network, we need to have a high-resolution 3-D velocity model of the Rock Springs Uplift site. Currently, such a velocity model is not available. LANL conducted some preliminary studies using an existing, preliminary velocity model obtained from smoothing root-mean-square (RMS) velocities. The RMS velocities were derived from interval velocities that were obtained using 1D data analysis of seismic data in the time domain.

For active seismic monitoring: LANL conducted elastic-wave sensitivity modeling for the optimal design of time-lapse active seismic surveys (VSP or surface seismic) using an existing, preliminary velocity model (**Figure 86**) illustrates the location of the proposed injection well at the Rock Springs Uplift carbon storage site. **Figure 87(a)** is a smoothed 2-D RMS compressional-wave velocity model along the East-West line crossing through the proposed injection well in the Phase II of the project. **Figure 87(b)** is the shear-wave velocity model for a Poisson medium ($\frac{V_p}{V_s} = \sqrt{3}$) and **Figure 87(c)** is the density, both derived from the compressional-wave velocity model. We defined a target monitoring region centered on the

proposed injection well, as shown in the white region in each panel of **Figure 87**, which is centered vertically at depth of 12,000 ft.

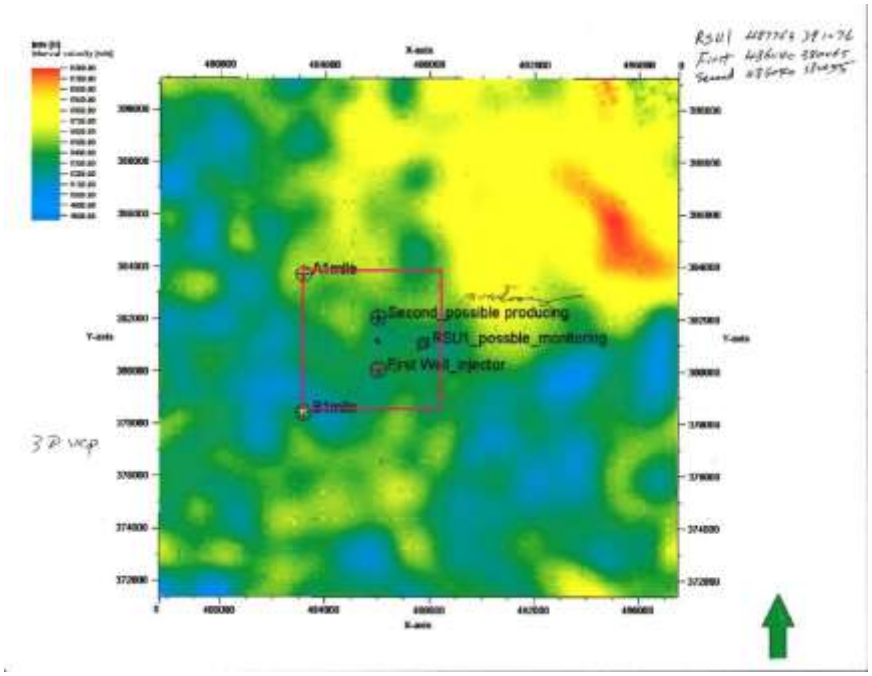

Figure 86: The location of the proposed injection well at the Rock Springs Uplift carbon storage site in southwest Wyoming.

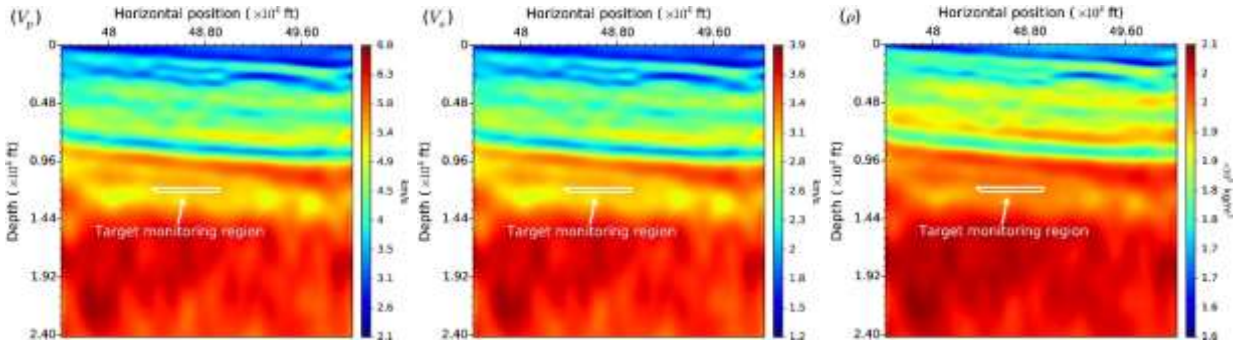

(a) (b) (c)

Figure 87: The compressional- and shear-wave velocities and the density model along an East-West line crossing through the proposed injection well at the Rock Springs Uplift carbon storage site in southwest Wyoming.

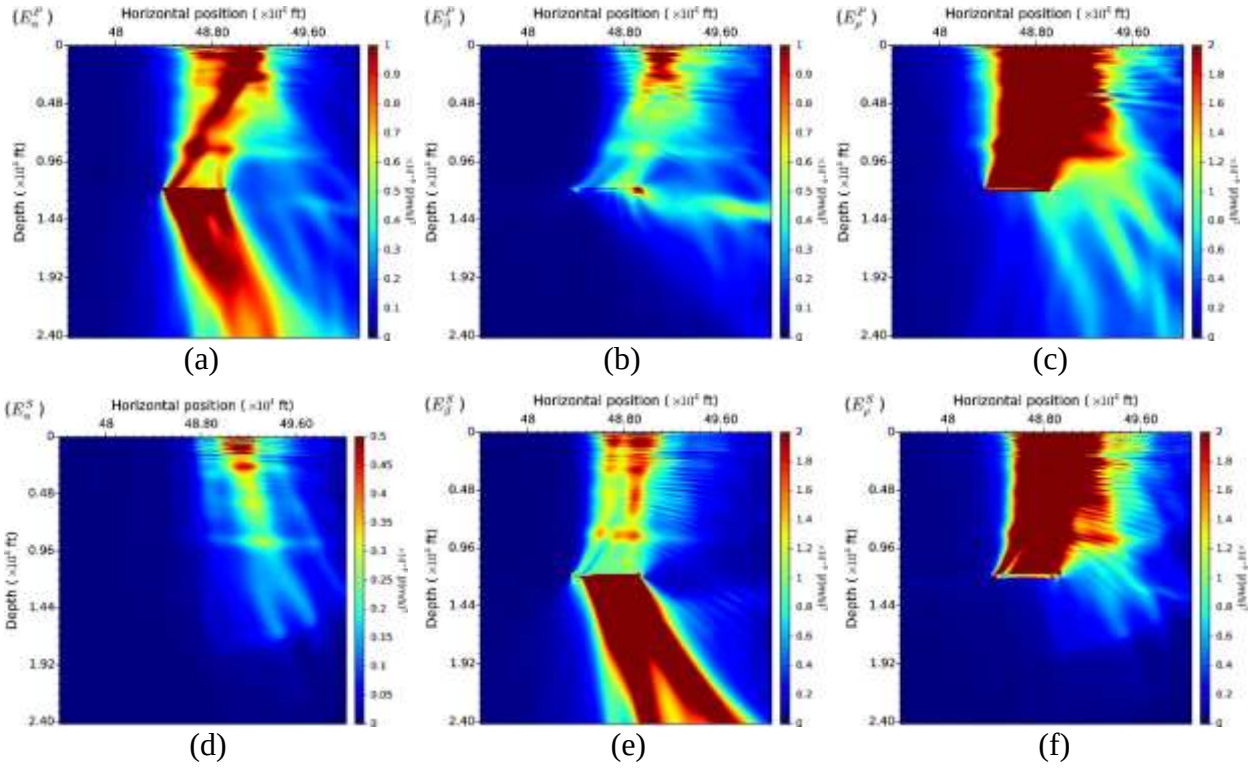

Figure 88: Simulated elastic-wave sensitivity energy distributions for the model and target monitoring region in **Figure 87**.

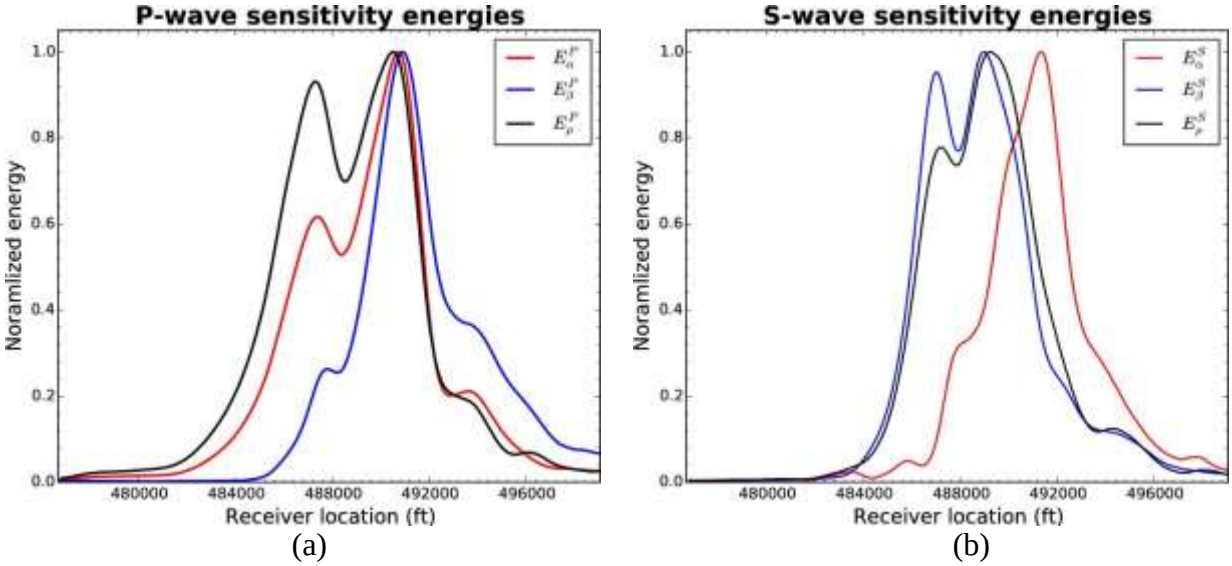

Figure 89: Normalized elastic-wave sensitivity energies along the surface of the mode in **Figure 87** for a shot point at 48,6000 ft. Geophones should be placed at locations where the elastic-wave sensitivity energies are significant for cost-effective time-lapse seismic monitoring.

We calculated elastic-wave sensitivities distributions for a source located at the horizontal position of 486000 ft at the top surface of the model in **Figure 87**. **Figure 88** shows the spatial distributions of our calculated elastic-wave sensitivity energies, and **Figure 89** displays the distributions of the elastic-wave sensitivity energies along the top surface of the model. These figures give the locations of surface seismic and VSP geophones to record the most significant information of time-lapse reservoir changes. If geophones are placed in locations where elastic-wave sensitivity energies are weak, it will compromise the effectiveness of time-lapse seismic monitoring. An accurate and high-resolution velocity model is needed for accurate calculation of elastic-wave sensitivities. This demonstrates again that it is important to obtain a high-resolution velocity model from the existing 3-D surface seismic data acquired at the Rock Springs Uplift site during the Phase II of the project.

For passive seismic monitoring: LANL designed an optimal microseismic monitoring network using the existing, preliminary 3-D velocity model for cost-effective monitoring of potential induced microseismicity within a target monitoring region centered in the proposed injection zone in Phase II of the project.

Figure 90 shows the top and side (north) projections of the true (red dots) and initial (blue dots) locations of microseismic events within a 3-D region centered at the proposed injection well location and the depth of 12,000 ft at the Rock Springs Uplift carbon storage site in southwest Wyoming. These event locations are used for the optimal design of a passive seismic monitoring network. The origin location (X,Y) = (0,0) in **Figure 90** is the proposed injection well location for Phase II of the project. The diameter of the true event distribution is 2 km. Ideally, we should relocate microseismic events from their initial event locations to the true locations using an enough number and optimally-distributed geophones. In practice, only a limited number of geophones are available for cost-effective monitoring, and there will be some errors in event locations.

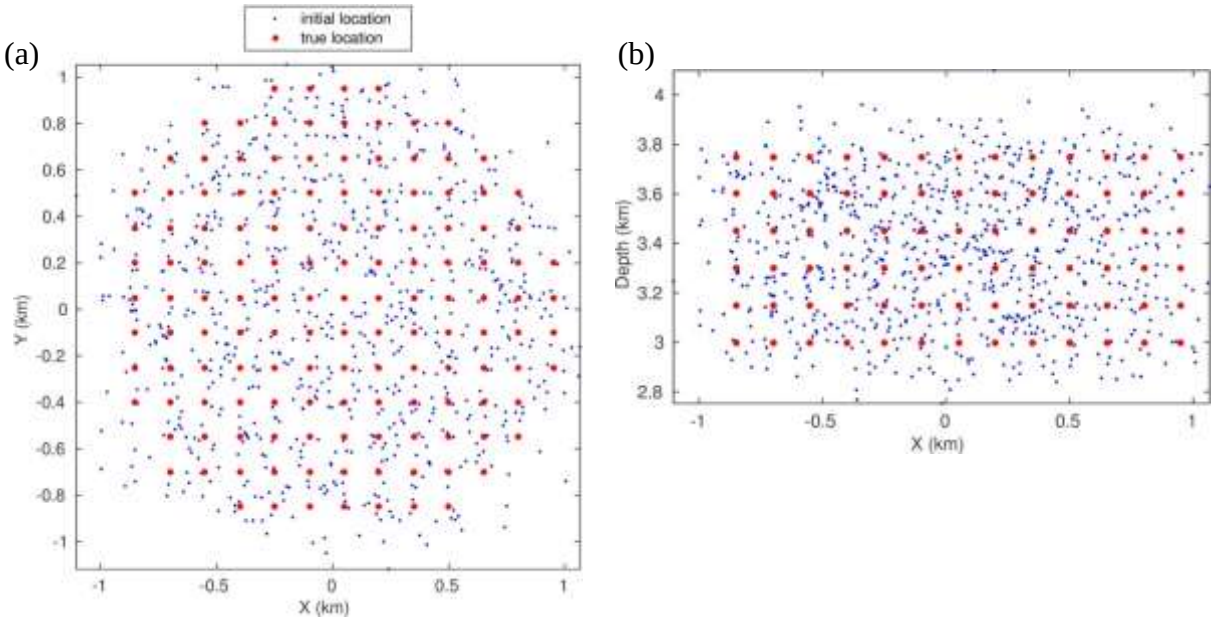

Figure 90: The top and side (north) projections of the true (red dots) and initial (blue dots) locations of microseismic events within a 3-D region centered at the proposed injection well location and the depth of 12,000 ft at the Rock Springs Uplift carbon storage site in southwest Wyoming. These event locations are used for the optimal design of a passive seismic monitoring network.

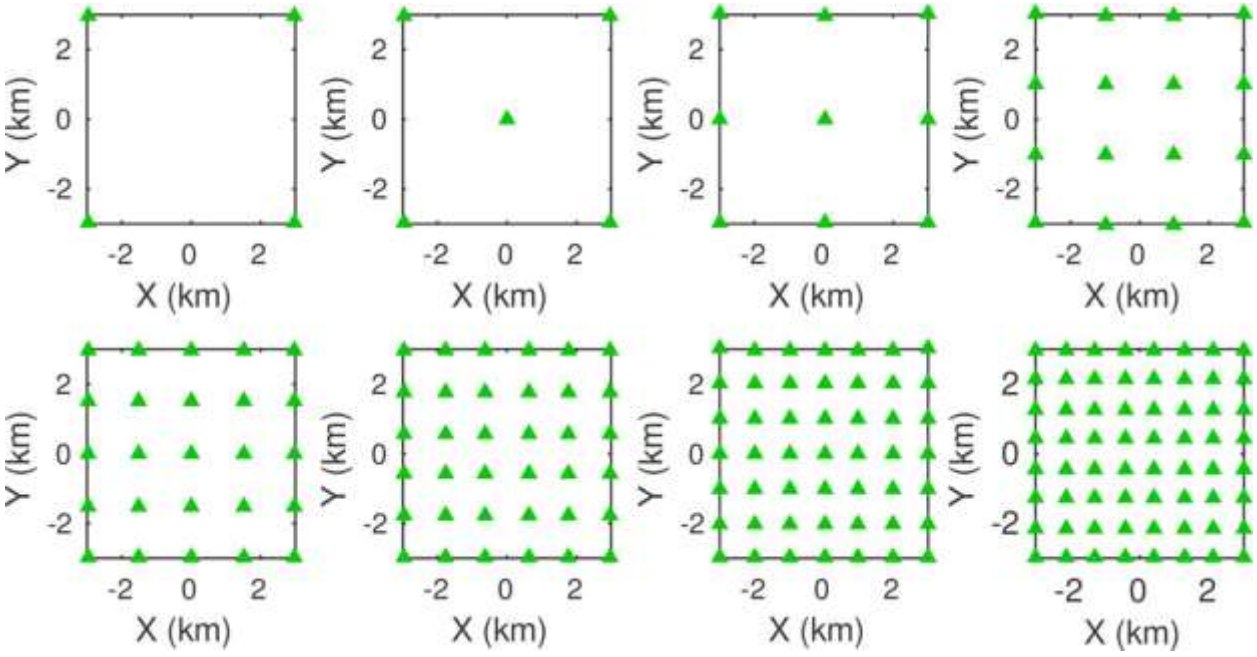

Figure 91: The green triangles in each panel are geophone locations used for the optimal design of a passive seismic monitoring network for monitoring potential induced microseismic events within the same 3-D region as **Figure 90**. The origin (0,0) is the proposed injection well location.

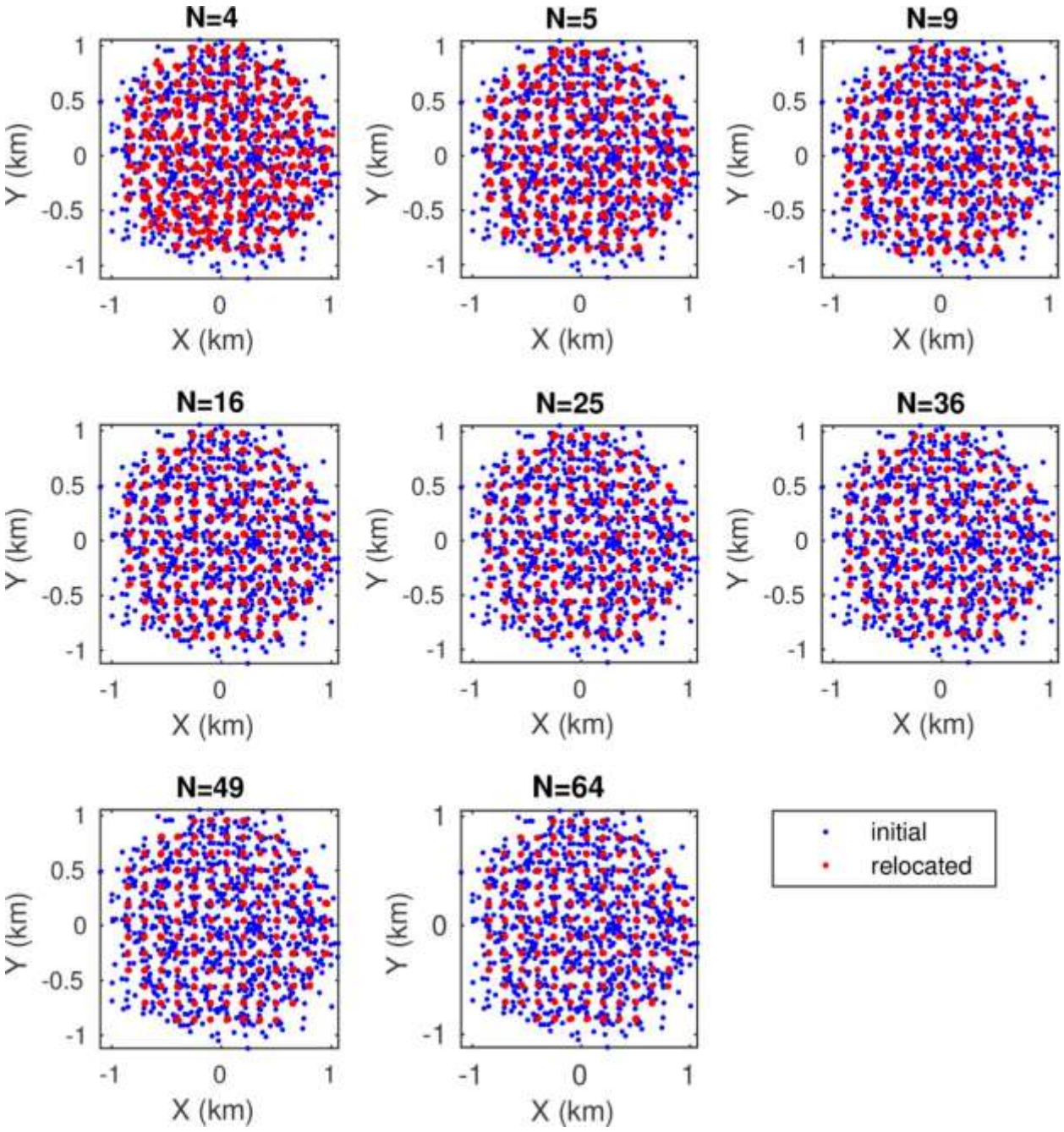

Figure 92: The top projections of the initial (blue dots) and relocated (red dots) microseismic events using the geophone distributions in **Figure 91.** "N" in each panel is the number of geophones used as shown in **Figure 91**. The origin (0,0) is the proposed injection well location.

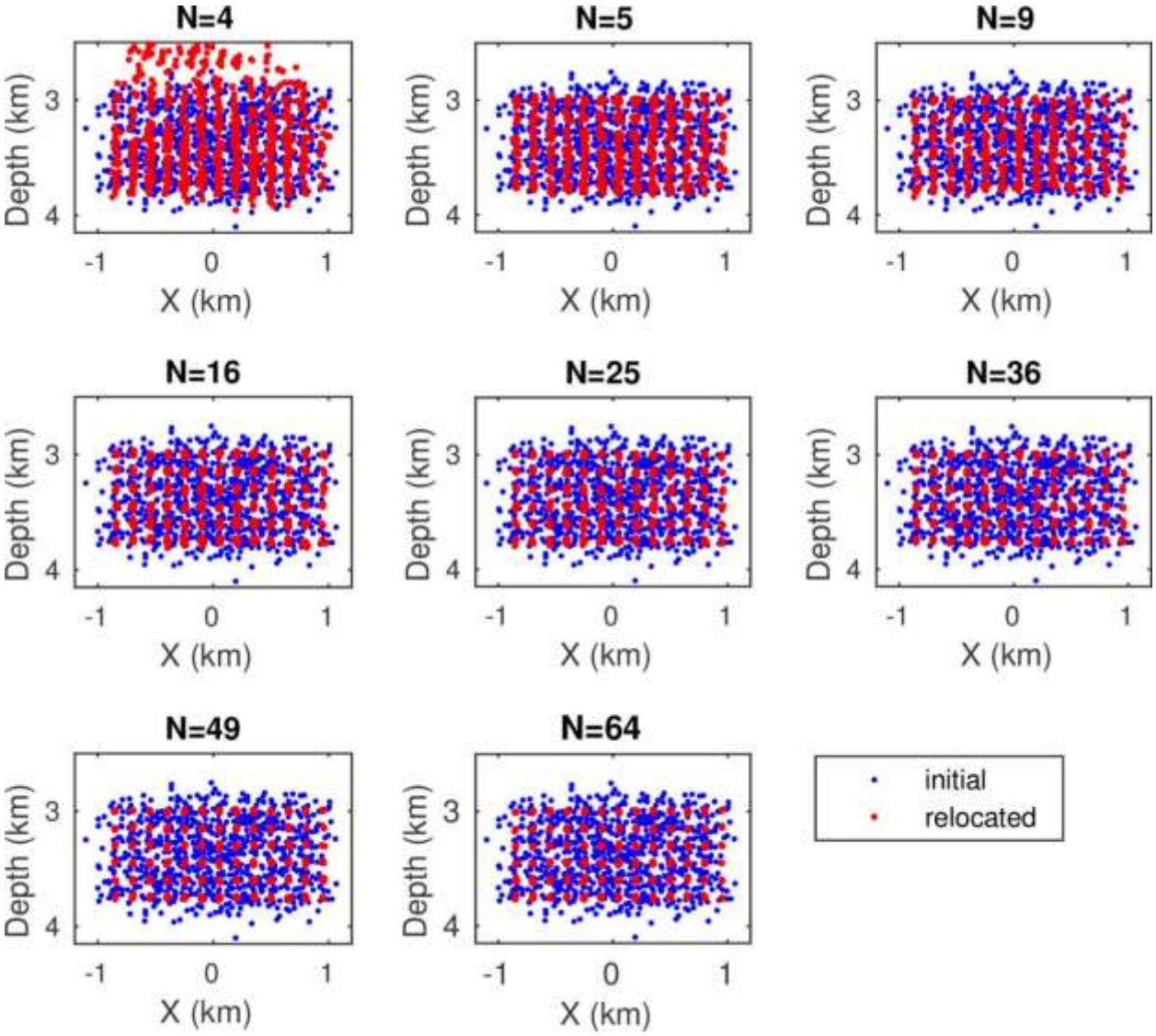

Figure 93: The side (north) projections of the initial (blue dots) and relocated (red dots) microseismic events using the geophone distributions in **Figure 91**. "N" in each panel is the number of geophones used as shown in **Figure 91**.

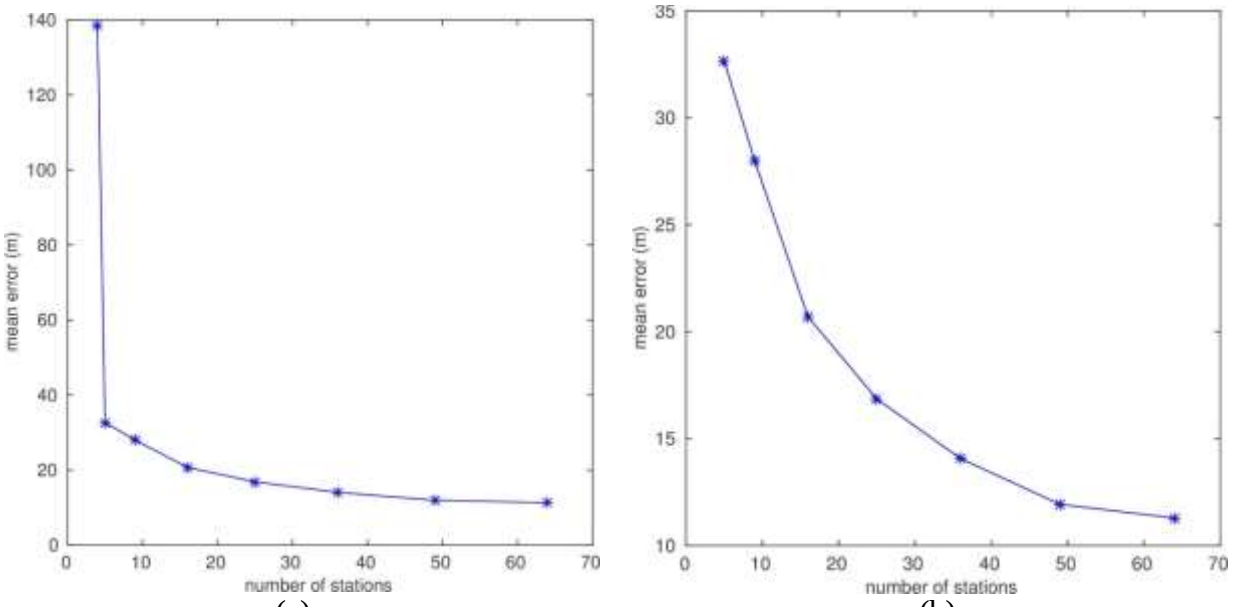

Figure 94: The mean location errors versus the number of geophones ranging from 4 to 64 in (a) and 5-64 in (b). A required number of geophones can be selected for an allowable mean location error of microseismic events.

We used the geophones distributed at the top surface as shown in **Figure 91** to relocate microseismic events in **Figure 90**, and the relocated microseismic events are shown in **Figure 92** and **Figure 93**. We then calculated the mean location errors, and **Figure 94** displays the averaged location errors versus the number of geophones used as shown in **Figure 91**. From **Figure 94**, we can choose the number of geophones needed for a given allowable mean location error of microseismic events. Again, an accurate, high-resolution velocity model derived from 3-D surface seismic data is needed for reliable estimation of mean location errors and the optimal design of passive seismic monitoring network. We can use the same methodology to study the optimal design using a random distribution of geophones and a high-resolution 3-D velocity model.

XVI. FEASIBILITY ASSESSMENT OF REPURPOSING EXISTING ASSETS AND NEW WELL DESIGN

A. Economic and technical feasibility of repurposing existing wells

The feasibility analysis for repurposing wells can be divided into two parts; repurposing the RSU#1, and repurposing wells outside of the state land section 16, where RSU#1 is located. Although a technical and economic analysis was original planned, the technical analyses showed that no wells could be repurposed to meet the project needs, so no economic analyses were conducted.

RSU#1

The first well analyzed was the RSU#1. The RSU#1 was drilled in 2011 as part of WY-CUSP (DE-FE0002142). The well was drilled and cased with a 16-inch conductor to 120 ft, a 10 ¾-inch surface casing set at 2000 ft, a 7-inch casing set at 9,750 ft, and a 3 ½-inch liner set at 12,810 ft (**Figure 95**). The liner was cemented into 7-inch casing, the 7-inch casing was cemented into the surface casing, and the surface and conductor casings were cemented to surface. The well was drilled as a characterization well, worked to collect seismic data, worked over to remove the geophones, and plugged and abandoned. Plugs were set from total depth through the Weber formation (11,150 ft) in the liner section and four plugs were set in the 7-inch casing at measured depths of 5,780-5,881 ft., 4,091-4,200 ft., 1,880-2,200 ft., and 50-250 ft.

During the workover processes the service provider was unable to remove two fish in the well (**Figure 95**). One fish was a "retrievable" packer that got stuck at 9,366 ft. The other fish consisted of approximately 2,817 feet of Kevlar cable and approximately 2,107 feet of 1 ½ coiled tubing.

The design of the RSU#1 and the fish remaining after workover operations make reentry and conversion of the well to a project well impossible. Based on the design, the 3 ½-inch liner between TD and 9,464 ft eliminates the well from being able to support an injection or production string sufficiently large to allow the volumes required for the project. The inside diameter of the liner (3 ½ inch, 9.2 lb/ft) is 2.992-inches and a drift diameter of 2.867-inches. The injection and production tubing required for the project has an outside diameter larger that the liner drift diameter at 2.875-inches (2 7/8-inch, 7.9 lb/ft tubing, see **Figure 95**) which would not fit even if a proprietary joint were employed that did not add additional diameter to the string. The fish in the well are another significant hurdle. The service provider attempted multiple times to remove both fish during workover operations. This indicates that they cannot likely be removed which precludes the RSU#1 from being reentered and converted to a monitoring well. It should also be noted that even without the fish in the well the small size of the liner would have precluded use as anything other than a monitoring well.

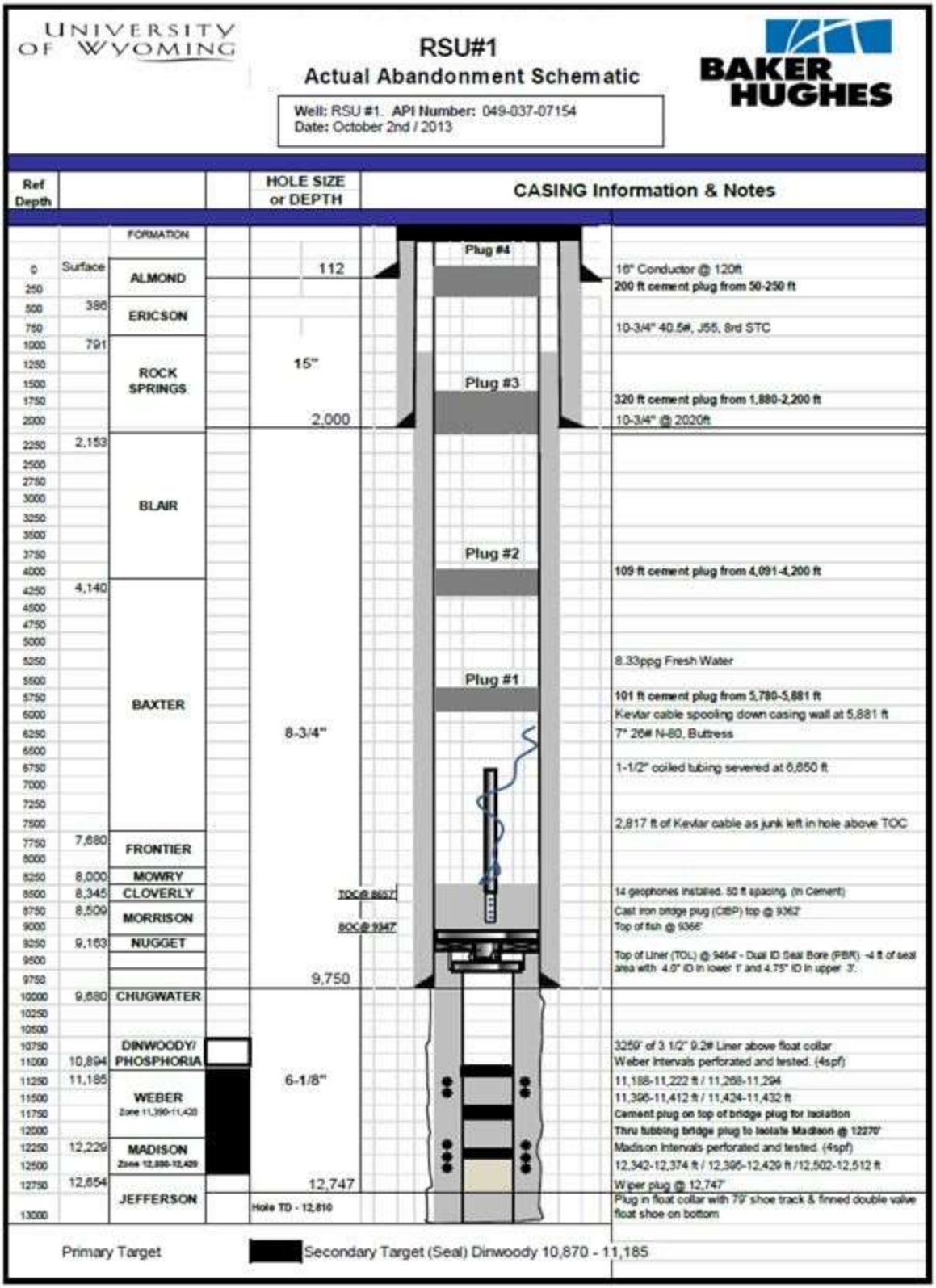

Figure 95: RSU#1 as it was plugged and abandoned

Other existing wells

A list of 33 wells was compiled by CMI as candidates for reentry and conversion (**Table 24**). All of the wells in the general area of the Rock Springs Uplift are outside of the state section (Section 16). The list was immediately narrowed to the wells in the adjacent sections to be able to best leverage the data collected from RSU#1 and the 3-D seismic survey of the area. The geology of the Rock Springs Uplift is heterogeneous. This heterogeneity dictates that the farther away CMI looks for existing wells the less likely they are to be represented by the existing subsurface data. Based on this the list of candidate wells was reduced from 33 wells to 8 wells (highlighted in green in Table 24).

Table 24: Possible existing candidate wells in the vicinity of RSU#1 (blue). Note: Green highlighted rows indicate wells in adjacent sections to section 16.

API NO.	COMPANY	T-R-S	TD
3721777	BP AMERICA PRODUCTION COMPANY	20-101-1 CSW	10,350
3721371	BP AMERICA PRODUCTION COMPANY	20-101-15 NWNW	8,727
3707154	RSU#1	20-101-16 SENE	12,810
3723254	ANADARKO E AND P COMPANY LP	20-101-19 NWSW	7,180
3721050	LUFF EXPLORATION	20-101-21 NWSW	7,188
3727184	GMT EXPLORATION COMPANY LLC	20-101-21 SESE	7,518
3720991	FOREST OIL CORPORATION	20-101-22 CSW	7,800
3720771	TRUE OIL LLC	20-101-26 NWNW	8,898
3726909	GMT EXPLORATION COMPANY LLC	20-101-26 NWSW BHL NWNW	7,752
3727389	GMT EXPLORATION COMPANY LLC	20-101-26 NWSW BHL SESE	7,875
3727015	GMT EXPLORATION COMPANY LLC	20-101-28 SESW	6,875
3727016	GMT EXPLORATION COMPANY LLC	20-101-28 SWNE	7,214
3726900	GMT EXPLORATION COMPANY LLC	20-101-29 SESW	6,840
3727260	TRUE OIL LLC	20-101-3 NESE	9,180
3720256	LUFF EXPLORATION	20-101-30 SENW	7,155
3727501	GMT EXPLORATION COMPANY LLC	20-101-30 SWNE	6,583
3725495	TRUE OIL LLC	20-101-4 NESE	8,884
3722801	PACIFIC ENTERPRISES OIL CO USA	20-101-4 NESE BHL SWSW 3	8,850
3720360	TRUE OIL LLC	20-101-4 SESW	7,917
3722793	TRUE OIL LLC	20-101-4 SESW	8,750
3720561	CODY ENERGY INC	20-101-5 SESE	8,720
3726542	GMT EXPLORATION COMPANY LLC	20-101-7 NWNE	8,000
3722308	SAMSON RESOURCES COMPANY	20-101-8 NENE	8,521
3724658	SAMSON RESOURCES COMPANY	20-101-8 NESW BHL CNW	8,600
3720408	TRUE OIL LLC	20-101-8 SENE	8,886
3720468	INDUSTRIAL GAS SERVICES INC	20-101-9 SENW	8,950
3722120	LEAR PETROLEUM EXPLORATION	21-100-32 SESW	9,900
3721492	FLORIDA GAS EXPLORATION CO	21-101-34 NESE	8,740
3720244	PRENALTA CORPORATION	21-101-34 SWSW	8,660
3720826	BP AMERICA PRODUCTION COMPANY	21-101-35 NWSE	8,848
3720224	PRENALTA CORPORATION	21-101-36 SESE	9,230
3721135	PRENALTA CORPORATION	21-101-36 SWSW	8,889
3720258	PRENALTA CORPORATION	20-101-18 SWSW	7,437

All 8 of the nearby wells were assessed with respect to ability to construct a project well using the existing infrastructure, each on an adjacent section (**Table 25**). All of the wells would require additional drilling to reach the Madison Limestone. Three of the wells are not available to the team because they are still in production (API numbers 3727184, 3722308, and 3724658). The other five wells are P&A'd and would require reentry to become project wells. Three wells of the P&A'd wells (API numbers 3721371, 3721050, and 3720991) had large sections of casing removed when they were abandoned. These wells are not likely candidates for reentry because of the added complication of finding and reconnecting to the production casing at depth. The two remaining P&A'd wells API No. 3720408 and 3720468 do not have large enough long string casing to be able to drill out from the original TD, set casing and then run a tubing string that is large enough to meet the project needs (2 7/8-inch tubing). Therefore, no existing wells meet the technical requirement of the project making an economic analysis unnecessary.

Table 25: Refined list of candidate wells analyzed to meet project technical needs

API NO.	COMPANY	T-R-S	TD	Long String Casing Size (in)	Next Bit Size (in)	Next Casing Size (in)	Tubing Size (in)	Status
3721371	BP AMERICA PRODUCTION COMPANY	20-101-15	8,727	5 1/2 (5,989 ft pulled)	4 1/2	3 1/2	1.9	P&A
3721050	LUFF EXPLORATION	20-101-21	7,188	4 1/2 (1,602 ft pulled)	3 7/8	2 3/8	1.05	P&A
3727184	GMT EXPLORATION COMPANY LLC	20-101-21	7,518	4 1/2	3 7/8	2 3/8	1.05	Producing
3720991	FOREST OIL CORPORATION	20-101-22	7,800	7 (set at 7595 ft)	6 1/8	4 1/2	2 3/8	P&A
3722308	SAMSON RESOURCES COMPANY	20-101-8	8,521	4 1/2	3 7/8	2 3/8	1.05	Producing
3724658	SAMSON RESOURCES COMPANY	20-101-8	8,600	5 1/2	4 1/2	3 1/2	1.9	Producing
3720408	TRUE OIL LLC	20-101-8	8,886	5 1/2	4 1/2	3 1/2	1.9	P&A
3720468	INDUSTRIAL GAS SERVICES INC	20-101-9	8,950	5 1/2	4 1/2	3 1/2	1.9	P&A

B. New Well Design and Cost Estimation

The project infrastructure will be constructed to illustrate that reservoir differential pressure changes and injectate plume movement can be controlled through variation of subsurface gradients created by injection and production. The project will have two wells; an injector and a production and monitoring well. This is the minimum configuration that can be used to validate the control of subsurface plumes. Each of the wells will be constructed in the same fashion. The Task is divided into eight subtasks. Subtasks 3.1 through 3.5 are planning and installation of wells and project infrastructure. Subtask 3.6 and 3.7 are injection and pressure management, respectively, and Subtask 3.8 is site closure.

Task 3 starts with finalizing the drilling plan. A base well design has been created during Phase I and a basic schedule and costing has been developed. The plan in Subtask 3.1 will detail all of the steps required to develop the site infrastructure. In will include a RACI chart to establish what project partners and stakeholders are **R**esponsible and **A**ccountable and who needs to be **C**onsult and **I**nformed. The planning will culminate with a drill well on paper (DWOP) exercise to ensure that all drilling service contractors know how they fit in to the overall process. Although the project is injecting water and will obtain a Class I non-hazardous UIC permit, all of the wells will be constructed to Class VI UIC standards to allow transition to CO_2 in a later project.

A design and associated cost was created for each well. The new wells were all assumed to be in the state section, (Section 16) to best leverage the existing knowledge of the RSU study site. Designing the project wells incorporated the existing data for the Madison Limestone at the site and CMI's ECLIPSE model generated for the project. The design used Schlumberger's PIPESIM to size the tubing required for injection and production, Schlumberger's Osprey (TDAS) to calculate loads on the well tubulars, and the results of corrosion modeling in OLI's corrosion analyzer to assess the effect of corrosion. Additional operational needs based on monitoring tools and equipment were also incorporated to finalize well designs. The costs of constructing the wells were calculated based in materials and services needed for each well.

Nodal Analysis

Nodal analyses were conducted for the injection well and production well using PIPESIM to quantify the size of tubing needed for each well. Sizing the tubing is the first step of the well design because each tubular (working from inside (tubing) to outside (conductor)) is sized based on the tubular inside.

Injection Well Nodal Analysis

The input data and injection rate requirement for the injection well are specified in **Table 26**. The Madison Limestone permeability, temperature, and injection zone depth were based on log and core measurements in RSU#1. The formation pressure was based on the steady-state ECLIPSE model of the site prepared for Phase 1.

Table 26: Injection well input data

	Madison Limestone
Depth of target zone (ft)	12,288 to 12,463
Temperature (°f)	204
Pressure (bar)	500 (7,252 psi)
kxy (mD)	5
Injection rate (Tonnes/year)	100,000

Four tubular sizes (**Table 27**) were used in the initial modeling to examine the injection of brine at rates of 100,000 tonnes/year (3.17 kg/s) and above.

Table 27: Injection tubing sizes used in PIPESIM nodal analyses

OD (inches)	**ID (Inches)**	**Linear mass (lb/ft)**
2.375	1.867	5.95
2.875	2.259	8.60
3.5	2.992	9.20
4	3.548	9.50

Nodal analysis using a wellhead pressure of 310 bar (4500 psi) and varying tubing size between 2.375 and 4 inches, indicates that all of the tubing sizes modeled are capable of meeting the injection requirement (**Figure 96**). However, the monitoring strategy calls for cased-hole pulsed neutron and formation resistivity logging, which rules out 2.375-inch tubing because the logging tools cannot pass through it to make measurements. Therefore, 2 7/8-inch 8.6 lb/ft tubing was selected for design.

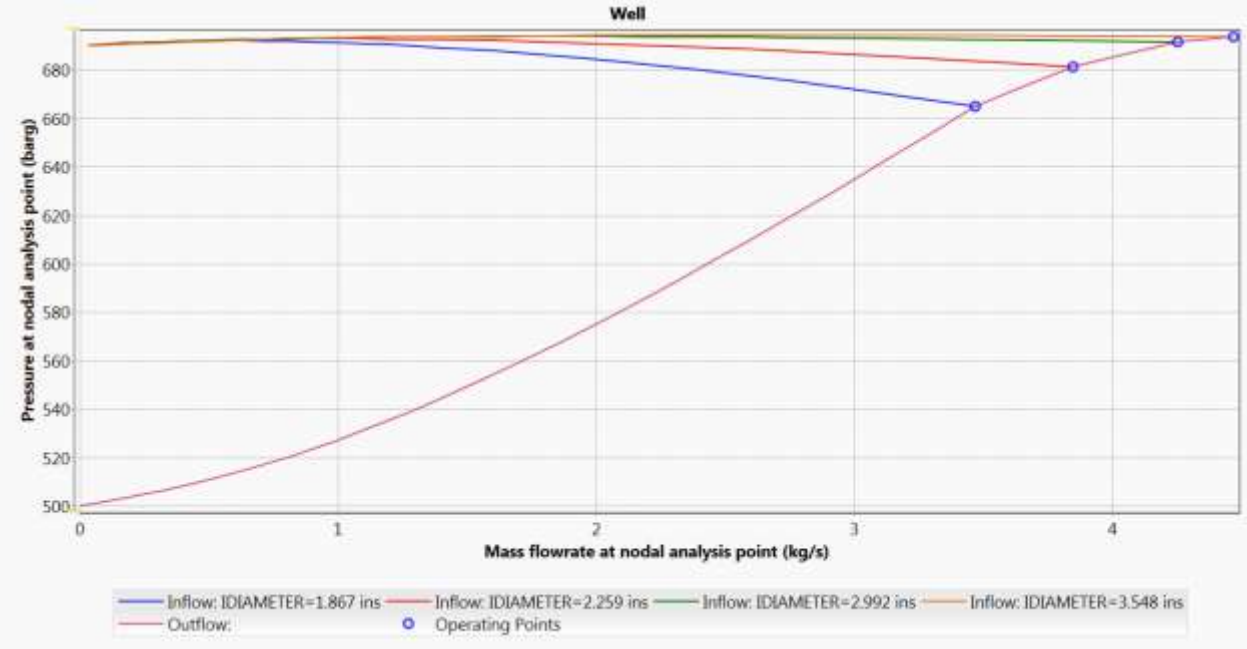

Figure 96: Injection well nodal analysis

Production Well Nodal Analysis

The input data and production requirement for the production well are specified in **Table 28**. The Madison Limestone permeability, temperature, and injection zone depth were based on log and core measurements in RSU#1 and are the same as in the injection well analysis. The formation pressure was also based on the steady-state ECLIPSE model of the site for Phase 1.

Table 28: Injection tubing sizes used in PIPESIM nodal analyses

	Madison Limestone
Depth of target zone (ft)	12,288 to 12,463
Temperature (°f)	204
Pressure (bar)	500 (7,252 psi)
kxy (mD)	5
Production rate (Tonnes/year)	50,000

Four tubular sizes (**Table 29**) were used in the initial modeling to examine the injection of water at a rate of 50,000 tonnes/year (1.58 kg/s).

Table 29: Production tubing sizes used in PIPESIM nodal analyses

OD (inches)	**ID (Inches)**	**Linear mass (lb/ft)**
2.375	1.867	5.95
2.875	2.259	8.60
3.5	2.992	9.20
4	3.548	9.50

Nodal analysis using a wellhead pressure of 6.9 bar (100 psi) and varying tubing sizes between 2.375 and 4 inches indicates that all of the tubing sizes modeled are capable of meeting the production requirement (**Figure 97**). However, like the injection well, the monitoring strategy in the production well calls for cased-hole pulsed neutron and formation resistivity logging, which rules out 2.375-inch tubing because the logging tools cannot pass through it to make measurements. Therefore, 2 7/8-inch 8.6 lb/ft tubing was selected for design.

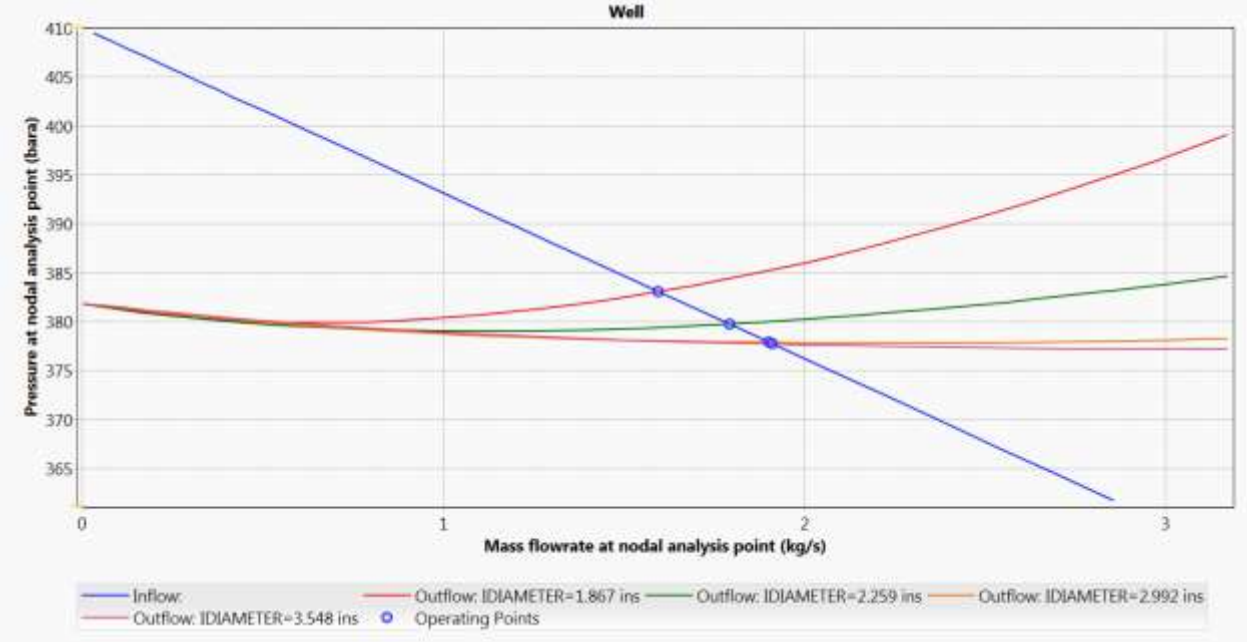

Figure 97: Production well nodal analysis

Casing and Tubing Design

Schlumberger's Osprey (TDAS) was used to analyze the likely forces on the well tubulars for the injection and production wells. The injector was assumed to have 9 5/8-inch surface casing set at 2,000 ft, 5 ½-inch casing set at 12,600 ft, and 2 7/8-inch tubing set at 12,200 ft. **Table 30** provides more detail on the tubulars.

Table 30: Assumed tubular string sizes for project wells

Well	Casing String	Casing OD (in)	Grade/Weight
All wells	Surface	9 5/8	J55 40lb/ft
	Injection	5 ½	L80 17lb/ft
	Tubing	2 7/8	L80 7.9lb/ft

Likely load cases were selected in Osprey to analyze the tubulars and estimate if they will be sufficiently robust for construction and operation. The load cases were for the injection well were:

<u>Surface Casing:</u>
Installed Load
1/3 Evacuation – 12,600 ft
Pressure Test – 2,000 ft

50 bbl Gas Kick – 12,600 ft
1/3 Replacement – 2,000 ft - Circulating
1/3 Replacement – 12,600 ft - Circulating
1/3 Replacement – 2,000 ft - Static
1/3 Replacement – 12,600 ft – Static

Injection Casing:

Installed Load
Cementing (Wet cement in the casing, water outside the casing)
Cementing (Brine inside the casing, wet cement outside the casing)

Injection Tubing:

Installed Load
Full Evacuation - Static
Injection

All of the proposed strings were sufficient to meet the project requirements with design factors for burst, collapse, tension, compressions, and Von Mises Ellipse (VME) above the design criteria. **Figure 98** shows a schematic of the VME design factors for the injection well. **Tables 31-33** provide the minimum design factors for pressure, axial load, and VME from all load cases. **Tables 34-36** provides the minimum calculated design factors for pressure, axial load, and VME for each of the load cases run.

Table 31: Minimum design factors and design criteria for the injection well surface casing

Load	Design Factor	Design Criteria	Failure Cause	MD (ft)	Position	Load Name	Item Name
Burst	1.4	1.25	Pipe Body	0	Below	1/3 Replacement - 12600 ft - Circulating	9-5/8 40.00 J55 LTC
Collapse	1.83	1	Plastic	1,999	Above	1/3 Evacuation - 12600 ft	9-5/8 40.00 J55 LTC
Tension	3.97	1.5	Jump Out	0	Below	1/3 Replacement - 12600 ft - Static	9-5/8 40.00 J55 LTC
Compression	6.88	1.2	Pin	1,999	Above	1/3 Evacuation - 12600 ft	9-5/8 40.00 J55 LTC
VME	1.41	1.25		0	Below	1/3 Replacement - 12600 ft - Circulating	9-5/8 40.00 J55 LTC

Table 32: Minimum design factors and design criteria for the injection well long-string casing

Load	Design Factor	Design Criteria	Failure Cause	MD (ft)	Position	Load Name	Item Name
Burst	2.26	1.25	Pipe Body	12,599	Above	Cementing (Cement in water out)	5-1/2 17.00 N80 LTC
Collapse	1.87	1	Plastic	12,599	Above	Cementing (Brine in cement out)	5-1/2 17.00 N80 LTC
Tension	1.62	1.5	Jump Out	0	Below	Cementing (Cement in water out)	5-1/2 17.00 N80 LTC
Compression	2.43	1.2	Pin	12,599	Above	Cementing (Brine in cement out)	5-1/2 17.00 N80 LTC
VME	1.65	1.25		0	Below	Cementing (Cement in water out)	5-1/2 17.00 N80 LTC

Table 33: Minimum design factors and design criteria for the injection well tubing

Load	Design Factor	Design Criteria	Failure Cause	MD (ft)	Position	Load Name	Item Name
Burst	2.36	1.25	Pipe Body	0	Below	Injection	2-7/8 7.90 L80 EUE
Collapse	1.88	1.1	Yield	12,200	Above	Full Evacuation - Static	2-7/8 7.90 L80 EUE
Tension	2.09	1.5	Pipe Body	0	Below	Installed Load	2-7/8 7.90 L80 EUE
Compression	6.95	1.2	Pipe Body	12,200	Above	Injection	2-7/8 7.90 L80 EUE
VME	1.79	1.25		12,200	Above	Injection	2-7/8 7.90 L80 EUE

Table 34: Minimum design factors for each injection well surface casing load case

Load Name	Pressure				Axial				VME		
	Load	DF	MD (ft)	Position	Load	DF	MD (ft)	Position	DF	MD (ft)	Position
Installed Load	Collapse	11.47	1,999	Above	Tension	9.29	0	Below	10	0	Below
1/3 Evacuation - 12600 ft	Collapse	1.83	1,999	Above	Compression	6.88	1999	Above	3.05	1999	Above
Pressure Test - 2000 ft	Burst	6.06	1,999	Above	Tension	8.59	0	Below	6.42	1999	Above
50 bbl Gas Kick - 12600 ft	Burst	1.52	1,999	Above	Tension	20.98	0	Below	1.51	1999	Above

1/3 Replacement - 2000 ft - Circulating	Burst	8.06	1,999	Above	Tension	9.08	0	Below	8.52	0	Below
1/3 Replacement - 12600 ft - Circulating	Burst	1.4	0	Below	Compression	7.19	1999	Above	1.41	0	Below
1/3 Replacement - 2000 ft - Static	Burst	8.06	1,999	Above	Tension	7.42	0	Below	7.69	0	Below
1/3 Replacement - 12600 ft - Static	Burst	1.4	0	Below	Tension	3.97	0	Below	1.54	0	Below

Table 35: Minimum design factors for each injection well long-string casing load case

Load Name	**Pressure**				**Axial**				**VME**		
	Load	**DF**	**MD (ft)**	**Position**	**Load**	**DF**	**MD (ft)**	**Position**	**DF**	**MD (ft)**	**Position**
Installed Load	Collapse	4.61	12,599	Above	Tension	2.12	0	Below	2.16	0	Below
Cementing (Cement in water out)	Burst	2.26	12,599	Above	Tension	1.62	0	Below	1.65	0	Below
Cementing (Brine in cement out)	Collapse	1.87	12,599	Above	Tension	1.62	0	Below	1.65	0	Below

Table 36: Minimum design factors for each injection well long-string casing load case

Load Name	**Pressure**				**Axial**				**VME**		
	Load	**DF**	**MD (ft)**	**Position**	**Load**	**DF**	**MD (ft)**	**Position**	**DF**	**MD (ft)**	**Position**
Installed Load					Tension	2.09	0	Below	1.87	0	Below
Full Evacuation - Static	Collapse	1.88	12,200	Above	Tension	2.37	0	Below	1.82	12,200	Above
Injection	Burst	2.36	0	Below	Tension	2.45	0	Below	1.79	12,200	Above

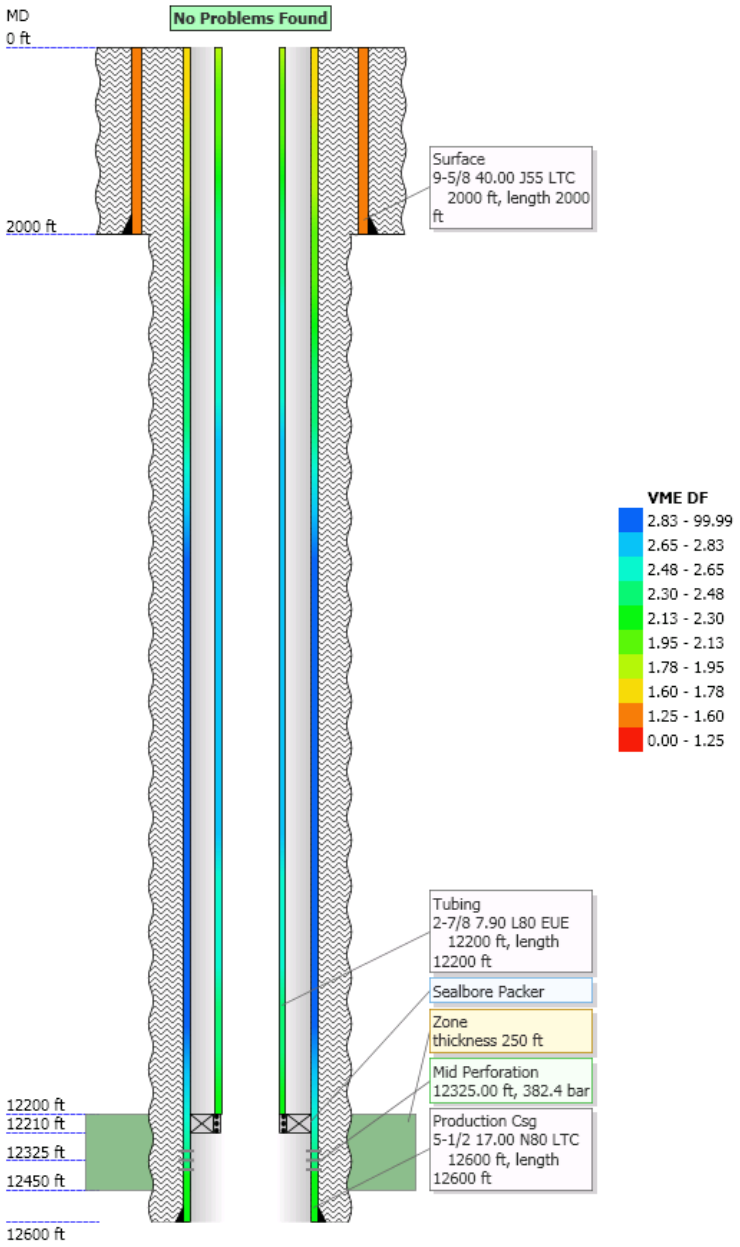

Figure 98 Schematic showing the VME design factor for each tubular string in the injection well.

The production well was assumed to have the same construction details as the injection well shown above in **Table 30**. Like the injection well, likely load cases were selected in Osprey to analyze the casing and estimate if it will meet the project requirements. The load cases for the surface casing were identical to those of the injection well surface casing. The load cases for the production casing and production tubing were:

Production Casing:
Installed Load
Surface Tubing Leak-Hot
Cementing (Wet cement in the casing, water outside the casing)
Cementing (Brine inside the casing, wet cement outside the casing)
Production Tubing:
Installed Load
Full Evacuation – Static
Full Evacuation – Hot
Gas Shut-In – Hot
Gas Shut-In -- Static
After Perforation

All of the proposed strings met the project requirements with design factors for burst, collapse, tension, compression, and VME above the design criteria. **Figure 99** shows a schematic of the VME design factors for the production well. **Tables 37 through 39** provide the minimum design factors for pressure, axial load, and VME from all load cases. **Tables 40 through 42** provides the minimum calculated design factors for pressure, axial load, and VME for each of the load cases run.

Table 37: Minimum design factors and design criteria for the production well surface casing

Load	Design Factor	Design Criteria	Failure Cause	MD (ft)	Position	Load Name	Item Name
Burst	1.4	1.25	Pipe Body	0	Below	1/3 Replacement – 12,600 ft - Circulating	9-5/8 40.00 J55 LTC
Collapse	1.83	1	Plastic	1999	Above	1/3 Evacuation – 12,600 ft	9-5/8 40.00 J55 LTC
Tension	3.97	1.5	Jump Out	0	Below	1/3 Replacement – 12,600 ft - Static	9-5/8 40.00 J55 LTC
Compression	6.88	1.2	Pin	1999	Above	1/3 Evacuation – 12,600 ft	9-5/8 40.00 J55 LTC
VME	1.41	1.25		0	Below	1/3 Replacement – 12,600 ft - Circulating	9-5/8 40.00 J55 LTC

Table 38: Minimum design factors and design criteria for the production well long-string casing

Load	Design Factor	Design Criteria	Failure Cause	MD (ft)	Position	Load Name	Item Name
Burst	1.56	1.25	Pipe Body	12,200	Above	Surface Tubing Leak - Hot	5-1/2 17.00 N80 LTC
Collapse	1.87	1	Plastic	12,599	Above	Cementing (Brine in cement out)	5-1/2 17.00 N80 LTC

Tension	1.62	1.5	Jump Out	0	Below	Cementing (Cement in water out)	5-1/2 17.00 N80 LTC
Compression	2.43	1.2	Pin	12,599	Above	Cementing (Brine in cement out)	5-1/2 17.00 N80 LTC
VME	1.57	1.25		12,200	Above	Surface Tubing Leak - Hot	5-1/2 17.00 N80 LTC

Table 39: Minimum design factors and design criteria for the production well tubing

Load	Design Factor	Design Criteria	Failure Cause	MD (ft)	Position	Load Name	Item Name
Burst	2.91	1.25	Pipe Body	0	Below	Gas Shut-In - Hot	2-7/8 7.90 L80 EUE
Collapse	2.33	1.1	Yield	12,200	Above	Full Evacuation - Hot	2-7/8 7.90 L80 EUE
Tension	2.14	1.5	Pipe Body	0	Below	Gas Shut-In - Static	2-7/8 7.90 L80 EUE
Compression	3.92	1.2	Pipe Body	12,200	Above	Full Evacuation - Hot	2-7/8 7.90 L80 EUE
VME	1.93	1.25		0	Below	Installed Load	2-7/8 7.90 L80 EUE

Table 40: Minimum design factors for each production well surface casing load case

Load Name	Pressure				Axial				VME		
	Load	DF	MD (ft)	Position	Load	DF	MD (ft)	Position	DF	MD (ft)	Position
Installed Load	Collapse	11.47	1,999	Above	Tension	9.29	0	Below	10	0	Below
1/3 Evacuation - 12600 ft	Collapse	1.83	1,999	Above	Compression	6.88	1999	Above	3.05	1999	Above
Pressure Test - 2000 ft	Burst	6.06	1,999	Above	Tension	8.59	0	Below	6.42	1999	Above
50 bbl Gas Kick - 12600 ft	Burst	1.52	1,999	Above	Tension	20.98	0	Below	1.51	1999	Above
1/3 Replacement - 2000 ft - Circulating	Burst	8.06	1,999	Above	Tension	9.08	0	Below	8.52	0	Below
1/3 Replacement - 12600 ft - Circulating	Burst	1.4	0	Below	Compression	7.19	1999	Above	1.41	0	Below

1/3 Replacement - 2000 ft - Static	Burst	8.06	1,999	Above	Tension	7.42	0	Below	7.69	0	Below
1/3 Replacement - 12600 ft - Static	Burst	1.4	0	Below	Tension	3.97	0	Below	1.54	0	Below

Table 41: Minimum design factors for each production well long-string casing load case

Load Name	**Pressure**				**Axial**				**VME**		
	Load	**DF**	**MD (ft)**	**Position**	**Load**	**DF**	**MD (ft)**	**Position**	**DF**	**MD (ft)**	**Position**
Installed Load	Collapse	4.61	12,599	Above	Tension	2.12	0	Below	2.16	0	Below
Surface Tubing Leak - Hot	Burst	1.56	12,200	Above	Tension	2.05	0	Below	1.57	12200	Above
Cementing (Cement in water out)	Burst	2.26	12,599	Above	Tension	1.62	0	Below	1.65	0	Below
Cementing (Brine in cement out)	Collapse	1.87	12,599	Above	Tension	1.62	0	Below	1.65	0	Below

Table 42: Minimum design factors for each production well tubing load case

Load Name	**Pressure**				**Axial**				**VME**		
	Load	**DF**	**MD (ft)**	**Position**	**Load**	**DF**	**MD (ft)**	**Position**	**DF**	**MD (ft)**	**Position**
Installed Load					Tension	2.15	0	Below	1.93	0	Below
Full Evacuation - Static	Collapse	2.34	12,200	Above	Tension	2.35	0	Below	2.11	0	Below
Full Evacuation - Hot	Collapse	2.33	12,200	Above	Tension	3.38	0	Below	2.34	12200	Above
Gas Shut-In - Hot	Burst	2.91	0	Below	Tension	2.69	0	Below	2.31	0	Below
Gas Shut-In - Static	Burst	3.04	0	Below	Tension	2.14	0	Below	1.98	0	Below
After Perforating	Burst	5.63	12,200	Above	Tension	2.33	0	Below	2.25	0	Below

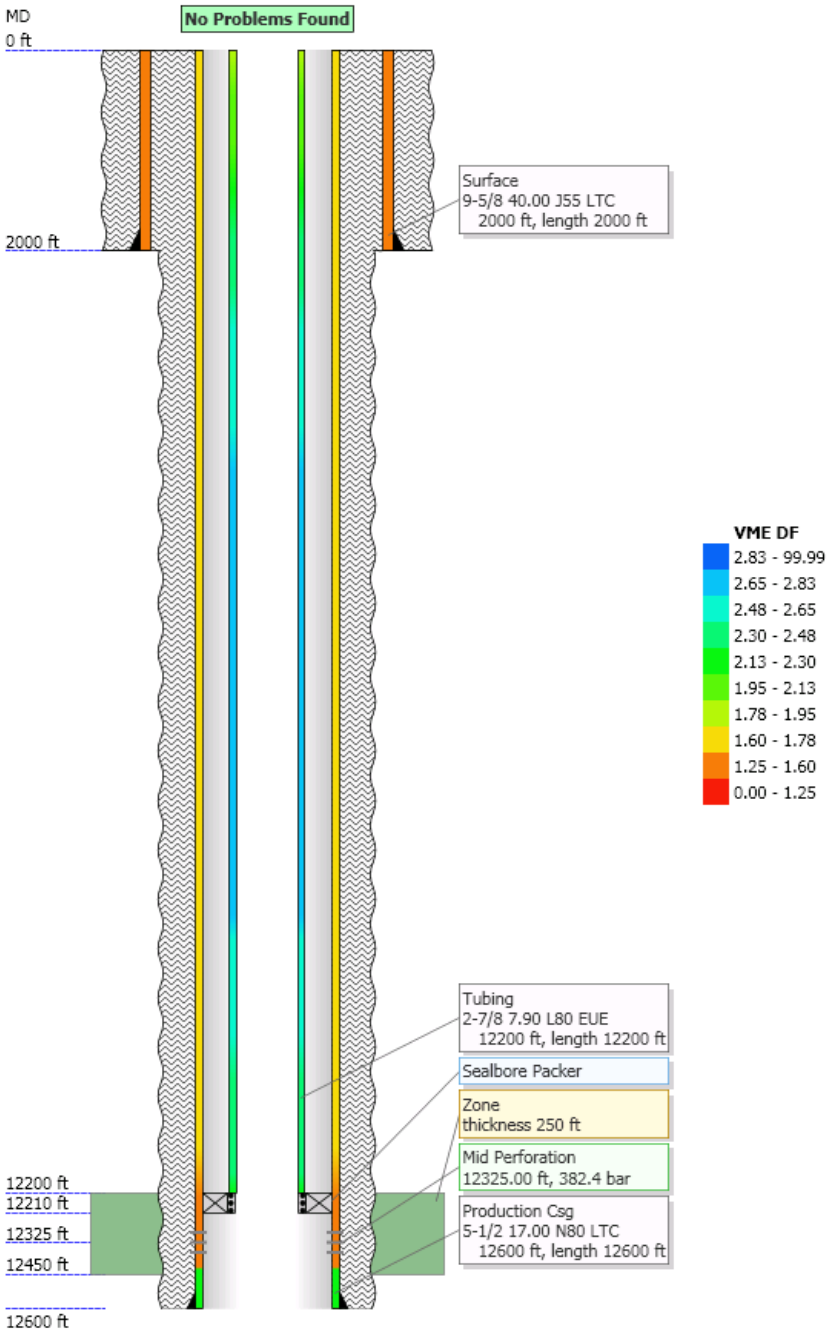

Figure 99: Schematic showing the VME design factor for each tubular string in the production well.

Scale and corrosion

Scale and formation incompatibility is not expected to be an issue. The injection fluid from the Jim Bridger power station is that same fluid that was used during hydraulic testing during the RSU#1 characterization, and no scaling or formation damage was observed. Production scale is also not expected based on the geochemistry of the Madison Formation. However, previous work on the scale in production in the RSU#1 indicates that if scale forms it will be dominated by $CaCO_3$.

Existing modeling on corrosion from exposure to brine was examined to address possible corrosion during operations for this project. Both flowing and shut-in conditions using the 2011 and 2012 brine sample geochemistries collected in RSU#1 were examined. The 2011 chemistry included less H_2S than the 2012 chemistry. Testing in RSU#1 resulted in a slight souring of the Madison Limestone. It is possible that this project could also sour the Madison. The results of the modeling showed that both mild steel (J55, L80, N80 and others) and 13-chrome steel perform sufficiently to be used as construction materials for the injection and production wells. **Figure 100** illustrates general corrosion rates for 2204, 304, 13-chrome, and mild steels under flowing conditions.

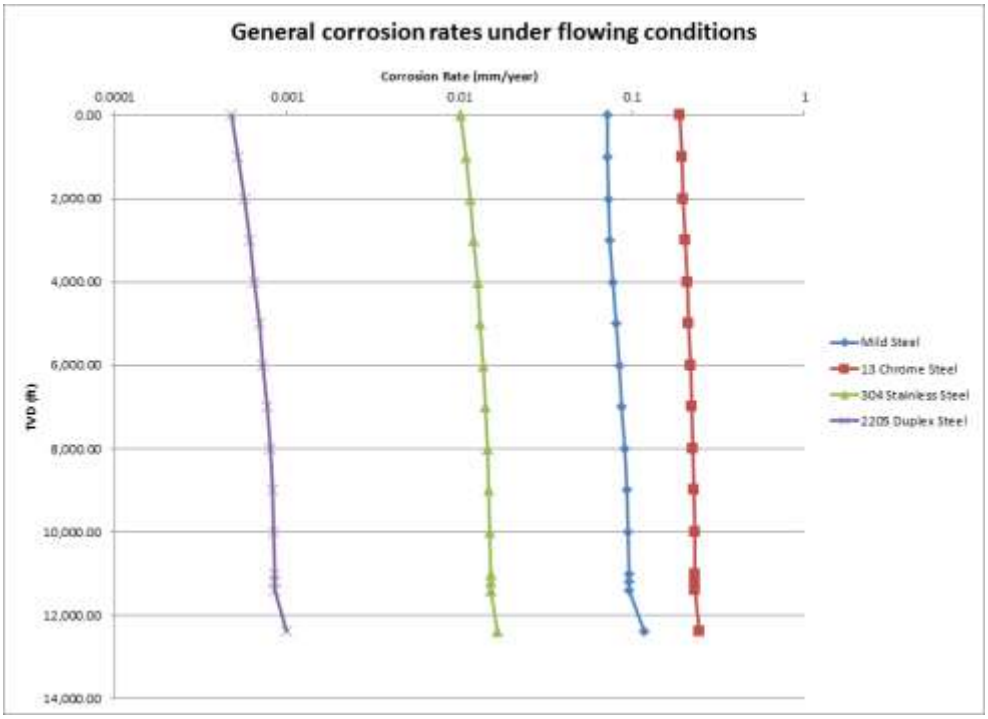

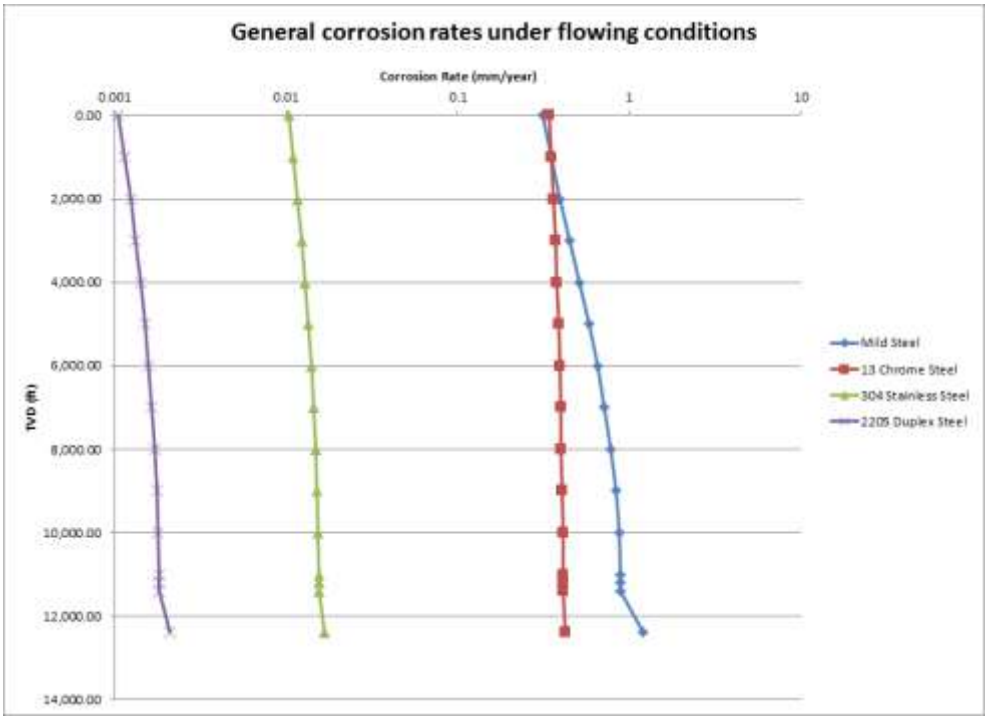

Figure 100: Simulated corrosion versus depth using the 2011 (top) and 2012 (bottom) geochemical data under flowing conditions

Well Design

The casing program for each well is detailed in **Table 43** and Figure **101**. The well design takes into account the nodal analyses data, the Osprey design factors, scale, and corrosion analysis. Each of the wells will be designed and constructed to meet UIC Class VI requirements in case a future project allows them to be used to inject CO_2. The lower 1,000 ft of the long-string in each well will be constructed using 13-chrome steel to provide better corrosion resistance in the injection zone. The upper portion of the long-string casings and the tubing strings will use L80 steel to provide better performance in case H_2S becomes an issue due to souring of the reservoir. The production tubing will 2 7/8-inch 7.9 lb/ft L80 with a packer set at 12,200 ft. This is slightly larger in inside diameter than what was used in the nodal analysis. It will perform as well or better that the tubing in the nodal analysis.

Each well will be fitted with a 5 Ksi wellhead (**Figure 101**) designed to meet all of the project injection, production, and monitoring requirements. Each wellhead will allow the measurement of pressure in the annulus between the casing and tubing. Each wellhead will have pass-throughs for the fiber optic lines and downhole pressure gauges, and a chemical injection line to allow anti-scale chemicals to be placed into the produced brine if scaling becomes an issue. The injection well will be fitted a 300Q-5H quintuplex plunger pump fitted with a Baldor Model ECP44256T-4, 250 HP, 1200 RPM, electric motor to allow injection up to 200,000 tonnes/year. Each casing string will be cemented to surface. Centralizers will be employed to ensure that the best possible cement job is obtained. The cement in the Madison will contain silica additive to provide CO_2-resistance by reacting out Portlandite that would otherwise result during the

hydration reaction. **Table 44** and **Table 45** show the lead and tail slurry designs for the surface casing cement and **Table 46** shows the single slurry planned for the long-string section.

Table 43: Casing and tubing details for both project wells

Well	Casing String	Bit Size (in)	Casing OD (in)	Grade/Weight	Thread	Set Depth (ft)	Comments
All wells	Conductor	17 ½	13 3/8	J55 61lb/ft	LTC	+/- 120’	Cement to surface
	Surface	12 ¼	9 5/8	J55 40lb/ft	LTC	+/- 2,000’	Cement to surface
	Injection	7 7/8	5 ½	L80 17lb/ft	LTC	+/- 11,800	Cement to surface
		7 7/8	5 ½	13Cr80 17lb/ft	VAM	+/-11,800 to +/-12,800	
	Tubing	-	2 7/8	L80 7.9lb/ft	LTC	+/- 12,200	Stabilized brine annular fluid

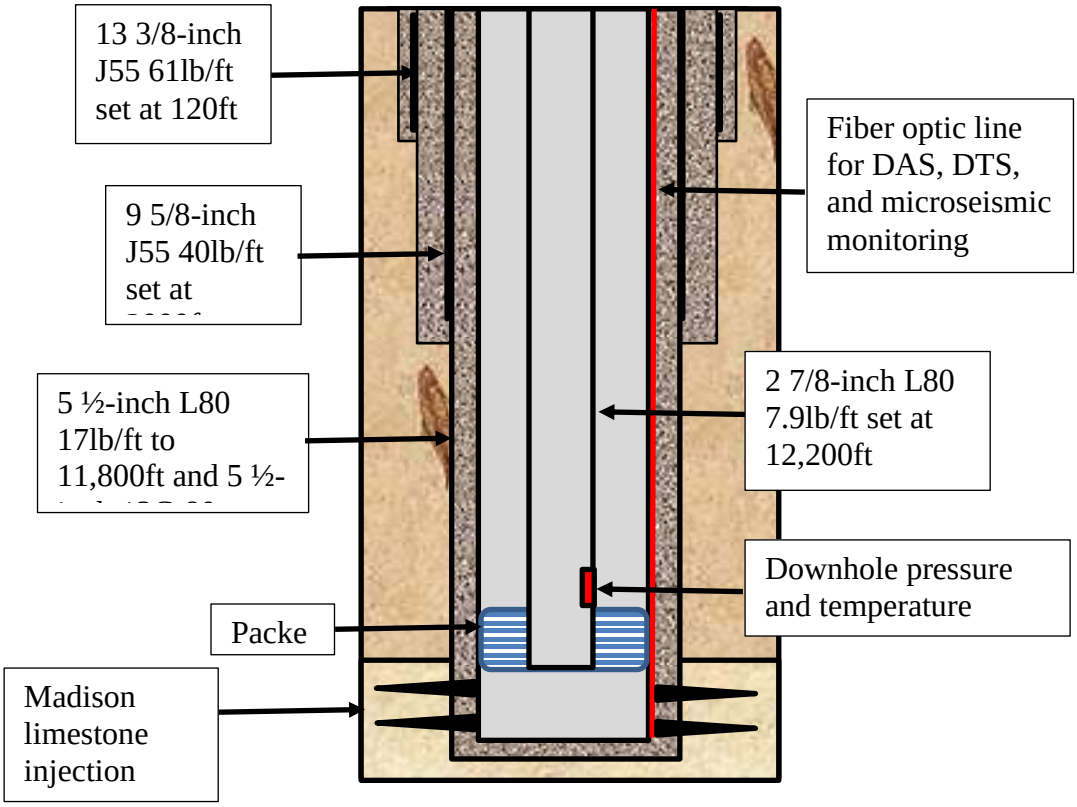

Figure 101: Well tubular diagram for both project wells

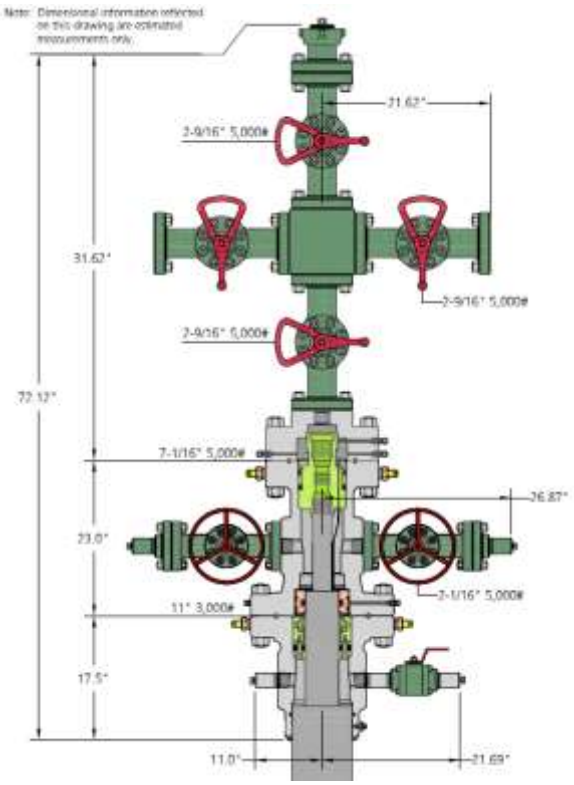

Figure 102: Initial wellhead design from Cameron for a 5 Ksi wellhead for both project wells

Table 44: Surface section lead slurry design

Lead Slurry (444 sacks, 94.0 lbm per sack of Blend)			
System		Conventional	
Density	12.50		lb/gal
Yield	2.11		ft3/sk
Mix Water	12.06		gal/sk
Mix Fluid	12.09		gal/sk
Total Volume	166.9		bbl
Additives	**Code**	**Description**	**Concentration**
D907	Cement	94.00	lb/sk BWOB
D013	Retarder	0.75	% BWOB
D029	Lost circ	0.25	lb/sk WBWOB
D047	Antifoam	0.03	gal/sk VBWOB
D079	Extender	2.00	% BWOB

Table 45: Surface section tail slurry design

Tail Slurry (134 sacks, 94.0 lbm per sack of Blend)			
System		Conventional	
Density	15.80		lb/gal
Yield	1.16		ft3/sk

Mix Water	5.07	gal/sk	
Mix Fluid	5.10	gal/sk	
Total Volume	27.7	bbl	
Additives	**Code**	**Description**	**Concentration**
D907	Cement	94.00	lb/sk BWOB
D013	Retarder	0.30	% BWOB
D029	Lost circ	0.25	lb/sk WBWOB
D047	Antifoam	0.03	gal/sk VBWOB

Table 46: Long-string section single slurry design

TXI Single Slurry (1717 sacks, 75.0 lbm per sack of Blend)			
System		Conventional	
Density	13.50	lb/gal	
Yield	1.68	ft3/sk	
Mix Water	8.10	gal/sk	
Mix Fluid	8.10	gal/sk	
Total Volume	514.3	bbl	
Additives	**Code**	**Description**	**Concentration**
D049	Cement	75.00	lb/sk BWOB
D013	Retarder	0.45	% BWOC
D046	Antifoam	0.50	% BWOC
D065	Dispersant	0.30	% BWOC
D066	Silica	35.00	% BWOC
D167	Fluid loss	0.40	% BWOC

The wells will be perforated in the Madison between, 12,250 ft and 12,425 ft. The perforating guns will be oriented to avoid damaging the fiber optic line in the Madison Limestone. Prior to injection, a mechanical integrity test (MIT) will be conducted in the injection well to meet UIC requirements and assure well integrity.

Each well will be constructed maximize scientific data collection for validation of pressure and plume management strategies. This will include open hole logging to characterize the formations adjacent to each well, drill stem tests (DSTs) and fluid sampling to characterize the hydraulic properties of the Madison Limestone, and time-lapse cased hole logging to characterize (collect a baseline) and then monitor pulsed neutron an resistivity responses to injection/production in each well. The open-hole logging is described in **Table 47** (The logging tools are presented as Schlumberger trade names).

Table 47: Open-hole logging details for both wells

Well Section	Logging Tool	Purpose
Surface	Platform Express	The Platform Express is similar to a triple combo tool. The tool has multiple modules that can be run to provide basic information about the formations in each well. The tool will provide gamma-ray and neutron porosity measurements in all sections of the borehole. It will provide caliper measurement in the borehole. And it will provide resistivity, self-potential data. All of this data will be comparable to the data collected in RSU #1 allowing the team to assess the heterogeneity/homogeneity of the project site.
	Borehole compensated sonic	A borehole compensated sonic module will be run with the PEX to collect shear and compressional slowness in the surface hole. These data will aid in tying the wells into seismic measurements and characterizing the heterogeneity/homogeneity of the site
Long-string	Platform Express (PEX)	Data collection will be the same as in the surface hole
	Sonic Scanner	The sonic scanner will be used to collect oriented anisotropic shear wave data over the wellbore. The tool uses short and long receiver spacing to enable characterization of rock properties. The tool will collect shear and compressional slowness data. The data from the logs will inform to team's geomechanical understanding of the site and allow tie-in of the wells to the existing 3-D seismic and the VSP surveys that will be collected.
	Fullbore Formation Micro Imager (FMI)	The FMI generates an electrical (microresistivity) image of the borehole in water-based muds. The tool uses four pads to contact the borehole and provide a high resolution measurement with image details to 50 microns. The FMI will be used to identify natural, drilling induced, and test induced fractures in the overburden and crystalline sections of the borehole.
	The Mechanical Sidewall Coring Tool (MSCT)	The MSCT will be used to collect sidewall cores in zones of interest. This will allow comparison to and validation of the new logs and comparison to the core collected in RSU 1. Difference and similarities between the RSU #1 core and new sidewall core will further aid in understanding the site heterogeneity/homogeneity.

DSTs will be performed in the Madison Limestone and possibly other formations before installing the long-string casing in each well to quantify hydraulic properties and identify reservoir boundaries.

Cased-hole logging will be performed during construction of each well to assess well integrity and monitor the plume of injected fluid. Well integrity will be assessed using a cement bond logging tool to measure the average cement bond and the Isolation Scanner ultrasonic logging tool to map the location, quality of cement, and cement bond radially along the well.

Cased-hole logging for monitoring of pressure and plume management will consist of time-lapse cased-hole formation resistivity logging and pulsed neutron logging. Each of these logging tools will be run at end of construction to collect a pre-operational baseline and then repeated during the operational period to assess injection/production related changes in the Madison Limestone. Each well will have a pressure transducer and temperature gauge above the packer in the tubing to provide continuous temperature and pressure data. Each well will also be completed with a fiber optic line cemented from the TD to surface behind the long-string casing. The fiber optic line will be used collect seismic survey data, microseismic data, distributed temperature data, and identify pressure plume arrival in different strata.

The construction of the production well will follow the same steps as the injection well with the exception that the production well will have an electric submersible pump (ESP) instead of an injection pump and an MIT will not be required before production. The initial plan for the ESP is a Summit ESP Series 400 250 stage pump.

The estimate to construct and complete the injection well was created based on similar projects and with advice of local drilling and service companies. Drilling time was also based on the drilling on drilling time for RSU#1 prior to coring. Rig time during drilling was estimated to be 17 days. **Table 48** provides the line items, references, and assumptions used to price the injection well. The injection well base costs are expected to be approximately $2.28 million.

Table 48: Injection Well Costs

Item	Quantity	Unit Price	Total	Reference
Conductor Casing	120	34.91	4,189.20	Estimate Based on Schlumberger Quote
Drilling	17	13,900.00	236,300.00	Estimate Based on Quote from True Drilling
Solids Control	17	2,405.00	40,885.00	Estimate Based on Quote from Clearwater
Solids Control Chemicals	1	3,000.00	3,000.00	Estimate Based on clarification of Quote from Clearwater
Surface cement	1	17,077.45	17,077.45	Estimate Based on Schlumberger Quote assuming only 50% discount
Primary cement	1	94,204.00	94,204.00	Estimate Based on Schlumberger Quote assuming only 50% discount
Cementing hardware	1	28,000.00	28,000.00	Estimate Based on Schlumberger Quote
Surface casing	2,000	25.91	51,820.00	Estimate Based on Schlumberger Quote
Long-string casing (12800-11800 ft)	1,000	36.56	36,560.00	Estimate Based on Schlumberger Quote
Long-string casing (11800-0)	11,800	11.05	130,390.00	Estimate Based on Tool Pusher Supply Company Quote
Tubing	12,200	5.42	66,124.00	Estimate Based on Tool Pusher Supply Company Quote
Packer	1	11,555.00	11,555.00	Estimate from Oilfield Tools Inc

Item	Quantity	Unit Price	Total	Reference
Wellhead	1	33,008.44	33,008.44	Estimate from Cameron
Surface hole OH Logs	1	10,318.03	10,318.03	Estimate Based on Schlumberger Quote
Surface hole CH logs	1	20,533.25	20,533.25	Estimate Based on Schlumberger Quote
Long-string OH logs	1	161,049.70	161,049.70	Estimate Based on Schlumberger Quote
Long-string CH Logs	1	95,372.12	953,72.12	Estimate Based on Schlumberger Quote
Mud	1	98,837.00	98,837.00	average of MMSS and AES Quotes
Mud logging	11	1,495.00	16,445.00	Estimate based on Schlumberger quote assuming 11 days of mud logging
Cuttings Hauling	1	19,592.41	19,592.41	Calculated using Freedom Oilfield Services Quote
Crew subsistence	374	20.00	7,480.00	Estimate Based on Quote from True Drilling
Conductor/mousehole/rathole				Included in Wyoming Casing Services Quote
Bits	1	102,730.00	102,730.00	Based on Previous Quote from Schlumberger
Conductor casing crew	1	11,310.00	11,310.00	Quote from Wyoming Casing Service
Surface casing crew	1	3,325.00	3,325.00	Quote from Wyoming Casing Service
Long-string casing crew	1	21,690.00	21,690.00	Quote from Wyoming Casing Service
Completion rig	1	78,440.00	78,440.00	Based on Quote from Basic Energy Services assuming 5 days
Perforating	1	86,746.46	86,746.46	Based on Schlumberger Quote
Infrastructure/other	25	495.00	12,375.00	Quote from Stallion Oilfield Services (assume 25 total days)
Pads/roads	1	56,553.47	56,553.47	Based of quote from Dan Hart Patrol (see subtask 3.2 explanation)
Fuel	17,600	3.00	52,800.00	Based on clarification from True Drilling on likely fuel usage of Rig 22
Pump	1	356,500.00	356,500.00	Based on quote from Fluid Systems Inc, assuming limited PM and Engineering
Mobilization/Demobilization	1	120,000.00	120,000.00	Based on quote from Black Hills Trucking
Crew Trailers	34	75.00	2,550.00	Based on clarification from True Drilling on crew numbers
Safety	1	31,883.00	31,883.00	Based on Quote from Casper Safety assuming 22 days of safety oversight
H2S Monitoring	1	10,000.00	10,000.00	Based on Quote from Casper Safety assuming 24 days of monitoring
Plug cement	1	50,000.00	50,000.00	Based on Schlumberger Quote
Plug Rig	1	78,440.00	78,440.00	Based on Quote from Basic Energy Services assuming 5 days
Site reclamation	1	19,908.64	19,908.64	Based of quote from Dan Hart Patrol and construction assumptions
		Total	**22,77,992.17**	

The cost of the production well was the similar to the injection well cost except the Fluid Systems Inc. pump was replaced by the SummitESP pump. The base cost of the production well was estimated at $2.17 Million.

XVII. APPENDICES

A. Complete Madison Formation Water Analyses

Analyses	Weber Formation Energy Labs (08/27/2011)	Weber Formation Core Labs (08/27/2011)	Weber Formation Energy Labs (12/14/12	Madison Limestone Energy Labs (08/27/2011)	Madison Limestone Core Labs (08/27/2011)	Madison Limestone Energy Labs (12/03/12)
Microbiological						
Heterotrophic (MPN/mL)	< 2	–	40	2	–	10
Major Ions						
pH	7.54	7.11	6.46	7.36	6.01	6.43
Alkalinity, Total as $CaCO_3$ (mg/L)	509	–	3030	1170	–	2620
Carbonate as CO_3 (mg/L)	ND	0	ND	ND	0	ND
Bicarbonate as HCO_3 (mg/L)	621	720	3690	1420	1,610	3190
Calcium (mg/L)	734	705	539	1190	1,280	1630
Chloride (mg/L)	60,900	61,830	57,400	50,300	52,290	51,600
Fluoride (mg/L)	11.5	8.4	6.1	3.5	13	2.8
Magnesium (mg/L)	37	40	45	158	170	195
Nitrogen, Ammonia as N (mg/L)	33.4	–	33.1	42	–	39
Nitrogen, Nitrate+Nitrite as N (mg/L)	0.1	ND	ND	ND	ND	0.1
Nitrogen, Nitrite as N (mg/L)	ND	ND	ND	ND	ND	ND
Phosphate	–	ND	–	–	ND	–
Potassium (mg/L)	–	1,940	1,910	–	4,210	3,780
Silicon (mg/L)	–	26	45.2	–	36	59.5
Sodium (mg/L)	40,700	43,250	36,500	29,000	32820	27,900
Strontium (mg/L)	–	26	14	–	67	51.1
Sulfate (mg/L)	11,600	10,320	6030	2,800	2,280	1,820
Non-Metals						
Dissolved inorganic carbon (mg/L)	144	–	786	355	–	724
Dissolved organic carbon (mg/L)	2.9	–	4.5	1	–	4.4
Total organic carbon (mg/L)	2.7	–	4.7	1	–	4.5
UV Absorbance at 254 nm (cm-1)	0.92	–	1.99	0.558	–	1.28
Total recoverable phenolics (mg/L)	0.61	–	0.16	0.05	–	0.7
Total cyanide (mg/L)	ND	–	0.098	ND	–	0.339
Sulfide (mg/L)	0.04		120	28	0	82
Sulfide as hydrogen sulfide (mg/L)	0.04	–	127	29	–	87
Physical properties						
Chemical oxygen demand (mg/L)	2420	–	9120	1940	–	3050
pH	7.54	7.11	6.46	7.36	6.01	6.43
Total dissolved solids @ 180 C (mg/L)	89,800	119,155	109,000	75,000	95,126	89,800

BOD (mg/L)	56.7	–	517	50.2	–	234
Sodium adsorption ratio	397	–	380	209	–	174
Metals						
Aluminum (mg/L)	ND	ND	3.5	ND	ND	1.9
Arsenic (mg/L)	0.095	–	0.444	1.76	–	0.376
Barium (mg/L)	ND	ND	14.3	1	ND	4.48
Beryllium (mg/L)	ND	–	0.007	ND	–	0.037
Bismuth (mg/L)	–	–	0.02	–	–	0.02
Boron (mg/L)	61.1	–	71.8	95.2	–	101
Borate (mg/L)	–	81		–	120	
Bromide (mg/L)	–	94	99	–	115	140
Cadmium (mg/L)	ND	ND	0.006	ND	ND	ND
Chromium (mg/L)	ND	ND	0.61	0.06	ND	0.576
Cobalt (mg/L)	0.02	ND	0.019	ND	ND	0.009
Copper (mg/L)	ND	ND	13.6	ND	ND	1.35
Iodide (mg/L)	–	ND	2	–	ND	ND
Iron (mg/L)	0.94	2.2	44.1	0.54	8.1	32.2
Lead (mg/L)	ND	ND	2.91	ND	ND	0.305
Lithium (mg/L)	92.8	100	90..5	91.9	105	91.6
Manganese (mg/L)	0.07	0.07	0.777	0.12	0.35	7.76
Mercury (mg/L)	ND	–	0.0006	ND	–	ND
Molybdenum (mg/L)	–	ND	–	–	ND	–
Nickel (mg/L)	ND	ND	0.093	ND	ND	0.03
Phosphorus	–	ND	–	–	ND	–
Selenium (mg/L)	0.0004	–	0.054	0.013	–	0.041
Silver (mg/L)	ND	–	ND	ND	–	0.001
Uranium (mg/L)	–	–	0.0187	–	–	0.0004
Vanadium (mg/L)	ND	–	0.26	ND	–	0.01
Zinc (mg/L)	0.26	–	4.58	0.4	–	2.1
Radionuclides						
Gross Alpha (pCi/L)	–	–	-400	–	–	157
Gross Beta (pCi/L)	–	–	1630	–	–	2990
Radium 226 (pCi/L)	–	–	24	–	–	39
Radium 228 (pCi/L)	–	–	14	–	–	1.2
Cesium 134 (pCi/L)	–	–	–	–	–	0
Cesium 137 (pCi/L)	–	–	–	–	–	0
Data Quality						
Anion/Cation Balance (± 5)	-3.15%	0.37%	-5.42%	-3.71%	2.61%	-4.57%
Organic Acids						
Acetate (mg/L)	–	5.5	–	–	0	–
Butyrate (mg/L)	–	0	–	–	0	–
Formate (mg/L)	–	5.4	–	–	1.7	–
Glycolate (mg/L)	–	0	–	–	0	–
Propionate (mg/L)	–	0	–	–	0	–
Valerate (mg/L)	–	0	–	–	0	–
Volatile organic compounds						
1,1,1,2-Tetrachloroethane (µg/L)	ND	–	ND	ND	–	ND

1,1,1-Trichloroethane (µg/L)	ND	–	ND	ND	–	ND
1,1,2,2-Tetrachloroethane (µg/L)	ND	–	ND	ND	–	ND
1,1,2-Trichloroethane (µg/L)	ND	–	ND	ND	–	ND
1,1-Dichloroethane (µg/L)	ND	–	ND	ND	–	ND
1,1-Dichloroethene (µg/L)	ND	–	ND	ND	–	ND
1,1-Dichloropropene (µg/L)	ND	–	ND	ND	–	ND
1,2,3-Trichlorobenzene (µg/L)	ND	–	ND	ND	–	ND
1,2,3-Trichloropropane (µg/L)	ND	–	ND	ND	–	ND
1,2,4-Trichlorobenzene (µg/L)	ND	–	ND	ND	–	ND
1,2,4-Trimethylbenzene (µg/L)	210	–	190	190	–	73
1,2-Dibromo-3-chloropropane (µg/L)	ND	–	ND	ND	–	ND
1,2-Dibromoethane (µg/L)	ND	–	ND	ND	–	ND
1,2-Dichlorobenzene (µg/L)	ND	–	ND	ND	–	ND
1,2-Dichloroethane (µg/L)	ND	–	ND	ND	–	ND
1,2-Dichloropropane (µg/L)	ND	–	ND	ND	–	ND
1,3,5-Trimethylbenzene (µg/L)	30	–	62	30	–	54
1,3-Dichlorobenzene (µg/L)	ND	–	ND	ND	–	ND
1,3-Dichloropropane (µg/L)	ND	–	ND	ND	–	ND
1,4-Dichlorobenzene (µg/L)	ND	–	ND	ND	–	ND
2,2-Dichloropropane (µg/L)	ND	–	ND	ND	–	ND
2-Chloroethyl vinyl ether (µg/L)	ND	–	ND	ND	–	ND
2-Chlorotoluene (µg/L)	ND	–	ND	ND	–	ND
4-Chlorotoluene (µg/L)	ND	–	ND	ND	–	ND
Benzene (µg/L)	ND	–	230	ND	–	13
Bromobenzene (µg/L)	ND	–	ND	ND	–	ND
Bromochloromethane (µg/L)	ND	–	ND	ND	–	ND
Bromodichloromethane (µg/L)	ND	–	ND	ND	–	ND
Bromoform (µg/L)	ND	–	ND	ND	–	ND
Bromomethane (µg/L)	ND	–	ND	ND	–	ND
Carbon tetrachloride (µg/L)	ND	–	ND	ND	–	ND
Chlorobenzene (µg/L)	ND	–	ND	ND	–	ND
Chlorodibromomethane (µg/L)	ND	–	ND	ND	–	ND
Chloroethane (µg/L)	ND	–	ND	ND	–	ND
Chloroform (µg/L)	ND	–	ND	ND	–	ND
Chloromethane (µg/L)	ND	–	ND	ND	–	ND
cis-1,2-Dichloroethene (µg/L)	ND	–	ND	ND	–	ND
cis-1,3-Dichloropropene (µg/L)	ND	–	ND	ND	–	ND
Dibromomethane (µg/L)	ND	–	ND	ND	–	ND
Dichlorodifluoromethane (µg/L)	ND	–	ND	ND	–	ND
Ethylbenzene (µg/L)	20	–	54	20	–	26
Hexachlorobutadiene (µg/L)	ND	–	ND	ND	–	ND
Isopropylbenzene (µg/L)	30	–	9	20	–	8.4
m+p-Xylenes (µg/L)	55	–	280	50	–	98
Methyl ethyl ketone (µg/L)	ND	–	280	ND	–	88
Methyl tert-butyl ether (MTBE) (µg/L)	ND	–	ND	ND	–	ND
Methylene chloride (µg/L)	ND	–	ND	ND	–	ND
n-Butylbenzene (µg/L)	57	–	44	40	–	53
n-Propylbenzene (µg/L)	ND	–	27	ND	–	28
Naphthalene (µg/L)	190	–	74	190	–	77
o-Xylene (µg/L)	ND	–	110	ND	–	66

p-Isopropyltoluene (µg/L)	ND	–	16	ND	–	15
sec-Butylbenzene (µg/L)	ND	–	15	ND	–	16
Styrene (µg/L)	ND	–	ND	ND	–	ND
tert-Butylbenzene (µg/L)	ND	–	ND	ND	–	ND
Tetrachloroethene (µg/L)	ND	–	ND	ND	–	ND
Toluene (µg/L)	ND	–	490	ND	–	86
trans-1,2-Dichloroethene (µg/L)	ND	–	ND	ND	–	ND
trans-1,3-Dichloropropene (µg/L)	ND	–	ND	ND	–	ND
Trichloroethene (µg/L)	ND	–	ND	ND	–	ND
Trichlorofluoromethane (µg/L)	ND	–	ND	ND	–	ND
Vinyl chloride (µg/L)	ND	–	ND	ND	–	ND
Xylenes (µg/L)		–	380		–	160
Organic Characteristics						
Oil and Grease (HEM) mg/L	270	–	1100	490	–	510
Compositional Analysis of Flash Gas						
Nitrogen (Mole %)	–	78.888	–	–	16.75	–
Carbon Dioxide (Mole %)	–	14.738	–	–	82.892	–
Hydrogen Sulfide (Mole %)	–	0	–	–	0	–
Methane (Mole %)	–	2.537	–	–	0.189	–
Ethane (Mole %)	–	0.297	–	–	0	–
Propane (Mole %)	–	0.213	–	–	0.021	–
Iso-Butane (Mole %)	–	0.043	–	–	0.004	–
N-Butane (Mole %)	–	0.071	–	–	0.011	–
Iso-Pentane (Mole %)	–	0.397	–	–	0.04	–
N-Pentane (Mole %)	–	0.02	–	–	0.004	–
Hexanes (Mole %)	–	2.119	–	–	0.006	–
Heptanes (Mole %)	–	0.244	–	–	0.015	–
Octanes (Mole %)	–	0.116	–	–	0.026	–
Nonanes (Mole %)	–	0.08	–	–	0.012	–
Decanes Plus (Mole %)	–	0.237	–	–	0.03	–

B. REFERENCES

Bakulin, A. and R. Calvert, 2006, The virtual source method: theory and case study: Geophysics, VOL. 71, no. 4, SI139–SI150

Bartos, Timothy, and L.L. Hallberg, 2010, *Chapter 5: Groundwater and Hydrogeologic Units* in *Available groundwater determination technical memorandum, Green River Basin Water Plan II. Report to the Wyoming Water Development Commission by the Wyoming State Geological Survey et al.*," David Copeland and Meg Ewald editors. pps. 5-1 – 5-94, Available 15 February 2016 at http://waterplan.state.wy.us/plan/green/2010/finalrept/.

Bell, D., 1998. Velocity Estimation for Pore Pressure Prediction, Pressure Regimes. *In* Huffman, A. and Bowers, G. (Eds). Sedimentary Basins and Their Prediction. *AAPG Memoir 76*.

Ben-Haim, Yakov. *Info-gap decision theory: decisions under severe uncertainty*. Academic Press, 2006.

Benke, Arthur C. and Colbert E. Cushing editors. 2005. *Rivers of North America*. Academic Press. pps 1168.

Bethke, C. M. (1996) geochemical reaction modeling: Concepts and applications. Oxford University press.

Biewick, Laura R.H. 2009. *Oil and Gas Development in Southwestern Wyoming—Energy Data and Services for the Wyoming Landscape Conservation Initiative (WLCI)* Accessed 1 February 2016 from http://pubs.usgs.gov/ds/437/downloads/pdf/WLCI.pdf.

Bowers, G. L., 1995. Pore pressure estimation from velocity data: Accounting for pore pressure mechanisms besides undercompaction. *SPE Drilling and Completion*, 10, 89–95.

Bowers, G.L., 2002. Detecting high overpressure. *The Leading Edge*, 21, 174-177.

Burba, J. L., and W. C. Baumann (1990) Intercalations of crystalline lithium aluminates. U.S. Patent 4,910,246.

Cameco, 2016. *Environment & Safety* Accessed 5 February 2016 from https://www.cameco.com/businesses/uranium-operations/usa/smith-ranch-highland/environment-safety.

Coblentz, D. and K. Karlstrom, 2011. Tectonic geomorphometrics of the western United States: Speculations on the surface expression of upper mantle processes, Geochem. Geophy. Geosystems, Vol. 12, no. 11, Q11002, doi:10.1029/2011GC003579

Daley, T.M., Freifeld, B.M., Ajo-Franklin, J., Dou, S., Pevzner, R., Shulakova, V., et al., 2013. Field testing of fiber optic distributed acoustic sensing (DAS) for subsurface seismic monitoring. The Leading Edge, vol. 32, no. 6, pp. 936-942.

Dix, C.H., 1955. Seismic Velocities from Surface Measurements. *Geophysics*, 20, 68-66.
DOE (2015) Work Proposal FWP0174: Best Practices Manual – Brines, Reservoir Management, and Water Treatment in CCUS Operations, Carbon Sequestration Program, October 30, 2015.

Doran, G. and L. Y. C. Leong (1998). Developing a Cost-Effective Environmental Solution for Produced Water and Creating a "New" Water Resource-Final Technical Report. Bakersfield, CA, ARCO Western Energy and Kennedy/Jenks Consultants**:** 248 pp.

Douglas, J., B. Edwards, V. Convertito, et al. (2013). Predicting ground motion from induced earthquakes in geothermal areas, *Bull. Seismol. Soc. Am. 103 (3),* 1875-1897.

Drever, J. I. (1982) The Geochemistry of Natural Waters. Prentice-Hall, Inc., 388 p.

Dutta, N.C., 2002. Geopressure prediction using seismic data: Current status and the road ahead. *Geophysics*, 67, 2012-2041.

Eaton, B. A., 1975. The equation for geopressure prediction from well logs. *SPE 5544*.

Energy Information Agency, 2015. *Domestic Uranium Production Report 3rd Quarter 2015.* Accessed 5 February 2016 from http://www.eia.gov/uranium/production/quarterly/pdf/qupd.pdf.

Feng, Q., Y. Miyai, H. Kanoh, and Kenta Ooi (1992) Li+ extraction with spinel-type lithium manganese oxides. Charaterization of redox-type ion exchange sites. Langmuir 8:1861-1867.

Freethey Geoffrey W., Gail E. Cordy, 1991. *Geohydrology of Mesozoic rocks in the Upper Colorado River Basin, in Arizona, Colorado, New Mexico, Utah and Wyoming, excluding the San Juan Basin: Regional aquifer-system analysis – Upper Colorado River Basin*. U.S. Geological Survey Professional

Ganshin, Y.V. and Surdam R.C, 2013, Utility of 3-D Seismic Attribute Analysis and VSP for Assessing Potential Carbon Sequestration Targets on the Rock Springs Uplift, Southwest Wyoming: in Ronald C. Surdam editor, Geological CO_2 Storage Characterization, Chapter 7, pp. 97-150, *Springer*.

Garrett, Donald E. (1996) Potash. Chapman and Hall, 734 pages.

Garrett, Donald E. (1998) Borates: Handbook of Deposits, Processing, Properties, and Use. Academic Press, 483 pages.

Garrett, Donald E. (2004) Handbook of Lithium and Natural Calcium Chloride. Elsevier, 476 pages.

Gebauer, D., A. Volkel, H. Colfen (2008) Stable prenucleation calcium carbonate clusters. Science 322:1819-1822.

Harp, Dylan R., and Velimir V. Vesselinov. "Contaminant remediation decision analysis using information gap theory." *Stochastic environmental research and risk assessment* 27, no. 1 (2013): 159-168.

Hill, Alistair (2015) Market drivers for commercial recovery of products from geothermal fluids. GNS Science Miscellaneous Series 81. www.gns.cri.nz

Humphreys, E. and **D. Coblentz**, 2007. North America Dynamics and Western U.S. Tectonics, Reviews of Geophysics, Vol. 45, RG3001, doi:10.1029/2005RG000181, 2007
J.C. Kammerer. 1990. *Largest Rivers in the United States.* Accessed 5 February 2016 from http://pubs.usgs.gov/of/1987/ofr87-242/.

Jiao Z., and Surdam R., 2013, Advances in estimating the geological CO2 storage capacity of the Madison Limestone and Weber Sandstone in the Rock Springs Uplift by utilizing detailed 3-D reservoir characterization and geological uncertainty reduction: in Surdam edit, Geological CO2 storage characterization, Springer Publication, p. 191-232.

Kamal, M. M., I*nterference and Pulse Testing – A Review*. Journal of Petroleum Technology, 2257-2270, December 1983.

Keister, Timothy CWT. Issued 2001. Revised 2008. *Cooling Water Management Basic Principles and Technology*. ProChemTech International, Inc. Accessed 11 January 2016 from: http://www.prochemtech.com/Literature/Technical/Basic_Cooling_Water_Management_II.pdf.

Kirschbaum, Mark et. al. 2002. *Assessment of Undiscovered Oil and Gas Resources of the Southwestern Wyoming Province, 2002.* Accessed 1 February 2016 from http://pubs.usgs.gov/fs/fs-145-02/fs-145-02.html.

Knudsen, S., G. Havsgard, and A. Berg, 2006, Flow-induced noise in fiber-optic 3C seismic sensors for permanent tubing-conveyed installations. 68th EAGE Conference. Extended Abstracts.

Korneev, V., and A. Bakulin, 2006, On the fundamentals of the virtual source method: Geophysics, 71, no. 3, A13–A17.

Lee, John C., *Well Testing*. Society of Petroleum Engineers, 1982

Leonard Rice Engineers Inc., 2009, *Consumptive use analysis.* Draft memo submitted to Wyoming State Engineer as part of the Wyoming Water Rights, Attribution Geodatabase Project, 27 June, 2009, pps 18.

Majer, E., V. Korneev, T. Daley, G. Li, T. Davis, J. Washbourne, and H. Merry, 2001, Weyburn field horizontal-to-horizontal crosswell seismic profiling: Part 1 – Planning and data acquisition, SEG Int'l Exposition and Annual Meeting, San Antonio, Texas, Sept. 9-14.

Mateeva, A., J. Lopez, J. Mestayer, P. Wills, B. Cox, and D. Kiyashchenko, et al., 2013, Distributed acoustic sensing for reservoir monitoring with VSP, *The Leading Edge*, vol. 32, no. 10, pp. 1278-1283.

McLaughlin, J. F., Ganshin, Y., Quillinan, S., Bentley, R., Jiao, Z., "Mitigating Risks Associated with Long-term CCUS: Characterizing the Geologic History and Heterogeneity of Sealing Strata." *Energy Procedia* 63 (2014): 4999-5009.

McLaughlin, J. F., Ramsey D. B., and Quillinan, S.A, . 2013. *Regional Geologic History, CO_2 Source Inventory and Groundwater Risk Assessment of a Potential CO_2 Sequestration Site on the Rock Springs Uplift in Southwest Wyoming*.

Oren, Yoram (2008) Capacitive deionization (CDI) for desalination and water treatment – past, present and future (a review). Desalination 228:10-29.

Pafeng, Josiane, Dario Grana, and Subhashis Mallick. "Joint Rock Physics Inversion of Elastic and Electric Attributes for Rock and Fluid Properties–A Real Data Example." 2014 SEG Annual Meeting. Society of Exploration Geophysicists, 2014.

Paper 1411–C. Accessed 1 February 2016 from http://pubs.usgs.gov/pp/1411c/report.pdf.
Pitzer, K. S. (1977) Electrolyte theory – Improvements since Debye and Huckel. Accounts. Chem. Res. 10:371-377.

Quillinan, S. A., and J. F. McLaughlin (2013) Reservoir fluid characterization of the Weber Sandstone and Madison Limestone on the Rock Springs Uplift in Southwest Wyoming. Chapter 8 in Geological CO_2 Storage Characterization, R. C. Surdam (ed.) Springer Science.

Rowe, D.R., and Abdel-Magid, 1995, *Handbook of Wastewater Reclamation and Reuse*, CRC Press, Inc. 550pp.

Sayers, C. M., G. M. Johnson, and G. Denyer, 2002, Predrill pore-pressure prediction using seismic data: *Geophysics,* 67, 1286–1292.

Schlumberger Limited. 2016. *Brine.* Accessed 1 February 2016 from http://www.glossary.oilfield.slb.com/Terms/b/brine.aspx.

Seccombe, J., Lager, A., Webb, K., Jerauld, G. and Fueg, E., 2008, *Improved Waterflood Recovery: LoSal™ EOR Field Evaluation.* SPE 113480.

Shukla, Khemraj, Priyank Jaiswal, and Subhashish Mallick. "A first-arrival wavelet based rotation strategy for 3D-3C Data: A Case Study from Rock Springs Uplift, Wyoming." Analysis 2 (2015): 1.

Spears and Associates, Inc., 2004, *Oilfield Market Report*. Tulsa, Oklahoma, www.spearsresearch.com.

Stone, I. P., R. E. Lee, C. R. Bradley and C. S. Larmat. (2016) Development of a Ground Motion Prediction Method for Carbon Dioxide Injection Induced Earthquakes. *Submitted to Engineering Geology (in Review)*

Sullivan Graham, E. J., S. Chu and R. J. Pawar (2014). The CO_2-PENS Water Treatment Module: Cost Profile and Importance Scenario Analysis for Understanding Treatment Processes. Thirteenth Annual Carbon Capture, Utilization, and Sequestration Conference, Pittsburgh, PA.

Sullivan Graham, E. J., S. Chu and R. J. Pawar (2015). "Probabilistic cost estimation methods for treatment of water extracted during CO_2 storage and EOR." International Journal of Greenhouse Gas Control 41: 316-327. Evans, Keith (2010) Lithium abundance – world lithium reserve. http://lithiumabundance.blogspot.com/

Surdam, RC and Jiao J. 2007. *The Rock Springs Uplift – an outstanding geological CO_2 sequestration site in southwest Wyoming*. Wyoming State Geological Survey Challenges in Geologic Resource Development No.2.

Surdam, RC editor, 2013. *Geological CO_2 Storage Characterization: The Key to Deploying Clean*

Fossil Energy Technology. Springer Environmental Science and Engineering. Pp 301.
Surdam, Ronald C., ed. Geological CO2 storage characterization: The key to deploying clean fossil energy technology. Springer Science & Business Media, 2013.

Suss, M. E., T. F. Baumann, W. L. Bourcier, C. M. Spadaccini, K. A. Rose, J. G. Santiago and M. Stadermann (2012) Capacitive desalination with flow-through electrodes. Energy and Env. Sci. 5:9511-9519.

Taner, M. T., and Koehler, F., 1969, Velocity spectra – digital computer derivation and applications of Terzaghi, K., 1943. *Theoretical soil mechanics.* John Wiley and Sons, New York.

Uranium Energy Corp, 2015. *In Situ Recovery (ISR).* Accessed 5 February 2016 from http://www.uraniumenergy.com/uranium/in_situ_leach/.

Ur-Energy, 2015. *Lost Creek* Accessed 5 February 2016 from http://www.ur-energy.com/lost-creek/.

USGS. 2013. *Water Data Report near Green River Utah.* Accessed 5 February 2016 from http://wdr.water.usgs.gov/wy2013/pdfs/09315000.2013.pdf.
Vledder, P., Fonseca, J. C., Wells, T. Gonzalez, I., Ligthelm, D., 2010, *Low salinity water flooding: Proof of wettability alteration on a field scale.* SPE 129564.

Wald, D.J. and T.I. Allen (2007). Topographic Slope as a Proxy for Seismic Site Conditions and Amplification, Bull. Seis. Soc. Am., Vol. 97, 1379-1395.

Washbourne, J., G. Li, and E. Majer, 2001, Weyburn field horizontal-to-horizontal crosswell seismic profiling: Part 2 – data processing, SEG Int'l Exposition and Annual Meeting, San Antonio, Texas, Sept. 9-14.

Wills, C. J., and Silva, W., 1998. Shear-wave velocity characteristics of geologic units in California, *Earthquake Spectra* **14** (3), 533–556.

Wills, C. J., Petersen, M., Bryant, W. A., Reichle, M., Saucedo, G. J., Tan, S., Taylor, G., and Treiman, J., 2000. A site-conditions map for California based on geology and shear-wave velocity, *Bull. Seismol. Soc. Am.* **90** (6B), S187–S208.

Wu, Wenting, et al. "Bayesian Facies Classification in a CO 2 Sequestration Study using Statistical Rock Physics Modeling of Elastic and Electrical Properties." 2015 SEG Annual Meeting. Society of Exploration Geophysicists, 2015.

WWC Engineering, 2010, *Green River Basin Plan submitted to the Wyoming Water Development Commission*, December 2010, pps 189.

Yu, F., Jin Y., Chen, K. P., and Chen, M., 2014. *Pore-pressure prediction in carbonate rock using wavelet transformation*: Geophysics, 79, D243-D252.